Title
Design and Synthesis of Novel Luciferin Architectures

Author
Steinhardt, Rachel

Publication Date
2015

Peer reviewed|Thesis/dissertation

UNIVERSITY OF CALIFORNIA,
IRVINE

Design and Synthesis of Novel Luciferin Architectures

DISSERTATION

submitted in partial satisfaction of the requirements
for the degree of

DOCTOR OF PHILOSOPHY

in Chemistry

by

Rachel Catherine Steinhardt

Dissertation Committee:
Professor Jennifer Prescher, Chair
Professor David Van Vranken
Professor James Nowick

2015

DEDICATION

To

my parents, family and friends

in recognition of their worth

and most of all to my wife, Genevieve

Enlightenment is like the moon reflected on the water.
The moon does not get wet, nor is the water broken.
Although its light is wide and great,
The moon is reflected even in a puddle an inch wide.
The whole moon and then entire sky
Are reflected in one dewdrop on the grass.
–Dogen

TABLE OF CONTENTS

LIST OF FIGURES

LIST OF TABLES

Rachel Steinhardt
Curriculum Vitae

Ph.D. Candidate, Chemistry
Prescher Lab
University of California, Irvine
3304 Natural Sciences 1
Irvine, CA 92697-2025

Education
Ph.D. Chemistry, 2015, University of California, Irvine
M.S. Chemistry, 2010, University of California, Santa Cruz
B.S. Genetics and Plant Biology, 2005, University of California, Berkeley

Research Experience
2010–Present Graduate Student with Prof. Jennifer Prescher, UC Irvine.

2009–2010 Graduate Student, organic chemistry lab of Prof. Scott Lokey, UC Santa Cruz. *Synthesized sulfenylated model peptides to improve cell permeability of linear and cyclic peptide-based drugs. Screened multidrug combinations for antibiotic efficacy in vancomycin resistant* S. aureus *and methecillin resistant* S. aureus.

2007–2009 Lab Technician, protein crystallography lab of Prof. Seth Rubin, UC Santa Cruz. *Crystallized complex of Retinoblastoma protein and peptide substrate. Performed kinetic analyses on enzyme-substrate interaction. Set up and maintained HPLC, FPLC.*

2005–2007 Scientist, Santa Cruz Biotechnology, Inc., antibody purification dept. *Independent projects: 1) Surface passivation and functionalization of mesoporus silica beads for antibody purification. 2) Creating an extended chemiluminescence reagent for proprietary production., Purified primary polyclonal antibodies, ran Western blots to demonstrate utility of reagents for catalog pictures, formulated secondary antibodies.*

2001–2003 UROP recipient, plant development lab of Prof, Z. R. Sung, UC Berkeley
Performed RT-PCR analyses to gauge phenotypic effects of new Arabidopsis *mutant. Cloned GFP fusion construct of mutant gene.*

1998–2001 Research assistant, neuropathology lab of Prof. Henry Poole, UC San Diego
Sole person responsible for assessing levels of neuronal demylination from microscopy images of subject in drug trial. Assisted in sample preparation for transmission electron microscopy.

Publications
7. **Steinhardt, R.C.**; Rathbun, C.M.; McCutcheon, D.C.; Krull, B.; Porterfield, W. B.; Furche, F.; Prescher, J.A. Building better luciferins through *ab initio* calculations. *Manuscript in preparation*

6. **Steinhardt, R.C.**; O'Neill, J.A.; McCutcheon, D.C; Prescher, J. A. Design and synthesis of an alkynyl luciferin analog for rapid assembly of bioluminescent probes *Manuscript in preparation.*

5. Book chapter: **Steinhardt**, **R.C.*,** McCutcheon, D.C.*, Prescher, J.A. Visualising chemical communication among migratory cells *in vivo*. *Manuscript in revision.*

4. McCutcheon, D.C.; Paley, M.A.; **Steinhardt, R.C.**; Prescher, J.A. Expedient synthesis of a electronically-modified luciferins for bioluminescence imaging. *J. Am. Chem. Soc.*, **2012**, *134*, 7604–7607.

3. Hirschi, A.; Cecchini, M.; **Steinhardt, R.C.**; Schamber, M.R.; Dick, F.A.; Rubin, S.M. An overlapping kinase and phosphatase docking site regulates activity of the retinoblastoma protein. *Nat. Struct. Mol. Bio.* **2010**, 17, 1051–1057.

2. Halpenny, G.M.; **Steinhardt, R.C.**; Okialda, K. A.; Mascharak, P.K. Characterization of pHEMA-based hydrogels that exhibit light-induced bactericidal effect via release of NO. J. Mater. Sci. Mater. Med. **2009**, *20*, 2353–2360.

1. Mizisin, A.P.; **Steinhardt, R.C.**; O'Brien, J.S.; Calcutt, N.A. TX14(A), a prosaposin-derived peptide, reverses established nerve disorders in streptozotocin-diabetic rats and prevents them in galactose-fed rats. *J. Neuropath. Exp. Neurol.* **2001**, *60*, 953–960.

Presentation

1. **Steinhardt, R.C.**; McCutcheon, D.C.; Paley, M.A.; O'Neill, J.M.; Prescher, J.A. "Clickable luciferins for bioluminescence imaging applications" *248th ACS National Meeting*, August 10-14 2014.

ABSTRACT OF THE DISSERTATION

Design and Synthesis of Novel Luciferin Architectures

By

Rachel Catherine Steinhardt

Doctor of Philosophy in Chemistry

University of California, Irvine, 2015

Professor Jennifer Prescher, Chair

Bioluminescence imaging using luciferase is a widely used technology. However, its scope is hampered by several limitations, most notably the lack of distinct luciferin-luciferase pairs suitable for multicomponent imaging. I addressed this problem by synthesizing novel luciferins which may be used by luciferase. Furthermore, I developed new techniques to evaluate whether a novel luciferin is intrinsically capable of emitting light.

Chapter 1: Optical imaging of biological processes

1.1 Introduction

Technologies have emerged within the imaging community that enable the non-destructive, real-time observation of dynamic cellular movements in vivo. Among the most popular of these approaches involve optical reporters. Optical imaging tools are uniquely suited to visualize cellular communication in living organisms [1-5]. These tools produce visible light that can report on cell motions and other behaviors [6-8]. Visible light is desirable for many in vivo applications owing to its non-toxicity (and thus biocompatability). Wavelengths in the 380-750 nm realm (UV-vis) have been used for decades in cell microscopy experiments and in vitrosame here, etc. assays to measure gene expression levels (Figure 1-1A). For imaging in live animals, though, more red-shifted light (>650 nm) is desirable. These wavelengths are less prone to absorption and scatter by endogenous chromophores and light, and can pass through tissues to be detected by sensitive cameras [9,10]. Mammalian tissues themselves emit few endogenous photons. Thus, optical probes can selectively report on a variety of cellular features. These probes—and how they have been used to understand biological functions—are the focus of this chapter.

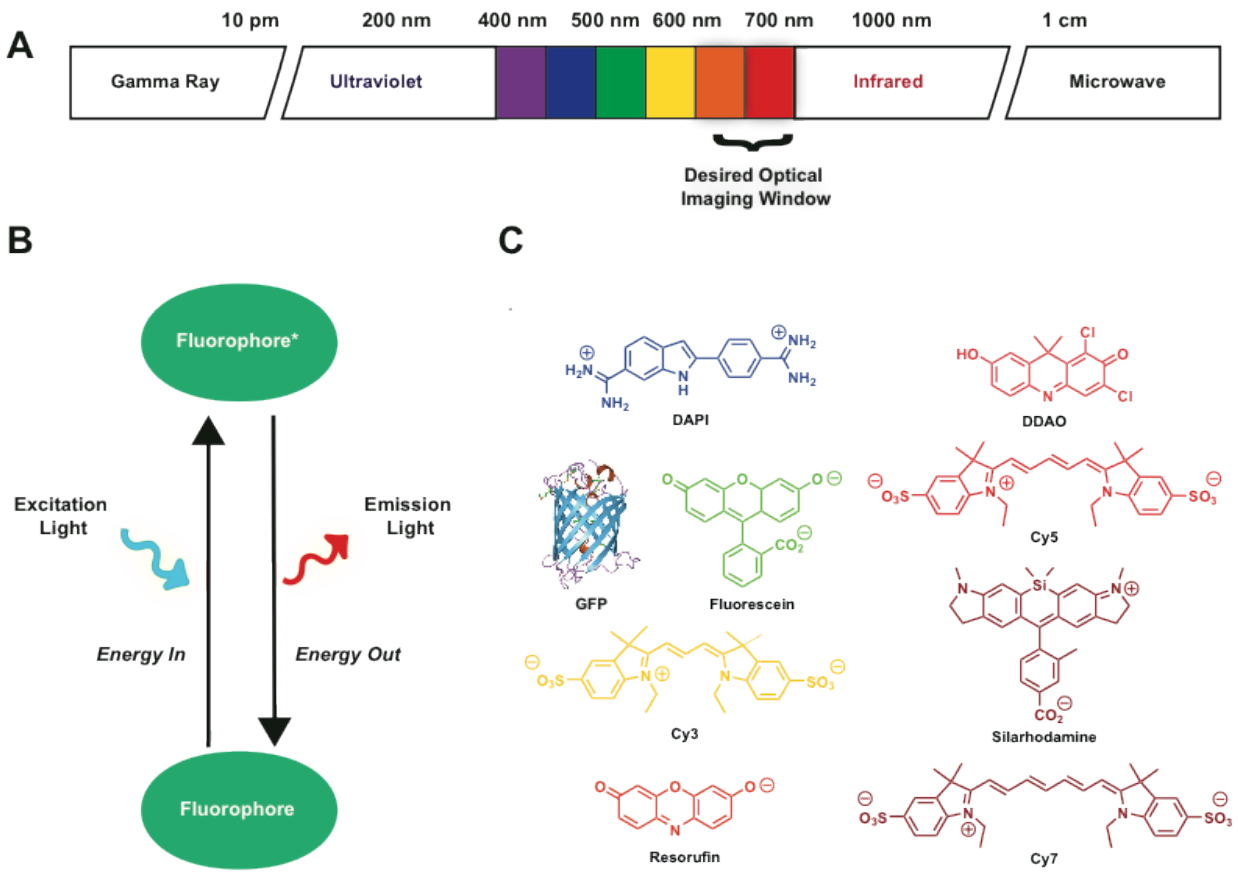

Figure 1-1. Considerations for fluorescence imaging. (A) The electromagnetic spectrum, with the desired window for in vivo optical imaging highlighted. (B) Fluorescent probes require excitation energy to emit light. Upon irradiation, the probes are electronically excited; relaxation to the ground state results in photon emission. (C) Examples of common fluorescent probes used for biological imaging.

For imaging cell-cell communication in vivo, most optical agents can be categorized as fluorescent or bioluminescent probes. Fluorescent probes emit light following absorption of incident photons (Figure 1-1B), and can be further sub-divided into two classes: small molecules (fluorophores) and fluorescent proteins (FPs) (Figure 1-1C). The bulk of FPs contain an internal chromophore produced from native amino acids upon protein folding [11]. For some FPs, the emission spectra are broad enough to include wavelengths that can escape tissue. Pushing these emission wavelengths farther into the red region is important for improved sensitivity and biocompatability. Over the years, both targeted and random mutagenesis have been used to diversify the palette of florescent proteins [4,11-14]. Some fluorescent proteins now excite and emit light in the red/near-infrared regime and are broadly useful for noninvasive imaging in whole organisms.

A complementary set of optical imaging probes comprises bioluminescent enzyme-substrate pairs. Like fluorescence imaging, bioluminescence imaging (BLI) has been useful for examining cellular and biological features in live organisms. BLI relies on a class of enzymes (luciferases) that catalyze light emission using small molecules substrates (Figure 1-2). Several luciferase-luciferin pairs have been identified in nature. The most popular for in vivo imaging derive from the North American firefly, *Photinus pyralis* (Fluc) [3,15]. Fluc catalyzes the oxidation of the small molecule D-luciferin, and emits yellow-green light. Other well-known luciferases derive from marine organisms, including *Renilla reniformis* (Rluc) and *Gaussia princeps* (Gluc). These enzymes catalyze the release of blue-green light using the small molecule coelenterazine [3,15]. Continued efforts to identify new luciferase-luciferin pairs in nature, and engineer non-natural ones, will expand the bioluminescent palette. However, the variations in

wavelength are not as dramatic as those for fluorescent molecules and dyes. This has somewhat limited the applicability of BLI for multi-component imaging [2,3].

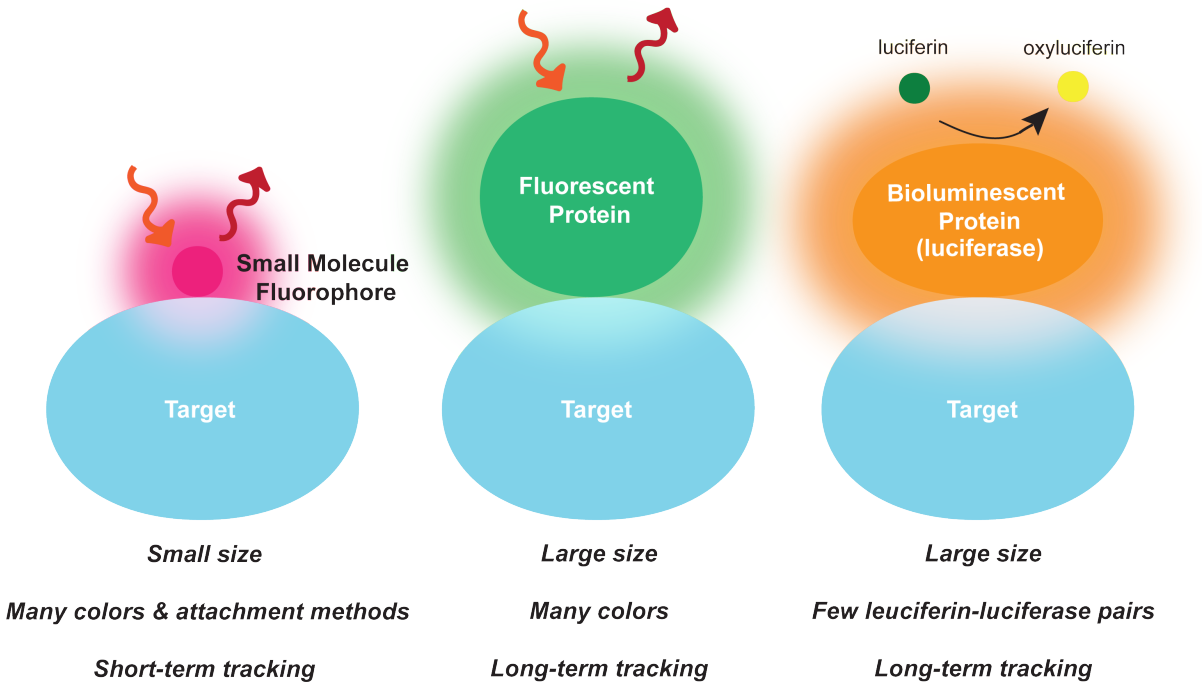

Figure 1-2. Common optical probes used in tracking cell communication and function. These include small molecule fluorophores, fluorescent proteins, and bioluminescent proteins (luciferases). Signature features of these probes are also listed.

1.2 Considerations for selecting an optical imaging modality

The photons produced by either fluorescent or bioluminescent probes must ultimately must be registered by a detector. Modern instrumentation offers a large linear range of photon detection, allowing very faint events to be visualized in concert with relatively bright ones [9,16]. In whole animal models, the number of photons reaching detector is influenced by overlying tissue and blood. Endogenous chromophores in these tissues and blood can both absorb and scatter light from the reporters. In general, the light reaching the detector falls off on a logarithmic scale with depth [9,10]. Transparent organisms avoid this problem; however, light penetration can be be limiting in studies that require mammalian tissues/organisms. In these latter cases, mathematical models can begin to deconvolute the diffusion of light within tissue. Based on these considerations, the ideal range for light transmission through tissue is in the near infrared range (650 – ~950 nm). Shorter wavelengths are absorbed by endogenous chromophores (melanin, hemoglobin, etc.) Longer wavelengths are absorbed by water.

Fluorescence microscopy can be reliably used to visualize cells over hundreds of micrometers, enabling studies of cell-to-cell contact in explanted tissues and small distances in live animals [17]. Fluorescence imaging over longer distances or depths remains difficult, though, owing to autofluorescence issues. Fluorescence microscopy also requires that investigators know where to look, that is, where and when to shine the excitation light [18]. The continued development of far-red emitting FPs is easing this requirement [19].

Imaging with bioluminescent probes, by contrast, does not rely on excitation light and can often be a better choice for imaging in thick tissues and animals. BLI has a very high signal-

to-noise ratio, due to virtually no photons being produced in mammalian tissue. The most commonly used luciferases (from the insect family) release light in the 600–650 nm range. While not absorbed well by hemoglobin, the wavelengths emitted are still subject to the diffusive effect of scattering that occurs as light descends deeper into tissue. The deeper the imaging source, the poorer the resolution. Thus BLI and noninvasive macroscopic imaging, in general, is a tradeoff between sensitivity and resolution.

The current depth limit of bioluminescence imaging (BLI) using firefly luciferase-luciferin is ~1-2 cm, and it is possible to use this technology without knowing the location of the imaging target *a priori*. BLI also requires an exogenous substrate and this can be limiting, based on cost and accessibility, as well as the bioavailability of the substrate. Bioluminescent probes are typically used for macroscale imaging in whole animals (due to low background signals), but are weak emitters. By contrast, fluorescent probes are more suitable for microscopic imaging owing to their requirement for excitation light. In fact, fluorescent and bioluminescent tools are often used in tandem to gain information across all length scales.

Optical reporters must often track with the cells of interest, requiring chemical or genetic "attachment" to the imaging target. Historically, small molecule fluorophores have been used to track cells for short-term imaging. These tools span a large spectrum of excitation and emission wavelength combinations [20]. For reasons mentioned above, those fluorophores whose excitation and emission wavelengths occur in the NIR tissue transmission window are particularly useful for in vivo imaging [21-23]. In addition to the traditional small organic molecules, fluorescent nanoparticles [24-26] and quantum dots [26,27] may also be used for in vivo imaging applications. Collectively, these tools can be appended covalently or non-

covalently (DiI, DiR, etc.) to cell surfaces. For cell-targeting probes, the dyes are often attached to antibodies via bioconjugation chemistries [28,29].

When the reporter probe needs to be used for long-term, serial tracking, genetic "attachment" is often more desirable. Genes encoding fluorescent or bioluminescent proteins can be incorporated into cells and animals, and the optical signatures of their encoded proteins can can "report" on desired biological process. Such genetic strategies can be used to mark cells or proteins for long-term visualization and monitor molecular events. Importantly, genetic tags propagate with cell division, providing stable sources of signal for longitudinal studies [30,31]. Genetic reporters can also be cloned into promoter regions of genes [32]. In these cases, the level of reporter produced parallels the transcription of the native gene. Several transgenic mice expressing these reporters are also readily available from commercial vendors.

1.3 Examples of cell communication with microscopic optical imaging tools

Cells exchange information via direct cell contacts and secreted small molecules. One of the most complex systems of cellular information exchange comprises immune function. Cell-cell contacts are required for basic immune function, including pathogen clearance mechanisms. Breakdowns in cellular communication also potentiate autoimmunity and other disease states. These phenomena are difficult to examine outside of living tissues or organisms. Capturing cell-cell communication in living systems is a paramount goal, and advances in imaging technologies and probes are bolstering efforts to examine such events. Fluorescence imaging tools, in particular, have been widely used to capture cell behaviors at microscopic scales. The bulk of examples described in this section focus on immunology.

Among immune cell types, T cells have been arguably the most well studied *in vivo*. These cells play central roles in both adaptive and innate immunity and T-cell based therapies are gaining traction in the clinic. T cells can be engineered to express fluorescent proteins and tracked in tissues and live organisms using fluorescence microscopy [33]. Their communication with other immune cells (including different T cell subtypes and B cells), in addition to their response to pathogens and malignant cells, are revealing new insights into the roles of immune function in human health and disease. Cahalan, Krummel, and others have shown that $CD4^+$ T cells form stable complexes with B cells in lymph tissue. The motile conjugates moved according in response to chemokine gradients for CCR7 [34] (Figure 1-3). Such discoveries were made possible using immune cells labeled differentially with fluorescent proteins. Numerous related studies have been performed to understand neutrophil trafficking patterns [35,36] and other immune cell behaviors

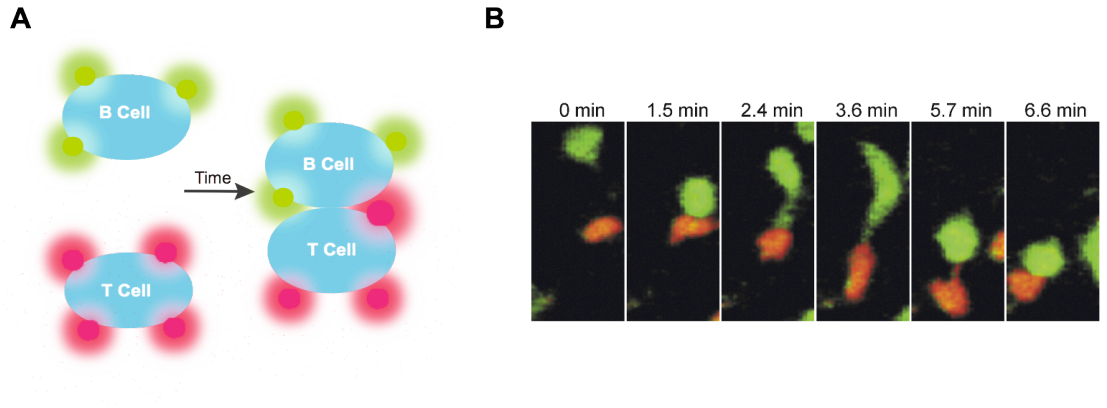

Figure 1-3. In vivo visualization of cell contacts. (A) Fluorescently labeled B (red) and T (green) cells were monitored over time. (B) Time-lapse images showing an encounter of a B cell and a T cell to form a conjugate. Image is reproduced with permission from [34].

More refined tracking studies are being enabled through advances in intravital microscopy. In these cases, microscope lenses can be juxtaposed next to tissues of interest to facilitate cell visualization in deeper locales [37]. Recent examples include imaging leukocytes to deconstruct the roles of selectins, integrins, and other endothelial markers involved in immune cell homing [38,39], and "serial killings" by single NK cells [40]. Fluorescent probes have also enabled detailed studies of antigen presentation by MHC molecules, a process central to the immune clearance of infection, along with lymphocyte proliferation in cell types which have proven difficult to image with traditional immunohistochemical staining [41,42]. In many cases, the same imaging tools can be used in combination with experimental therapies to judge efficacy and mechanistic targeting [43].

Beyond basic tracking of immune cells, imaging tools have enabled immune cell interactions with cancer cells and infectious agents to be readily visualized [44]. For example, intravital microscopy revealed a new role for perivascular macrophages in staph infections. These cells were observed to work closely with neutrophils in skin infected with *S. aureus* [45]. Such interactions would have gone unnoticed in studies outside of living organisms. Optical imaging tools are also aiding virus-immune cell interactions. In one example, the roles of $CD8^+$ T cells and dendritic cells in H1N1 influenza infection were examined using GFP labeled T cells and YFP labeled dendritic cells [43]. In related work, fluorescently labeled murine leukemia virus enabled researchers the observation of a viral synapse in vivo [46]. In another striking example, fluorescently labeled HIV particles were imaged in humanized mice to determine that infected T cells migrated readily and formed stable synapses [47]. These studies showcase the obvious strengths of genetically encoded imaging tags to visualize detailed biological processes.

Beyond cell tracking, optical reporters (especially FP's) can be co-opted for readouts on *gene expression* relevant to signal transduction and cell-cell communication. For example, Alves *et al.* were able to use intravital microscopy to follow YFP expression driven by the interleukin-7 (IL-7) promoter in the murine thymus [41]. IL-7 is difficult to visualize with conventional immunohistochemistry due to its low level of expression [42]. The imaging results provided a new level of insight into the spatiotemporal dynamics of IL-7 expression, which has implications both for T-cell development, as well as thymic morphology. The reporter gene construct also revealed IL-7 expression in several tissue types, as well as colocalization of IL-7 expressing cells and $CD8^+$ T cells, which require IL-7 in order to home to bone marrow. Optical tools have also been used to report on cascades of gene expression relevant to inflammation [48,49]. Multicomponent tracking experiments related to inflammation have also been performed. In one example, Matheu *et al*. labeled both H1N1 influenza specific $CD8^+$ T cells and dendritic cells [43]. The researchers were then able to observe the dynamics of the "cytokine storm" implicated in the increased virulence for this strain of flu.

In addition to monitoring cells and gene expression, optical reporters can be co-opted for direct visualization of the biomolecules involved in communication. Dynamic fluctuations in chemokines and other immune signaling molecules can dramatically influence immune cell behavior [50]. Visualizing levels of these probes can therefore provide direct insight into immune function. Most approaches to imaging and quantifying signaling molecules rely on antibody conjugates. Cleverly designed sensors can also report on biomolecule abundance. Several of these tools rely on fluorescence resonance energy transfer (FRET) for signal generation (Figure 1-4A). FRET involves the transfer of energy from one excited state molecule (donor) to a second molecule (the acceptor), with the released photon matching the emission

spectrum of the acceptor (Figure 1-4A). When the donor chromophore (i.e., small molecule dye or FP) and acceptor chromophore are far apart, excitation of the donor results in the characteristic emission wavelength of the donor. When the donor and acceptor are in close contact (i.e., 10–100 angstroms), excitation of the donor results in emission of the *acceptor* due to FRET. Thus, the ratio of acceptor to donor emissions (FRET ratio) directly reports on the distance between the two chromophores.

FRET imaging has been extensively applied to unravel protein-protein interactions relevant to signal transduction and receptor dimerization [51,52]. In these cases, the donor and acceptor fluorophores are appended to the candidate interacting proteins. FRET principles have also been used to design unique sensors to report on small molecule metabolites [53,54]. In one example, Mues *et al.* used a FRET-based genetically encoded calcium reporter gene to report on calcium levels in activated T cells. This genetically encoded reporter was used to monitor the cytosolic calcium levels of T cells in various situations and milieus in vivo, which enabled greater understanding of the activation patterns of T cells in a multiple sclerosis model (Figure 1-4) [55].

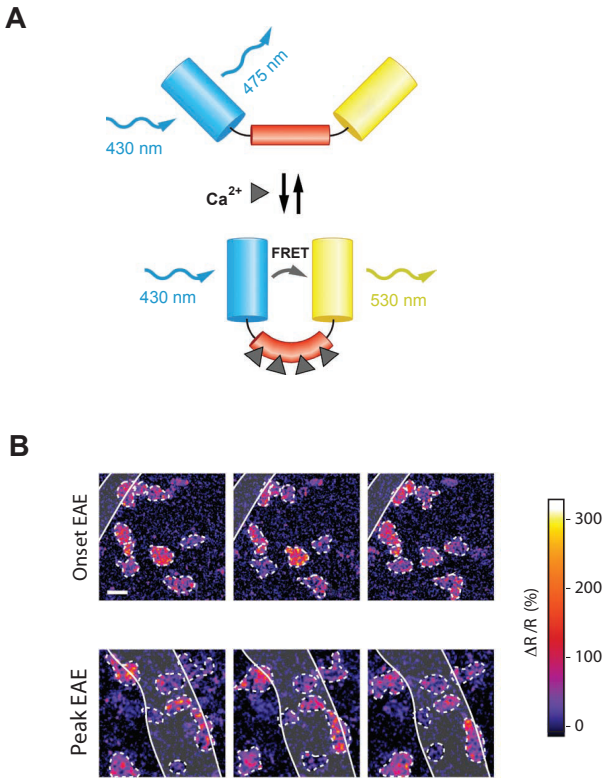

Figure 1-4. FRET sensors can be used to probe immune cell function in vivo. (A) A calcium-based FRET sensor comprising two fluorescent proteins joined by a calcium-responsive linker. When calcium ions bind, a conformational change re-positions the fluorescent proteins and FRET is observed. (B) The genetically encoded calcium sensor was used to image calcium concentrations in extravasated T cell clusters. Images were collected in inflamed spinal cords during onset of EAE (top panel) and peak EAE (bottom panel). EAE: mouse experimental autoimmune encephalitis, a murine multiple sclerosis model. ΔR/R: fractional fluorescence changes in the emission ratio. Both images are reproduced with permission from [55].

1.4 Macroscale visualization of cellular function with bioluminescent tools

Despite numerous advances in optical imaging over the past fifty years, our ability to resolve molecular and microscopic events in tissues and whole organisms remains limited. This is primarily due to the scattering of visible light by lipids and other biomolecules in opaque tissues, a phenomenon that broadens the area of signal perceived by the detector. Scattering can be partially ameliorated with physical methods, including mechanical disruption and dissolution [56], but these procedures are typically not compatible with serial imaging experiments requiring intact, living tissues. Intravital microscopy circumvents the need for disrupting tissue structures by placing the optical source and detector near the tissue of interest. Surgically implanted windows can further reduce interference from overlying tissues and resolve issues due to autofluorescence [17]. While providing unrivaled insight into microscopic cell interactions in living tissues, these techniques are invasive and not readily accessible to all researchers. Furthermore, these techniques require *a priori* knowledge of when and where to image.

Bioluminescence imaging (BLI) with luciferase-luciferin pairs, by contrast, is more suited to monitor biological processes in intact animals. Indeed, luciferase-labeled cells have been used to monitor cell trafficking patterns in diverse fields. Similar to microscopic imaging with FPs, several facets of immunology and methods for disease treatment have been monitored in vivo using BLI [57,58]. Improved luciferase reporters are enabling even more sensitive imaging in mouse models. Rabinovich and coworkers recently reported that as few as ten T-cells expressing an optimized luciferase can be imaged in some mouse models post-implantation [59]. This exquisite sensitivity has been capitalized on to track other immune cell classes, including NK cell homing to tumor stroma BLI [60]. Recently, the Negrin group examined the roles of

regulatory T cells (Tregs) and natural killer T (NKT) in immune function (Figure 1-5A). Using adoptive transfer of luciferase-labeled CD4(+) NKT cells in a murine model of allogeneic hematopoietic cell transplantation (HCT) the authors monitored the migration of the cells first to lymphoid tissues then to graft-versus-host disease (GVHD) target tissues. GVHD entails donor cells attack host tissue following transplantation. The study found that adoptively transferred NKT cells survive over 100 days and unlike conventional T cells do not cause significant GVHD-related morbidity or mortality. Furthermore, mixing in just 10,000 NKT cells to large boluses of T cells suppressed GVHD, demonstrating clinical potential in reducing GVHD in HCT [61]. While macroscale views of these cells could be readily gleaned, dissection and ex vivo analyses (with conventional fluorescent probes) were necessary to capture microscopic information.

The ability to sensitively visualize immune cell homing has similarly proved to be a tremendous boon to adoptive cell transfer studies in preclinical cancer models [61]. These therapies involve isolating a patient's white blood cells and engineering the cells *ex vivo* to improve their tumor-killing and homing efficacies. The modified cells are then re-introduced into the patient [57]. In a recent example, Tsukahara *et al.* utilized BLI to examine chimeric T cell engineering and its relevance to adoptive cell transfer. Human T cells were engineered to express CD19 receptors. CD19 is a cell surface protein that assembles with the B cell antigen receptor in order to decrease the threshold for antigen receptor-dependent stimulation. When these cells reinfused into mice bearing $CD19^{+}Fluc^{+}$ tumors, tumor proliferation was markedly reduced as judged by bioluminescence imaging [62].

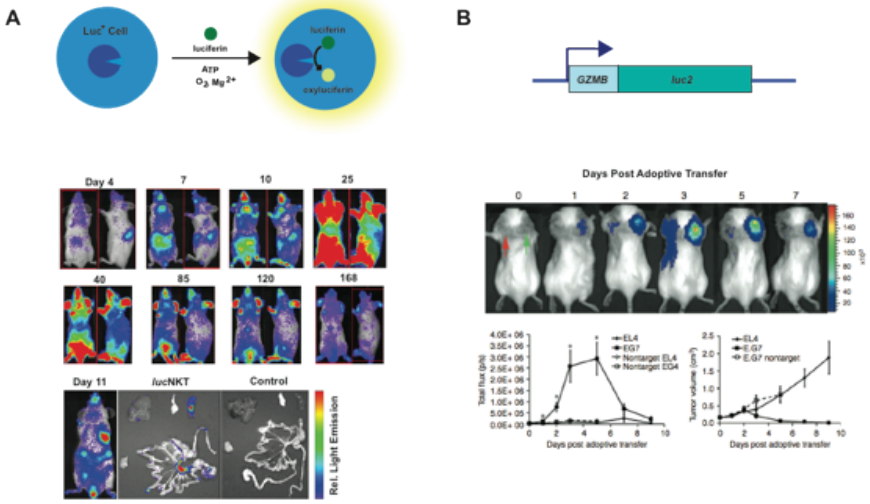

Figure 1-5. Luciferase probes can be used to track cell populations and gene expression patterns in vivo. (A) In graft-versus-host disease (GVHD) models, NKT (luc^+) cells were observed in the spleen and lymph nodes, then the skin and other organs. The total photons emitted from the luc+ cells peaked at day 25, and then declined steadily. Imaging of excised organs indicated NKT cells trafficked to the spleen and mesenteric lymph nodes on day 11. (B) Bioluminescence imaging was used to monitor T cell effector function in response to tumor antigens in vivo. T cell activation was monitored using a luc2 reporter gene, driven by a granzyme B promoter. Mice were implanted with two cancer cell lines, EL4 (thyroma cell line) and its derivative EG7 (EL4 cells stably express chicken OVA cDNA). An adoptive T cell transfer was performed on the tumor bearing mice, with $CD8^+$ T cells responsive to OVA. Bioluminescent signal in the EG7 tumor was more robust than in the non-targeted EL4 tumor. Peak signal intensity from the target tumor coincided with tumor regression. OVA: ovalbumin. Image (A) is reproduced with permission from [61]. Image (B) reproduced with permission from [72].

Unlike fluorescence technologies, bioluminescence has been largely limited to monitoring one cell type or biological feature at a time. Only a handful of distinct luciferase-luciferin pairs have been optimized for use in heterologous organisms. While these bioluminescent probes often emit different colors of light, they remain difficult to distinguish in living organisms, where the depth of the source and various tissue properties influence the

"color" of light observed by the detector. Luciferases that catalyze light emission with chemically distinct molecules can be more readily discerned, and some have been used in tandem. In one example, T cells expressing Gluc could be readily visualized accumulating within Fluc-expressing tumor cells [63]. Sequential application of coelenterazine and luciferin (the Gluc and Fluc substrates, respectively) enabled both populations of cells to be imaged simultaneously. Similar bioluminescent pairs have been used to track Treg and effector T cell functions [64], differential tumor growth [65], mesenchymal stem cell interactions with tumor stroma, and interaction of the immune system with fungal infections such as *Aspergillis* and *Candida* [66-70]. While fruitful, these studies still remain arduous, as substrates must often be supplied sequentially and given ample time to clear.

Similar to fluorescence imaging, BLI has been applied to studies of gene expression patterns [71]. Various promoters have been used to drive luciferase expression, including those involved in T cell activation [72] and B cell proliferation [73], in addition to tumor progression [74], and other pathologies [75]. In a recent example, T cell activation was monitored by transfecting T cells with a granzyme B promoter-luciferase reporter construct (Figure 1-5B). Granzyme B was used because of its known correlation with T cell activation. It should be noted that the researchers subsequently had to apply two rounds of signal amplification in order to detect the luciferase signal in a BLI platform. Researchers were then able to observe T cell activation in response to an antigenic tumor, the peak of which correlated with tumor regression [72]. In all cases, BLI provided a facile readout of gene expression levels across entire organisms.

While less common, BLI can also be used to track individual proteins and other biomolecules relevant to immune function. In one example, the Serganova lab monitored the

abundance of HIF-1α, a transcription factor that is overexpressed in many human cancers, using an Fluc fusion. The chimeric protein enabled sensitive imaging of the abundance and stability of HIF-1a *in cellulo* and in xenograft models [76]. Luciferase fusions have also been used to interrogate the canonical Wnt signaling pathway. The Wnt pathway regulates various aspects of development, including immune cell differentiation and becomes dysregulated in a variety of cancers [77]. In this network, β-catenin (β-cat) acts as a transcriptional activator of numerous host transcription factors. Usually marked for degradation, β-cat stabilization enables propagation of Wnt signaling. To study the posttranslational stabilization of β-cat, Naik *et al.* developed two bioluminescent fusion reporters, a β-cat click beetle luciferase (β-cat-CBG) and β-cat firefly luciferase (β-cat-FLuc). The researchers were able to observe modulators of β-cat activity and global β-cat levels, as well as processing, and downstream transcriptional activity by using further reporters [78].

Beyond direct detection, biomolecules can be visualized using bioluminescent sensors. Many of these exploit BRET in which bioluminescent emission excites a longer-wavelength fluorophore (Figure 1-6A). Analogous to FRET, the emission spectrum of the luciferase must overlap with the excitation of the fluorophore or FP. When the two light emitting molecules are in close proximity, the emission of the longer wavelength fluorophore is observed. Using an optimized version of Rluc (Rluc8) and a yellow-fluorescent protein (Venus) linked by pro-IL-1β, the Pelegrin group developed a BRET sensor for caspase-1 activity (Figure 1-6B). Caspase-1 modulates several inflammatory signaling molecules, including the proapopotic chemokine IL-1β in macrophages and other immune cells. IL-1β becomes activated upon caspase-1 cleavage of the proprotein form (pro-IL-1β). When the BRET sensor was expressed in cells with low levels of active caspase, the BRET pair remained in close proximity, evidenced by the emission

of yellow light. The blue photons emitted by Rluc8 acting upon coelentrazine are absorbed by Venus which emits lower-energy yellow light. When the BRET sensor is cleaved by caspase-1, Rluc is free to diffuse away from Venus and blue light is observed upon coelentrazine administration. The ratio of blue to yellow light in each case is a measure of caspase-1 activity and IL-1β activation, which indicates changes in the inflammatory response [79].

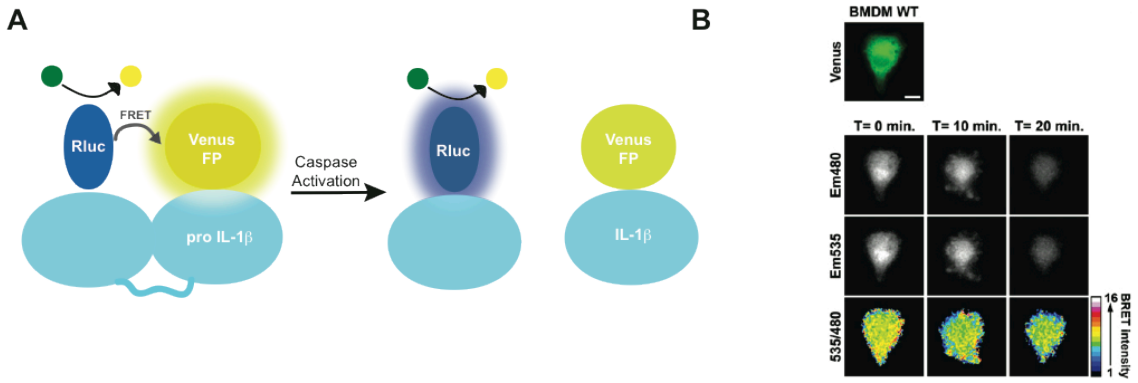

Figure 1-6. BRET probes can report on immune cell function. (A) A BRET sensor for IL-1β formation (mediated by caspase activity) was devised. Before pro IL-1β is cleaved, the two parts of the pro protein, labeled with Rluc and Venus fluorescent protein, are in close proximity. In this scenario, Rluc serves as the excitation source for Venus fluorescence. Once the pro protein is cleaved to mature IL-1β, Rluc is no longer in close enough proximity to Venus fluorescent protein, and Rluc light emission is observed. (B) The BRET sensor was used to image IL-1β processing in primary bone marrow-derived macrophages (BMDM). Macrophages were monitored at 480 nm (Rluc emission) and 535 nm (Venus emission), after being administered the Rluc substrate, coelenterazine. The bottom row is a pseudo colored for the 480/535 BRET ratio. Image (B) is reproduced with permission from [79].

1.5 Next-generation tools for imaging immune cell communication

The need to monitor cells at all length scales to capture chemical communication is driving the development of new tools and technologies. Work in the fluorescence realm is already well under way. As noted above, brighter, more photostable, and red-shifted FPs are being produced [80-82], along with metabolite-responsive FP's [54,83]. New chemistries to efficiently produce dyes and attach them to cells and other imaging targets are also being developed [20,84]. New fluorescence imaging technologies based on reconstitution of split GFP or enzymatic tagging of intracellular interactions have enabled rapid identification of direct cell contact in synapses [84-86].

In the bioluminescence realm, new luciferins and luciferases are also being engineered to track multiple cell types and for more sensitive imaging. The majority of this work to date has focused on identifying new luciferases, although many remain poorly characterized. Continued optimization of these luciferases for expression and stability is also increasing their sensitivity for use in vivo. Within well-characterized luciferase families, standard molecular biology techniques are being used to optimize reaction kinetics and, in some cases, provide altered colors or other desirable characteristics such as prolonged light emission [87-90].

More recently, the focus has turned to the luciferin itself. The luciferin small molecule is the bioluminescent light-emitter, thus efforts to modify its structure and enzyme utilization are attractive. Urano and coworkers developed several new luciferin derivatives by appending fluorophores to the aromatic core [91]. Upon luciferase utilization, BRET to the pendant fluorophore red shifts the light emission. The Miller and Prescher labs have similarly explored nitrogenous luciferins [92,93]. Moerner and Urano have also developed heterocyclic variants (Figure 1-7) [94]. Most have altered emission spectra, and are on par with D-luciferin in terms

of enzyme utilization. Additionally, one of the cyclic amino luciferin derivatives exhibits enhanced bioavailability in mouse models [95]. Studies on novel luciferins rely on efficient syntheses of these new compounds. To this end, the Prescher lab has developed method to quickly access several novel luciferins [93].

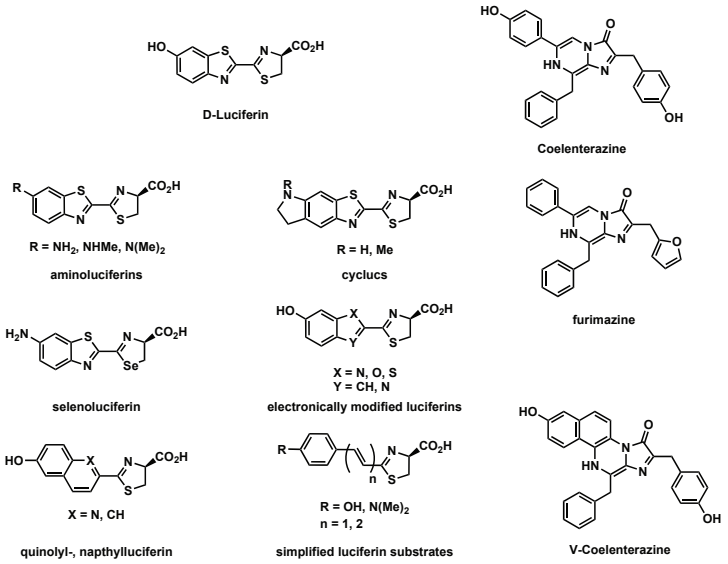

Figure 1-7. Collection of luciferin analogs for bioluminescence imaging.

Despite these efforts to identify improved luciferins, multispectral imaging with BLI remains difficult. As mentioned above, light emission in rodent models is skewed by tissue depth, complicating the interpretation of wavelength. Thus, multi-component bioluminescence imaging and efforts to map cell-cell contacts with distinct luciferase and luciferin pairs are complicated. In recent years, alternative methods to capture these events have been reported. For example, "split" versions of luciferase have been used to map cell interactions and detect chemokine receptor-ligand interactions [96]. The Prescher group extended this technology to probing direct cell-cell contacts in living systems [97].

In a related strategy, we crafted bioluminescent tools that produce light only when two cells interact (Figure 1-8). These tools comprise "caged" probes—luciferins outfitted with appendages (i.e., "cages") that preclude binding to luciferase [98]. In the presence of "activator" cells capable of removing the cage (e.g., via selective enzymatic activity), active luciferin is liberated and available for use by luciferase-expressing ("reporter") cells. Reporter cells nearest the activator cells consume the most substrate; thus, light intensity correlates with the proximity of the two populations (Figure 1-8). For example, a galactose-caged luciferin (Lugal) was synthesized to monitor the proximity between β-galactosidase (β-gal)-expressing activator cells and luciferase-expressing reporter cells in tumor models [99]. When activator cells were localized to sites of metastases, Lugal administration signaled the invasion of luciferase-expressing tumor cells in mice (Figure 1-8B) fix [100]. This study enabled sensitive imaging of cell-cell interactions not possible with traditional toolsets. Further extensions of "caged" luciferin technology and other methods to visualize cellular interactions promise to refine our views of organismal biology and disease.

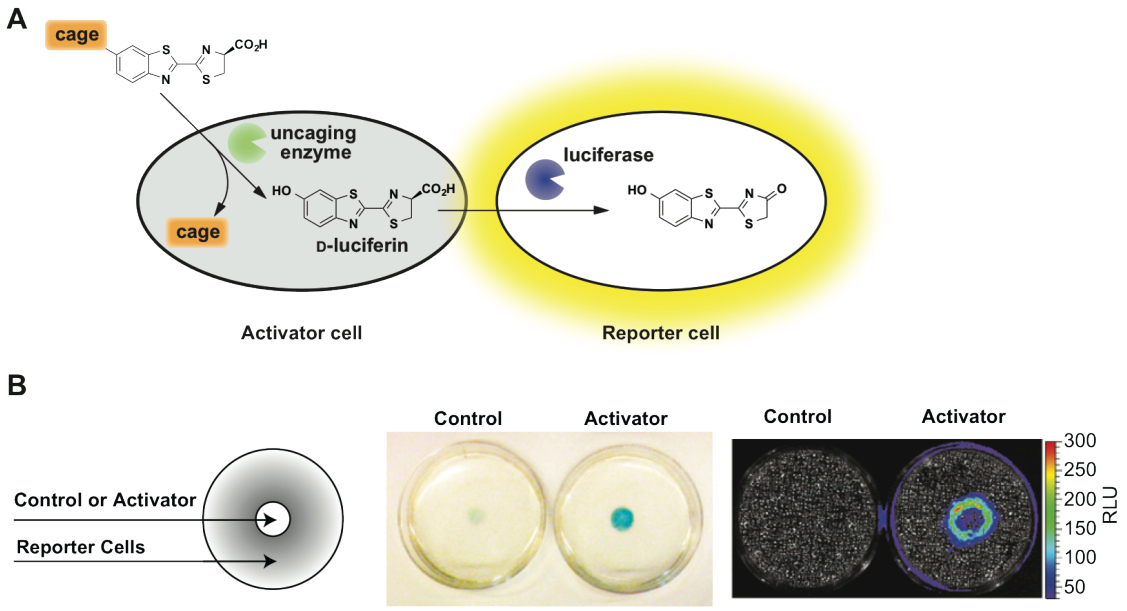

Figure 1-8. Immune cell interactions can be visualized with proximity reporters. (A) A proximity probe ("caged" luciferin) enters an activator cell, where it is liberated by an uncaging enzyme. Free luciferin can diffuse out of the cell. If a luc^{+} reporter cell is nearby, the uncaged substrate can be used to produce light. Robust light production is only observed when the activator and reporter cells are in close proximity. (B) An in vitro assay of the uncaging process. Activator or control cells in matrigel were plated in the center of a Petri dish. Luciferase reporter cells were plated in a monolayer surrounding the activator or control cells. The plates were incubated with a reporter substrate that shows location of uncaging enzyme activity (center). The caged luciferin was administered, and BLI was performed on the plates. Light emission was shown to correlate with the proximity of reporter cells to activator cells. Images were reproduced with permission from [100]

1.6 Objectives of this study

Optical imaging technologies have revolutionized our understanding of immunity and living systems by enabling researchers to visualize biological features in real time. As highlighted above, there is shortage of tools for imaging in vivo and, in particular, cellular communication networks in vivo. To address these issue I sought to develop new luciferins toward enabling multi-target tracking and detection.

The objectives of my thesis work included the following:

1. Develop novel syntheses of richly functionalized luciferins, towards the creation of compound libraries.
2. Characterize the biochemical and physical chemical properties of these new compounds.
3. Develop methods to predict robust, light-emitting luciferins for the development of unique bioluminescent enzyme-substrate pairs.

1.7 References

(1) Luker, G. D.; Luker, K. E. Optical imaging: current applications and future directions. *J. Nucl. Med.* **2008**, *49*, 1–4.

(2) Prescher, J. A.; Contag, C. H. Guided by the light: visualizing biomolecular processes in living animals with bioluminescence. *Curr. Opin. Chem. Biol.* **2010**, *14*, 80–89.

(3) Paley, M. A.; Prescher, J. A. Bioluminescence: a versatile technique for imaging cellular and molecular features. *MedChemComm* **2014**, *5*, 255–267.

(4) Day, R. N.; Davidson, M. W. The fluorescent protein palette: tools for cellular imaging. *Chem. Soc. Rev.* **2009**, *38*, 2887-2921.

(5) Hilderbrand, S. A.; Weissleder, R. Near-infrared fluorescence: application to in vivo molecular imaging. *Curr. Opin. Chem. Biol.* **2010**, *14*, 71–79.

(6) Hochgräfe, K.; Mandelkow, E.-M. Making the brain glow: in vivo bioluminescence imaging to study neurodegeneration. *Mol. Neurobiol.* **2013**, *47*, 868–882.

(7) Gross, S.; Piwnica-Worms, D. Spying on cancer: molecular imaging in vivo with genetically encoded reporters. *Cancer Cell* **2005**, *7*, 5–15.

(8) Germain, R. N.; Robey, E. A.; Cahalan, M. D. A decade of imaging cellular motility and interaction dynamics in the immune system. *Science* **2012**, *336*, 1676–1681.

(9) Rice, B. W.; Cable, M. D.; Nelson, M. B. In vivo imaging of light-emitting probes. *J. Biomed. Opt.* **2001**, *6*, 432–440.

(10) Cheong, W. F.; Prahl, S. A.; Welch, A. J. A review of the optical properties of biological tissues. *J. Quant. Elec.,* **1990**, *26*, 2166–2185.

(11) Chudakov, D. M.; Matz, M. V.; Lukyanov, S.; Lukyanov, K. A. Fluorescent proteins and their applications in imaging living cells and tissues. *Physiol. Rev.,* **2010**, *90*, 1103–1163.

(12) Shaner, N. C.; Steinbach, P. A.; Tsien, R. Y. A guide to choosing fluorescent proteins. *Nat. Methods* **2005**, *2*, 905–909.

(13) Filonov, G. S.; Piatkevich, K. D.; Ting, L.-M.; Zhang, J.; Kim, K.; Verkhusha, V. V. Bright and stable near-infrared fluorescent protein for in vivo imaging. *Nat. Biotechnol.* **2011**, *29*, 757–761.

(14) Yu, D.; Gustafson, W. C.; Han, C.; Lafaye, C. L.; Noirclerc-Savoye, M.; Ge, W.-P.; Thayer, D. A.; Huang, H.; Kornberg, T. B.; Royant, A.; Jan, L. Y.; Jan, Y. N.; Weiss, W. A.; Shu, X. An improved monomeric infrared fluorescent protein for neuronal and tumour brain imaging. *Nat. Commun.* **2014**, *5,* 1–7.

(15) Adams Jr, S. T.; Miller, S. C. Beyond D-luciferin: expanding the scope of bioluminescence imaging in vivo. *Curr. Opin. Chem. Biol.* **2014**, *21*, 112–120.

(16) Kim, J. B.; Urban, K.; Cochran, E.; Lee, S.; Ang, A.; Rice, B.; Bata, A.; Campbell, K.; Coffee, R.; Gorodinsky, A.; Lu, Z.; Zhou, H.; Kishimoto, T. K.; Lassota, P. Non-invasive detection of a small number of bioluminescent cancer cells in vivo. *PLoS One* **2010**, *5*, e9364.

(17) Pittet, M. J.; Weissleder, R. Intravital imaging. *Cell* **2011**, *147*, 983–991.

(18) Yushchenko, D. A.; Schultz, C. Tissue clearing for optical anatomy. *Angew. Chem. Int. Ed.* **2013**, *52*, 10949–10951.

(19) Nienhaus, K.; Nienhaus, G. U. Fluorescent proteins for live-cell imaging with super-resolution. *Chem. Soc. Rev.* **2014**, *43*, 1088–1106.

(20) Lavis, L. D.; Raines, R. T. Bright ideas for chemical biology. *ACS Chem. Biol.* **2008**, *3*, 142–155.

(21) Lavis, L. D.; Raines, R. T. Bright building blocks for chemical biology. *ACS Chem. Biol.* **2014**, *9*, 855–866.

(22) Lu, H.; Mack, J.; Yang, Y.; Shen, Z. Structural modification strategies for the rational design of red/NIR region BODIPYs. *Chem. Soc. Rev.* **2014**, *43*, 4778–4823.

(23) Adams, K. E.; Ke, S.; Kwon, S.; Liang, F.; Fan, Z.; Lu, Y.; Hirschi, K.; Mawad, M. E.; Barry, M. A.; Sevick-Muraca, E. M. Comparison of visible and near-infrared wavelength-excitable fluorescent dyes for molecular imaging of cancer. *J. Biomed. Opt.* **2007**, *12*, 024017.

(24) Yao, J.; Yang, M.; Duan, Y. Chemistry, biology, and medicine of fluorescent nanomaterials and related systems: new insights into biosensing, bioimaging, genomics, diagnostics, and therapy. *Chem. Rev.* **2014**, *114,* 6130–6178.

(25) Weissleder, R.; Nahrendorf, M.; Pittet, M. J. Imaging macrophages with nanoparticles. *Nat. Mater.* **2014**, *13*, 125-138.

(26) Peng, F.; Su, Y.; Zhong, Y.; Fan, C.; Lee, S. T.; He, Y. Silicon nanomaterials platform for bioimaging, biosensing, and cancer therapy. *Acc. Chem. Res.* **2014**, *47*, 612–623.

(27) S. Lidke, D.; Nagy, P.; J. Arndt-Jovin, D. Current protocols in cell biology; John Wiley & Sons, Inc.: 2001.

(28) Kalia, J.; Raines, R. T. Advances in bioconjugation. *Curr. Org. Chem.* **2010**, *14*, 138–147.

(29) Biju, V. Chemical modifications and bioconjugate reactions of nanomaterials for sensing, imaging, drug delivery and therapy. *Chem. Soc. Rev.* **2014**, *43*, 744–764.

(30) Contag, C. H.; Jenkins, D.; Contag, P. R.; Negrin, R. S. Use of reporter genes for optical measurements of neoplastic disease in vivo. *Neoplasia* **2000**, *2*, 41–52.

(31) Mandl, S.; Schimmelpfennig, C.; Edinger, M.; Negrin, R. S.; Contag, C. H. Understanding immune cell trafficking patterns via in vivo bioluminescence imaging. *J. Cell Biochem. Suppl.* **2002**, *39*, 239–248.

(32) Bhaumik, S.; Lewis, X. Z.; Gambhir, S. S. Optical imaging of Renilla luciferase, synthetic Renilla luciferase, and firefly luciferase reporter gene expression in living mice. *J. Biomed. Opt.* **2004**, *9*, 578–586.

(33) Favicchio, R.; Zacharakis, G.; Oikonomaki, K.; Zacharopoulos, A.; Mamalaki, C.; Ripoll, J. Kinetics of T-cell receptor-dependent antigen recognition determined in vivo by multi-spectral normalized epifluorescence laser scanning. *J. Biomed. Opt.* **2012**, *17*, 76–131.

(34) Okada, T.; Miller, M. J.; Parker, I.; Krummel, M. F.; Neighbors, M.; Hartley, S. B.; O'Garra, A.; Cahalan, M. D.; Cyster, J. G. Antigen-engaged B cells undergo chemotaxis toward the T zone and form motile conjugates with helper T cells. *PLoS biol.* **2005**, *3*, e150.

(35) Baker, D. W.; Zhou, J.; Tsai, Y.-T.; Patty, K. M.; Weng, H.; Tang, E. N.; Nair, A.; Hu, W.-J.; Tang, L. Development of optical probes for in vivo imaging of polarized macrophages during foreign body reactions. *Acta Biomater.* **2014**, *10*, 2945–2955.

(36) Qiu, Y.; Palankar, R.; Echeverría, M. A.; Medvedev, N.; Moya, S. E.; Delcea, M. Design of hybrid multimodal poly (lactic-co-glycolic acid) polymer nanoparticles for neutrophil labeling, imaging and tracking. *Nanoscale* **2013**, *5*, 12624–12632.

(37) Kolaczkowska, E.; Kubes, P. Neutrophil recruitment and function in health and inflammation. *Nat. Rev. Immunol.* **2013**, *13*, 159–175.

(38) Ley, K.; Laudanna, C.; Cybulsky, M. I.; Nourshargh, S. Getting to the site of inflammation: the leukocyte adhesion cascade updated. *Nat. Rev. Immunol.* **2007**, *7*, 678–689.

(39) Zarbock, A.; Ley, K. New insights into leukocyte recruitment by intravital microscopy. *Curr. Top. Microbiol. Immunol.* **2009**, *334*, 129–152.

(40) Choi, P. J.; Mitchison, T. J. Imaging burst kinetics and spatial coordination during serial killing by single natural killer cells. *Proc. Natl. Acad. Sci. U. S. A.* **2013**, *110*, 6488–6493.

(41) Alves, N. L.; Richard-Le Goff, O.; Huntington, N. D.; Sousa, A. P.; Ribeiro, V. S.; Bordack, A.; Vives, F. L.; Peduto, L.; Chidgey, A.; Cumano, A.; Boyd, R.; Eberl, G.; Di Santo, J. P. Characterization of the thymic IL-7 niche in vivo. *Proc. Natl. Acad. Sci. U. S. A.* **2009**, *106*, 1512–1517.

(42) Mazzucchelli, R. I.; Warming, S.; Lawrence, S. M.; Ishii, M.; Abshari, M.; Washington, A. V.; Feigenbaum, L.; Warner, A. C.; Sims, D. J.; Li, W. Q.; Hixon, J. A.; Gray, D. H.; Rich, B. E.; Morrow, M.; Anver, M. R.; Cherry, J.; Naf, D.; Sternberg, L. R.; McVicar, D. W.; Farr, A. G.; Germain, R. N.; Rogers, K.; Jenkins, N. A.; Copeland, N. G.; Durum, S. K. Visualization and identification of IL-7 producing cells in reporter mice. *PLoS ONE* **2009**, *4*, e7637.

(43) Matheu, M. P.; Teijaro, J. R.; Walsh, K. B.; Greenberg, M. L.; Marsolais, D.; Parker, I.; Rosen, H.; Oldstone, M. B. A.; Cahalan, M. D. Three phases of cd8 t cell response in the lung following h1n1 influenza infection and sphingosine 1 phosphate agonist therapy. *PLoS ONE* **2013**, *8*, e58033.

(44) Boissonnas, A.; Licata, F.; Poupel, L.; Jacquelin, S. b.; Fetler, L.; Krumeich, S.; Thréy, C.; Amigorena, S. B.; Combadière, C. CD8+ tumor-infiltrating t cells are trapped in the tumor-dendritic cell network. *Neoplasia* **2013**, *15*, 85.

(45) Abtin, A.; Jain, R.; Mitchell, A. J.; Roediger, B.; Brzoska, A. J.; Tikoo, S.; Cheng, Q.; Ng, L. G.; Cavanagh, L. L.; von Andrian, U. H.; Hickey, M. J.; Firth, N.; Weninger, W. Perivascular macrophages mediate neutrophil recruitment during bacterial skin infection. *Nat. Immunol.* **2014**, *15*, 45–53.

(46) Sewald, X.; Gonzalez, D. G.; Haberman, A. M.; Mothes, W. In vivo imaging of virological synapses. *Nat. Commun.* **2012**, *3*, 1320.

(47) Murooka, T. T.; Deruaz, M.; Marangoni, F.; Vrbanac, V. D.; Seung, E.; von Andrian, U. H.; Tager, A. M.; Luster, A. D.; Mempel, T. R. HIV-infected T cells are migratory vehicles for viral dissemination. *Nature* **2012**, *490*, 283–287.

(48) Dorward, D. A.; Lucas, C. D.; Rossi, A. G.; Haslett, C.; Dhaliwal, K. Imaging inflammation: molecular strategies to visualize key components of the inflammatory cascade, from initiation to resolution. *Pharmacol. Ther.* **2012**, *135*, 182–199.

(49) Rajasekaran, S.; Kao, V. Y.; Chen, M. R.; Yang, A. L.; Hsu, C. H.; Chen, C. T.; Lin, K. M. Detection of experimentally induced pulmonary granuloma inflammation in monocyte chemoattractant protein-1 reporter mice. *Mol. Imaging Biol.* **2010**, *12*, 163–173.

(50) Griffith, J. W.; Sokol, C. L.; Luster, A. D. Chemokines and chemokine receptors: positioning cells for host defense and immunity. *Ann. Rev. Immunol.* **2014**, *32*, 659–702.

(51) Stirnweiss, A.; Hartig, R.; Gieseler, S.; Lindquist, J. A.; Reichardt, P.; Philipsen, L.; Simeoni, L.; Poltorak, M.; Merten, C.; Zuschratter, W.; Prokazov, Y.; Paster, W.; Stockinger, H.; Harder, T.; Gunzer, M.; Schraven, B. T cell activation results in conformational changes in the src family kinase lck to induce its activation. *Sci. Signal.,* **2013**, *6*, 283.

(52) Yamasaki, S.; Ishikawa, E.; Sakuma, M.; Ogata, K.; Sakata-Sogawa, K.; Hiroshima, M.; Wiest, D. L.; Tokunaga, M.; Saito, T. Mechanistic basis of pre-T cell receptor-mediated autonomous signaling critical for thymocyte development. *Nat. Immunol.* **2006**, *7*, 67–75.

(53) Ting, A. Y.; Kain, K. H.; Klemke, R. L.; Tsien, R. Y. Genetically encoded fluorescent reporters of protein tyrosine kinase activities in living cells. *Proc. Natl. Acad. Sci. U. S. A.* **2001**, *98*, 15003–15008.

(54) Park, J. G.; Palmer, A. E. Quantitative measurement of Ca^{2+} and Zn^{2+} in mammalian cells using genetically encoded fluorescent biosensors. *Meth. Mol. Biol.* **2014**, *1071*, 29–47.

(55) Mues, M.; Bartholomaus, I.; Thestrup, T.; Griesbeck, O.; Wekerle, H.; Kawakami, N.; Krishnamoorthy, G. Real-time in vivo analysis of T cell activation in the central nervous system using a genetically encoded calcium indicator. *Nat. Med.* **2013**, *19*, 778–783.

(56) Chung, K.; Wallace, J.; Kim, S. Y.; Kalyanasundaram, S.; Andalman, A. S.; Davidson, T. J.; Mirzabekov, J. J.; Zalocusky, K. A.; Mattis, J.; Denisin, A. K.; Pak, S.; Bernstein, H.; Ramakrishnan, C.; Grosenick, L.; Gradinaru, V.; Deisseroth, K. Structural and molecular interrogation of intact biological systems. *Nature* **2013**, *497*, 332–337.

(57) Badr, C. E.; Tannous, B. A. Bioluminescence imaging: progress and applications. *Trends. Biotechnol.* **2011**, *29*, 624–633.

(58) Cao, Y.-A.; Wagers, A. J.; Beilhack, A.; Dusich, J.; Bachmann, M. H.; Negrin, R. S.; Weissman, I. L.; Contag, C. H. Shifting foci of hematopoiesis during reconstitution from single stem cells. *Proc. Natl. Acad. Sci. U. S. A.* **2004**, *101*, 221–226.

(59) Rabinovich, B. A.; Ye, Y.; Etto, T.; Chen, J. Q.; Levitsky, H. I.; Overwijk, W. W.; Cooper, L. J.; Gelovani, J.; Hwu, P. Visualizing fewer than 10 mouse T cells with an enhanced

firefly luciferase in immunocompetent mouse models of cancer. *Proc. Natl. Acad. Sci. U. S. A.* **2008**, *105*, 14342–14346.

(60) Knorr, D. A.; Bock, A.; Brentjens, R. J.; Kaufman, D. S. Engineered human embryonic stem cell-derived lymphocytes to study in vivo trafficking and immunotherapy. *Stem Cells Dev.* **2013**, *22*, 1861.

(61) Leveson-Gower, D. B.; Olson, J. A.; Sega, E. I.; Luong, R. H.; Baker, J.; Zeiser, R.; Negrin, R. S. Low doses of natural killer T cells provide protection from acute graft-versus-host disease via an IL-4-dependent mechanism. *Blood* **2011**, *117*, 3220–3229.

(62) Tsukahara, T.; Ohmine, K.; Yamamoto, C.; Uchibori, R.; Ido, H.; Teruya, T.; Urabe, M.; Mizukami, H.; Kume, A.; Nakamura, M.; Mineno, J.; Takesako, K.; Riviere, I.; Sadelain, M.; Brentjens, R.; Ozawa, K. CD19 target-engineered T-cells accumulate at tumor lesions in human B-cell lymphoma xenograft mouse models. *Biochem. Biophys. Res. Commun.* **2013**, *438*, 84–89.

(63) Santos, E. B.; Yeh, R.; Lee, J.; Nikhamin, Y.; Punzalan, B.; Punzalan, B.; Perle, K. L.; Larson, S. M.; Sadelain, M.; Brentjens, R. J. Sensitive in vivo imaging of T cells using a membrane-bound Gaussia princeps luciferase. *Nat. Med.* **2009**, *15*, 338–344.

(64) Lewandrowski, G. K.; Magee, C. N.; Mounayar, M.; Tannous, B. A.; Azzi, J. Bioluminescent imaging; Springer: 2014, 211.

(65) Charles, J. l. P.; Fuchs, J.; Hefter, M.; Vischedyk, J. B.; Kleint, M.; Vogiatzi, F.; Schäfer, J. A.; Nist, A.; Timofeev, O.; Wanzel, M.; Stiewe, T. Monitoring the dynamics of clonal tumour evolution in vivo using secreted luciferases. *Nat. Commun.* **2014**, *5*.

(66) Hasenberg, M.; Krappmann, S.; Gunzer, M. Human fungal pathogens; Springer: 2014, 141.

(67) Donat, S.; Hasenberg, M.; Schafer, T.; Ohlsen, K.; Gunzer, M.; Einsele, H.; Loffler, J.; Beilhack, A.; Krappmann, S. Surface display of Gaussia princeps luciferase allows sensitive fungal pathogen detection during cutaneous aspergillosis. *Virulence* **2012**, *3*, 51–61.

(68) Vecchiarelli, A.; d'Enfert, C. Shedding natural light on fungal infections. *Virulence* **2012**, *3*, 15–17.

(69) Vande Velde, G.; Kuchariková, S. A.; Schrevens, S.; Himmelreich, U.; Van Dijck, P. Towards non-invasive monitoring of pathogen-host interactions during Candida albicans biofilm formation using in vivo bioluminescence. *Cell. Microbiol.* **2014**, *16*, 115–130.

(70) Maguire, C. A.; Bovenberg, M. S.; Crommentuijn, M. H.; Niers, J. M.; Kerami, M.; Teng, J.; Sena-Esteves, M.; Badr, C. E.; Tannous, B. A. Triple bioluminescence imaging for in vivo monitoring of cellular processes. *Mol. Ther. Nucleic Acids* **2013**, *2*, e99.

(71) Chen, Z. H.; Zhao, R. J.; Li, R. H.; Guo, C. P.; Zhang, G. J. Bioluminescence imaging of DNA synthetic phase of cell cycle in living animals. *PLoS ONE* **2013**, *8*, e53291.

(72) Patel, M. R.; Chang, Y. F.; Chen, I. Y.; Bachmann, M. H.; Yan, X.; Contag, C. H.; Gambhir, S. S. Longitudinal, noninvasive imaging of T-cell effector function and proliferation in living subjects. *Cancer Res.* **2010**, *70*, 10141–10149.

(73) Zangani, M.; Carlsen, H.; Kielland, A.; Os, A.; Hauglin, H.; Blomhoff, R.; Munthe, L. A.; Bogen, B. Tracking early autoimmune disease by bioluminescent imaging of NF-kappaB activation reveals pathology in multiple organ systems. *Am. J. Pathol.* **2009**, *174*, 1358-1367.

(74) Bhang, H. E.; Gabrielson, K. L.; Laterra, J.; Fisher, P. B.; Pomper, M. G. Tumor-specific imaging through progression elevated gene-3 promoter-driven gene expression. *Nat. Med.* **2011**, *17*, 123–129.

(75) Watts, J. C.; Giles, K.; Oehler, A.; Middleton, L.; Dexter, D. T.; Gentleman, S. M.; DeArmond, S. J.; Prusiner, S. B. Transmission of multiple system atrophy prions to transgenic mice. *Proc. Natl. Acad. Sci. U. S. A.* **2013**, *110*, 19555–19560.

(76) Moroz, E.; Carlin, S.; Dyomina, K.; Burke, S.; Thaler, H. T.; Blasberg, R.; Serganova, I. Real-time imaging of HIF-1alpha stabilization and degradation. *PloS ONE* **2009**, *4*, e5077.

(77) Klaus, A.; Birchmeier, W. Wnt signalling and its impact on development and cancer. *Nat. Rev. Cancer* **2008**, *8*, 387–398.

(78) Naik, S.; Piwnica-Worms, D. Real-time imaging of beta-catenin dynamics in cells and living mice. *Proc. Natl. Acad. Sci. U. S. A.* **2007**, *104*, 17465–17470.

(79) Compan, V.; Baroja-Mazo, A.; Bragg, L.; Verkhratsky, A.; Perroy, J.; Pelegrin, P. A genetically encoded IL-1beta bioluminescence resonance energy transfer sensor to monitor inflammasome activity. *J. Immunol.* **2012**, *189*, 2131–2137.

(80) Shaner, N. C.; Lambert, G. G.; Chammas, A.; Ni, Y.; Cranfill, P. J.; Baird, M. A.; Sell, B. R.; Allen, J. R.; Day, R. N.; Israelsson, M.; Davidson, M. W.; Wang, J. A bright monomeric green fluorescent protein derived from Branchiostoma lanceolatum. *Nat. Methods* **2013**, *10*, 407–409.

(81) Shaner, N. C.; Lin, M. Z.; McKeown, M. R.; Steinbach, P. A.; Hazelwood, K. L.; Davidson, M. W.; Tsien, R. Y. Improving the photostability of bright monomeric orange and red fluorescent proteins. *Nat. Methods* **2008**, *5*, 545–551.

(82) Chu, J.; Haynes, R. D.; Corbel, S. Y.; Li, P.; Gonzalez-Gonzalez, E.; Burg, J. S.; Ataie, N. J.; Lam, A. J.; Cranfill, P. J.; Baird, M. A.; Davidson, M. W.; Ng, H.-L.; Garcia, K. C.; Contag, C. H.; Shen, K.; Blau, H. M.; Lin, M. Z. Non-invasive intravital imaging of cellular differentiation with a bright red-excitable fluorescent protein. *Nat. Methods* **2014**, *11*, 572–578.

(83) Zhong, S.; Navaratnam, D.; Santos-Sacchi, J. A genetically-encoded YFP sensor with enhanced chloride sensitivity, photostability and reduced pH interference demonstrates augmented transmembrane chloride movement by gerbil prestin (SLC26a5). *PLoS ONE* **2014**, *9*, e99095.

(84) Uttamapinant, C.; White, K. A.; Baruah, H.; Thompson, S.; Fernández-Suárez, M.; Puthenveetil, S.; Ting, A. Y. A fluorophore ligase for site-specific protein labeling inside living cells. *Proc. Natl. Acad. Sci. U. S. A.* **2010**, *107*, 10914–10919.

(85) Liu, D. S.; Loh, K. H.; Lam, S. S.; White, K. A.; Ting, A. Y. Imaging trans-cellular neurexin-neuroligin interactions by enzymatic probe ligation. *PLoS ONE* **2013**, *8*, e52823.

(86) Feinberg, E. H.; VanHoven, M. K.; Bendesky, A.; Wang, G.; Fetter, R. D.; Shen, K.; Bargmann, C. I. GFP reconstitution across synaptic partners (GRASP) defines cell contacts and synapses in living nervous systems. *Neuron* **2008**, *57*, 353–363.

(87) Branchini, B. R.; Magyar, R. A.; Murtiashaw, M. H.; Anderson, S. M.; Helgerson, L. C.; Zimmer, M. Site-directed mutagenesis of firefly luciferase active site amino acids: a proposed model for bioluminescence color. *Biochemistry* **1999**, *38*, 13223–13230.

(88) Viviani, V. R.; Amaral, D. T.; Neves, D. R.; Simoes, A.; Arnoldi, F. G. The luciferin binding site residues C/T311 (S314) influence the bioluminescence color of beetle luciferases through main-chain interaction with oxyluciferin phenolate. *Biochemistry* **2013**, *52*, 19–27.

(89) De, A.; Loening, A. M.; Gambhir, S. S. An improved bioluminescence resonance energy transfer strategy for imaging intracellular events in single cells and living subjects. *Cancer Res.* **2007**, *67*, 7175–7183.

(90) Degeling, M. H.; Bovenberg, M. S.; Lewandrowski, G. K.; de Gooijer, M. C.; Vleggeert-Lankamp, C. L.; Tannous, M.; Maguire, C. A.; Tannous, B. A. Directed molecular evolution

reveals Gaussia luciferase variants with enhanced light output stability. *Anal. Chem.* **2013**, *85*, 3006–3012.

(91) Kojima, R.; Takakura, H.; Ozawa, T.; Tada, Y.; Nagano, T.; Urano, Y. Rational design and development of near-infrared-emitting firefly luciferins available in vivo. *Angew. Chem. Int. Ed.* **2013**, *52*, 1175–1179.

(92) Reddy, G. R.; Thompson, W. C.; Miller, S. C. Robust light emission from cyclic alkylaminoluciferin substrates for firefly luciferase. *J. Am. Chem. Soc.* **2010**, *132*, 13586–13587.

(93) McCutcheon, D. C.; Paley, M. A.; Steinhardt, R. C.; Prescher, J. A. Expedient synthesis of electronically modified luciferins for bioluminescence imaging. *J. Am. Chem. Soc.* **2012**, *134*, 7604–7607.

(94) Conley, N. R.; Dragulescu-Andrasi, A.; Rao, J.; Moerner, W. E. A selenium analogue of firefly D-luciferin with red-shifted bioluminescence emission. *Angew. Chem. Int. Ed.* **2012**, *51*, 3350–3353.

(95) Evans, M. S.; Chaurette, J. P.; Adams Jr, S. T.; Reddy, G. R.; Paley, M. A.; Aronin, N.; Prescher, J. A.; Miller, S. C. A synthetic luciferin improves bioluminescence imaging in live mice. *Nat. Methods* **2014**, *11*, 393–395.

(96) Luker, K. E.; Luker, G. D. Split Gaussia luciferase for imaging ligand-receptor binding. *Methods Mol. Biol.* **2014**, *1098*, 59–69.

(97) Jones, K. A.; Li, D. J.; Hui, E.; Sellmyer, M. A.; Prescher, J. A. Visualizing cell proximity with genetically encoded bioluminescent reporters. *ACS Chem. Biol.* **2015**, *10*, 933–938.

(98) Li, J.; Chen, L.; Du, L.; Li, M. Cage the firefly luciferin! - a strategy for developing bioluminescent probes. *Chem. Soc. Rev.* **2013**, *42*, 662–676.

(99) Wehrman, T. S.; von Degenfeld, G.; Krutzik, P. O.; Nolan, G. P.; Blau, H. M. Luminescent imaging of beta-galactosidase activity in living subjects using sequential reporter-enzyme luminescence. *Nat. Methods* **2006**, *3*, 295–301.

(100) Sellmyer, M. A.; Bronsart, L.; Imoto, H.; Contag, C. H.; Wandless, T. J.; Prescher, J. A. Visualizing cellular interactions with a generalized proximity reporter. *Proc. Natl. Acad. Sci. U. S. A.* **2013**, *110*, 8567–8572.

Chapter 2: Design and synthesis of an alkynyl luciferin analog for bioluminescence imaging

2.1 Introduction

Bioluminescence is a versatile imaging platform with applications ranging from metabolite biosensing to whole animal imaging [1,2]. At the heart of this technology are enzymes (luciferases) that catalyze the oxidation of small molecule substrates (luciferins) [3,4]. During each enzymatic transformation, an electronically excited oxyluciferin is generated that emits a photon of light upon relaxation to the ground state [5]. Since mammalian cells and tissues do not produce large numbers of photons in the absence of incident light, bioluminescence can provide an exquisitely sensitive readout on biological processes in these environments [6]. Indeed, luciferase-luciferin pairs have been widely used to report on enzyme activities and gene expression patterns in live cells and tissue lysates [1,2]. Additionally, since bioluminescence does not require an excitation source, this technology is well suited for noninvasive imaging in whole animals, where delivery of excitation light is often inefficient or impractical [1,7-10].

The most widely used luciferases for cell and animal imaging originate from the insect family [2]. These enzymes, including firefly luciferase (Fluc), catalyze the oxidation of D-luciferin (**1**) and release ~500-600 nm light (Figure 2-1a) [4,5]. Wavelengths of this sort can penetrate the skin of small rodents and be detected by sensitive cameras, making insect luciferases attractive for imaging in vivo. Indeed, Fluc and related enzymes have been expressed in a variety of tissue and cell types, and when exposed to D-luciferin, light is produced [1,2]. D-

luciferin is also sufficiently bioavailable in rodents [11] and has been used extensively in preclinical models [12,13].

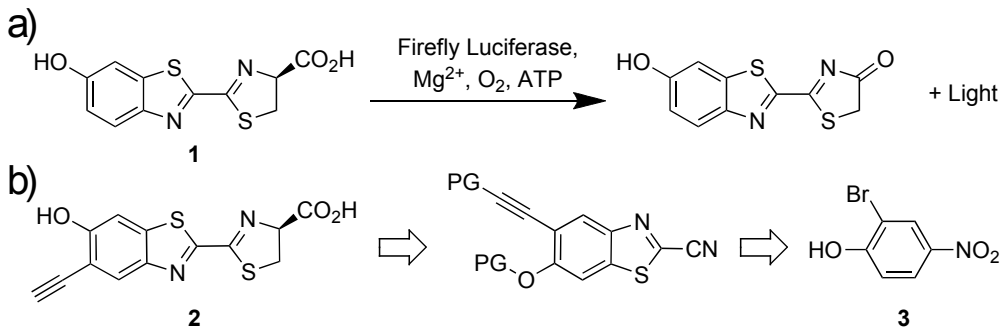

Figure 2-1. a) The luciferase-catalyzed oxidation of D-luciferin (**1**) produces visible light. b) Retrosynthetic analysis of alkynyl luciferin (PG= protecting group).

2.2 Results and discussion

Because of the sensitivity and user-friendly features of bioluminescence, there has been much interest in expanding the scope of the technology [10,14]. Several efforts have been directed toward identifying other naturally occuring luciferase-luciferin pairs for multi-component imaging [1]. The instability and poor tissue penetrance of many luciferins has been prohibitive in many cases. Other attempts have focused on generating luciferases that provide altered emission spectra. For example, several insect luciferases have been engineered to emit different colors of light (ranging from ~500-650 nm) with D-luciferin [15-22]. While these wavelengths can be adequately resolved in vitro, they cannot be easily discriminated in vivo, where tissue absorption and scatter modulate the color of light that ultimately reaches the detector.

Compared to luciferase engineering efforts, there has been less work invested in crafting new luciferins. Substrate engineering is an obvious strategy to broaden the scope of bioluminescence technology, though, as the luciferin molecules can be modified to emit different colors of light or be selectively utilized by unique luciferases [23-27]. In some cases, the substrates have proven remarkably cell and tissue permeant and, thus, well suited for in vivo work [28]. In the majority of cases, though, the engineered substrates remain poor substrates for the enzyme. Mutant luciferases can be developed to more efficiently process unnatural substrates [29], but these studies typically require access to large quantities of molecules that are difficult to synthesize.

Continued efforts to develop unique bioluminescent tools would benefit from rapid access to diverse collections of light-emitting luciferins. These scaffolds have been notoriously difficult to synthesize owing to their electron-rich and highly substituted cores. Late-stage modifications to luciferin molecules are also complicated. For example, most attempts to dervitize D-luciferin (**1**) have focused on altering the 6′-position via alkylation or acylation chemistries [11, 30, 31]. While facile, these strategies have produced scaffolds that are somewhat limited in scope. Electron donation is required for robust emission and, thus, the 6′-position is particularly sensitive to modification. Indeed, many 6′-substituted luciferins comprise electron-withdrawing substituents that dampen light output [30].

We aimed to develop a bioluminescent probe modified at an alternative ring position. We were initially drawn to the 5′-alkyne derivative (**2**) shown in Figure 2-1b. In previous work, 5′-fluoro and other small substituents were shown to be well tolerated by Fluc and minimally perturbing to the bioluminescent reaction [24]. Our initial modeling analyses also suggested that the alkyne would be sterically accommodated in the luciferase active site (Figure 2-2a).

Similarly, computational data [32] suggested that the installation of the alkynyl functional group in conjugation with the benzothiazole could permit the alkyne to extend the pi system of the luciferin chromophore, resulting in red shifted light (Figure 2-2b).

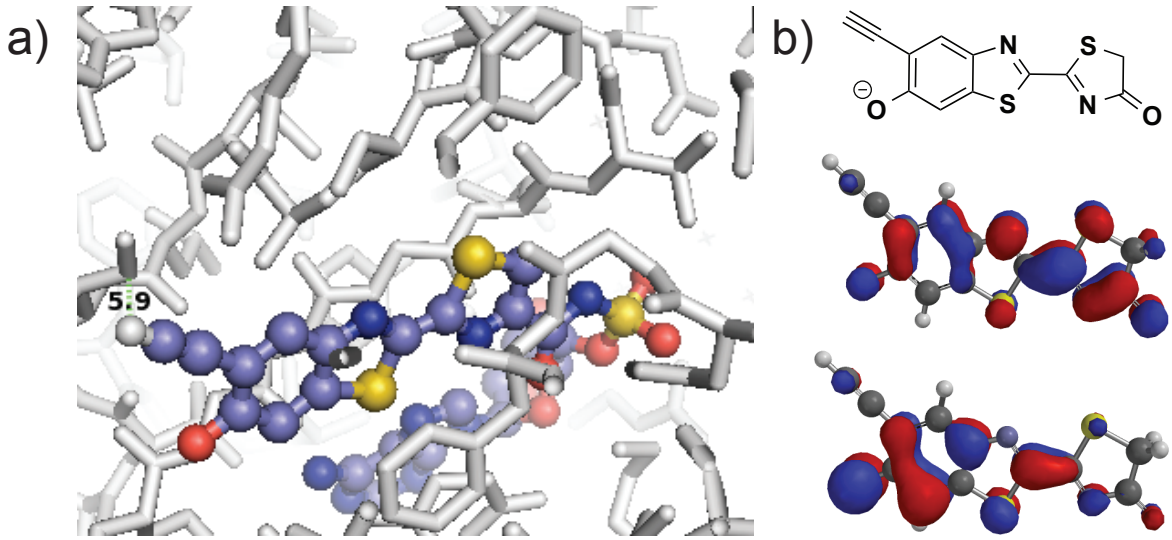

Figure 2-2. *In silico* analyses of D-luciferin. a) Overlay of **2** with firefly luciferase structure (PDB ID: 4G36) suggests that the alkyne motif will be tolerated. b) DFT predictions of (B3LYP/6-311**) of the HOMO (middle) and LUMO (bottom) of a possible structure of oxyluciferin (top) suggest the participation of the alkyne in these molecular orbitals, which may contribute to the red shift in the light emssion observed (for computational details please see the Materials and Methods).

We were further attracted to alkyne **2** as its benzothiazole core could be accessed using C–H activation chemistry, as previously reported by our group [33-37]. The functionalized luciferin still presented some synthetic challenges, though. Electron-rich heterocycles like **2** are susceptible to non-specific oxidation and are thus difficult to handle and prepare on scale. Methods to produce highly substituted benzothiazoles are also rare. To access the desired heterocycle, we began with tri-substituted phenol **3**. The hydroxy substituent was first protected with a mesyl group (Scheme 2-1) [38]. Other classic phenol protecting groups (e.g., silyl and methyl) were explored, but most proved either incompatible with subsequent transformations (in the case of bulky silyl groups) or difficult to remove later on in the synthesis (in the case of methyl groups). Mesylate **4** was ultimately subjected to Sonogashira conditions for alkyne installation. Notably, this reaction was readily scalable and provided decagram quantities of **5** (Scheme 2-2). The nitro group of **5** was reduced using iron filings and glacial acetic acid [39] to reveal aniline **6** in good yield and purity.

Scheme 2-1. Installation of the alkyne substituent.

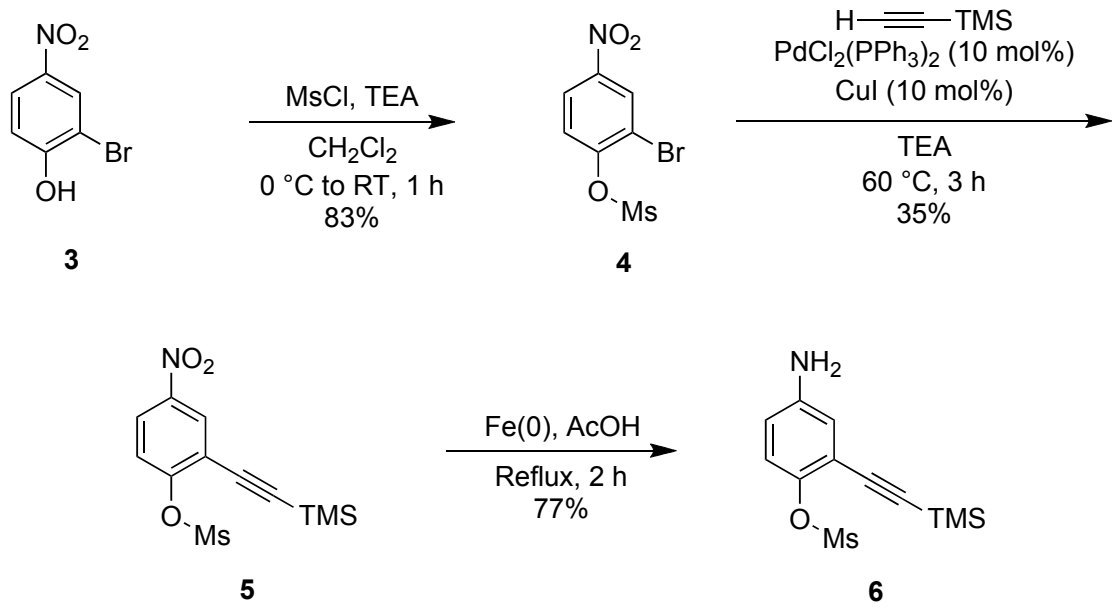

Scheme 2-2. Gram-scale synthesis of mesylate 5.

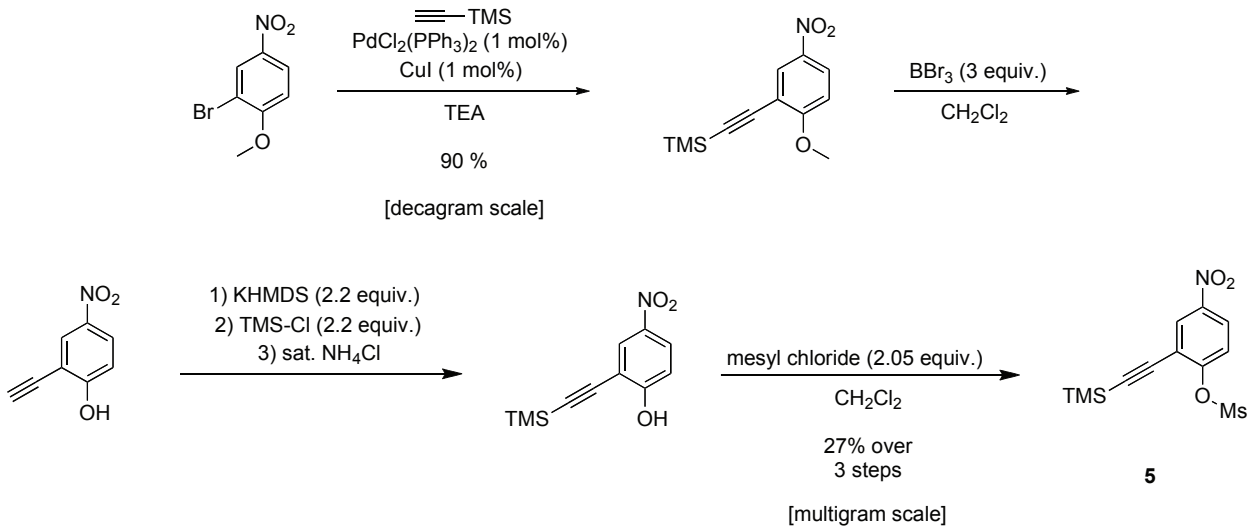

Compound **6** was then treated with Appel's salt **7**, and the resulting adduct was fragmented with resin-linked PPh_3 to yield thioamide **9** (Scheme 2-3) [40]. It should be noted that while other bulky nucleophiles (e.g, DBU and DBA) [41] can be used for such fragmentations, they resulted in premature deprotection of the mesyl group and reduced overall yields in this case. Subsequent cyclization of thioamide **9** via palladium- and copper-catalyzed C–H activation [42] provided **10** in 61% yield. Attempts to isolate **10** directly from **8** via thermal cyclization resulted in product decomposition and were not pursued further. The desired alkyne luciferin **2** was ultimately isolated following mesyl group removal [43] and cysteine condensation. Importantly, luciferin **2** was stable for weeks as a solid material and in aqueous solution.

Scheme 2-3. Synthesis of alkyne luciferin 2 using C–H activation chemistry.

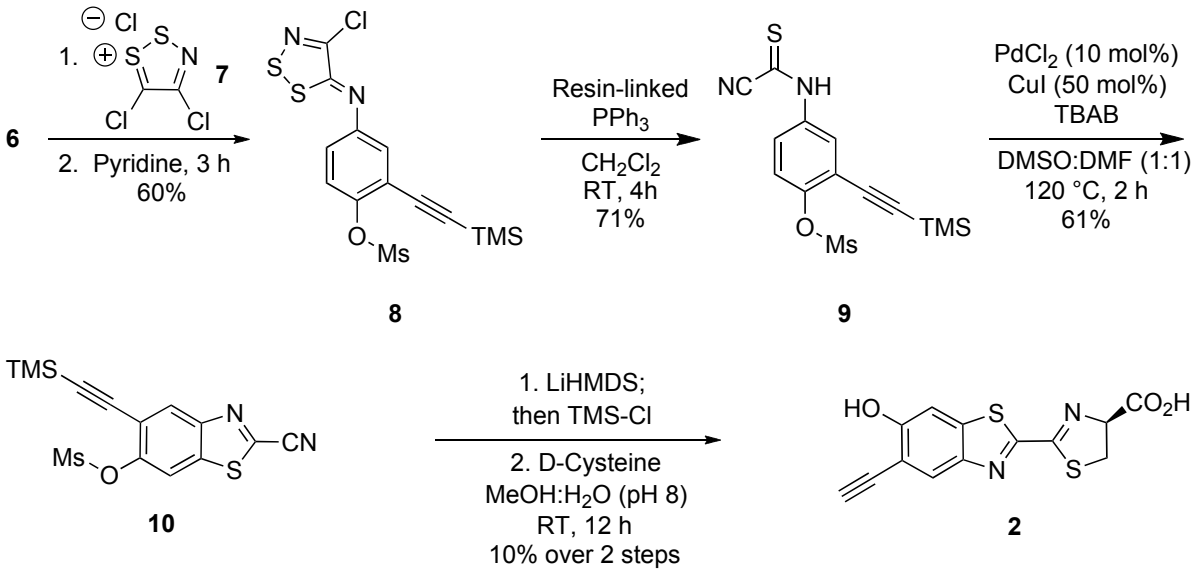

Luciferin **2** was also found to be a viable substrate for firefly luciferase (Fluc). When **2** was incubated with Fluc in the presence of ATP, bioluminescent light was observed. Light emission was both concentration-dependent and sustained. The overall photon output from **2** is weaker than that observed with D-luciferin (the native substrate), but on par with other luciferin analogs used in biological assays (Figures 2-3) [24]. Interestingly, the bioluminescence emission spectrum of 2 is substantially red-shifted compared to D-luciferin (λ_{max} = 610 nm at 25 °C, Figure 2-4). In fact, the emission wavelengths are on par with some of the most red-shifted luciferins used in BLI: aminoluciferin [27, 31] and CycLuc2 [27, 28, 31].

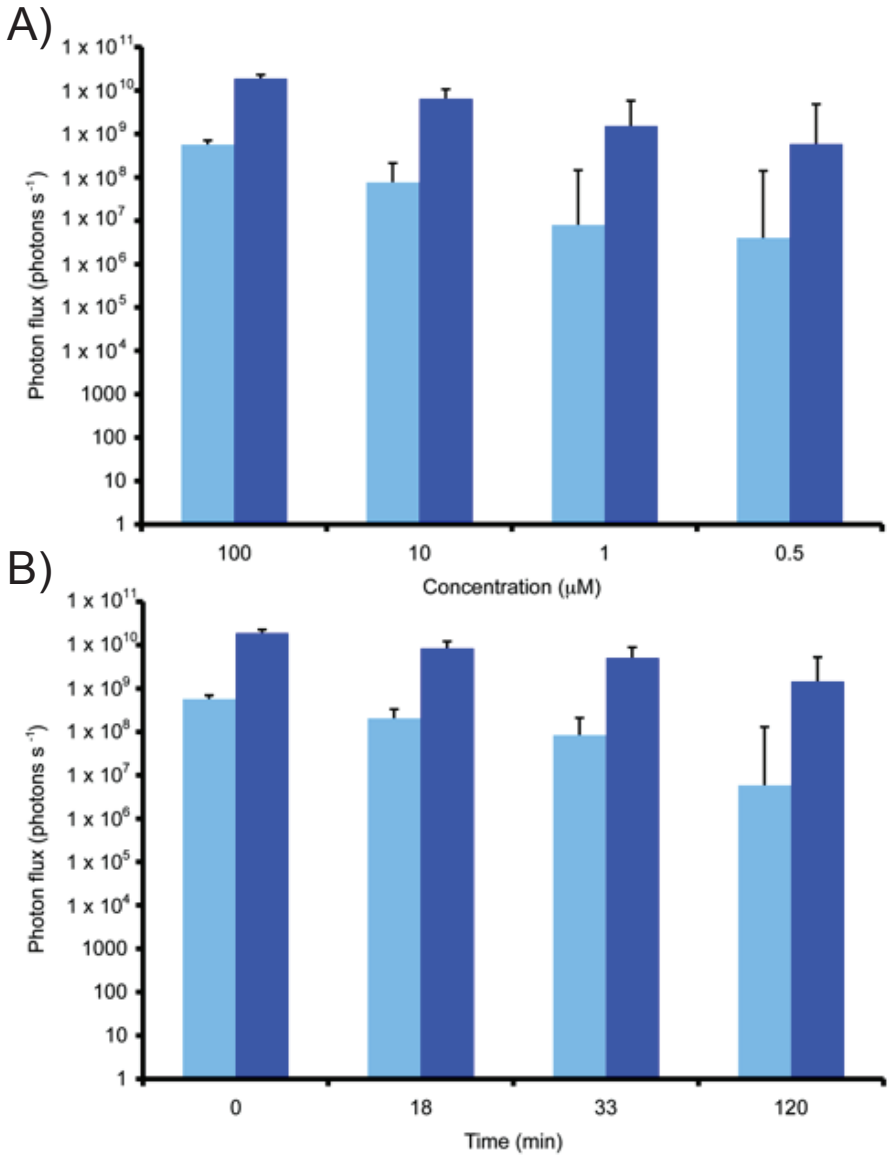

Figure 2-3. Alkynyl luciferin 2 is a weaker light emitter than D-luciferin. A) Total photon flux for the bioluminescent reactions of alkynyl luciferin **2** (light blue bars) or D-luciferin (dark blue bars) with firefly luciferase (Fluc). Assays were performed in triplicate using black 96-well plates (BD Bioscience). Each well contained purified Fluc (2 mg), luciferin substrate (0-100 mM), ATP (1 mM, Sigma Aldrich), coenzyme A (0.5 mM, Calbiochem), and reaction buffer (20 mM Tris-HCl pH 7.6, 0.5 mg/mL BSA, 0.1 mM EDTA, 1 mM TCEP, 2 mM $MgSO_4$), totaling 100 mL. All reaction components were pre-mixed prior to Fluc addition. B) Total photon flux for the bioluminescent reactions of alkynyl luciferin **2** (100 mM, light blue bars) or an equimolar amount of D-luciferin (dark blue bars) monitored over time. Assays were conducted as in A).

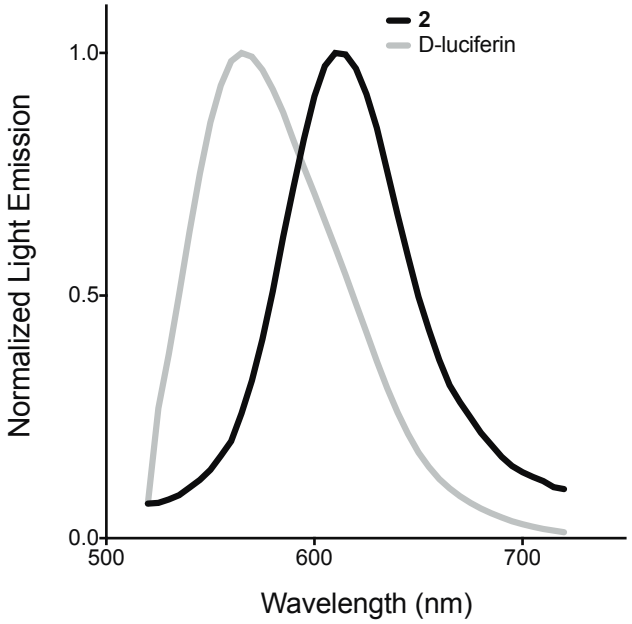

Figure 2-4. Normalized bioluminescence spectra for alkynyl luciferin **2** (λ_{max} 610 nm) and D-luciferin **1** (λ_{max} 565nm). Samples (100 μM) were combined with *Photinus pyralis* luciferase (10 μg) in bioluminescence buffer and monitored at 25 °C.

Based on the ease of synthesis and favorable spectral properties of **2**, we anticipated that the probe would be useful for biological imaging applications both in vitro and in vivo. To test this hypothesis, we first evaluated the probe with recombinant Fluc. We found that **2** was a light emitting substrate (Figure 2-5a), and able sustain photon production over time (Figure 2-5b). The alkynyl probe also appeared to be reasonably tolerated by the enzyme, with an apparent K_m of 8.5 ± 1 μM, and an apparent V_{max} of $130 \pm 5 \times 10^6$ photons s^{-1} (Figure 2-6).

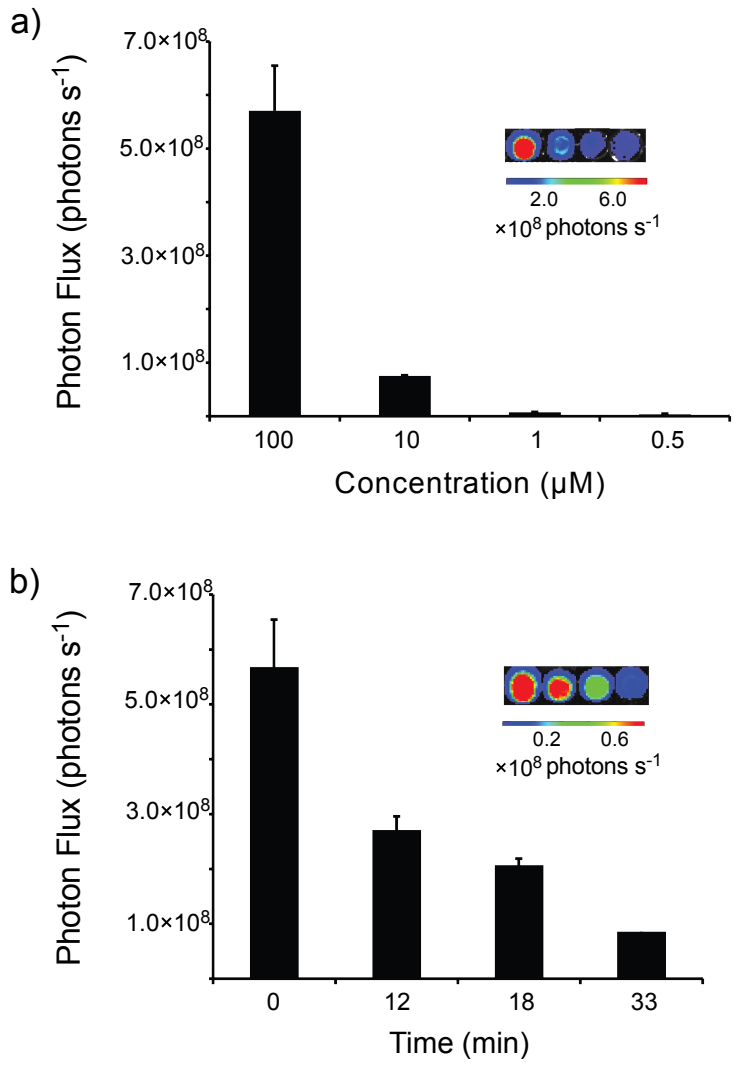

Figure 2-5. a) Alkynyl luciferin **2** produces light upon incubation with Fluc. Samples of analog **2** (0.5-100 μM) were mixed with Fluc, ATP, and CoA in pH 8 buffer in 96-well plates. Light emission was measured using a cooled CCD camera. Sample images are shown in the inset. b) Analog **2** exhibits sustained light emission. Photon production from samples of **2** (100 μM), Fluc, ATP, and CoA (in black-walled 96-well plates) were monitored over time. Light emission was quantified over time, and sample images are shown. For a–b, error bars represent the standard deviation of the mean for three replicate experiments.

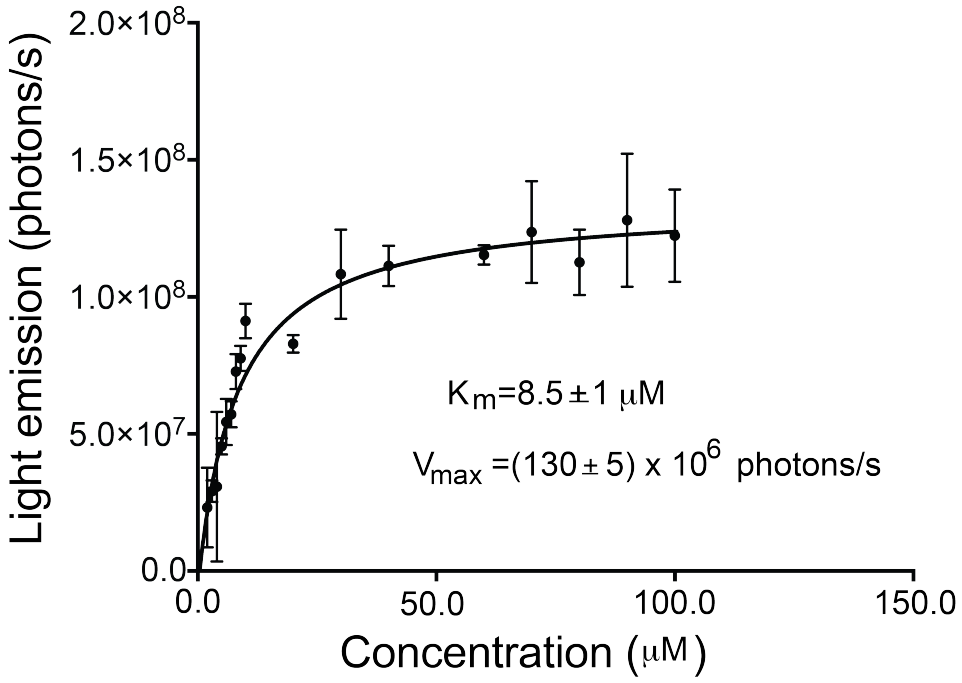

Figure 2-6. Alkynyl luciferin 2 is a viable substrate for Fluc. Luciferin **2** (0-150 mM) was incubated with purified Fluc (2 μg), ATP (1 mM), coenzyme A (0.5 mM), and light emission was monitored. For further details see materials and methods. Reactions were performed in triplicate. Error bars represent the standard deviation of the mean for n > 3 experiments.

The luciferin analog also performed well in cell assays. Luciferase-expressing HEK293 cells were incubated with various doses of **2**, a similar trend was observed to the in vitro experiment (Figure 2-7a), indicating that alkynyl luciferin was cell permeable. The light emission was sustained over 2 h (Figure 2-7b), which is a desirable characteristic for BLI applications.

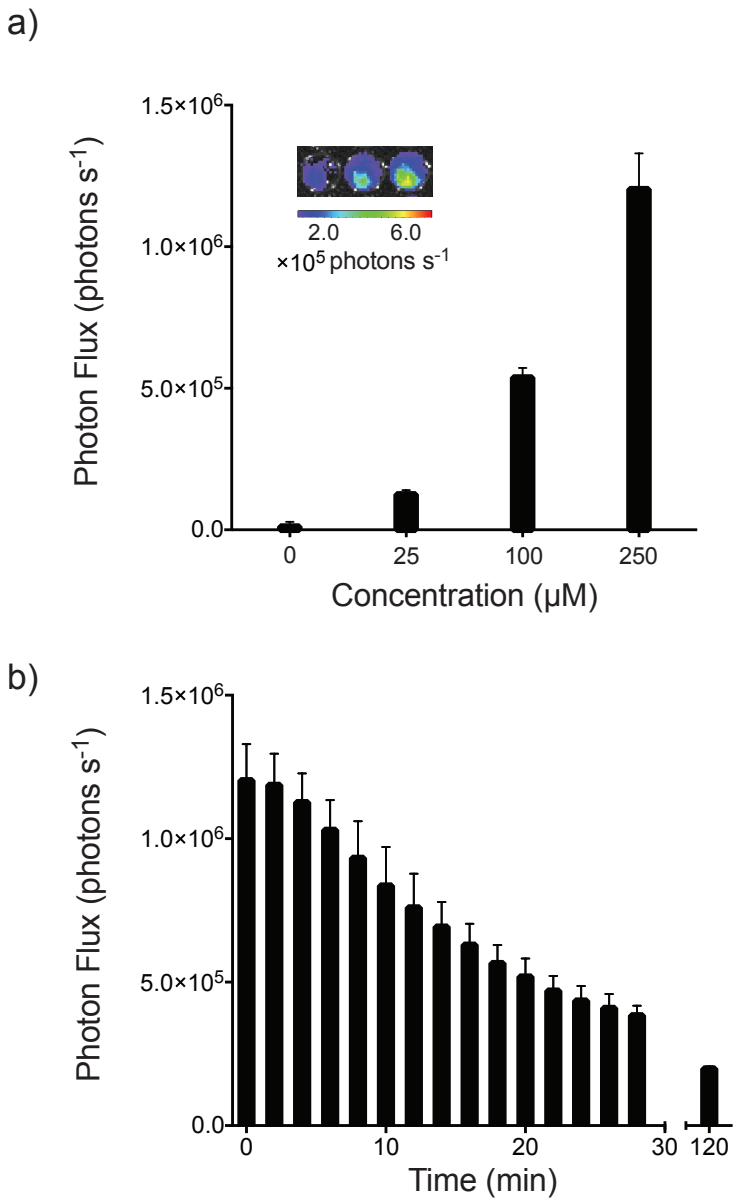

Figure 2-7. a) Alkynyl luciferin **2** produces light when incubated with HEK293 cells. Doses of analog **2** (25 to 250 μM) in PBS were added to the cells (100,000 cells per well in 96 well plates). Sample images are shown (inset). b) Analog **2** exhibits sustained light emssion with HEK293 cells. Photon production from a dose of **2** (250 μM) in HEK293 cells (100,00 cells per well in 96 well plates) was monitored over time. For a, error bars represent the standard deviation of the mean for 6 replicate experiments. For b, error bars represent the standard deviation of the mean for 3 replicate experiments.

We also recognized that the alkyne provided a convenient handle for late-stage diversification and potential access to diverse pools of light-emitting luciferins. Alkynes can be "clicked" with various azido appendages via copper-catalyzed azide-alkyne cycloaddition (i.e., CuAAC). Azides and alkynes are well-behaved in complex settings and "click" chemistry conditions are mild enough to be performed in the presence of numerous functional groups [44-46]. Indeed, preliminary evidence suggested compound **2** was readily modified with azido appendages via CuAAC (Figures 2-8–2-11, Scheme 2-4). We found that azide-alkyne cycloaddition proceeds in aqueous solvents and in the absence of copper ligands. However, excess copper was necessary in most cases, likely due to metal chelation with the ring nitrogen atoms. When alkyne **2** was "clicked" with a fluorogenic azide [47], robust fluorescence was observed (Figures 2-8–2-10). The excitation and emission spectra of the ligated product also differed from those of the starting alkyne **2** (Figures 2-9 and 2-10), indicating successful ligation. Other model azides were also successfully ligated to the alkynyl core via CuAAC (Scheme 2-4, Figure 2-11).

Collectively, these data indicate that alkynyl luciferin **2** can be modified with appendages at the 5′-position. We envision using this approach to produce libraries of analogs that can be screened for altered wavelengths of emission or selective processing by mutant luciferases. Recent crystallographic analyses have also revealed Fluc amino acids in close proximity to the 5′ carbon of a bound luciferin intermediate [22,48]. These amino acids could potentially be mutated to complement more bulky, steric appendages on the luciferin ring, thereby facilitating the development of new substrate-specific (i.e., orthogonal) bioluminescent tools.

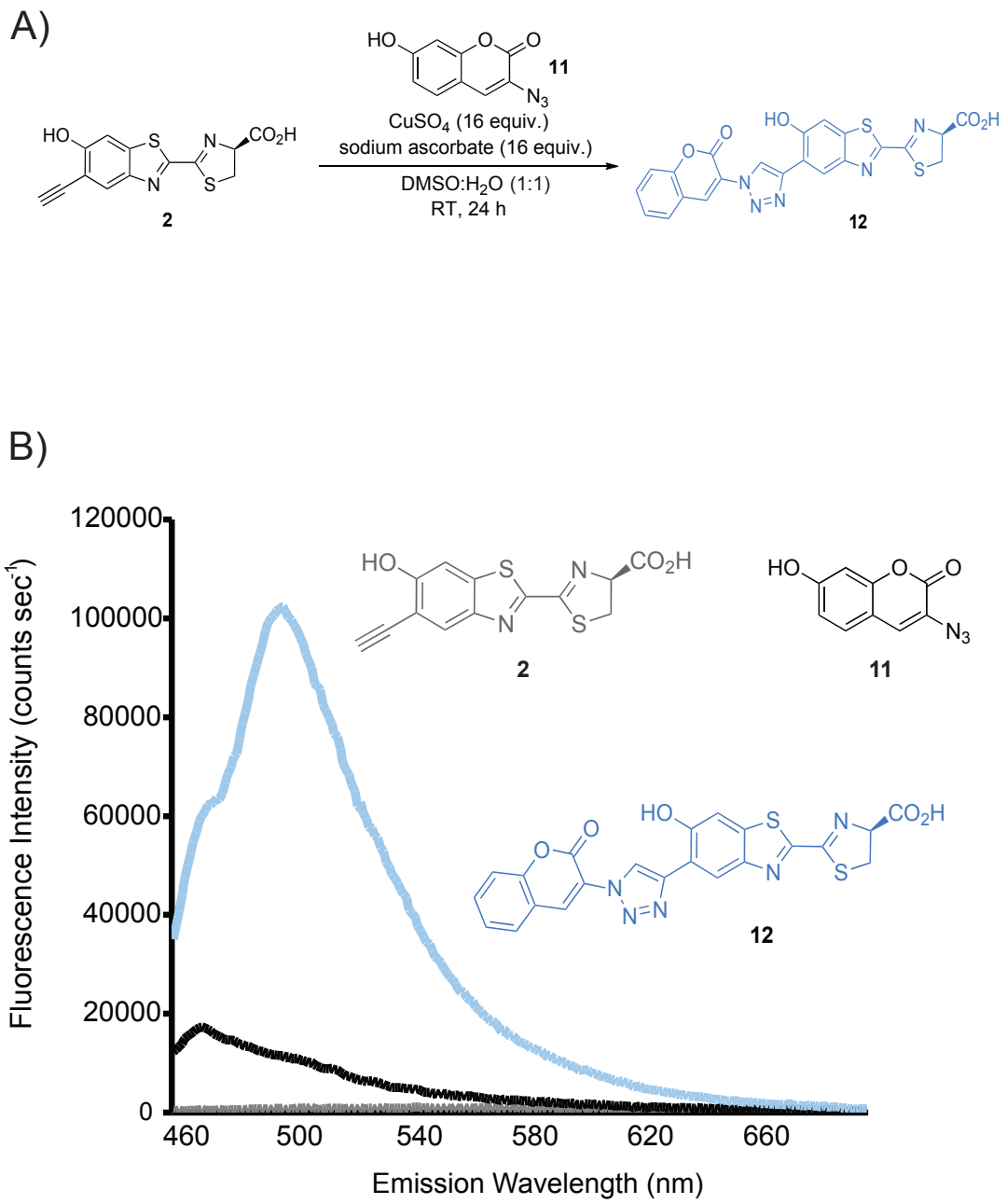

Figure 2-8: A) Modification of luciferin **2** via "click" chemistry. Azide **11** was reacted with **2** to generate fluorescent adduct **12**. B) Fluorescence emission spectra of alkyne **2** with sodium ascorbate and copper sulfate only (gray line), azide **11** with sodium ascorbate and copper sulfate only (dark blue line) and the reaction mixture of **2, 11,** sodium ascorbate and copper sulfate to provide **12** (light blue line). All spectra were acquired using an excitation wavelength of l=444 nm.

A)

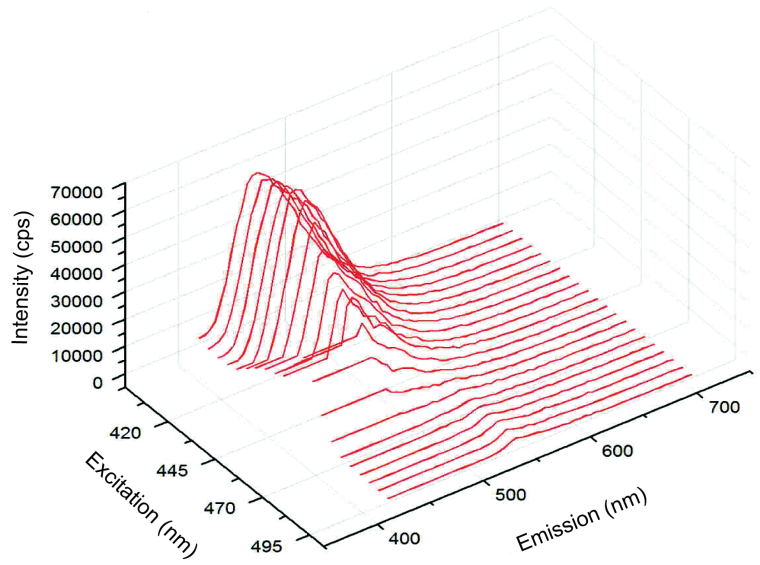

B)

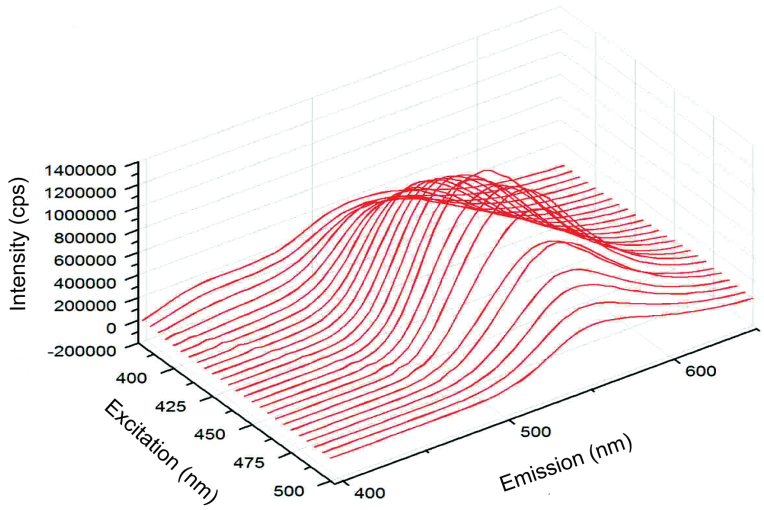

Figure 2-9. Unique fluorescence spectra observed for "click" reaction control samples. A) Excitation and emission spectra for the reaction mixture containing azide **11** (10 mM in DMSO). B) Excitation and emission spectra for the reaction mixture containing alkynyl luciferin **2** (10 mM), $CuSO_4$ (160 mM), and sodium ascorbate (160 mM), but no azide **11**, in DMSO. For (A)-(B), cps is defined as counts per second.

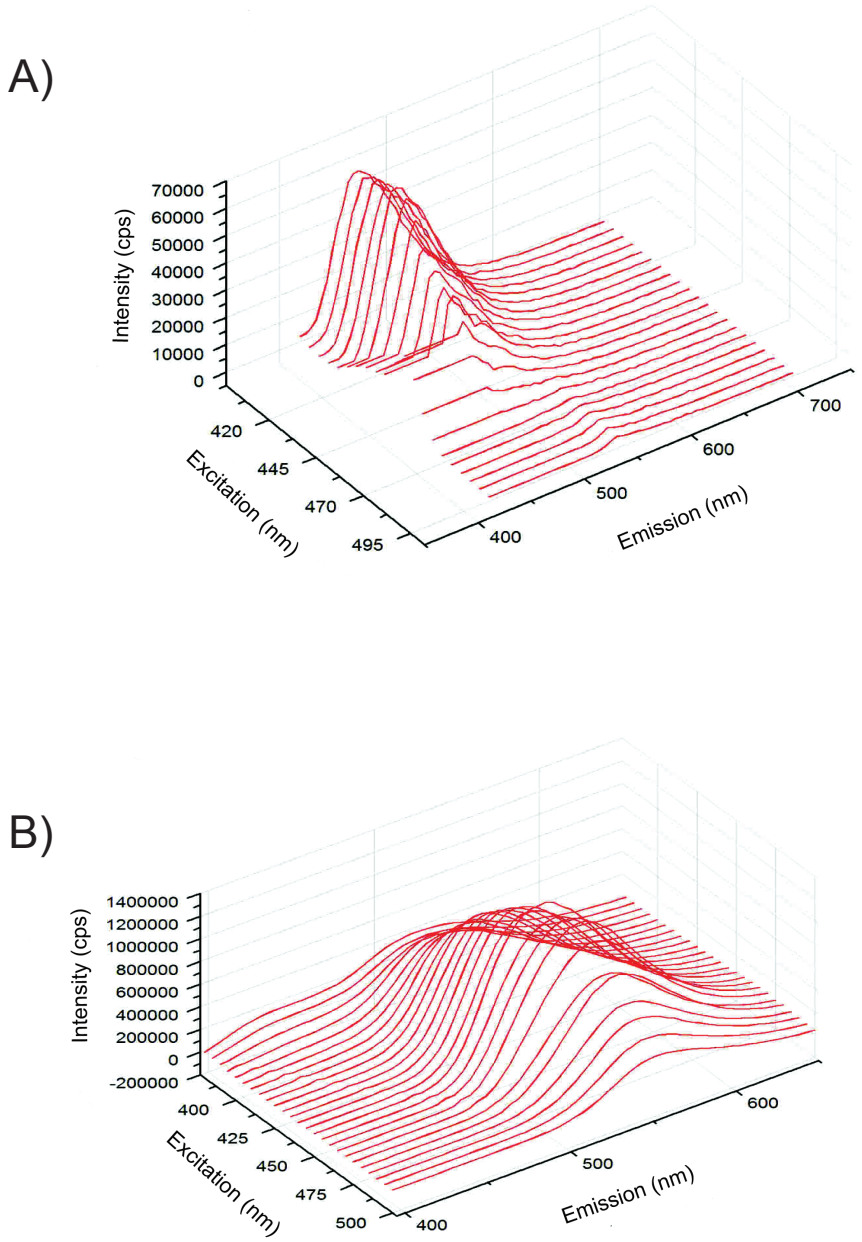

Figure 2-10. Unique fluorescence spectra observed for "click" reaction control samples. A) Excitation and emission spectra for azide **11** (10 mM) in DMSO containing $CuSO_4$ (160 mM) and sodium ascorbate (160 mM), but no alkyne **2**. B) Excitation and emission spectra for alkyne **2** (10 mM) in DMSO, without the addition of copper or ascorbate. For (A)-(B), cps is defined as counts per second.

Scheme 2-4. Additional "click" reactions performed with luciferin 2 and various azides.

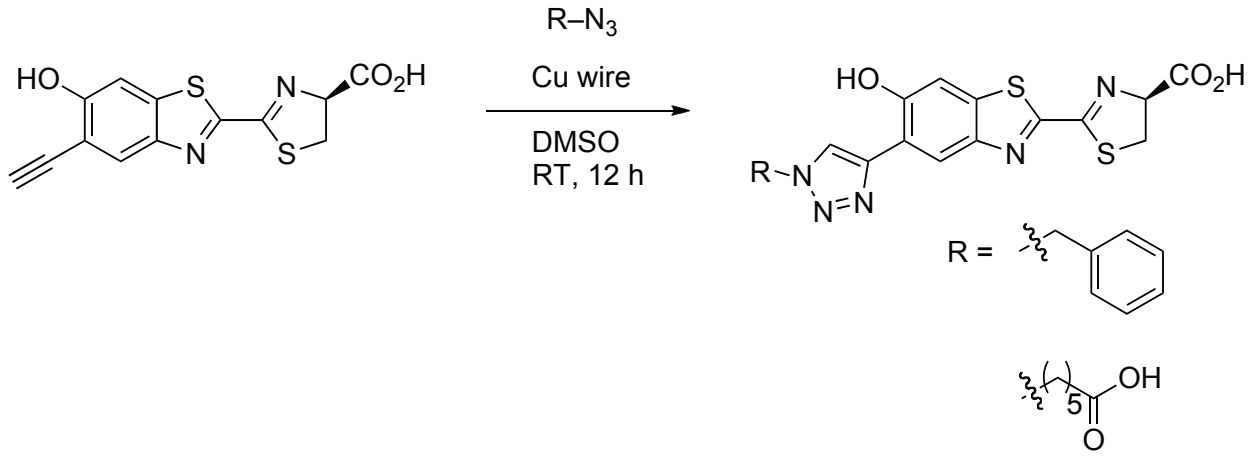

A)

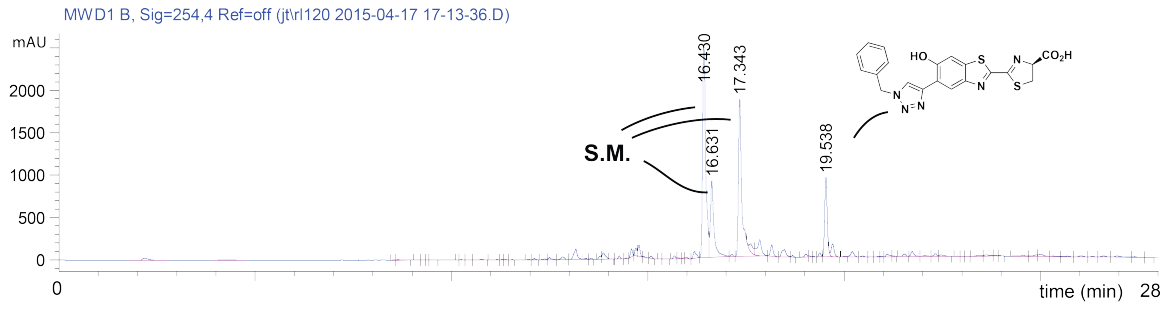

B)

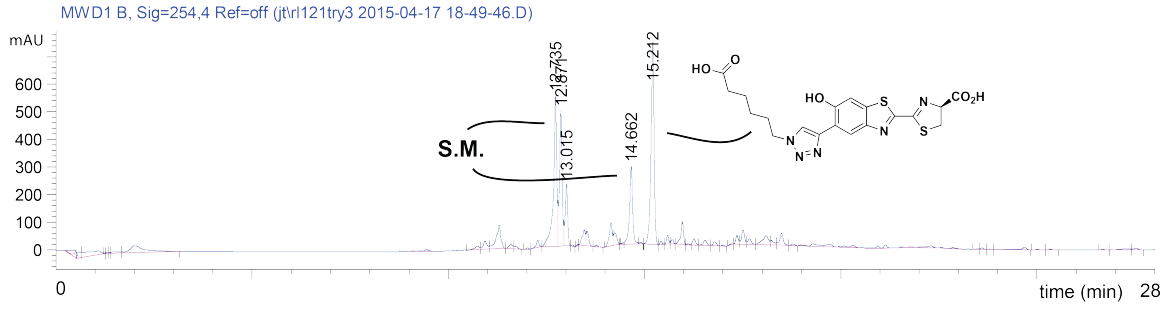

Figure 2-11. HPLC analysis of CuAAC reactions with alkyne 2 and model azides. A) Reaction mixture of **2** and benzyl azide at t = 8 h. B) Reaction mixture of **2** and azidohexanoic acid at t = 8 h. S. M. = copper complexes of starting material.

2.3 Conclusions

In conclusion, we identified an alkyne-modified luciferin for use in bioluminescence assays. The alkyne scaffold is isolable in reasonable yields and quantities and is a functional light emitter with luciferase. The alkynyl probe can also be selectively modified with azido appendages via CuAAC. Such luciferins could eventually be used for multi-component in vivo imaging. Strategies to produce luciferins to date have generally been quite tedious owing to the non-divergent nature of their syntheses and the difficulties in accessing the highly substituted benzothiazole cores. Thus, the installation of a readily modifiable chemical handle (e.g., an alkyne) at the 5′ position addresses these difficulties and provides a platform for both late-stage diversification and rapid expansion of the luciferin toolkit. The alkynyl luciferin will also bolster efforts to generate "activatable" forms of luciferin for biosensing applications in cells and live organisms [49, 50]. Such designer luciferin analogs will further expand the scope of bioluminescence imaging.

2.4 Materials and methods

General experimental procedures

All reactions were performed in flame- or oven-dried glassware under positive pressure of nitrogen or argon unless otherwise noted. Dichloromethane, dimethylacetamide, *N*,*N*-dimethylformamide, triethylamine, and toluene were dried by columns packed with activated alumina on a solvent purification system. Anhydrous pyridine and DMSO were purchased from Acros Organics in AcroSeal™ bottles. All reagents were used as purchased without further

purification. 4,5-Dichloro-1,2,3-dithiazol-1-ium chloride (Appel's salt) [33], benzyl azide [51], azidohexanoic acid [52], and 3-azido-7-hydroxy-2*H*-chromen-2-one [47] were synthesized according to a published procedures. Thin layer chromatography (TLC) was performed on Merck 60 F_{254} pre-coated silica gel plates, and plates were visualized with UV light and ninhydrin stain when appropriate. Flash-column chromatography was performed using silica gel (60 Å, 230-240 mesh, Merck KGA). HPLC runs were conducted on a Varian ProStar equipped with UV-Vis Detector. Analytical runs were performed using an Agilent Polaris 5 C18-A column (4.6 x 150 mm, 5 μM) with a 1 mL/min flow rate, eluting with 10-90% acetonitrile (with 0.1% TFA) over 28 min. Separations were monitored at 254 nm. NMR spectra were recorded with Bruker Advanced spectrometers using deuterated solvents. ^{1}H NMR spectra were recorded at 400 or 500 MHz as indicated. ^{13}C spectra were recorded at 125 MHz. ^{1}H NMR data are reported in the following order: chemical shift (δ ppm), multiplicity, coupling constant (Hz), and integration. ^{13}C NMR data are reported in terms of chemical shift. Infrared spectra were recorded using a Thermo Scientific iD5 ATR infrared spectrophotometer. High-resolution mass spectra were obtained from the UC Irvine Mass Spectrometry Facility. The abbreviations used can be found in the document *JOC Standard Abbreviations and Acronyms*.

General bioluminescence imaging

All images were acquired using an IVIS Lumina (Xenogen) system equipped with a cooled CCD camera. Exposure times ranged from 1-5 s. The captured images were analyzed using Living Image software (Xenogen) and Microsoft Excel.

Light emission assays with recombinant luciferase

Assays were performed in triplicate using black 96-well plates (BD Bioscience). Each well contained purified Fluc (2 mg), luciferin substrate (0-100 mM), ATP (1 mM, Sigma Aldrich), coenzyme A (0.5 mM, Calbiochem), and reaction buffer (20 mM Tris-HCl pH 7.6, 0.5 mg/mL BSA, 0.1 mM EDTA, 1 mM TCEP, 2 mM $MgSO_4$) to a final volume of 100 μL. All reaction components were pre-mixed prior to Fluc addition. Light emission was monitored using an IVIS Lumina as described above. For kinetic assays, non-linear regression to a Michaelis-Menten model was performed using robust outlier determination (GraphPad Prism program, www.graphpad.com).

Bioluminescence emission spectra

Emission spectra were recorded on a Horiba Jobin-Yvon FluoroMax®-4 spectrometer. The excitation and emission slits were adjusted to 0 and 29.4 nm, respectively. Emission data were collected at 5 nm intervals from 500-750 nm at room temperature. Light emission was measured in counts per second (cps), and the acquisition time for each sample was 15 s per wavelength. The luciferin (100 μM) was incubated in a cuvette (10 mm path length) with ATP (1 mM), LiCoA (0.5 mM) and reaction buffer (see above) totaling 900 μL. Purified Fluc (10 μg) was added immediately prior to data acquisition.

Fluorescence imaging

Fluorescence spectra for all luciferin analogs were recorded on a Horbia Jobin-Yvon FluoroMax®-4 spectrometer. Pure compounds were diluted to 0.01 mM with DMSO, and reaction mixtures were diluted with DMSO to 0.01 mM product, assuming the reaction had gone to completion. Excitation and emission slit widths were both 1 nm.

Synthetic Experimental Procedures

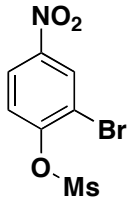

Chemical Formula: $C_7H_6BrNO_5S$
Molecular Weight: 296.10

2-Bromo-4-nitrophenyl methanesulfonate (4)

To a flask of 2-bromo-4-nitrophenol (5.16 g, 23.8 mmol) under argon was added dry CH_2Cl_2 and triethylamine (4.90 g, 48.4 mmol). Methanesulfonyl chloride (3.25 g, 28.4 mmol) was then added slowly over 15 min. After 1 h, the reaction was quenched (1 M $NaHSO_4$) and washed with 1 M $NaHSO_4$ (3 x 50 mL), saturated ammonium chloride (1 x 50 mL), and brine (3 x 50 mL). The organic layers were dried over $MgSO_4$, filtered, and concentrated *in vacuo*. The crude residue was purified via flash-column chromatography (eluting with 7:3 hexanes:ethyl acetate) to yield **4** as a light yellow solid (5.89 g, 84%). ^{1}H NMR (500 MHz, DMSO) δ 8.64 (d, J = 2.5 Hz, 1H), 8.36 (dd, J = 9.0, 3.0 Hz, 1H), 7.82 (d, J = 9.0 Hz, 1H), 3.66 (s, 3H); ^{13}C NMR (125 MHz, DMSO) δ 151.3, 146.6, 129.5, 125.3, 125.0, 117.4, 39.8; IR (thin film) 3108.8, 3012.0, 1511.7, 1371.8, 1335.0, 1174.9, 1280.2, 972.9, 884.8, 851.6, 735.0 cm^{-1}.

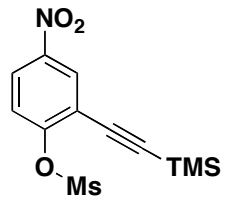

Chemical Formula: $C_{12}H_{15}NO_5SSi$
Molecular Weight: 313.40

4-Nitro-2-((trimethylsilyl)ethynyl)phenyl methanesulfonate (5)

Following the general method of Cappelli and coworkers [53], a flame-dried round-bottom flask was flushed with argon and charged with 2-bromo-1-methanesufonyl-4-nitrobenzene **4** (1.02 g, 3.46 mmol), bis(triphenylphosphine)palladium(II) dichloride (0.25 g, 350 μmol), and copper(I) iodide (67 mg, 350 μmol). The flask was again flushed with argon and capped with a rubber septum. Dry triethylamine (40 mL) and ethynyltrimethylsilane (0.490 mL, 3.47 mmol) were then added by syringe. The flask was heated in a 60 º C oil bath under positive argon pressure for 3 h, and the reaction was monitored by TLC. Upon completion, the reaction mixture was filtered through a pad of Celite and diluted with ethyl acetate (100 mL). The solution was then washed with a saturated NH_4Cl solution (2 x 100 mL), brine (1 x 100 mL), dried with $MgSO_4$, filtered, and concentrated *in vacuo* to give **5** as a grey solid. (0.38 g, 35%) ^{1}H NMR (400 MHz, $CDCl_3$) δ 8.41 (d, J = 2.8 Hz, 1H), 8.25 (dd, J = 9.2, 2.8 Hz, 1H), 7.55 (d, J = 8.8 Hz, 1H), 3.30 (s, 3H), 0.30 (s, 9H); ^{13}C NMR (125 MHz, $CDCl_3$) δ 153.7, 146.0, 129.3, 125.0, 124.3, 118.9, 104.1, 96.0, 39.5, –0.3; HRMS (CI) *m/z* calcd for $C_{12}H_{19}O_5N_2SSi$ $[M+NH_4]^+$ 331.0784, found 331.0788.

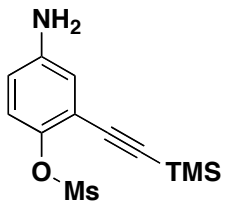

Chemical Formula:
$C_{12}H_{17}NO_3SSi$
Molecular Weight: 283.42

4-Amino-2-((trimethylsilyl)ethynyl)phenyl methanesulfonate (6)

Following the general method of Shen and Driver [39], a solution of **5** (0.22 g, 0.70 mmol) in acetone (5 mL) was added to a solution of iron

powder (0.250 g, 4.50 mmol) and glacial acetic acid (4 mL) in water (10 mL). The mixture was heated at reflux for 2 h, then filtered hot through a pad of Celite. The reaction mixture was neutralized with a saturated Na_2CO_3 solution and extracted with EtOAc (50 mL). The organic layer was washed with saturated EDTA (2 x 50 ml) to remove any additional iron species, followed by water (1 x 50 mL) and brine (1 x 50 mL). The organic layer was dried with $MgSO_4$, filtered, and concentrated *in vacuo* to give **6** as a brown oil (0.121 g, 63%). ^{1}H NMR (400 MHz, DMSO) δ 6.99 (d, J = 8.8 Hz, 1H), 6.63 (d, J = 2.8 Hz, 1H), 6.57 (dd, J = 8.8, 2.8 Hz, 1H), 5.37 (br s, 2 H), 3.25 (s, 3H), 0.20 (s, 9H); ^{13}C NMR (125 MHz, DMSO) δ 148.3, 140.0, 124.0, 117.4, 117.2, 115.7, 101.2, 98.9, 38.6, 0.22; HRMS (CI) *m/z* calcd for $C_{12}H_{21}N_2O_3SSi$ $[M+NH_4]^+$ 301.1042, found 301.1039.

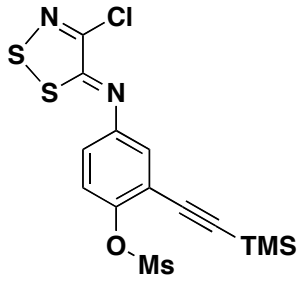

Chemical Formula: $C_{14}H_{15}ClN_2O_3S_3Si$
Molecular Weight: 419.01

(*Z*)-4-(4-Chloro-5*H*-1,2,3-dithiazol-5-ylideneamino)-2-((trimethylsilyl)ethynyl)phenyl methanesulfonate (8)

Following the general procedure of Micaelidou and Koutentis [41], to a flask of **6** (58.1 mg, 0.205 mmol), was added Appel's salt **7** (4,5-dichloro-1,2,3-dithiazol-1-ium chloride, 51.0 mg, 0.245 mmol), quickly followed by an argon flush. Anhydrous CH_2Cl_2 (5 mL) was immediately added and the reaction was stirred at room temperature for 5 min under positive argon pressure. Upon consumption of starting material, anhydrous pyridine (36 mg, 0.45 mmol) was slowly added. The reaction mixture was allowed to stir overnight and then loaded onto a silica gel column. The crude material was purified using flash-column chromatography (eluting with 8:2 hexanes:EtOAc) to afford **8** as a

dark brown oil (52 mg, 61%). ^{1}H NMR (400 MHz, $CDCl_3$) δ 7.47 (d, *J* = 8.8 Hz, 1H), 7.37 (d, *J* = 2.8 Hz, 1H), 7.22 (dd, *J* = 8.8 Hz, 2.4 Hz, 1H), 3.26 (s, 3H), 0.29 (s, 9H); ^{13}C NMR (125 MHz, DMSO) δ 162.2, 150.6, 147.2, 147.2, 125.3, 124.1, 122.5, 119.0, 101.7, 99.5, 39.3, 0.1; HRMS (ESI+) *m/z* calcd for fragment $C_{13}H_{19}O_3N_2S_2Si$ $[M+NH_4]^+$ 343.0606, found 343.0603.

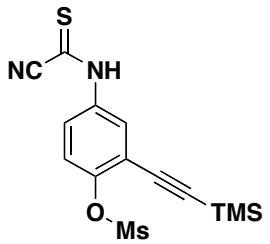

Chemical Formula: $C_{14}H_{16}N_2O_3S_2Si$
Molecular Weight: 352.50

4-(Cyanocarbonothioylamino)-2-((trimethylsilyl)ethynyl)phenyl methanesulfonate (9)

Note: This compound degrades quickly. Following the general procedure of Besson *et al.* [40], a flask containing **8** (0.104 g, 0.248 mmol) was flushed with argon. Resin-linked triphenylphosphine (0.42 g, 0.51 mmol assuming an average loading of 1.2 mmol/g resin) and anhydrous CH_2Cl_2 (3 mL) were added. The reaction mixture was agitated for 2.5 h under argon at room temperature. The crude mixture was purified via flash-column chromatography (eluting with 7:3 hexanes:EtOAc) to afford **9** as a dark yellow oil (0.062 g, 0.18 mmol, 71%) The product was used immediately in next reaction.

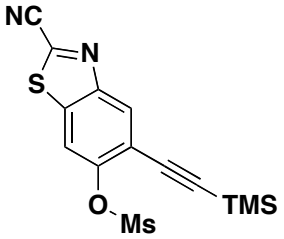

Chemical Formula: $C_{14}H_{14}N_2O_3S_2Si$
Molecular Weight: 350.49

2-Cyano-5-((trimethylsilyl)ethynyl)benzo[*d*]thiazol-6-yl methanesulfonate (10)

Following the general procedure of Inamoto and coworkers [42], a flask containing **9** (16.4 mg, 46.5 μmol was charged with palladium(II) chloride (1 mg, 6 μmol), copper(I) iodide (5.0 mg, 26 μmol), and tetrabutylammonium bromide (0.031 g, 98 μmol), followed by an argon flush. Anhydrous DMF (0.22 mL) and DMSO (0.22 mL)

were then added. The reaction was heated at 120 ˚C for 3h. The crude mixture was filtered over a pad of Celite and extracted with Et_2O (5 mL). The organic phase was then washed with NH_4Cl (1 x 15 mL), water (1 x 10 mL), and brine (1 x 10 mL), dried by $MgSO_4$, filtered, and concentrated *in vacuo*. The concentrated mixture was purified by flash-column chromatography (eluting with 8:2 hexanes:EtOAc) to afford **10** as a brown solid (10.0 mg, 61%). ^{1}H NMR (500 MHz, $CDCl_3$) δ 8.43 (s, 1H), 8.07 (s, 1H), 3.36 (s, 3H), 0.37 (s, 9 H); ^{13}C NMR (125 MHz, $CDCl_3$) δ 150.4, 148.8, 138.8, 136.1, 130.2, 118.4, 116.5, 112.3, 103.0, 98.0, 39.1, –0.3; HRMS (ESI+) *m/z* calcd for $C_{15}H_{19}N_2O_3S_2SiNa$ $[M+Na+CH_3OH]^+$ 405.0375, found 405.0374.

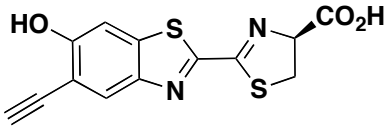

Chemical Formula: $C_{13}H_8N_2O_3S_2$
Molecular Weight: 304.34

(*S*)-2-(5-Ethynyl-6-hydroxybenzo[*d*]thiazol-2-yl)-4,5-dihydrothiazole-4-carboxylic acid (2)

To a flask of **10** (58 mg, 0.16 mmol) in dry THF (2 mL) under argon at –78 ˚C was added a 1.0 M solution of LiHMDS in THF (0.26 mL), followed immediately by TMS chloride (29 mg, 0.26 mmol). The reaction was allowed to warm to room temperature, and then quenched (1 M $NaHSO_4$). The mixture was extracted with EtOAc (20 mL) and then washed with 1 M $NaHSO_4$ (2 x 20 mL) and brine (1 x 20 mL), dried with $MgSO_4$, filtered, and concentrated *in vacuo*. The concentrated mixture was then purified via flash-column chromatography (eluting with 8:2 hexanes:EtOAc) to yield 6-hydroxy-5-((trimethylsilyl)ethynyl)benzo[d]thiazole-2-carbonitrile as a brown solid which was used immediately in the next step. To a solution of 6-hydroxy-5-((trimethylsilyl)ethynyl)benzo[d]thiazole-2-carbonitrile (0.02 g, 0.08 mmol) in degassed methanol was added a solution of D-cysteine (0.015 g, 0.097 mmol) in degassed 0.05 M

phosphate buffer (pH 8.0). The reaction was stirred under N_2 overnight. The mixture was then concentrated *in vacuo*, dissolved in a solution of sodium carbonate (pH 9), and filtered through cotton wool. The filtrate was then cooled to 0 ˚C, and HCl was added until a precipitate formed. The resultant brown precipitate was collected to provide **2** as a brown solid (4.4 mg, 20 μmol, 18%) ^{1}H NMR (500 MHz, CD_3OD) δ 8.09 (s, 1H), 7.44 (s, 1H), 5.43 (s, 1H), 3.78 (m, 3H); ^{13}C NMR (125 MHz, CD_3OD) δ 177.7, 165.6, 158.2, 144.3, 138.3, 127.6, 111.6, 107.4, 82.9, 80.1, 67.9, 36.5, 30.3; IR (thin film) 3371.7, 3283.7, 2918.3, 2850.3, 2359.6, 1593.5, 1489.0, 1435.8, 1280.4, 1205.5, 1027.7, 880.7, 857.8, 668.0 cm^{-1}; HRMS (ESI–) *m/z* calcd for $C_{13}H_7N_2O_3S_2$ [M–H]$^-$ 302.9898, found 302.9905.

HPLC trace:

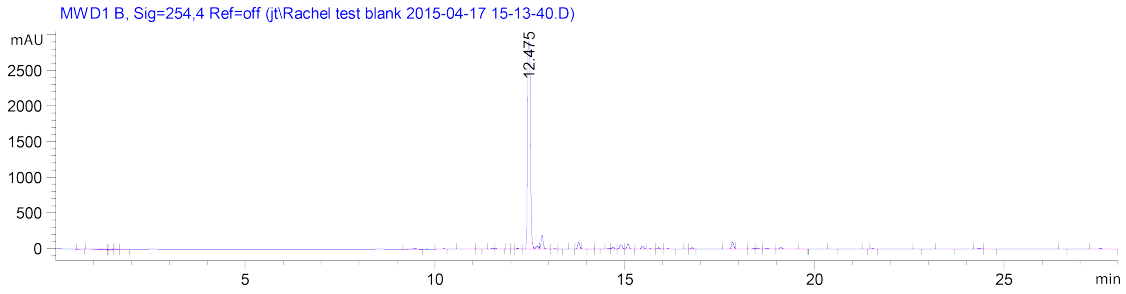

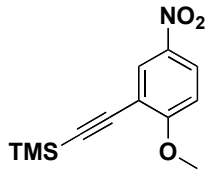

S-1

((2-Methoxy-5-nitrophenyl)ethynyl)trimethylsilane (S1)

Following the general method of Cappelli and coworkers [53] a flame-dried round bottom flask was flushed with argon gas and charged with 2-bromo-1-methoxy-4-nitrobenzene (9.95 g, 42.9 mmol), dichlorobis(triphenylphosphine) palladium (0.31 g, 0.43 mmol), and copper(I) iodide (0.085 g, 0.45 mmol). The flask was again flushed with argon and sealed with a rubber septum. Dry triethylamine (250 mL) and ethynyltrimethylsilane (6.10 mL, 43.0 mmol) were then added via syringe. The flask was heated in a 60 ºC oil bath under positive argon pressure for 3 h, and the reaction was monitored by TLC. Upon completion, the reaction mixture was filtered through a pad of Celite and diluted with EtOAc (200 mL). The filtrate was washed with saturated NH_4Cl (2 x 100 mL) and brine (1 x 100 mL), then dried with $MgSO_4$, filtered, and concentrated *in vacuo* to provide **S1** as a grey solid. (13.0 g, 90%). ^{1}HNMR (400 MHz, $CDCl_3$) δ 8.33 (d, J = 2.7 Hz, 1H), 8.19 (dd, J = 9.2, 2.8 Hz, 1H), 6.93 (d, J = 9.2 Hz, 1H), 3.99 (s, 3H), 0.29 (s, 9H); ^{13}C NMR (125 MHz, $CDCl_3$) δ 164.9, 140.9, 129.8, 125.8, 113.5, 110.3, 101.5, 98.5, 56.7, –0.09; IR (thin film) 2987, 2161, 1579, 1521 cm^{-1}; HRMS (CI) *m/z* calcd for $C_{12}H_{15}NO_3Si$ $[M]^+$ 249.0821, found 249.0821.

Procedure for converting methyl ether 5

To a flame dried round bottom flask containing the 2-bromo-4-nitroaniline (7.47 g, 30.0 mmol) under argon, was added 200 mL of dry CH_2Cl_2. The temperature was reduced to –78 ˚C. To this mixture was slowly added 90 mL (90 mmol) of 1 M BBr_3 solution in dry CH_2Cl_2. The reaction was allowed to warm and stir at room temperature for 12 h. The reaction was then

quenched with 1.0 M $NaHSO_4$, washed with 1.0 M $NaHSO_4$ (2 x 250 mL), saturated NH_4Cl (1 x 250 mL) and brine (1 x 250 mL). Filtered through a pad of Celite and diluted with EtOAc (200 mL). The filtrate was washed with saturated NH_4Cl (2 x 100 mL) and brine (1 x 100 mL), then dried with $MgSO_4$, filtered, and concentrated *in vacuo*. The crude material was purfied by flash-column chromatography (eluting with 1:1 EtOAc:hexanes) to afford the crude phenol as a brown solid, which was carried on immediately. A flask containing the crude phenol (4.40 g, 27.0 mmol) was flushed with argon, and 30 mL dry THF was added. The flask was then cooled to –78 ˚C. A solution of KHMDS (1.0 M in THF 59.0 mL) was added, followed by trimethylsilyl chloride (7.53 mL, 59.0 mmol). The reaction was allowed to warm to room temperature, then quenched (1 M $NaHSO_4$). The mixture was extracted with EtOAc (40 mL), and the organic fractions were combined, washed with 1 M $NaHSO_4$ (2 x 60 mL) and brine (1 x 60 mL), then dried with $MgSO_4$, filtered, and concentrated *in vacuo*. The concentrated material was purified via flash-column chromatography (eluting with 7:3 hexanes:EtOAc) to yield the protected alkynyl compound as a brown solid. This solid was taken on directly to the next step. To a flask of the protected alkynyl compound (2.62 g, 11.0 mmol), was added dry CH_2Cl_2 (25 mL), followed by anhydrous diisopropylethylamine (2.97 g, 23.0 mmol). Methanesulfonyl chloride (1.80 mL, 23.0 mmol) was then added slowly over the course of 10 min, and the reaction was allowed to stir for an additional 15 min. The reaction was then washed with 1 M $NaHSO_4$ (2 x 25 mL), saturated ammonium NH_4Cl (1 x 25 mL) and brine (1 x 25 mL). The organic layers were combined and dried with $MgSO_4$, then filtered and concentrated to yield a yellow-orange oil. This material was purified via flash-column chromatography (eluting with 8:2 hexanes:ethyl acetate) to give **5** (2.5 g, 27% over 3 steps).

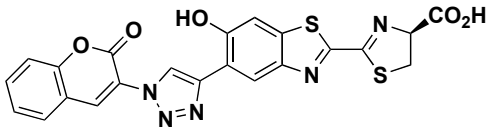

Chemical Formula: $C_{22}H_{13}N_5O_5S_2$
Molecular Weight: 491.50

(*S*)-2-(6-hydroxy-5-(1-(2-oxo-2*H*-chromen-3-yl)-1*H*-1,2,3-triazol-5-yl)benzo[*d*]thiazol-2-yl)-4,5-dihydrothiazole-4-carboxylic acid (12)

Following the general method of Sivakumar, *et al.*[47], 10 μL of a solution comprising coumarin azide (1 mM) **11**, alkyne **2** (1 mM), $CuSO_4$ (16 mM) and sodium ascorbate (16 mM) in 1:1 DMSO:H_2O was prepared. The mixture was allowed to incubate at room temperature for 24 h prior to dilution with DMSO (final concentration of 0.01 mM in DMSO) and fluorescence measurement.

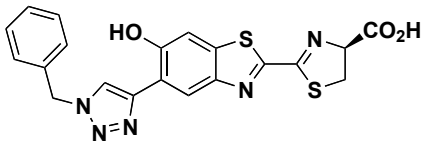

Chemical Formula: $C_{20}H_{15}N_5O_3S_2$
Molecular Weight: 437.49

(*S*)-2-(5-(1-benzyl-1H-1,2,3-triazol-4-yl)-6-hydroxybenzo[*d*]thiazol-2-yl)-4,5-dihydrothiazole-4-carboxylic acid (S7)

Following the general procedure of Himo, *et al.* [54], alkyne **2** (2.0 mg, 5.8 μmol) was added to a vial containing benzyl azide (2.5 μL, 8.8 μmol), copper ribbon (20 mg), and anhydrous DMSO. The vial was then sealed and allowed to stir at room temperature for 8 h. The reaction mixture was diluted with ethyl acetate (5 mL), then washed with 1 M $NaHSO_4$ (1 x 5 mL) and ammonium chloride (1 x 5 mL). The organic layer was concentrated *in vacuo.* The crude material was dissolved in a minimal volume of acetonitrile and analyzed by HPLC. HPLC analysis showed12% conversion. HRMS (ESI+) *m/z* calcd for $C_{20}H_{16}N_5O_3S_2$ $[M + H]^+$ 438.0695, found 438.0690.

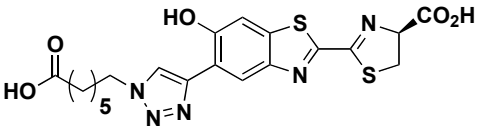

Chemical Formula: $C_{19}H_{19}N_5O_5S_2$
Molecular Weight: 461.51

(*S*)-2-(5-(1-(5-carboxypentyl)-1H-1,2,3-triazol-4-yl)-6-hydroxybenzo[*d*]thiazol-2-yl)-4,5-dihydrothiazole-4-carboxylic acid (S8)

Following the general procedure of Himo *et al*. [54], alkyne **2** (2.0 mg, 5.8 μmol) was added to a vial containing azidohexanoic acid (6.0 μL, 8.8 μmol), copper ribbon (30 mg), and anhydrous DMSO. The vial was then sealed and allowed to stir at room temperature for 8 h. The reaction mixture was diluted with ethyl acetate (5 mL), washed with 1 M $NaHSO_4$ (1 x 5 mL) and ammonium chloride (1 x 5 mL). The organic layer was concentrated *in vacuo*. The crude material was dissolved in a minimal volume of acetonitrile and analyzed by HPLC, showing 40% conversion. Nominal mass (ESI+) *m*/*z* found for $C_{19}H_{20}N_5O_5S_2$ $[M + H]^+$ 462.1, and $C_{19}H_{19}N_5O_5S_2Na$ $[M + Na]^+$ 484.0.

2.5 References

(1) Paley, M. A.; Prescher, J. A. Bioluminescence: a versatile technique for imaging cellular and molecular features. *MedChemComm.* **2014**, *5*, 255–267.

(2) Prescher, J. A.; Contag, C. H. Guided by the light: visualizing biomolecular processes in living animals with bioluminescence. *Curr. Opin. Chem. Biol.* **2010**, *14*, 80–89.

(3) Viviani, V. R. The origin, diversity, and structure function relationships of insect luciferases. *CMLS* **2002**, *59*, 1833–1850

(4) Hastings, J. W. Chemistries and colors of bioluminescent reactions: a review. *Gene* **1996**, *173*, 5–11.

(5) Fraga, H. Firefly luminescence: a historical perspective and recent developments. *Photochem. Photobiol. Sci.* **2008**, *7*, 146–158.

(6) Rice, B. W.; Cable, M. D.; Nelson, M. B. In vivo imaging of light-emitting probes. *J. Biomed. Opt.* **2001**, *6*, 432–440.

(7) Tinkum, K. L.; White, L. S.; Marpegan, L.; Herzog, E.; Piwnica-Worms, D.; Piwnica-Worms, H. Forkhead box O1 (FOXO1) protein, but not p53, contributes to robust induction of p21 expression in fasted mice. *J. Biol. Chem*. *288*, 27999–28008.

(8) Takakura, H.; Hattori, M.; Takeuchi, M.; Ozawa, T. Visualization And Quantitative Analysis Of G Protein-Coupled Receptor Arrestin Interaction In Single Cells And Specific

Organs Of Living Mice Using Split Luciferase Complementation. *ACS Chem. Biol.* **2012**, *7*, 901–910.

(9) Hattori, M.; Haga, S.; Takakura, H.; Ozaki, M.; Ozawa, T. Sustained accurate recording of intracellular acidification in living tissues with a photo-controllable bioluminescent protein. *Proc. Natl. Acad. Sci. U. S. A.* **2013**, *110*, 9332–9337.

(10) Dothager, R. S.; Flentie, K.; Moss, B.; Pan, M. H.; Kesarwala, A.; Piwnica-Worms, D. Advances in bioluminescence imaging of live animal models. *Curr. Opin. Biotechnology* **2009**, *20*, 45–53.

(11) Shinde, J. Perkins, C. H. Contag, *Biochemistry* **2006**, *45*, 11103–11112

(12) Contag, C. H.; Bachmann, M. H. Advances in in vivo bioluminescence imaging of gene expression. *Annu. Rev. Biomed. Eng.* **2002**, *4*, 235–260.

(13) Sacco, A.; Doyonnas, R.; Kraft, P.; Vitorovic, S.; Blau, H. M. Self-renewal and expansion of single transplanted muscle stem cells. *Nature* **2008**, *456*, 502–506.

(14) Villalobos, V.; Naik, S.; Bruinsma, M.; Dothager, R. S.; Pan, M.-H.; Samrakandi, M.; Moss, B.; Elhammali, A.; Piwnica-Worms, D. Dual-color click beetle luciferase heteroprotein fragment complementation assays. *Annu. Rev. Biomed. Eng.* **2007**, *9*, 321–349.

(15) Branchini, B. R.; Ablamsky, D. M.; Davis, A. L.; Southworth, T. L.; Butler, B.; Fan, F.; Jathoul, A. P.; Pule, M. A. Red-emitting luciferases for bioluminescence reporter and imaging applications. *Anal. Biochem.* **2010**, *396*, 290–297.

(16) Branchini, B. R.; Ablamsky, D. M.; Murtiashaw, M. H.; Uzasci, L.; Fraga, H.; Southworth, T. L. Thermostable red and green light-producing firefly luciferase mutants for bioluminescent reporter applications. *Anal. Biochem.* **2007**, *361*, 253–262.

(17) Branchini, B. R.; Southworth, T. L.; Khattak, N. F.; Michelini, E.; Roda, A. Red- and green-emitting firefly luciferase mutants for bioluminescent reporter applications. *Anal. Biochem.* **2005**, *345*, 140–148.

(18) Leevy, W. M.; Gammon, S. T.; Jiang, H.; Johnson, J. R.; Maxwell, D. J.; Jackson, E. N.; Marquez, M.; Piwnica-Worms, D.; Smith, B. D. Optical imaging of bacterial infection in living mice using a fluorescent near-infrared molecular probe. *J. Am. Chem. Soc.* **2006**, *128*, 16476.

(19) Rabinovich, B. A.; Ye, Y.; Etto, T.; Chen, J. Q.; Levitsky, H. I.; Overwijk, W. W.; Cooper, L. J.; Gelovani, J.; Hwu, P. Visualizing fewer than 10 mouse T cells with an enhanced firefly luciferase in immunocompetent mouse models of cancer. *Proc. Natl. Acad. Sci. U. S. A.* **2008**, *105*, 14342–14346.

(21) Mezzanotte, L.; Que, I.; Kaijzel, E.; Branchini, B.; Roda, A.; Lowik, C. Sensitive dual color in vivo bioluminescence imaging using a new red codon optimized firefly luciferase and a green click beetle luciferase. *PLoS ONE* **2011**, *6*, e19277.

(22) Nakatsu, T.; Ichiyama, S.; Hiratake, J.; Saldanha, A.; Kobashi, N.; Sakata, K.; Kato, H. Structural basis for the spectral difference in luciferase bioluminescence. *Nature* **2006**, *440*, 372–376.

(23) Branchini, B. R.; Hayward, M. M.; Bamford, S.; Brennan, P. M.; Lajiness, E. J. Naphthyl- and quinolylluciferin: green and red light emitting firefly luciferin analogues. *Photochem. Photobiol.* **1989**, *49*, 689–695.

(24) Takakura, H.; Sasakura, K.; Ueno, T.; Urano, Y.; Terai, T.; Hanaoka, K.; Tsuboi, T.; Nagano, T. Development of luciferin analogues bearing an amino group and their application as BRET donors. *Chem. Asian. J.* **2010**, *5*, 2053.

(25) Jathoul, A. P.; Grounds, H.; Anderson, J. C.; Pule, M. A. A dual-color far-red to near-infrared firefly luciferin analogue designed for multiparametric bioluminescence imaging. *Angew. Chem. Int. Ed.* **2014**, *53*, 13059–13063.

(26) Kojima, R.;, H.; Ozawa, T.; Tada, Y.; Nagano, T.; Urano, Y. Rational design and development of near-infrared-emitting firefly luciferins available in vivo. *Angew. Chem. Int. Ed.* **2013**, *52*, 1175–1179.

(27) Mofford, D. M.; Reddy, G. R.; Miller, S. C. Aminoluciferins extend firefly luciferase bioluminescence into the near-infrared and can be preferred substrates over D-luciferin. *J. Am. Chem. Soc.* **2014**, *136*, 13277–13282.

(28) Evans, M. S.; Chaurette, J. P.; Adams Jr, S. T.; Reddy, G. R.; Paley, M. A.; Aronin, N.; Prescher, J. A.; Miller, S. C. A synthetic luciferin improves bioluminescence imaging in live mice. *Nat. Methods* **2014**, *11*, 393–395.

(29) Harwood, K. R.; Mofford, D. M.; Reddy, G. R.; Miller, S. C. Identification of mutant firefly luciferases that efficiently utilize aminoluciferins. *Chem. Biol*. **2013**, *18*, 1649–1657.

(30) Woodroofe, C. C.; Shultz, J. W.; Wood, M. G.; Osterman, J.; Cali, J. J.; Daily, W. J.; Meisenheimer, P. L.; Klaubert, D. H. N-Alkylated 6'-aminoluciferins are bioluminescent substrates for Ultra-Glo and QuantiLum luciferase: new potential scaffolds for bioluminescent assays. *Biochemistry* **2008**, *47*, 10383.

(31) Reddy, G. R.; Thompson, W. C.; Miller, S. C. Robust light emission from cyclic alkylaminoluciferin substrates for firefly luciferase. *J. Am. Chem. Soc.* **2010**, *132*, 13586–13587.

(32) SPARTAN Student v. 5.0.2. SPARTAN Student v. 5.0.2 Wavefunction, Inc.

(33) Appel, R.; Janssen, H.; Siray, M.; Knoch, F. Synthese und Reaktionen des 4,5-Dichlor-1,2,3-dithiazolium-chlorids. *Chem. Ber.* **1985**, *118*, 1632.

(34) McCutcheon, D. C.; Paley, M. A.; Steinhardt, R. C.; Prescher, J. A. Expedient synthesis of electronically modified luciferins for bioluminescence imaging. *J. Am. Chem. Soc.* **2012**, *134*, 7604–7607.

(35) Besson, T.; Guillard, J.; Rees, C. W. Rapid synthesis of 2-cyanobenzothiazole, isothiocyanate and cyanoformanilide derivatives of dapsone. *J. Chem. Soc., Chem. Commun.* **1995**, 1419–1420.

(36) Koutentis, P. A.; Koyioni, M.; Michaelidou, S. S. The conversion of [(4-chloro-5H-1,2,3-dithiazol-5-ylidene)amino]azines into azine fused thiazole-2-carbonitriles. *Org. Biomol. Chem.* **2010**, *11*, 621–629

(37) Akhavan-Tafti, H.; De Silva, R.; Wang, G.; Eickholt, R. A.; Gupta, R.; Kaanumalle, L. S.; Google Patents.

(38) Looker, J. H.; Thatcher, D. N. The utility of the methanesulfonyl blocking group. A new synthesis of p-hydroxyphenylacetic acid. *J. Org. Chem.* **1954**, *19*, 784–788.

(39) Shen, M.; Driver, T. G. Iron(II) bromide-catalyzed synthesis of benzimidazoles from aryl azides. *Org. Lett.* **2008**, *10*, 3367–3370.

(40) Besson, T.; Emayan, K.; Rees, C. W. 3,1-Benzoxazin-4-ones, 3,1-benzothiazin-4-ones and N-arylcyanothioformamides. *J. Chem. Soc., Chem. Commun.* **1995**, 1419–1420.

(41) Michaelidou, S. S.; Koutentis, P. A. The synthesis of 2-cyano-cyanothioformanilides from 2-(4-Chloro-5H-1,2,3-dithiazol-5-ylideneamino)benzonitriles Using DBU. *Synthesis* **2009**, 4167–4174.

(42) Inamoto, K.; Hasegawa, C.; Hiroya, K.; Doi, T. Palladium-catalyzed synthesis of 2-substituted benzothiazoles via a C-H functionalization/intramolecular C-S bond formation process. *Org. Lett.* **2008**, *10*, 5147–5150.

(43) Ritter, T.; Stanek, K.; Larrosa, I.; Carreira, E. M. Mild cleavage of aryl mesylates: methanesulfonate as potent protecting group for phenols. *Org. Lett.* **2004**, *6*, 1513–1514.

(44) Kolb, H. C.; Finn, M. G.; Sharpless, K. B. Click chemistry: diverse chemical function from a few good reactions. *Angew. Chem. Int. Ed.* **2001**, *40*, 2004–2021

(45) Baskin, J. M.; Prescher, J. A.; Laughlin, S. T.; Agard, N. J.; Chang, P. V.; Miller, I. A.; Lo, A.; Codelli, J. A.; Bertozzi, C. R. Copper-free click chemistry for dynamic in vivo imaging. *Proc. Natl. Acad. Sci. U. S. A.* **2007**, *104*, 16793–16797

(46) Patterson, D. M.; Nazarova, L. A.; Prescher, J. A. Finding the right (bioorthogonal) chemistry. *ACS Chem. Biol.*, **2014**, *9*, 592–605.

(47) Sivakumar, K.; Xie, F.; Cash, B. M.; Long, S.; Barnhill, H. N.; Wang, Q. A fluorogenic 1,3-dipolar cycloaddition reaction of 3-azidocoumarins and acetylenes. *Org. Lett.* **2004**, *6*, 4603–4606.

(48) Sundlov, J. A.; Fontaine, D. M.; Southworth, T. L.; Branchini, B. R.; Gulick, A. M. Crystal structure of firefly luciferase in a second catalytic conformation supports a domain alternation mechanism. *Biochemistry,* **2014,** *51*, 6493.

(49) Li, J.; Chen, L.; Du, L.; Li, M. Cage the firefly luciferin! - a strategy for developing bioluminescent probes. *Biochemistry*, **2014,** *51*, 6493-6495.

(50) Yao, H.; So, M. K.; Rao, J. A bioluminogenic substrate for in vivo imaging of beta-lactamase activity. *Angew. Chem. Int. Ed.* **2007**, *46*, 7031–7034.

(51) Alvarez, S. G.; Alvarez, M. T. A practical procedure for the synthesis of alkyl azides at ambient temperature in dimethyl sulfoxide in high purity and yield. *Synthesis* **1997**, 413.

(52) Zhang, Y.; Chakraborty, M.; Cerda-Smith, C. G.; Bratton, R. N.; Maurer, N. E.; Senser, E. M.; Novak, M. Chemistry of ring-substituted 4-(benzothiazol-2-yl)phenylnitrenium ions from antitumor 2-(4-aminophenyl)benzothiazoles. *J. Org. Chem.*, *78*, 6992.

(53) Capelli, L.; Manini, P.; Pezzella, A.; Napolitano, A.; d'Ischia, M. Efficient synthesis of 5,6-dihydroxyindole dimers, key eumelanin building blocks, by a unified o-ethynylaniline-based strategy for the construction of 2-linked biindolyl scaffolds. *J. Org. Chem.* **2009**, *74,* 7191.

(54) Himo, F.; Lovell, T.; Hilgraf, R.; Rostovtsev, V. V.; Noodleman, L.; Sharpless, K. B.; Fokin, V. V. Copper(I)-catalyzed synthesis of azoles. Dft study predicts unprecedented reactivity and intermediates. *J. Am. Chem. Soc.* **2005**, *127*, 210.

Chapter 3: Building better bioluminescent reporters through *ab initio* calculations

3.1 Introduction

Recent years have seen a surge of interest in accessing novel luciferin scaffolds for bioluminescence imaging (BLI) [1-5]. BLI relies on the enzyme-catalyzed production of light via luciferase enzymes and luciferin small molecules [6]. This reaction has been routinely used *in vitro* and *in vivo* for monitoring diverse biological processes [7]. However, a limited supply of robust, light-emitting luciferins has stymied efforts to visualize multicellular networks and other interactions.

We and others are attempting to fill this void with new luciferin architectures for both multi-spectral and multi-component imaging [7,8]. Our efforts have been focused on developing analogs of D-luciferin, the native light-emitting substrate for firefly luciferase (Fluc) [1]. Fluc catalyzes the activation and subsequent oxidation of D-luciferin, releasing photons of yellow-green light (Figure 3-1) [6]. While the mechanism of photon release remains controversial and the subject of intense investigation, the most accepted version involves initial activation of the luciferin substrate (as a luciferyl-AMP anhydride) [6,9-13]. Subsequent oxidation of this intermediate, followed by CO_2 release results in a singlet excited-state (S_1) oxyluciferin; this compound then emits light as it relaxes to a singlet ground state (S_0). Fluc can also catalyze light emission with a range of D-luciferin analogs [7], and a similar mechanism is believed to be operative.

The most robust, light-emitting analogs harbor common features: strong electron-donating groups at the 6' position, extended pi systems, and rigid cores [14,15]. However, plenty

of analogs exist that meet these criteria, yet remain poor light emitters [4,14,16]. Some notable examples include heterocyclic luciferins (including benzimidazole and benxoxazole variants). Most of these molecules emit less light than D-luciferin when incubated with Fluc [1,17,18]. Whether the reduced bioluminescent intensities are due to inefficient processing by Fluc, or the inability of the luciferin to access an appropriate electronic excited state (S_1) remains difficult to deconvolute. These uncertainties have confounded the development of new useful luciferin analogs; there is no guarantee that a desired scaffold will be able to reach the appropriate electronic excited state or emit light efficiently from that state. Thus, an important long-term goal involves predicting viable light-emitting scaffolds prior to chemical synthesis. Accurate predictions would avoid time-consuming syntheses, streamlining the production of new bioluminescent tools.

There are several challenges involved in predicting robust luciferin emitters. Bioluminescent light production is a complex, multi-step process that involves *chemical* activation (versus the light-based excitation of fluorescence), thus, traditional fluorescence parameters do not apply. In this particular case, the light-emitting species is an oxyluciferin, the unstable—and difficult to access—product of the chemical activation [19]. For these reasons, we turned to computational tools to aid in the design of desirable luciferin architectures. We employed time-dependent density functional theory [20] (TDDFT) to compute the adiabatic emission of oxyluciferin from the first singlet excited state (S_1) to the ground state (S_0). The predicted oscillator strength of this de-excitation served as an indirect measure for the chemiluminscence intensity. These data identified scaffolds that were likely to be robust light emitters, and upon synthesizing compounds of interest, we confirmed the predictions using

standard biochemical and BLI assays, even in live cells. This method will aid in the design of new synthetic targets with desired optical properties.

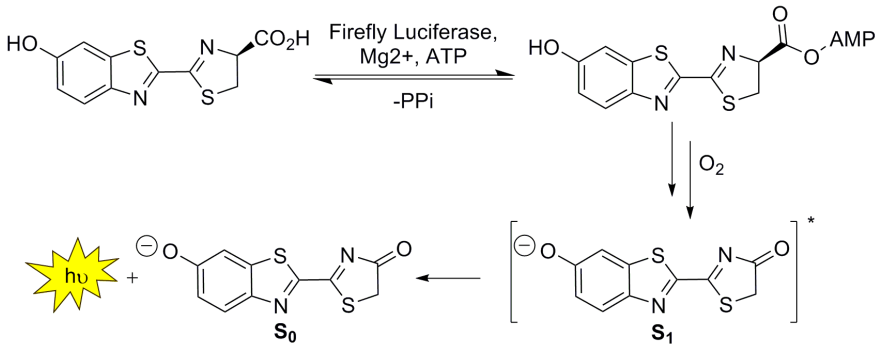

Figure 3-1. Mechanism of luciferase-mediated light production. Fluc catalyzes the adenylation/activation and oxidation of D-luciferin to oxyluciferin, releasing light in the process. The reaction proceeds through an excited state (S_1) oxyluciferin intermediate. Relaxation of this molecule to the ground state (S_0) is accompanied by photon release.

3.2 Results and discussion

3.2a Oscillator strengths correlate with known robust bioluminescent emitters.

We first calibrated our computational results by calculating the emission intensity of known luciferin analogs (Table 3-1). The predicted values correlated with the known bioluminescent emission intensities in most cases. For example, D-luciferin analogs lacking an electron-donating group at the 6′ position were predicted to have low oscillator strengths. Such compounds are known to be poor bioluminescent emitters [14,21,22]. By contrast, D-luciferin analogs with 6′–amino substituents—known robust light emitters—were predicted to have oscillator strengths on par with (or in some cases better than) the native Fluc substrate. In the case of **6′–dimethylaminoLuc**, the steric bulk of the methyl groups can force an out-of-plane twisting, thereby breaking the conjugation across the molecule and drastically lowering its emission strength [23-28]. Similar decreased light emission has been observed for 6′-alkylated luciferins, including **6′–methoxyLuc**, in addition to some fluorophores [28-30].

Table 3-1. Comparison of calculated oscillator strengths and bioluminescence emission intensities for known luciferins.

Compound		Name	Oscillator Strength[a]	Rel. BLI[b]
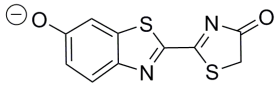		**D–Luc**	100	100
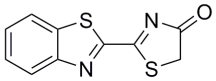		**6'–deoxyLuc**	1.4	<0.01[c]
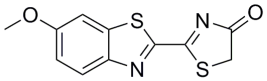		**6'–methoxyLuc**	57.2	<0.01
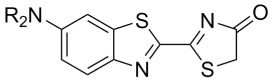	R_1, R_2 = H	**6'–aminoLuc**	91.9	61
	R_1 = Me R_2 = H	**6'–MeNHLH$_2$**	94.9	101
	R_1, R_2 = Me	**6'–Me$_2$NLH$_2$**	102.9	1
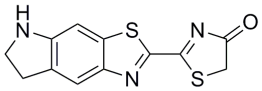	R = H	**CycLuc1**	127.6	38
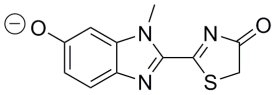		**NMeBenzLuc**	0.282	0.01

[a]Calculated as a theoretical maximum. [b]Bioluminescence was measured using 100 μM luciferin and 1 μg recombinant luciferase. [c]no signal exceeding background was observed.

3.2b Oscillator strengths predict novel bioluminescent emitters.

Encouraged by these results, we used the same methodology to predict the emission strengths for novel luciferin architectures. These compounds included various electronically and sterically modified luciferins (Table 3-2). This latter category included scaffolds with substituents at the 4′, 5′, and 7′ positions on the D-luciferin core.

Table 3-2. Calculated oscillator strengths and measured bioluminescent photon production for novel luciferin analogs.

Compound	Name	Oscillator Strength[a]	Rel. BLI[b]	Rel. CLI[c]
	D-Luc	100	100	100 ± 11
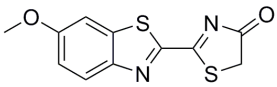	**6'–methoxyLuc**	57.2	<0.01[d]	0.157 ± 0.029
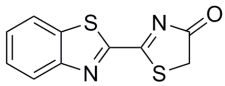	**6'–deoxyLuc**	1.4	<0.01	0.99 ± 0.11
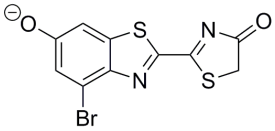	**4'–BrLuc**	86.1	3.1	5.31 ± 0.45
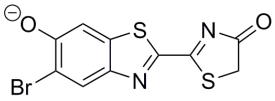	**5'–BrLuc**	104	46.0	15.1 ± 2.4
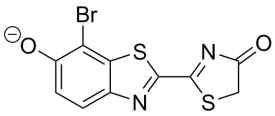	**7'–BrLuc**	79.3	3.4	15.8 ± 2.0
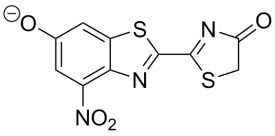	**4'–NO_2Luc**	25.8	0.5	0.47 to 0.06[e]
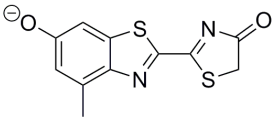	**4'–MeLuc**	93.3	34.3	46.5 ± 10.4

[a]Calculated as a theoretical maximum. [b]Bioluminescence was measured using 100 μM luciferin and 1 μg recombinant luciferase. [c]Chemiluminescence was measured at approximately 25 μM luciferin and 0.05 M KOPh in DMSO (see SI for further details). [d]no signal exceeding background was observed. [e]A range of measured values is given due to compound instability.

As expected, the calculated oscillator strengths for the 6′–deoxy compound (**6′–deoxyLuc**) and nitro-substituted scaffold **4′–NO_2Luc** were substantially lower than D-luc. Both **6′–deoxyLuc** and **4′–NO_2Luc** reduce the amount of electron density at the 6′ position of the luciferin ring; this type of modification is known to reduce luciferin light output [31,32]. Since the *bioluminescent* properties of these analogs are unknown, the reduction in light emission predicted by DFT could imply an inherent reduction in the light-emitting potential of the compound (as noted above). To avoid this confounding issue, we utilized a traditional *chemiluminescent* assay to measure their intrinsic abilities to produce light (Figure 3-2) [33-35]. This non-enzymatic process mimics the enzymatic reaction itself, involving formation of an activated ester intermediate, followed by oxidation [36]. Indeed, White and others have previously shown that the luciferin excited state can be attained by treating activated luciferin esters (as AMP surrogates) with base (e.g., KOPh), in the absence of enzyme [33]. We were able to recapitulate these results, observing strong emission from the activated ester of D-luciferin. Control compounds (e.g., **6′–methoxyLuc** and **6′–deoxyLuc)** with weaker electron donation into the aromatic ring (a key feature of luciferins) did not produce this level of emission.

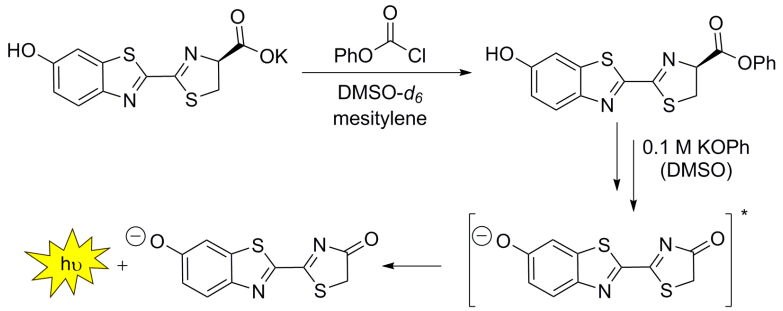

Figure 3-2. Chemiluminescent light production from luciferin analogs. Luciferin acids can be chemically activated to labile esters. Subsequent H-atom abstraction/oxidation generates light-emitting species. This procedure mimics the bioluminescent reaction mediated by Fluc.

3.2c DFT model, chemiluminescence and biochemical analyses reveal sites for orthogonal probe development.

More interesting patterns emerged with the sterically modified compounds. DFT analyses were performed on a series of luciferins comprising modifications at the 4′, 5′, and 7′ positions. In initial surveys, the site of substitution was predicted to minimally impact emission for a given substituent. However, the electron-withdrawing/donating character of the substituent itself was predicted to greatly impact the strength of the emission (i.e., the more electron-withdrawing substituents correlated with the weakest oscillator strengths). We decided to move forward with the bromo-substituted compounds (**4′–BrLuc**, **5′–BrLuc**, and **7′–BrLuc**) for experimental validation. Bromo substituents are inductive electron-withdrawing groups, yet ortho/para-directors in classic organic transformations. Thus, they fall in the "middle-of-the-road" considering their electronic impact. Methyl groups are classified solely as inductive donors, while nitro groups are classified as resonance acceptors. Bromo substituents are also suffi sufficiently large to present a steric barrier for enzyme utilization and thus help us deconvolute the role of electronics vs. enzymatic processing. Last, these substituents offer unique opportunities for further analog development – as chemical handles for important classes of cross-coupling reactions.

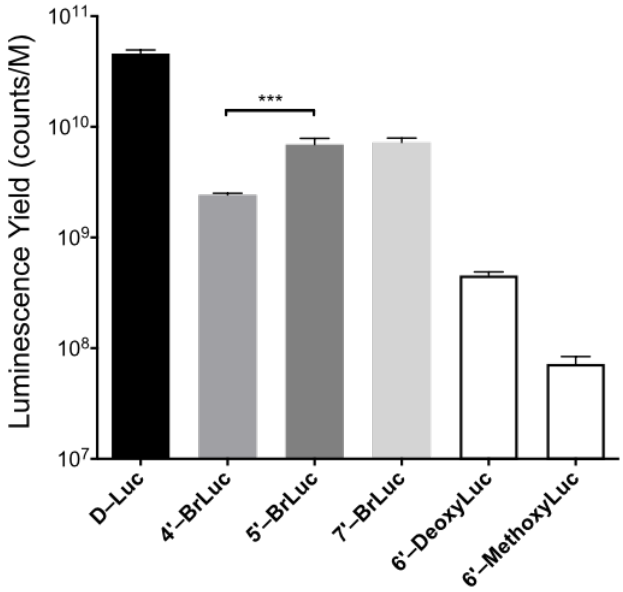

Figure 3-3. Bromo-substituted luciferins are capable of chemiluminescent photon production. Measured counts were normalized to concentration. Error bars represent the standard error in the mean of at least 18 measurements over three days ***$p < 0.001$ (t-test)

When the bromo luciferins were subjected to the chemiluminescence assay pictured in Figure 3-2, light emission was observed for all compounds. The intensity of photon production was lower than that of D-luciferin, which was predicted by the DFT calculations (Figure 3-3). Within the analog series, the **5′–BrLuc** and **7′–BrLuc** compounds exhibited nearly the same levels of chemiluminescence. The photon emission values for the 4′-substituted luciferin (**4′–BrLuc**) were somewhat lower, but on par with the other two isomers (**5′**, and **7′**). The reduction in chemiluminescence relative to **D-Luc** can be attributed to electronic effects due to the presence of bromine. DFT calculations revealed two low-lying states that may play a major role in the deactivation of luciferin emission: (1) a triplet ground state and (2) a singlet twisted intramolecular charge-transfer (TICT) excited state (Figure 3-4).

Figure 3-4. Ordering of relevant spin and geometric states. In order to reconcile the differences in experimental and computational results for the BromoLuc series, **4′–NO_2Luc**, and **6′–methoxyLuc**, the ground and excited electronic states were studied in both the planar and twisted geometric states of the neutral and anionic species; both singlet and triplet states were included to help rationalize possible intruder states that may be responsible for the quenching of the chemiluminescence. Electronic states were computed at the geometry of the first singlet excited state, which was confirmed to be a minimum by numerical frequency analysis. In the case of neutral **4′–BrLuc**, no twisted S_1 minimum was found. This picture gives relative energetics of the different electronic states at the assumed emissive nuclear configuration.

For the native D-Luciferin, both the twisted and the planar S_1 state are relatively isolated from other states. Given that our model can reasonably predict the emission strength of native luciferin, the isolated nature of the S_1 state helps to establish a baseline by demonstrating that it is less probable that there is some other electronic state lower in energy that can be accessed. In the case of the anionic **7′–BrLuc**, one observes a very small separation between the planar S_1 state and the twisted triplet ground state, which could account for the considerable decrease in experimentally measured emission. The planar S_1 state for the other bromo-substiuted luciferin molecules seems to be modestly isolated, but there could be a distribution of protonated and deprotonated luciferin whose different accessible electronic states could cause interference. For both protonation states of **4′–NO_2Luc**, the S_1 planar state is very near in energy to the twisted S_1 state. Considering finally **6′–methoxyLuc**, there seem to be no nearby electronic states, but there is a low-lying planar triplet state that could act as a channel for nonradiative decay. The overall environment in solution is complex compared to our model and many factors besides those described here could be in effect; however, electronic states in both the planar and twisted configurations are definitely accessible under photoexcitation and provide a reasonable explanation for the quenching of chemiluminescence.

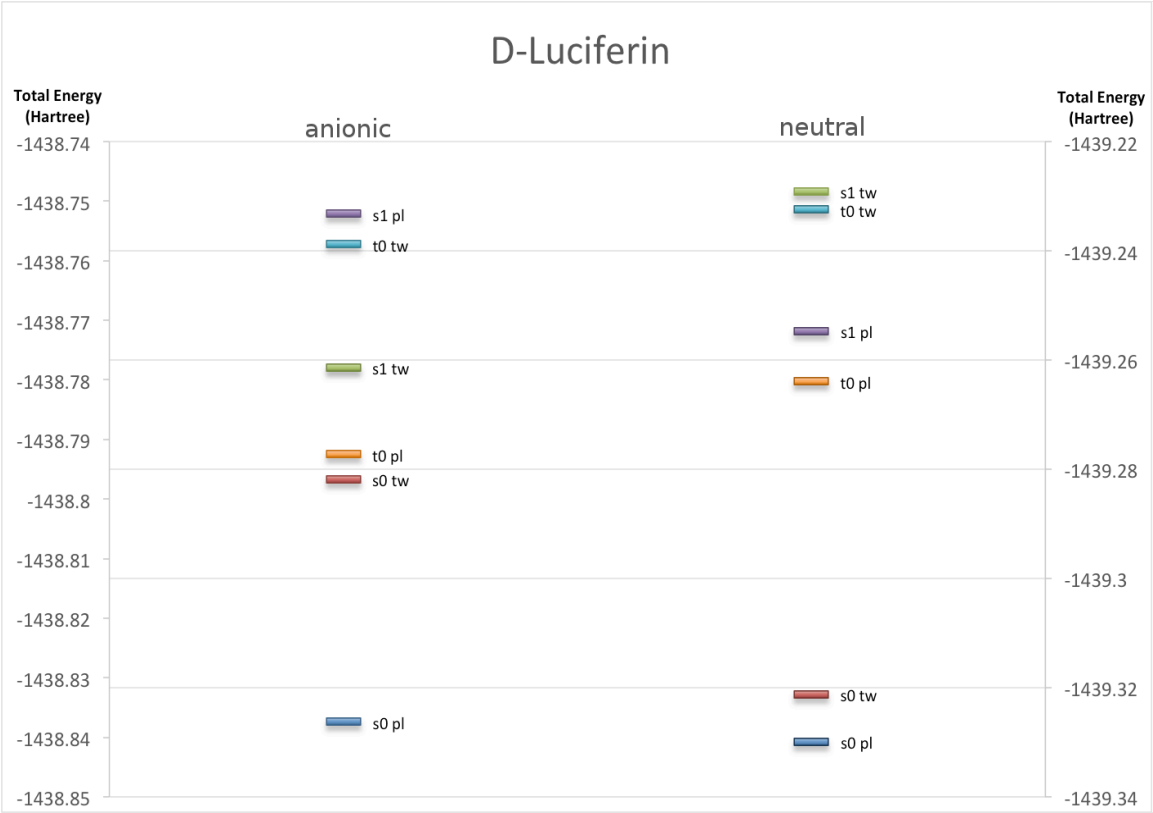
D-Luciferin
Total Energy (Hartree)
anionic
neutral
Total Energy (Hartree)
-1438.74
-1438.75
-1438.76
-1438.77
-1438.78
-1438.79
-1438.8
-1438.81
-1438.82
-1438.83
-1438.84
-1438.85
-1439.22
-1439.24
-1439.26
-1439.28
-1439.3
-1439.32
-1439.34
s1 pl
t0 tw
s1 tw
t0 pl
s0 tw
s0 pl
s1 tw
t0 tw
s1 pl
t0 pl
s0 tw
s0 pl

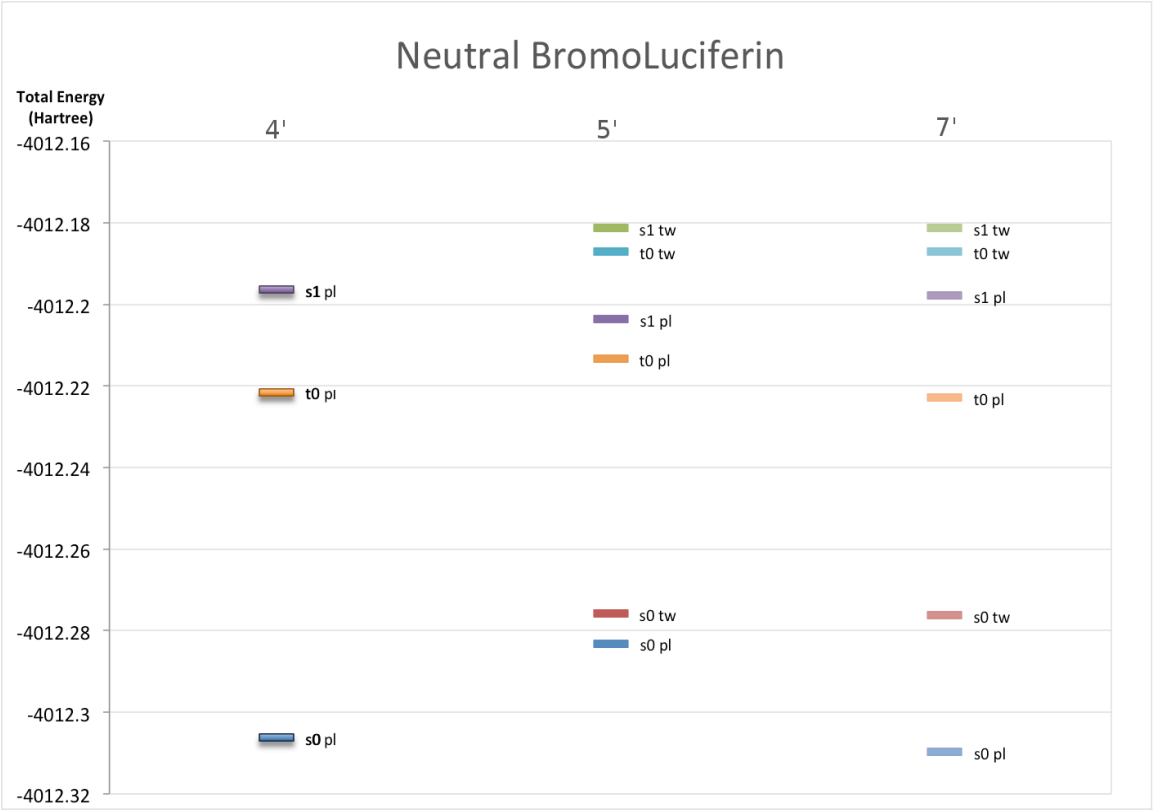
Neutral BromoLuciferin
Total Energy (Hartree)
4'
5'
7'
-4012.16
-4012.18
-4012.2
-4012.22
-4012.24
-4012.26
-4012.28
-4012.3
-4012.32
s1 pl
t0 pl
s0 pl
s1 tw
t0 tw
s1 pl
t0 pl
s0 tw
s0 pl
s1 tw
t0 tw
s1 pl
t0 pl
s0 tw
s0 pl

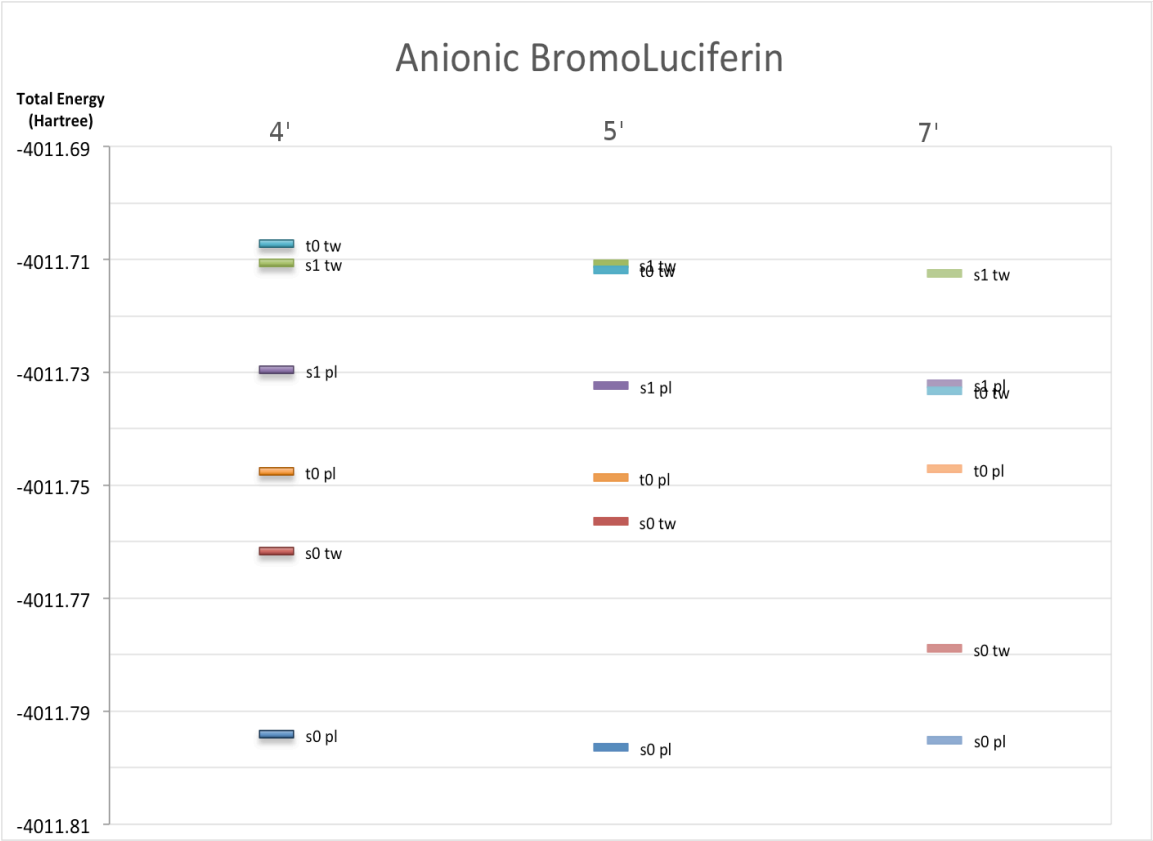
Anionic BromoLuciferin
Total Energy (Hartree)
-4011.69
-4011.71
-4011.73
-4011.75
-4011.77
-4011.79
-4011.81
4'
5'
7'
t0 tw
s1 tw
s1 pl
t0 pl
s0 tw
s0 pl

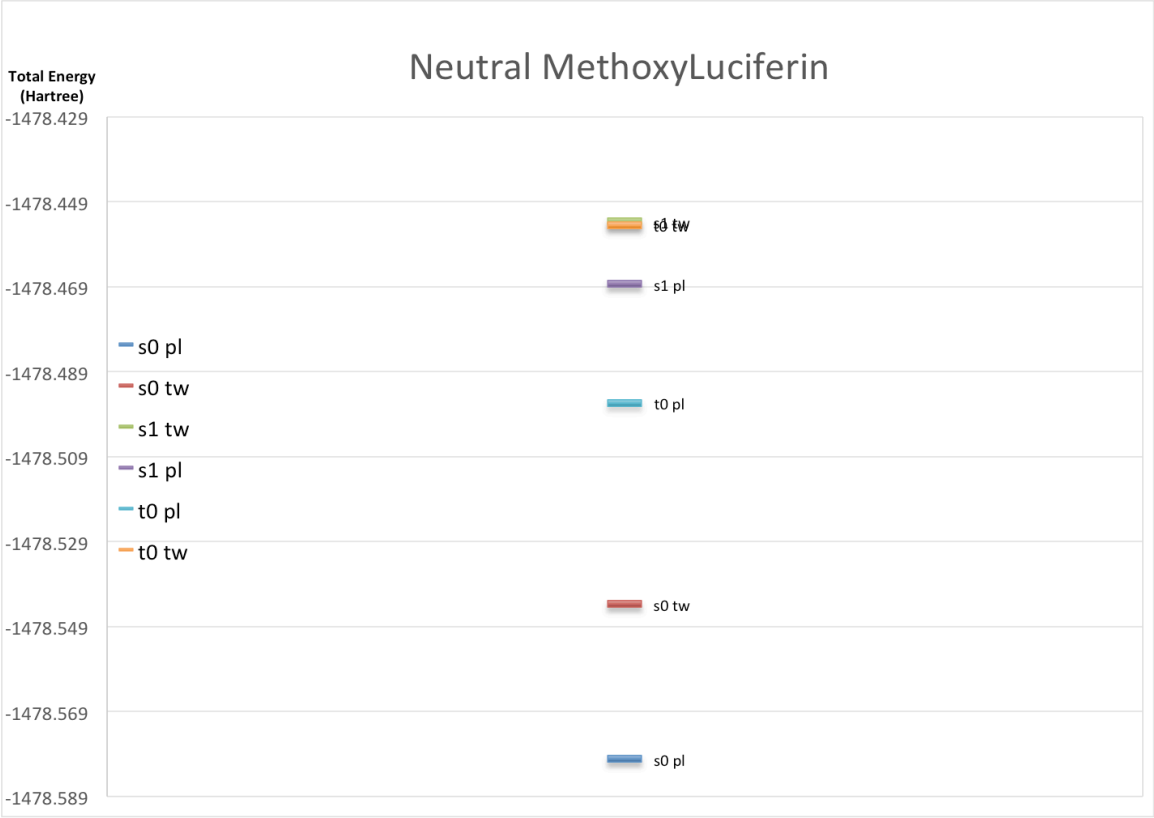
Neutral MethoxyLuciferin
Total Energy (Hartree)
-1478.429
-1478.449
-1478.469
-1478.489
-1478.509
-1478.529
-1478.549
-1478.569
-1478.589
s0 pl
s0 tw
s1 tw
s1 pl
t0 pl
t0 tw

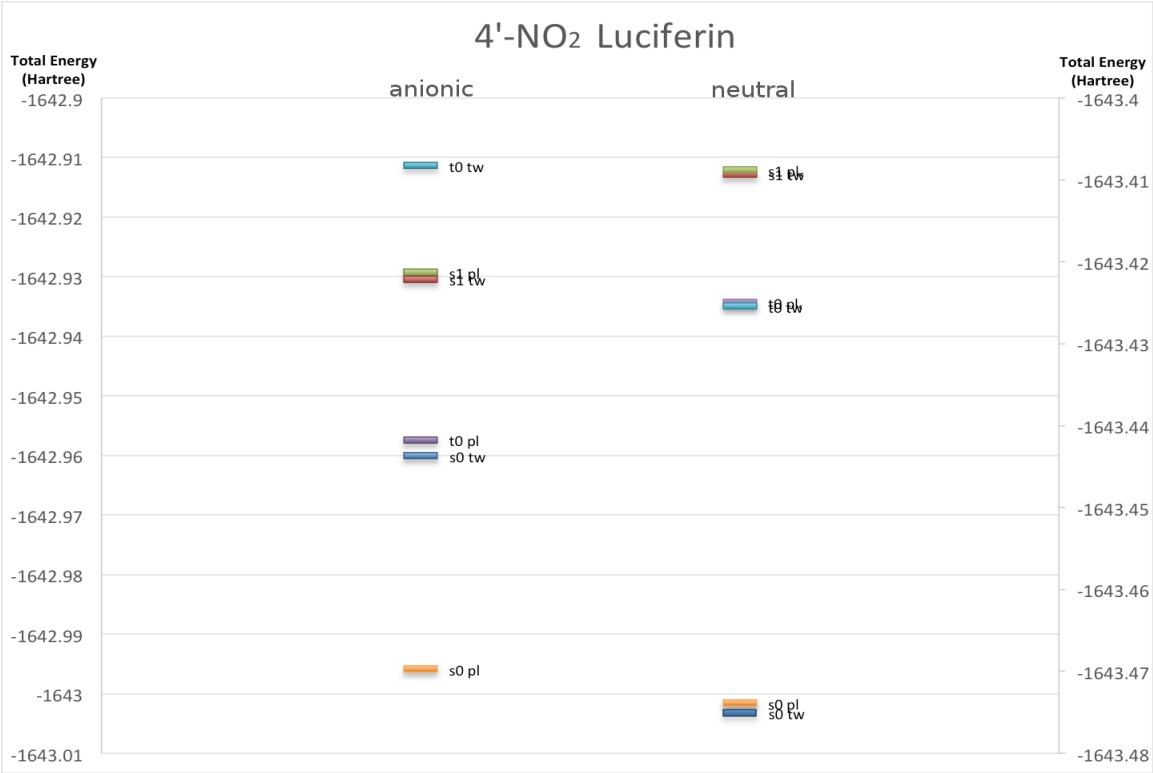
4'-NO2 Luciferin
Total Energy (Hartree)
Total Energy (Hartree)
anionic
neutral
-1642.9
-1642.91
-1642.92
-1642.93
-1642.94
-1642.95
-1642.96
-1642.97
-1642.98
-1642.99
-1643
-1643.01
-1643.4
-1643.41
-1643.42
-1643.43
-1643.44
-1643.45
-1643.46
-1643.47
-1643.48
t0 tw
s1 pl
s1 tw
t0 pl
s0 tw
s0 pl
s1 pl
s1 tw
t0 pl
t0 tw
s0 pl
s0 tw

It is well known that in the case of (1) intersystem crossing leads to non-radiative relaxation and (2) that TICT states display near-zero oscillator strength ("dark") due to the broken conjugation of the pi-system [25]. Luciferins with groups that can twist out of plane may have a lower-lying energetically twisted excited state responsible for the observed 'dark' behavior. In chemiluminescence experiments, one would expect the emission profile to derive from a Boltzmann-like distribution of torsional angles, only some of which are light-emitting, while the computational results represent a single excitation from a discrete nuclear configuration (either planar or twisted). TICT states may be underappreciated in luciferin emission and have important ramifications for orthogonal probe development (Figure 3-4).

From a chemiluminscence perspective, both the experimental and computational data suggest that an increase in emission intensity can be achieved by chemical modification at many positions on the luciferin core, as long as the electronic requisites are met by the appendage. However, if this extra steric bulk yields poor *bioluminscence*, the reduction in light emission must be attributed to poor enzyme utilization rather than an inherent inability to reach the necessary excited state. When the three bromo analogs were analyzed with recombinant Fluc, a significant reduction in bioluminescent light emission was observed for both **7′–BrLuc** and **4′–BrLuc**. **5′–BrLuc** retained robust light emission. This suggests that the **5′–BrLuc** analog is more efficiently processed by Fluc than the **4′** or **7′** isomers (since chemiluminescent data suggest that the compounds are roughly capable of producing the same numbers of photons). Other luciferin analogs with rather bulky groups at the 5′ position are also known to be processed efficiently by Fluc [37]. Indeed, recent crystal structure analyses of Fluc suggest that its active site has sufficient room to accommodate steric appendages at the 5′ and 6′ positions, but tends to be too crowded to fit large modifications at the **4′** and **7′** positions [38-40]. Our results establish a

crucial precedence that luciferin scaffolds may be poor substrates for the native enzyme, but still capable of emission from a chemically-accessed excited state.

3.2d Experimental characterization of bromoluciferins

Crystal structure analyses also suggest that backbone/steric clashes prevent the utilization of **4′–BrLuc** and **7′–BrLuc**. To elucidate which aspect of the enzymatic process (binding vs. catalytic turnover) might be precluding use of the analogs, we measured the K_m and relative k_{cat} parameters for each of the transformations (Table 3-3). Interestingly, the K_m for **4′–BrLuc** was on par with D–luciferin, but the relative k_{cat} for this analog was 50-fold reduced compared to the native substrate. This finding is corroborated by crystal structure data, indicating room for a halogen atom to dock – the modification likely interferes with subsequent motion of the enzyme required for catalysis. The relative k_{cat} for **7′–BrLuc** was similarly low compared to **D–Luc**. The K_m for **7′–BrLuc** was also higher than **D–Luc**, suggesting that the **7′** substituted analog does not bind the active site as efficiently. Gratifyingly, the enzymatic parameters measured for **5′–BrLuc** were on par with those for **D–Luc**.

The bioluminescence spectra for all bromo luciferins were red-shifted from that of **D–Luc**, while the fluorescence spectra were virtually identical (Figure 3-5). These data further suggest that the luciferin analogs can access alternate excited state geometries and relaxation pathways.

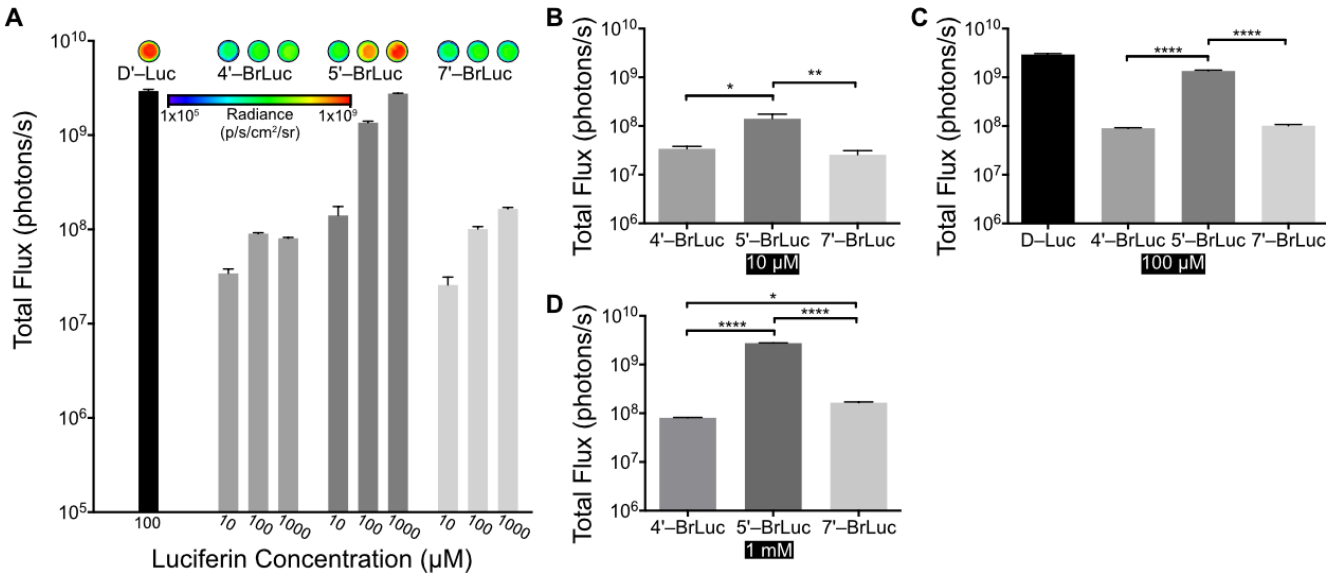

Figure 3-5. A) Differential bioluminescent photon production is observed with the series of bromoluciferins and recombinant luciferase (conc. nM) Sample images are included. Error bars represent the standard deviation of three replicates. B-D) Statistical analysis of the data given in A). B) 10 μM concentration. C) 100 μM concentration. D) 1 mM concentration. *$p < 0.1$ (ANOVA), **$p < 0.01$ (ANOVA), ****$p < 0.0001$ (ANOVA)

Table 3-3. Enzymatic parameters for Fluc-catalyzed oxidation of bromo analogs.

Compound	K_m (μM)	Rel k_{cat}[a]
D–Luc	3.07 ± 0.80	100 ± 0.3
4'–BrLuc	2.47 ± 0.92	1.8 ± 0.4
5'–BrLuc	6.72 ± 0.31	104 ± 2.2
7'–BrLuc	17.3 ± 8.8	1.9 ± 0.4

[a]Expressed as the ratio of the corresponding compound with **D–Luc**.

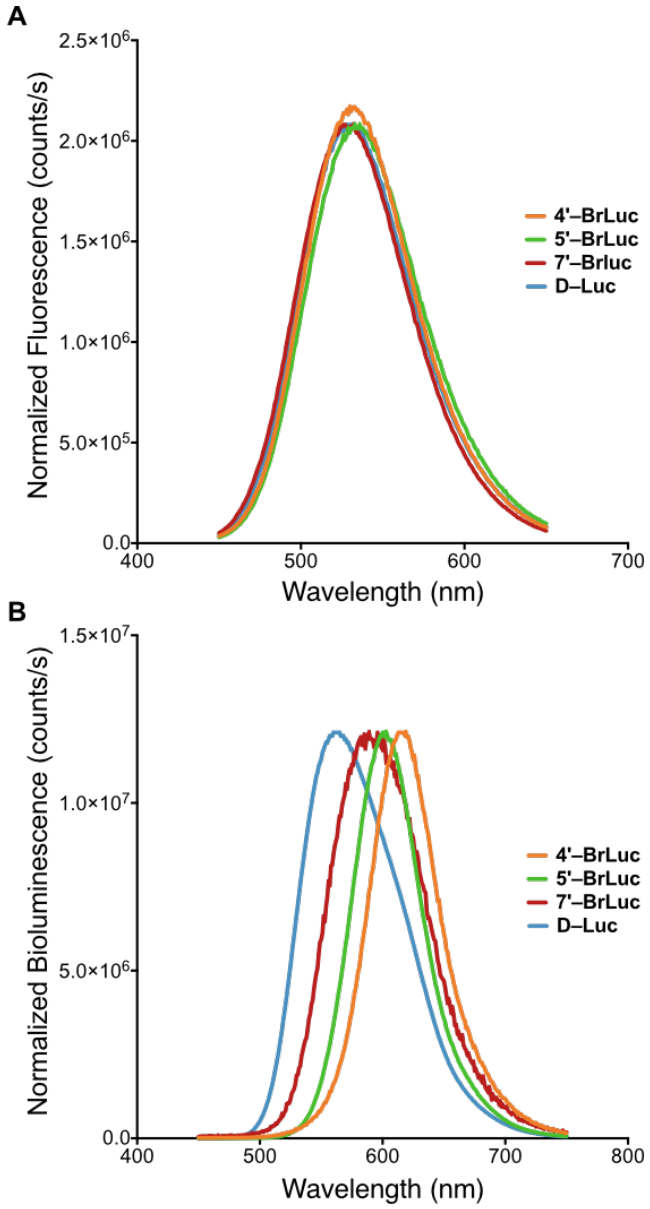

Figure 3-6. Optical analyses of luciferin analogs. A) Fluorescence spectra of D-luciferin and bromo analogs using 365-nm excitation light (pH 7.6). B) Bioluminescence spectra of **D–Luc** and the bromo analogs at pH 7.6.

Collectively, DFT calculations and in vitro assays suggested that the **5′**-brominated analog would be suitable for BLI, while the **4′** and **7′** isomers were good starting points for orthogonal probe development. These compounds were further analyzed in cells. When the brominated compounds were incubated with Fluc-expressing HEK293 cells, robust light emission was observed from cultures treated with **5′–BrLuc**. Minimal light was produced with **4′–BrLuc** and **7′–BrLuc**, consistent with the in vitro data. Interestingly, the light emission observed with **5′–BrLuc** was similar to **D–Luc**. These data suggest that **5′–BrLuc** may have superior cell permeability compared to the native probe. Though it performed worse than **D–Luc** in vitro, it performs better in cellulo at lower concentrations, implying superior cell permeability.

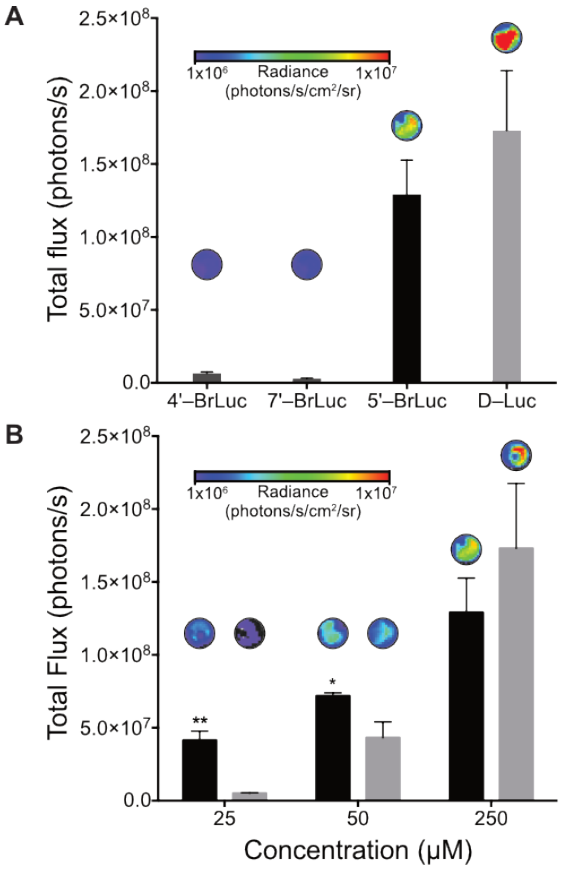

Figure 3-7. **Differential bioluminescent photon production is similarly observed with Fluc-expressing cells treated with series of bromoluciferins.** Compounds were administered to HEK293 sells stably expressing Fluc with a concentration of 100,000 cells per well. Imaging was performed at 37 °C. Compounds were diluted to the indicated concentration in PBS pH 7.4. For further details see supporting information. Sample images are included. (A) Peak emission for all analogs at 100 μM concentration. (B) Dose response comparison between **5′–BrLuc** (black) and **D–Luc** (grey). Error bars represent the standard deviation of three runs. $*p < 0.1$, $**p < 0.01$ (*t*-test).

3.3 Conclusions

Limitations in multi-spectral and multi-component emission have spurred the development of luciferins with altered emission wavelengths, conjugation, caged probe development, and orthogonal pairs. The efficient development of such probes has been confounded by a lack of accurate models to predict robust light-emitting luciferins. Here, we report a direct link between density functional calculations and experimental results that allows for the *a priori* assessment of the light-emitting efficacy of new luciferin analogs with moderate reliability. Our simulations predict that a variety of sterically and electronically modified luciferins should be good bioluminescent emitters. Enzymatic assays confirmed that the molecules retained their ability to bind the enzyme, but were poorly turned over by luciferase itself. It has also not escaped our attention that these groups can be further sterically modified using traditional cross-coupling reactions. These experiments are ongoing in our laboratory and will be reported in due course. Collectively, these studies provide a rational basis for new luciferin design.

3.4 Materials and methods

3.4a Expression and purification of Fluc

Firefly luciferase was expressed and purified as previously described [1].

3.4b Bioluminescence kinetic measurements

Measurements were acquired on a Tecan F200 Pro injection port luminometer with a neutral density filter. Reactions were performed in black 96-well flat-bottom plates (Grenier). Bioluminescence buffer [41] (93.5 μL of 20 mM Tris-HCl pH 7.6, 2 mM $MgSO_4$, 2 mM ATP,

0.1 mM EDTA, 1 mM TCEP, 0.5 mg/mL BSA) was added to each well, followed by conenzyme A (0.5 μL of a 100 mM solution) and luciferin substrate (1 μL of a 0.01-100 mM solution in DMSO). The luminescence from each well was measured for 30 s prior to the addition of Fluc (5 μL of a 1 μg/μL solution in bioluminescence buffer). Following the addition of Fluc, luminescence was recorded every 0.1 s over a 1-min period. Samples were analyzed in triplicate and multiple runs were performed. The emission maxima were determined by averaging the largest photon outputs from five independent runs. K_m and relative k_{cat} values were determined using nonlinear regression analyses and robust fit outlier removal in GraphPad Prism (version 6.0f for Macintosh, GraphPad Software).

3.4c Bioluminescence imaging (in vitro)

Imaging was performed using an IVIS Lumina (Xenogen) system equipped with a cooled CCD camera. Reactions were performed in black 96-well flat-bottom plates (Grenier). Bioluminescence buffer (93.5 μL) was added to each well, along with coenzyme A (0.5 μL of a 100 mM solution) and luciferin substrate (1 μL of a 0.5-100 mM solution in DMSO). To initiate photon production, Fluc (5 μL of a 1 μg/mL solution in bioluminescence buffer) was added to each well. The plate was then briefly agitated and placed in the IVIS instrument. The bioluminescent output was recorded every 5-30 s over a 45-75 min time period. Measurements were performed in triplicate.

3.4d Bioluminescence imaging (in cellulo)

HEK-293 cells stably expressing Fluc (provided by the Contag Lab, Stanford) were grown in DMEM media supplemented with fetal bovine serum (FBS, 10%) penicillin (10

units/mL), and streptomycin (10 mg/mL). The cells were cultured in a CO_2 (5%) incubator at 37 ºC. Imaging was performed using an IVIS Lumina (Xenogen) system equipped with a heated stage (37 ºC) and a cooled CCD camera. Reactions were performed in black 96-well flat-bottom plates (Grenier) with 100,000 cells per well. Luciferin (50 μL of 2X stock in PBS, pH 7.4) was added to each well and bioluminescence images were acquired as above.

3.4e Bioluminescence emission spectra

Emission spectra for D-luciferin and all analogs were recorded on a FluoroMax-4 spectrometer (Horiba Jobin-Yvon). Luciferin (10 μL of a 100 μM solution in bioluminescence buffer) and Fluc (10 μL of a 1 mg/mL solution in bioluminescence buffer) along with coenzyme A (5 μL of a 100 mM solution) were placed in a 10 mm path length quartz cuvette (1 mL total volume). Emission data were collected from 450-750 nm (1 nm intervals) at room temperature. The acquisition times were 0.1 s/wavelength. The spectra were then normalized to D-luciferin and plotted.

3.4f General chemiluminescence procedure

Phenyl esters of each luciferin analog were prepared following the basic procedure of Kim *et al* [42]. In brief, the potassium salt of each luciferin (6.0 μmol) was added to an oven-dried, two-dram vial containing a small stir bar. Deuterated dimethylsulfoxide (0.55 mL) containing a mesitylene internal standard (0.275 μL) was then added and the luciferin was dissolved with stirring (5 min). Phenylchloroformate (0.76 μL, 6.0 μmol) was subsequently added and a brief color change was observed in most cases. The solutions were stirred for an additional 5 min. A portion of each solution (5 μL) was reserved, and the remainder was added to

an NMR tube for analysis. The NMR sample was kept at ambient temperature until luminometer measurements were made (see below). At that point, the NMR sample was frozen (-73 °C) to preserve the contents of the tube. At a later time, each tube was thawed and a ^{1}HNMR spectrum was immediately acquired (2 scans, 20 s relaxation delay). The concentration of each luciferin phenyl ester was determined via comparison to the internal standard (mesitylene, see Figure 3-7).

The reserved portion of each luciferin ester solution was diluted to 0.5 mL with anhydrous dimethylsulfoxide, and 50 μL of this solution was added to six wells of a black 96-well flat-bottom plate (Greiner). Chemiluminescence values were acquired on a Tecan Infinite F200 PRO plate-reading luminometer. Data were acquired for 1.5 s prior to injection of potassium phenoxide solution (50 μL of a of 0.1 M solution). The phenoxide solution was prepared via dissolution of potassium *tert*-butoxide (112 mg) and phenol (94 mg) in anhydrous dimethylsulfoxide (10 mL) with stirring (30 min). The total volume in each well was 100 μL. After the addition of base, luminescence data were collected for an additional 50 s (100 ms integration times were used). Relative luminescence yields were determined via trapezoidal integration of the data (Figure 3-8).

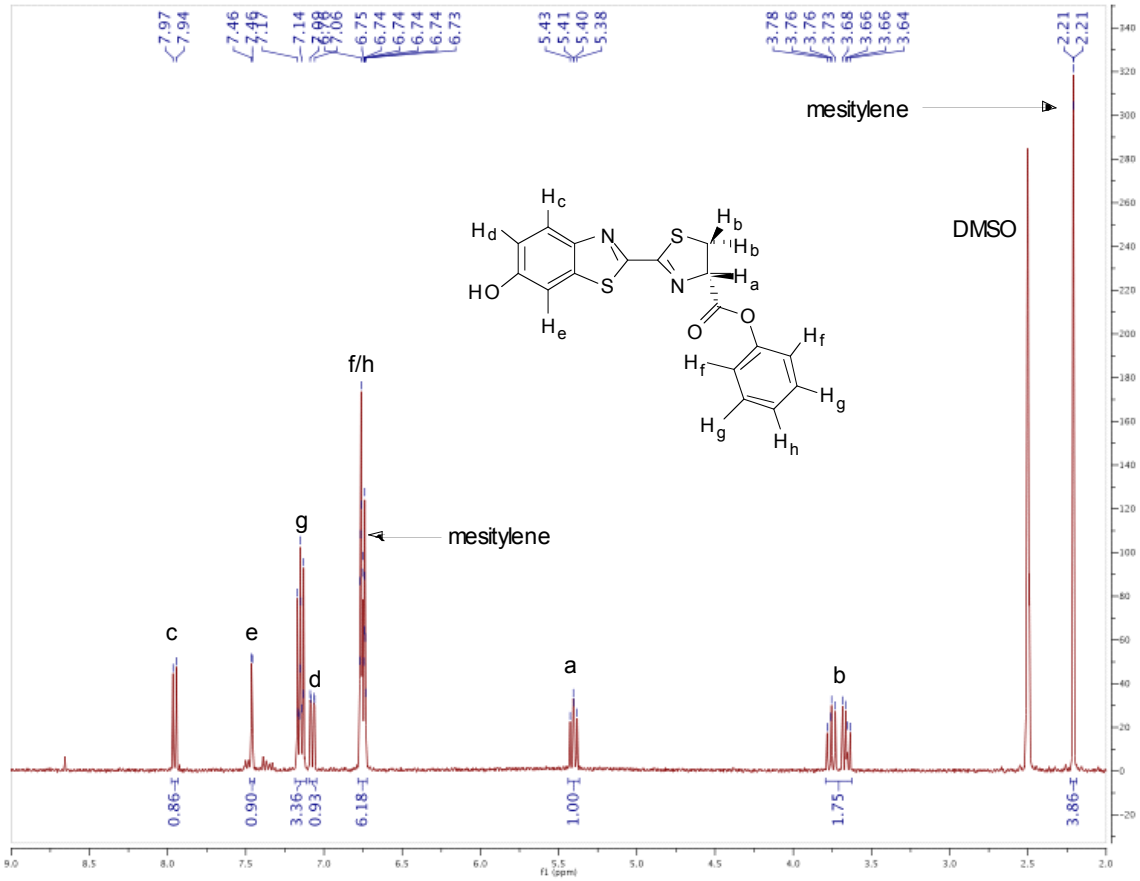

Figure 3-8. Representative ^{1}H NMR spectrum of a luciferin phenyl ester prepared as described.

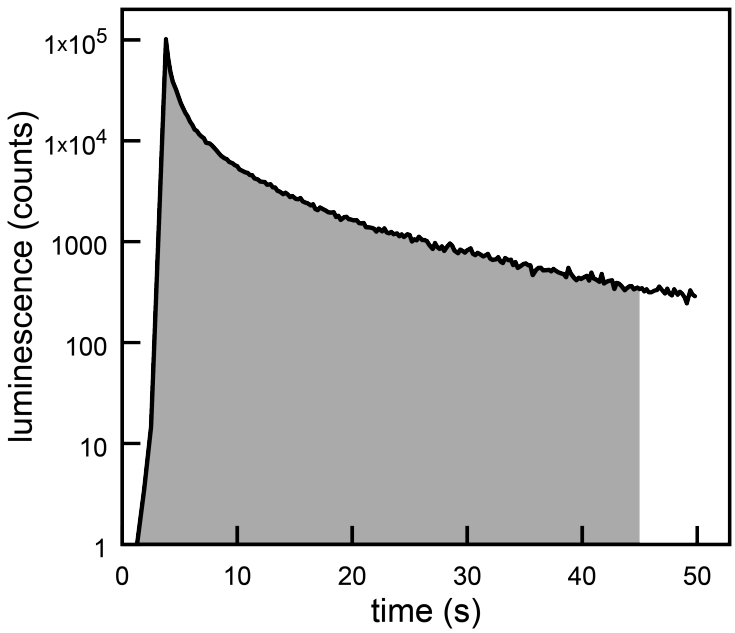

Figure 3-9. Representative luminescence data following the addition of base to the phenyl ester of D-luciferin. The shaded area denotes the region used for trapezoidal integration.

3.4g General experimental procedures

All reactions were performed in flame- or oven-dried glassware under positive pressure of nitrogen or argon unless otherwise noted. Dichloromethane, dimethylacetamide, *N*,*N*-dimethylformamide, triethylamine, and toluene were dried by columns packed with activated alumina on a solvent purification system. Anhydrous pyridine and DMSO were purchased from Acros Organics in AcroSeal™ bottles. All reagents were used as purchased without further purification. 4,5-Dichloro-1,2,3-dithiazol-1-ium chloride (Appel's salt) was synthesized according to a published procedure[43] and stored in a desiccator. Thin layer chromatography (TLC) was performed on Merck 60 F_{254} pre-coated silica gel plates, and TLC plates were visualized with UV light and ninhydrin stain when appropriate. Flash-column chromatography was performed using silica gel (60 Å, 230-240 mesh, Merck KGA). NMR spectra were recorded with Bruker Advanced spectrometers using deuterated solvents. ^{1}H NMR spectra were recorded at 400 or 500 MHz as indicated. ^{13}C NMR spectra were recorded at 125 MHz. ^{1}H NMR data are reported in the following order: chemical shift (δ ppm), multiplicity, coupling constant (Hz), and integration. ^{13}C NMR data are reported in terms of chemical shift. Infrared spectra were recorded using a Thermo Scientific iD5 ATR infrared spectrophotometer. High-resolution mass spectra were obtained from the UC Irvine Mass Spectrometry Facility. The abbreviations used can be found in the document JOC Standard Abbreviations and Acronyms.

3.4h Synthetic Procedures

Scheme 3-1: Synthesis of brominated luciferins.

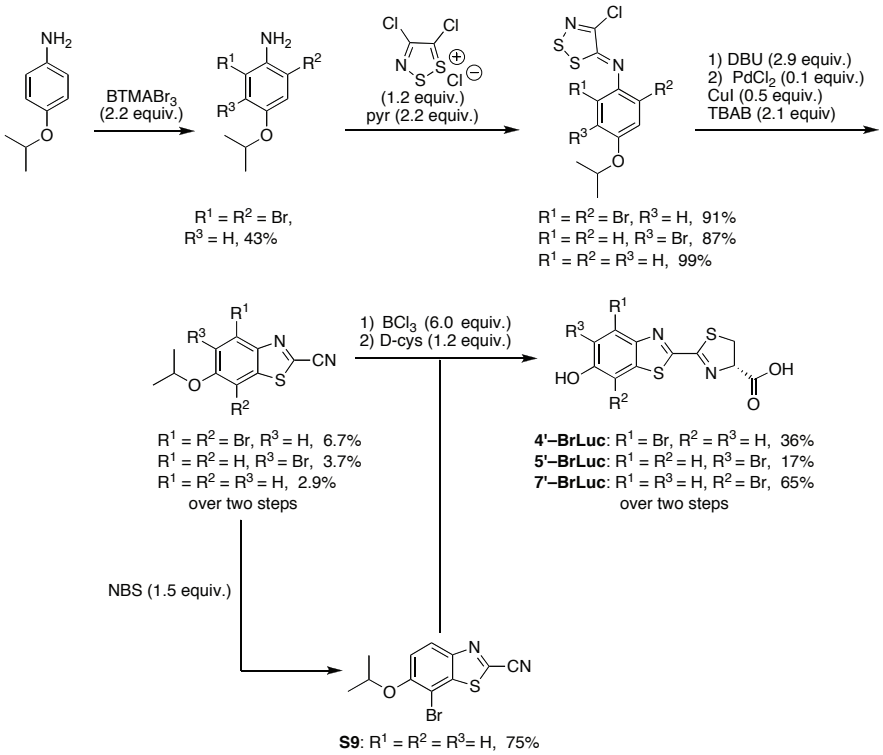

3-Bromo-4-isopropoxyaniline

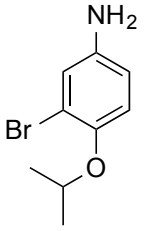

$C_9H_{12}BrNO$
230.10

Following the general method of Shen and Driver [44], to a flask of 2-bromo-1-isopropoxy-4-nitrobenzene [45] was added iron filings (0.15 g, 0.56 mmol) followed by acetone (3 mL) and water (10 mL). Glacial acetic acid (1 mL) was then added, and the mixture was heated at reflux for 3 h. The mixture was then diluted with ethyl acetate (20 mL) and washed with saturated sodium carbonate (2 x 20 mL), ammonium chloride (2 x 20 mL), and brine. The organic layer was then dried with $MgSO_4$, filtered, and concentrated *in vacuo*. The residue was purified *via* flash-column chromatography (eluting with 8:2 hexanes:ethyl acetate) to yield 3-bromo-4-isopropoxyaniline (72 mg, 57%) as a brown oil. The spectra matched those reported [46].

2,6-Dibromo-4-isopropoxyaniline

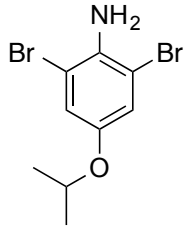

$C_9H_{11}Br_2NO$
Mol. Wt.: 309.00

Following the procedure of Popney and Guan, to a solution of 4-isopropoxy aniline (1.20 g, 7.90 mmol) in CH_2Cl_2 (66 mL) and methanol (22 mL) was added calcium carbonate (3.03 g, 30.0 mmol), followed by benzyltrimethylammonium tribromide (6.53 g, 16.0 mmol). The reaction proceeded at room temperature for 2 h. The reaction was quenched with a 1 M solution of $Na_2S_2O_3$ (2 x 100 mL), water (2 x 100 mL) and brine (1 x 100 mL), dried with $MgSO_4$, and concentrated *in vacuo*. The concentrated mixture was then purified by flash-column chromatography (eluting with 8:2 hexanes:ethyl acetate) to afford the title compound (1.02 g, 3.30 mmol, 43%) as an orange oil. ^{1}H NMR (400 MHz, $CDCl_3$) δ 7.03 (s, 2H), 4.34 (septet, J = 6.1 Hz, 1H), 1.29 (d, J = 6.1 Hz, 6H); ^{13}C NMR (500 MHz, $CDCl_3$) δ 150.2, 136.4, 120.9, 109.0, 72.0, 22.0; HRMS (CI) *m/z* calcd for $C_9H_{12}Br_2NO$ $[M+H]^+$ 309.9265, found 309.9274.

3.4i Representative procedure for the synthesis of Appel's salt adducts.

(Z)-2,6-Dibromo-N-(4-chloro-5H-1,2,3-dithiazol-5-ylidene)-4-isopropoxyaniline

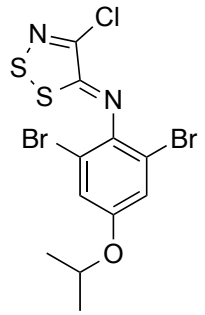

$C_{11}H_9Br_2ClN_2OS_2$
Mol. Wt. 444.59

Following the general method of Michaelidou and Koutentis [47], to a flask of the dibromoaniline (0.94 g, 3.3 mmol) under argon was added Appel's salt (4,5 dichloro-1,2,3-dithiazol-1-ium chloride) (0.83 g, 4.0 mmol) followed by anhydrous CH_2Cl_2 (15 mL) and anhydrous pyridine (0.59 mL, 7.30 mmol). The reaction mixture was stirred at room temperature for 2 h, then loaded onto silica gel and purified *via* flash-column chromatography (eluting with 8:2 hexanes:ethyl acetate) to yield the title compound (1.28 g, 91%) as a brown oil. ^{1}H NMR (400 MHz, DMSO-d_6) δ 7.33 (s, 2H), 4.66 (septet, J = 6.0 Hz, 1H), 1.23 (d, J = 6.0 Hz, 6H); ^{13}C NMR (500 MHz, $CDCl_3$) δ 164.8, 155.8, 146.7, 142.8, 120.3, 113.6, 71.3, 22.0; HRMS (ESI-TOF)$^+$ *m/z* calcd for $C_{11}H_{10}Br_2ClN_2OS_2$ $[M+H]^+$ 442.8290, found 442.8295.

(Z)-3-Bromo-N-(4-chloro-5H-1,2,3-dithiazol-5-ylidene)-4-isopropoxyaniline

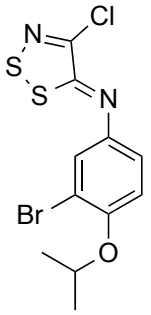

$C_{11}H_{10}BrClN_2OS_2$
Mol. Wt. 365.70

Isolated as a brown oil (0.92 g, 87%). ^{1}H NMR (400 MHz, DMSO-d_6) δ 7.52, (s, 1H), 7.28 (s, 2H), 4.72 (septet, J = 4.8 Hz, 1H), 1.34 (d, J = 4.8 Hz, 6H); ^{13}C NMR (500 MHz, $CDCl_3$) δ 159.2, 152.5, 147.5, 144.5, 125.2, 121.0, 116.6, 113.3, 72.1, 22,3; HRMS (CI) *m/z* calcd for $C_{11}H_{10}BrClN_2OS_2$ $[M+H]^+$ 364.9185, found 364.9189.

(Z)-N-(4-Chloro-5H-1,2,3-dithiazol-5-ylidene)-4-isopropoxyaniline

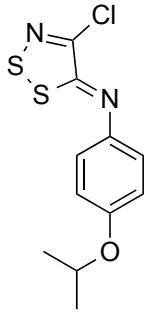

$C_{11}H_{11}ClN_2OS_2$
Mol. Wt. 286.80

Isolated as a brown oil (2.84 g, 99%). ^{1}H NMR (400 MHz, DMSO-d_6) δ 7.20 (d, J = 8.9 Hz, 2 H), 7.01 (d, J = 8.9 Hz, 2 H), 4.61 (septet, J = 6.0 Hz, 1 H), 1.25 (d, J = 6.0 Hz, 6 H); ^{13}C NMR (500 MHz, DMSO-d_6) δ 156.6, 156.4, 147.8, 142.9, 122.3, 116.9, 70.0, 22.3; HRMS (ESI-TOF)$^+$ m/z calcd for $C_{11}H_{11}ClN_2OS_2$ $[M+H]^+$ 287.0080, found 287.0084.

3.4j Representative procedure for the fragmentation and cyclization of Appel's salt adducts.

4-bromo-6-isopropoxybenzo[d]thiazole-2-carbonitrile

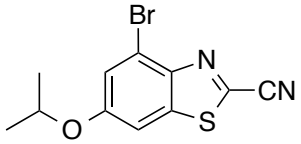

$C_{11}H_9BrN_2OS$
Mol. Wt. 297.17

Following the general procedure of Micaelidou and Koutentis [47], a flask containing the dibrominated Appel adduct (0.28 g, 0.6 mmol) was flushed with dry nitrogen and charged with CH_2Cl_2 (5 mL). The flask was cooled to 0 °C in an ice bath and DBU (0.29 mL, 1.9 mmol) was added. The reaction mixture was allowed to stir for 5 min, then adsorbed to silica gel. The crude mixture was purified by plug-style flash-column chromatography: the plug with the adsorbed reaction mixture was washed with hexanes and was then eluted with 7:3 hexanes:ethyl acetate to afford the thioamide which was immediately used in the next reaction. (Note: this compound degrades quickly and best yields are realized by moving the compound immediately on to the cyclization protocol that follows).

Following the general procdure of Inamoto and cowerkers [48], to a flask containing (2,6-dibromo-4-isopropoxyphenyl)carbamothioyl cyanide (0.24 g, 0.6 mmol) (based on crude

yield from fragmentation procedure), was added palladium(II) chloride (11 mg, 64 μmol), copper(I) iodide (60 mg, 0.3 mmol), and tetrabutyl ammonium bromide (0.43 g, 1.3 mmol). The flask was flushed with dry nitrogen, and then DMF (8 mL) and DMSO (8 mL) were added. The reaction was heated at 125 °C for 2 h. The mixture was then diluted with ethyl acetate (40 mL) and washed with 1 M $NaHSO_4$ (1 x 40 mL), water (3 x 40 mL), ammonium chloride (1 x 40 mL) and brine. The organic layer was then dried with $MgSO_4$, and concentrated *in vacuo*. The concentrate was then purified with flash-column chromatography (eluting with 9:1 hexanes:ethyl acetate) to yield the title compound (33 mg, 6.7% over two steps) as a brown solid. ^{1}H NMR (400 MHz, $CDCl_3$) δ 7.45, (d, J = 2.3 Hz, 1H), 7.29 (d, J = 2.3 Hz, 1H), 4.64 (septet, J = 6.0 Hz, 1H), 1.40 (d, J = 6.0 Hz, 6H); ^{13}C NMR (500 MHz, $CDCl_3$) δ 159.0, 145.2, 137.7, 133.6, 122.9, 119.2, 112.8, 104.3, 71.7, 21.9; HRMS (ESI-TOF)$^+$ *m/z* calcd for $C_{11}H_9BrN_2OS$ $[M+H]^+$ 350.9779, found 350.9783.

5-Bromo-6-isopropoxybenzo[d]thiazole-2-carbonitrile

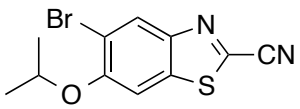

$C_{11}H_9BrN_2OS$
Mol. Wt. 297.17

Isolated as a brown solid (79 mg, 4% over two steps). ^{1}H NMR (400 MHz, $CDCl_3$) δ 8.40 (s, 1H), 7.36 (s, 1H), 4.69 (septet, J = 6.0 Hz, 1 H), 1.47, (d, J = 6.0 Hz, 6H); ^{13}C NMR (500 MHz, $CDCl_3$) δ 155.2, 146.9, 136.1, 134.4, 129.3, 115.9, 113.0, 104.4, 73.0, 21.8; HRMS (CI) *m/z* calcd for $C_{11}H_9BrN_2OS$ $[M+H]^+$ 296.9697, found 296.9694.

6-Isopropoxybenzo[d]thiazole-2-carbonitrile

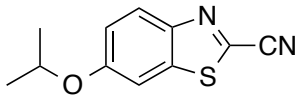

$C_{11}H_{10}N_2OS$
Mol. Wt. 218.27

Isolated as a brown solid (48 mg, 3% over two steps). ^{1}H NMR (400 MHz, $CDCl_3$) δ 8.07 (d, *J* = 9.1 Hz, 1H), 7.34 (d, *J* = 2.4 Hz, 1 H), 7.20 (dd, *J* = 9.1, 2.5 Hz, 1H), 4.66 (septet, *J* = 5.3 Hz, 1H), 1.41 (d, *J* = 5.3 Hz, 1H); ^{13}C NMR (500 MHz, $CDCl_3$) δ 158.9, 146.7, 137.5, 126.0, 119.6, 113.3, 104.9, 71.1, 21.9; HRMS (CI) *m/z* calcd for $C_{11}H_{10}N_2OS$ $[M+H]^+$ 236.0858, found 236.0864.

7-Bromo-6-isopropoxybenzo[d]thiazole-2-carbonitrile

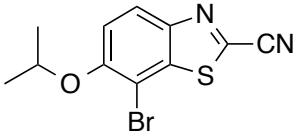

$C_{11}H_9BrN_2OS$
Mol. Wt. 297.17

To a flask of 6-isopropoxybenzo[d]thiazole-2-carbonitrile (0.13 g, 0.6 mmol) was added *N*-bromosuccinimide (0.16 g, 0.9 mmol) followed by CH_3CN (15 mL). The reaction mixture was stirred for 12 h. The mixture was then extracted with ethyl acetate (30 mL), and washed with water (3 x 60 mL) and brine (1 x 60 mL), dried with $MgSO_4$, filtered, and concentrated *in vacuo* to yield the title compound (0.14 g, 75%). ^{1}H NMR (400 MHz, DMSO-d_6) δ 8.22 (d, *J* = 11.4 Hz, 1H), 7.60 (d, *J* = 11.5 Hz, 1H), 4.88 (septet, *J* = 6.0 Hz, 1H), 1.31 (d, *J* = 6.0 Hz, 6H); ^{13}C NMR (500 MHz, $CDCl_3$) δ 155.3, 145.7, 134.2, 124.7, 116.4, 113.0, 103.3, 73.7, 22.2; HRMS (CI) *m/z* calcd for $C_{11}H_9BrN_2OS$ $[M+H]^+$ 296.9697, found 296.9696.

3.4k Representative procedure for the deprotection of the 6-isopropoxybenzothiazole-2-carbonitriles and condensation of the 6'-hydroxybenzothiazole-2-carbonitrle compounds with D-cysteine (7′–BrLuc, 4′–BrLuc, 5′–BrLuc).

(S)-2-(7-Bromo-6-hydroxybenzo[d]thiazol-2-yl)-4,5-dihydrothiazole-4-carboxylic acid (7′–BrLuc)

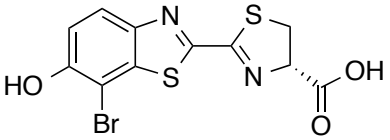

7'–BrLuc
$C_{11}H_7BrN_2O_3S_2$
Mol. Wt. 359.22

To a flask of 7-bromo-6-isopropoxybenzo[d]thiazole-2-carbonitrile (52 mg, 18 μmol) was added anhydrous CH_2Cl_2 (5 mL) and a 1.0 M solution of BCl_3 in hexanes (1.00 mmol, 1.06 mL) was added slowly. The mixture was stirred at room temperature under nitrogen for 24 h. The reaction was then quenched with a saturated solution of ammonium chloride (10 mL), extracted into ethyl acetate (30 mL), washed with saturated ammonium chloride (2 x 30 mL) and brine (1 x 30 mL). The organic layer was dried with $MgSO_4$, filtered, and concentrated *in vacuo*. The concentrate was then purified with flash-column chromatography (eluting with 1:1 hexanes:ethyl acetate) to yield the title compound which was used immediately in the following step.

To a flask of 7-bromo-6-hydroxybenzo[d]thiazole-2-carbonitrile (33 mg, 13 μmol) (based on crude yield isolated according to the procedure above) in degassed methanol (2 mL) under nitrogen was added D-cysteine (24 mg, 14 μmol) in degassed 0.05 M phosphate buffer, pH 8.0. The mixture was allowed to stir at room temperature, under nitrogen, overnight. The mixture was then acidified with 1 M $NaHSO_4$ (10 mL). The mixture was then extracted with ethyl acetate (20 mL), washed with saturated ammonium chloride (2 x 20 mL) and brine (1 x 20 mL), dried with $MgSO_4$, and concentrated *in vacuo* to yield the title compound (41.0 mg, 65% over two steps) as

a yellow solid. Note: this compound was treated with 1.0 equiv. of anhydrous K_2CO_3 in water and lyophilized if the compound was to be further esterified in the chemiluminescence assay. ^{1}H NMR (500 MHz, D_2O) δ 7.56 (d, *J* = 8.9 Hz, 1H), 6.89 (d, *J* = 8.9 Hz, 1H), 5.17 (m, 1H), 3.76 (m, 1 H), 3.55 (m, 1H); ^{13}C NMR (500 MHz, D_2O) δ 180.6, 168.4, 164.4, 157.0, 144.6, 142.9, 125.7, 123.4, 103.7, 82.7, 39.1. Note: it is extremely difficult to obtain high resolution mass spectrometry for this compound due to its multiple fragmentation pathways [49].

(S)-2-(4-Bromo-6-hydroxybenzo[d]thiazol-2-yl)-4,5-dihydrothiazole-4-carboxylic acid

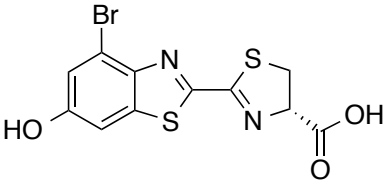

4'–BrLuc
$C_{11}H_7BrN_2O_3S_2$
Mol. Wt.: 359.22

(14 mg, 17% over two steps) as a yellow solid. ^{1}H NMR (500 MHz, D_2O) δ 7.01 (m, 2H), 5.21 (m, 1H), 3.84 (m, 1H), 3.64 (m, 1H); ^{13}C NMR (500 MHz, D_2O) δ 180.4, 168.3, 169.8, 159.3, 146.7, 139.9, 123.3, 119.2, 109.0, 82.8, 39.3. Note: it is extremely difficult to obtain high resolution mass spectrometry for this compound due to its multiple fragmentation pathways [49].

(S)-2-(5-Bromo-6-hydroxybenzo[d]thiazol-2-yl)-4,5-dihydrothiazole-4-carboxylic acid

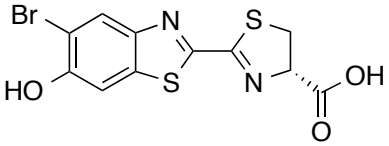

5'–BrLuc
$C_{11}H_7BrN_2O_3S_2$
Mol. Wt.: 359.22

(16 mg, 36% over two steps) as a yellow solid. ^{1}H NMR (500 MHz, D_2O) δ 7.81 (s, 1H), 7.12 (s, 1H), 5.20 (apparent t, *J* = 8.6 Hz, 1H), 3.81 (m, 1H), 3.60 (m, 1H); ^{13}C NMR (500 MHz, D_2O) δ 180.0, 168.2, 160.4, 158.8, 147.4, 139.0, 129.1, 116.2, 110.1, 82.8, 39.1. Note: it is extremely difficult to obtain high resolution mass spectrometry for this compound due to its multiple fragmentation pathways [49].

Scheme 3-2: Synthesis of (*S*)-2-(benzothiazol-2-yl)-4,5-dihydrothiazole-4-carboxylic acid (**6′–deoxyLuc**)

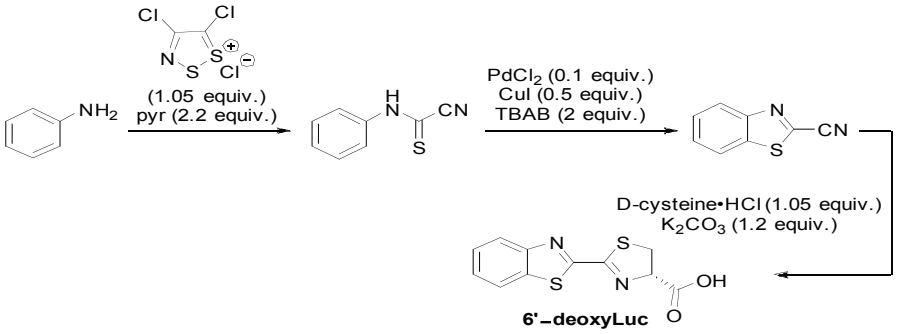

Phenylcarbamothioyl cyanide.

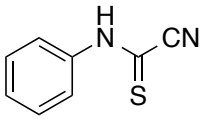

$C_8H_6N_2S$
Mol. Wt. 162.21

A dry, nitrogen-purged round bottom flask containing a stir bar and anhydrous tetrahydrofuran (30 mL) was charged with aniline (0.91 mL, 10 mmol), and 4,5-dichloro-1,2,3-dithiazol-1-ium chloride (Appel's salt, 2.19 g, 10.5 mmol). The resulting solution was stirred at room temperature for 40 min and pyridine (1.66

mL, 20.5 mmol) was subsequently added. When complete starting material consumption was observed by TLC analysis, a solution of sodium thiosulfate pentahydrate (3.2 g, 20 mmol) in 15 mL water and CH_3CN (15 mL) were added. The solution was stirred, and when complete consumption of the intermediate was observed by TLC, the reaction mixture was diluted with ethyl acetate, washed with saturated $NaHSO_4$, and dried with $MgSO_4$. The mixture was filtered, concentrated by rotary evaporation and purified by flash column chromatography (eluting with 10% ethyl acetate in hexanes) to yield the title compound (0.75 g, 46%) as a brown solid. ^{1}H NMR (500 MHz, $CDCl_3$, mixture of tautomers) δ 9.51 (s, 1H), 7.78 (d, J = 8.3 Hz, 1H), 7.57 – 7.28 (m, 4H), 1.75 (s, 1H). ^{13}C NMR (126 MHz, $CDCl_3$) δ 165.8, 162.0, 137.0, 136.9, 130.2, 129.5, 129.0, 128.5, 122.9, 122.6, 113.7, 112.1.

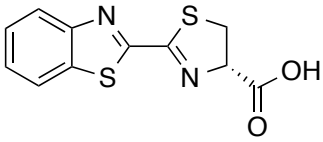

6'–deoxyLuc
$C_{11}H_8N_2O_2S_2$
Mol. Wt.: 264.32

(*S*)-2-(Benzothiazol-2-yl)-4,5-dihydrothiazole-4-carboxylic acid (6′–deoxyLuc)

Benzothiazole-2-carbonitrile (222 mg, 1.38 mmol) was dissolved in CH_3CN (6 mL) and a solution of K_2CO_3 (228 mg, 1.65 mmol), D-cysteine hydrochloride monohydrate (252 mg, 1.45 mmol), and water (3 mL) was added dropwise with stirring. After 45 min, the CH_3CN was removed via rotary evaporation and hydrochloric acid (1 M) was added until the solution was acidic. Upon addition of acid, a cream colored precipitate was observed. The solid was collected by filtration, washed with water, and dried under high vacuum to isolate **6′–deoxyLuc** (319 mg, 88%) as an off white solid. Note: this compound was treated with 1.0 equiv. of anhydrous K_2CO_3 in water and lyophilized if the compound was to be further esterified in the chemiluminescence assay. ^{1}H

NMR (500 MHz, DMSO-d_6) δ 8.16 (ddd, J = 28.6, 7.7, 0.5 Hz, 1H), 7.57 (dtd, J = 19.7, 7.4, 1.2 Hz, 1H), 4.94 (at, J = 9.0 Hz, 1H), 3.77 (dd, J = 10.4, 8.2 Hz, 1H), 3.51 (t, J = 10.0 Hz, 1H). ^{13}C NMR (126 MHz, DMSO-d_6) δ 169.88, 162.15, 159.35, 152.67, 135.05, 126.87, 126.85, 123.76, 122.71, 83.98, 36.27; HRMS (ESI$^+$) calcd for $C_{11}H_8N_2O_2S_2$ [M + Na]$^+$ 324.9484, found 324.9479.

Scheme 3-3: Synthesis of (*S*)-2-(6-hydroxy-4-methylbenzo[*d*]thiazol-2-yl)-4,5-dihydrothiazole-4-carboxylic acid (**4′–MeLuc**)

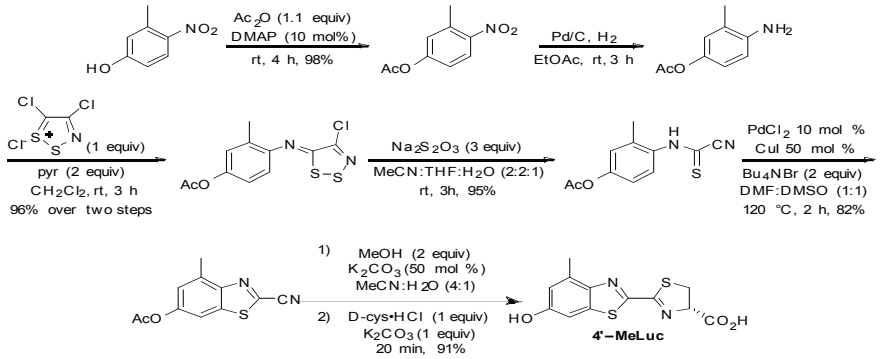

4-[(4-Chlorodithiazol-5-ylidene)amino]phenyl acetate

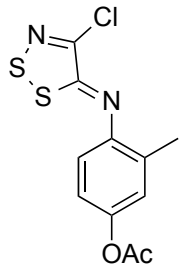

$C_{11}H_9ClN_2O_2S_2$
Mol. Wt. 300.77

3-Methyl-4-nitrophenyl acetate (9.76 g, 50.0 mmol) was dissolved in EtOAc (500 mL) and the vessel purged with N_2 before 10% Pd/C (974 mg) was added. The solution was then sparged with H_2 then stirred under an atmosphere of H_2. Upon consumption of starting material, the heterogeneous catalyst was removed by celite filtration and the solvent removed *in vacuo*. The residual colorless oil was taken up in dry CH_2Cl_2 and Appel's salt (10.8 g, 52.5 mmol) was added. The mixture was stirred initially for 1 h before dry pyridine was added

then stirred for an additional 2 h at r.t. Upon completion the solvent was removed *in vacuo* and the crude residue purified over a plug of silica using gradient elution (100% hexanes to 2:1 hexanes:EtOAc). The dithiazole (14.5 g) was isolated as a bright yellow solid in 96 % yield over two steps. ^{1}H NMR (400 MHz, $CDCl_3$) δ 7.12 (d, J = 8.5, 1H), 7.05 (d, J = 2.5, 1H), 7.01 (dd, J = 8.5, 2.5, 1H), 2.30 (s, 3H), 2.27 (s, 3H); ^{13}C NMR (125 MHz, $CDCl_3$) δ 169.6, 158.3, 148.7, 148.1, 147.6, 132.6, 124.3, 120.2, 116.8, 21.3, 18.0; HRMS (ESI$^+$) calcd for $C_{11}H_9O_2N_2S_2ClNa$ $[M + H]^+$ 322.9692, found 322.9682.

4-(1-Cyanomethanethioamide-N-(3-methylphenyl acetate)

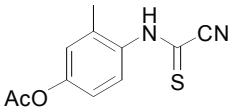

$C_{11}H_{10}N_2O_2S$
Mol. Wt. 234.27

The dithiazole (14.5 g, 48.2 mmol) was dissolved in (1:1 MeCN:THF, 386 mL) and stirred rapidly as a solution of $Na_2S_2O_3$ (23.0 g, 145 mmol) in H_2O (96.0 mL) was added. The mixture was vigorously stirred at rt for 3 h when TLC (hexanes:EtOAc, 3:1) showed consumption of starting material. The biphasic solution was quickly filtered to remove sulfur then the organics were evaporated *in vacuo*. The residual aqueous phase was acidified with 1M $NaHSO_4$ and the resultant precipitate vacuum filtered. The solids were washed with chilled H_2O (2 x 100 mL) and once dry provided the thioamide (10.7 g, 95%) as a bright yellow solid. The compound was characterized as a mixture of tautomers. ^{1}H NMR (400 MHz, $CDCl_3$) δ 7.49-7.37 (m, 1H), 7..06-6.96 (m, 2H), 7.02 (m, 2H), 2.35-2.20 (m, 6H); ^{13}C NMR (125 MHz, $CDCl_3$) δ 170.5, 169.7, 167.6, 164.7, 151.0, 150.3, 135.6, 134.9, 133.6, 132.2, 127.1, 127.0, 124.7, 124.5, 120.8, 120.1, 113.5, 112.0, 21.3, 18.2, 18.0; HRMS (ESI$^-$) calcd for $C_{11}H_9O_2N_2S$ $[M - H]^-$ 233.0385, found 233.0388.

(2-Cyano-4-methyl-1,3-benzothiazol-6-yl) acetate.

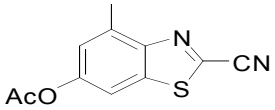

S15
$C_{11}H_8N_2O_2S$
Mol. Wt. 232.26

Compound was prepared according to our previously published method [50].

^{1}H NMR (400 MHz, acetone-d_6) δ 7.88 (dd, J = 2.2, 0.6, 1H), 7.32 (dd, J = 2.2, 0.9, 2H), 2.75 (s, 3H), 2.32 (s, 3H); ^{13}C NMR (125 MHz, acetone-d_6) δ 170.1, 152.5, 150.9, 137.6, 137.5, 137.2, 124.6, 114.4, 114.1, 21.5, 18.7; HRMS (ESI$^-$) calcd for $C_{11}H_9O_2N_2S$ [M – H]$^-$ 233.0385, found 233.0388.

4′–MeLuc

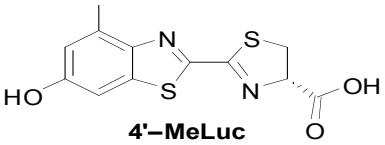

4'–MeLuc
$C_{14}H_{12}N_2O_4S_2$
Mol. Wt. 336.38

The nitrile (232 mg, 1.00 mmol) was taken up in MeCN (4 ml) and a solution of K_2CO_3 (209 mg, 1.51 mmol) in MeOH (80.8 µl, 2.00 mmol) and H_2O (1 ml) was added. The mixture was stirred at rt until TLC (hexanes:EtOAc, 2:1) showed consumption of starting material. D-Cysteine•HCl•H_2O was added to the reaction and the mixture stirred for an additional 15 min. The reaction was acidified with 1M $NaHSO_4$ and the precipitate collection by vacuum filtration. The precipitate was washed with chilled H_2O and once dried gave **4′–MeLuc** (268 mg, 91%) as an off-white solid. ^{1}H NMR (500 MHz, acetone-d_6) δ 12.1 (br s, 1H), 7.92 (d, J = 9.1, 1.5H), 7.48 (d, J = 8.9, 0.4H), 7.02 (m, 2H), 3.84 (s, 3H); ^{13}C NMR (125 MHz, acetone-d_6) δ 162.4, 160.0, 132.1, 125.4, 115.2, 114.9, 56.2.

3.4k Computational Details

Density functional theory (DFT) structural optimizations of the singlet ground state S0 and the first singlet excited state (S1) were performed using the hybrid-GGA functional, PBE0 [51] in the gas phase. Basis sets of double-zeta quality with polarization and diffuse functions [52] (def2-SVPD) were necessary to bind the additional electron of the anionic structures. Analytical force constant calculations [20] for the ground state and numerical force constant calculations were performed to verify minima by the absence of imaginary vibrational modes. Constrained excited state geometry optimizations were performed by fixing the out-of-plane bending angle of the carbon-carbon single bond connecting the two thiazoline rings to 0° and adjusting the torsional angle between the nitrogens in each ring. All calculations were performed with the quantum chemistry package TURBOMOLE [53,54].

3.4l Molecular orbitals involved in the emission of luciferin analogs.

For each luciferin analogue, we report the molecular orbitals involved in the emission "de-excitation" from the S_1 excited state geometry. All orbitals are plotted with a contour value of 0.05au. The primary contribution to the excitation is a HOMO to LUMO transition that tends to have pi-pi character originating on the anionic oxygen attached to the benzothiazoline with the transition dipole moment pointing towards the thiazoline motif. In the case of luciferin that are electron poor at the 6' position of the benzothiazoline, e.g. 6'-deoxyLuc, no such character is observed and corroborates the notion that an electron rich moiety is necessary for strong emission.

Compound	HOMO	LUMO
D-Luc	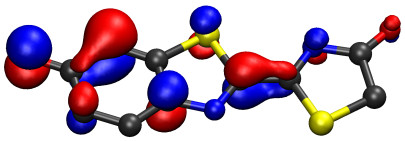	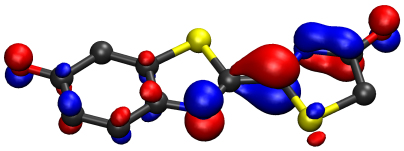
6'-aminoLuc	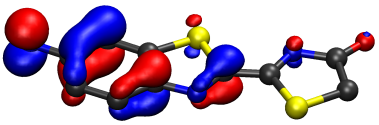	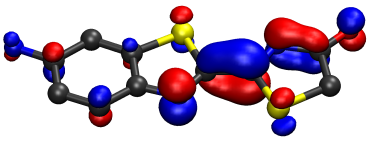
6'-MeNHLH2	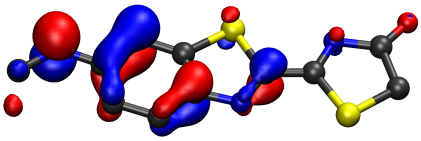	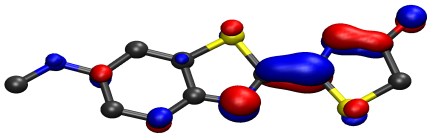
6'-Me2NLH2	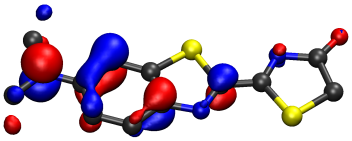	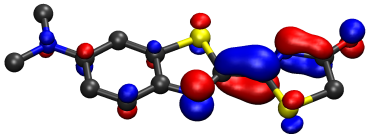
CyoLuc-1	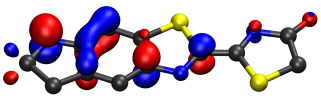	
CyoLuc-2	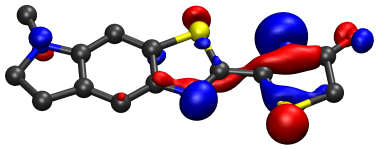	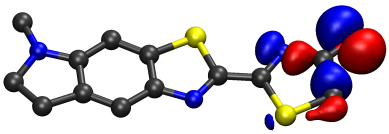

NmeBenzLuc	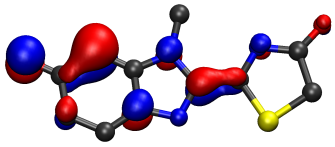	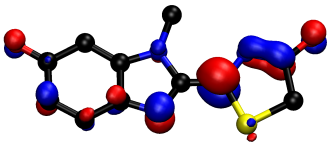
4-BrLuc	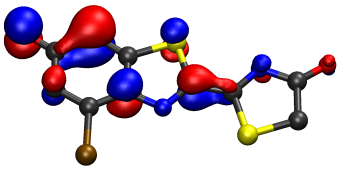	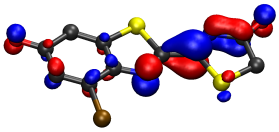
5-BrLuc	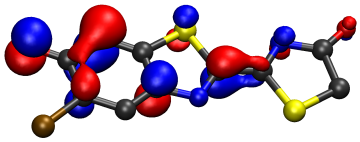	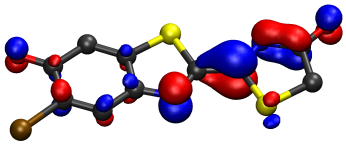
7-BrLuc	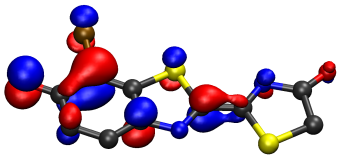	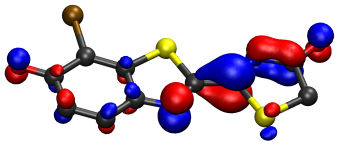
4-MeLuc	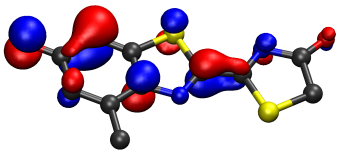	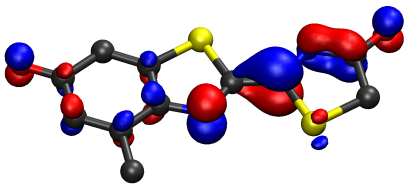
4-NO2Luc	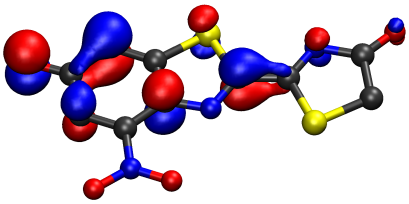	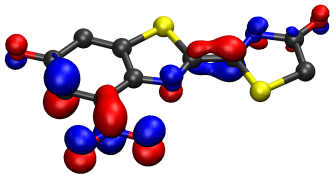

PhLuc	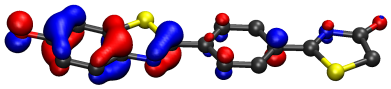	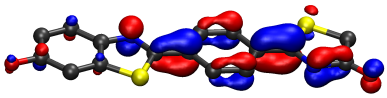
6' - deoxyLuc	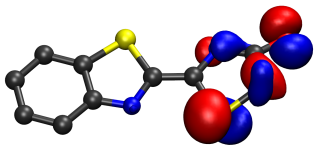	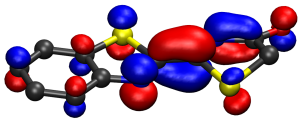
6' – methoxyLuc	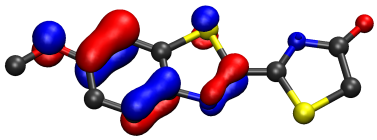	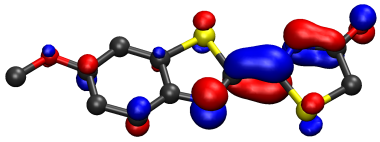

Note: for further computational details, please see Appendix D.

3.5 References

(1) McCutcheon, D. C.; Paley, M. A.; Steinhardt, R. C.; Prescher, J. A. Expedient synthesis of electronically modified luciferins for bioluminescence imaging. *J. Am. Chem. Soc*. **2012**, *134*, 7604.

(2) Conley, N. R.; Dragulescu-Andrasi, A.; Rao, J.; Moerner, W. E. A selenium analogue of firefly d-luciferin with red-shifted bioluminescence emission. *Angew. Chem. Int. Ed.* **2012**, *51*, 3350.

(3) Evans, M. S.; Chaurette, J. P.; Adams Jr, S. T.; Reddy, G. R.; Paley, M. A.; Aronin, N.; Prescher, J. A.; Miller, S. C. A synthetic luciferin improves bioluminescence imaging in live mice. *Nat Methods* **2014,** *11*, 393.

(4) Kojima, R.;, H.; Ozawa, T.; Tada, Y.; Nagano, T.; Urano, Y. Rational design and development of near-infrared-emitting firefly luciferins available in vivo. *Angew. Chem. Int. Ed.* **2013**, *52*, 1175.

(5) Mofford, D. M.; Reddy, G. R.; Miller, S. C. Aminoluciferins extend firefly luciferase bioluminescence into the near-infrared and can be preferred substrates over D-luciferin. *J. Am. Chem. Soc.* **2014**, *136*, 13277.

(6) Fraga, H. Firefly luminescence: a historical perspective and recent developments. *Photochem. Photobiol. Sci.* **2008**, *7*, 146.

(7) Paley, M. A.; Prescher, J. A. Bioluminescence: a versatile technique for imaging cellular and molecular features. *MedChemComm.* **2014**, *5*, 255.

(8) Adams Jr, S. T.; Miller, S. C. Beyond D-luciferin: expanding the scope of bioluminescence imaging in vivo. *Curr. Opin. Chem. Biol.* **2014**, *21*, 112.

(9) Rhodes, W. C.; Mc, E. W. The synthesis and function of luciferyl-adenylate and oxyluciferyl-adenylate. *J. Biol. Chem.* **1958**, *233*, 1528.

(10) Marques, S. M.; Esteves da Silva, J. C. Firefly bioluminescence: a mechanistic approach of luciferase catalyzed reactions. *IUBMB Life* **2009**, *61*, 6.

(11) Inouye, S. Firefly luciferase: an adenylate-forming enzyme for multicatalytic functions. *Cell. Mol. Life Sci.*, **2006,** *67*, 387.

(12) Mofford, D. M.; Reddy, G. R.; Miller, S. C. Latent luciferase activity in the fruit fly revealed by a synthetic luciferin. *Proc. Natl. Acad. Sci. U. S. A.* **2014**, *111*, 4443.

(13) Branchini, B. R.; Behney, C. E.; Southworth, T. L.; Fontaine, D. M.; Gulick, A. M.; Vinyard, D. J.; Brudvig, G. W. Experimental support for a single electron-transfer oxidation mechanism in firefly bioluminescence. *J. Am. Chem. Soc.*, **2015**, *137*, 7592.

(14) White, E. H.; Worther, H.; Field, G. F.; McElroy, W. D. Analogs of firefly luciferin. *J. Org. Chem.* **1965**, *30*, 2344.

(15) White, E. H.; Roswell, D. F. Analogs and derivatives of firefly oxyluciferin, the light emitter in firefly bioluminescence. *Photochem. Photobiol.* **1991**, *53*, 131.

(16) Branchini, B. R.; Hayward, M. M.; Bamford, S.; Brennan, P. M.; Lajiness, E. J. Naphthyl- and quinolylluciferin: green and red light emitting firefly luciferin analogues. *Photochem. Photobiol.* **1989**, *49*, 689.

(17) Woodroofe, C. C.; Meisenheimer, P. L.; Klaubert, D. H.; Kovic, Y.; Rosenberg, J. C.; Behney, C. E.; Southworth, T. L.; Branchini, B. R. Novel heterocyclic analogues of firefly luciferin. *Biochemistry*, **2008,** *51*, 9807.

(18) Reddy, G. R.; Thompson, W. C.; Miller, S. C. Robust light emission from cyclic alkylaminoluciferin substrates for firefly luciferase. *J. Am. Chem. Soc.,* **2010**, *132*, 13586.

(19) Maltsev, O. V.; Nath, N. K.; Naumov, P.; Hintermann, L. Why is firefly oxyluciferin a notoriously labile substance? *Angew. Chem. Int. Ed.*, **2014** , *53*, 847.

(20) Bauernschmitt, R. d.; Ahlrichs, R. Treatment of electronic excitations within the adiabatic approximation of time dependent density functional theory. *Chem. Phys. Lett.* **1996**, *256*, 454.

(21) Leitao, J. M.; Esteves da Silva, J. C. Firefly luciferase inhibition. *J. Photochem. Photobiol. B*, **2006**, *101*, 1.

(22) da Silva, L. P.; Esteves da Silva, J. C. G. Kinetics of inhibition of firefly luciferase by dehydroluciferyl-coenzyme A, dehydroluciferin and l-luciferin. *Photochem. Photobiol. Sci.*, **2008**, *10*, 1039.

(23) Lakowicz, J. R. *Principles of fluorescence spectroscopy*; Springer Science & Business Media, 2007.

(24) Lippert, E.; LuDer, W.; Boos, H.; Mangini, A. In *Advances in Molecular Spectroscopy*; Pergamon: 1962, p 443.

(25) Grabowski, Z. R. R., K.; Siemiarczuk, A.; Cowley, D.J.; Baumann, W. *Nouv. J. Chem.* **1979**, *3*, 443.

(26) Grabowski, Z. R.; Dobkowski, J. Twisted intramolecular charge transfer (TICT) excited states: energy and molecular structure. *Pure Appl. Chem.* **1983**, *55*, 245.

(27) Grabowski, Z. R.; Dobkowski, J.; Kuehnle, W. Model compounds in study of the photophysical behaviour of carbonyl derivatives of N,N-dimethylaniline. *J. Mol. Struct.* **1984**, *114*, 93.

(28) Grabowski, Z. R.; Rotkiewicz, K.; Rettig, W. Structural changes accompanying intramolecular electron transfer:, focus on twisted intramolecular charge-transfer states and structures. *Chem. Rev.* **2003**, *103*, 3899.

(29) Grimm, J. B.; English, B. P.; Chen, J.; Slaughter, J. P.; Zhang, Z.; Revyakin, A.; Patel, R.; Macklin, J. J.; Normanno, D.; Singer, R. H.; Lionnet, T.; Lavis, L. D. A general method to improve fluorophores for live-cell and single-molecule microscopy. *Nat. Methods*, **2015**, *12*, 244.

(30) Vogel, M.; Rettig, W.; Sens, R. d.; Drexhage, K. H. Structural relaxation of rhodamine dyes with different N-substitution patterns: a study of fluorescence decay times and quantum yields. *Chem. Phys. Lett.* **1988**, *147*, 452.

(31) Morton, R. A.; Hopkins, T. A.; Seliger, H. H. Spectroscopic properties of firefly luciferin and related compounds; an approach to product emission. *Biochemistry* **1969**, *8*, 1598.

(32) White, E. H.; Rapaport, E.; Seliger, H. H.; Hopkins, T. A. The chemi- and bioluminescence of firefly luciferin: an efficient chemical production of electronically excited states. *Bioorg. Chem.* **1971**, *1*, 92.

(33) White, E. H.; Steinmetz, M. G.; Miano, J. D.; Wildes, P. D.; Morland, R. Chemi- and bioluminescence of firefly luciferin. *J. Am. Chem. Soc.* **1980**, *102*, 3199.

(34) White, E. H.; Rapaport, E.; Hopkins, T. A.; Seliger, H. H. Chemi- and bioluminescence of firefly luciferin. *J. Am. Chem. Soc.* **1969**, *91*, 2178.

(35) Seliger, H.; McElroy, W. Chemiluminescence of firefly luciferin without enzyme. *Science* **1962**, *138*, 683.

(36) Shimomura, O.; Goto, T.; Johnson, F. H. Source of oxygen in the CO2 produced in the bioluminescent oxidation of firefly luciferin. *Proc. Natl. Acad. Sci. U. S. A.* **1977**, *74*, 2799.

(37) Takakura, H.; Sasakura, K.; Ueno, T.; Urano, Y.; Terai, T.; Hanaoka, K.; Tsuboi, T.; Nagano, T. Development of luciferin analogues bearing an amino group and their application as BRET donors. *Chem. Asian. J.*, **2012**, *5*, 2053.

(38) Sundlov, J. A.; Fontaine, D. M.; Southworth, T. L.; Branchini, B. R.; Gulick, A. M. crystal structure of firefly luciferase in a second catalytic conformation supports a domain alternation mechanism. *Biochemistry*, **2012,** *51*, 6493.

(39) Auld, D. S.; Lovell, S.; Thorne, N.; Lea, W. A.; Maloney, D. J.; Shen, M.; Rai, G.; Battaile, K. P.; Thomas, C. J.; Simeonov, A.; Hanzlik, R. P.; Inglese, J. Molecular basis for the high-affinity binding and stabilization of firefly luciferase by PTC124. *Proceedings of the National Academy of Sciences U. S. A.* **2008**, *107*, 4878.

(40) Auld, D. S.; Southall, N. T.; Jadhav, A.; Johnson, R. L.; Diller, D. J.; Simeonov, A.; Austin, C. P.; Inglese, J. Characterization of chemical libraries for luciferase inhibitory activity. *J. Med. Chem.* **2008**, *51*, 2372.

(41) Reddy, G. R.; Thompson, W. C.; Miller, S. C. Robust light emission from cyclic alkylaminoluciferin substrates for firefly luciferase. *J. Am. Chem. Soc*. **2010** *132*, 13586.

(42) Kim, S.; Lee, J. I.; Kim, Y. C. A simple and mild esterification method for carboxylic acids using mixed carboxylic-carbonic anhydrides. *J. Org. Chem.* **1985**, *50*, 560.

(43) Appel, R.; Janssen, H.; Siray, M.; Knoch, F. Synthese und Reaktionen des 4,5-Dichlor-1,2,3-dithiazolium-chlorids. *Chemische Berichte* **1985**, *118*, 1632.

(44) Shen, M.; Driver, T. G. Iron(II) bromide-catalyzed synthesis of benzimidazoles from aryl azides. *Org. Lett.* **2008**, *10*, 3367.

(45) Patrick, D. A.; Ismail, M. A.; Arafa, R. K.; Wenzler, T.; Zhu, X.; Pandharkar, T.; Jones, S. K.; Werbovetz, K. A.; Brun, R.; Boykin, D. W.; Tidwell, R. R. Synthesis and antiprotozoal activity of dicationic m-terphenyl and 1,3-dipyridylbenzene derivatives. *J. Med. Chem.* **2010**, *56*, 5473.

(46) Rix, D.; Clavier, H.; Coutard, Y.; Gulajski, L.; Grela, K.; Mauduit, M. Activated pyridinium-tagged ruthenium complexes as efficient catalysts for ring-closing metathesis. *J. Organomet. Chem.* **2006**, *691*, 5397.

(47) Michaelidou, S. S.; Koutentis, P. A. The synthesis of 2-cyano-cyanothioformanilides from 2-(4-chloro-5H-1,2,3-dithiazol-5-ylideneamino)benzonitriles using DBU. *Synthesis* **2009**, *2009*, 4167.

(48) Inamoto, K.; Hasegawa, C.; Hiroya, K.; Doi, T. Palladium-catalyzed synthesis of 2-substituted benzothiazoles via a C-H functionalization/intramolecular C-S bond formation process. *Org. Lett.* **2008**, *10*, 5147.

(49) Oba, Y.; Yoshida, N.; Kanie, S.; Ojika, M.; Inouye, S. Biosynthesis of firefly luciferin in adult lantern: decarboxylation of L-cysteine is a key step for benzothiazole ring formation in firefly luciferin synthesis. *PLoS ONE*, *8*, e84023.

(50) McCutcheon, D. C.; Porterfield, W. B.; Prescher, J. A. Rapid and scalable assembly of firefly luciferase substrates. *Org. Biomol. Chem.*, *13*, 2117.

(51) Perdew, J. P.; Ernzerhof, M.; Burke, K. Rationale for mixing exact exchange with density functional approximations. *J. Chem. Phys.* **1996**, *105*, 9982.

(52) Rappoport, D.; Furche, F. Property-optimized Gaussian basis sets for molecular response calculations. *J. Chem. Phys.*, *133*, 134105.

(53) F. Furche, R. A., C. Hättig, W. Klopper, M. Sierka and F. Weigend *WIREs Comp. Mol. Chem.* **2014**, *4*, 91.

(54) GmbH *TURBOMOLE V6.2 2010, a development of University of Karlsruhe and Forschungszentrum Karlsruhe GmbH, 1989-2007, TURBOMOLE GmbH, since 2007; available from* http://www.turbomole.com.

Chapter 4: Diversifying the luciferin scaffold with metal-based cross-coupling reactions

4.1 Introduction

Expanding the bioluminescent toolkit requires access to diverse luciferin architectures. As noted in earlier chapters, these scaffolds have been notoriously difficult to synthesize from a common route. We thus aimed to identify more expedient methods to prepare libraries of functional luciferins. We hypothesized that cross coupling reactions could enable streamlined syntheses. These reactions have broad utility in organic synthesis, the Suzuki and Stille reactions were the specific transformations which best fit our requirements. We sought to examine whether cross-coupling methodologies could be used to readily prepare luciferins with extended pi system to provide rapid access to luciferins with novel properties. For these studies, we examined methodologies to build off the 2'-position of the benzothiazole ring based on computational data.

Many cross coupling reactions have also been used in catalytic transformations. Catalytic reactions with the luciferin scaffold could be problematic due to multiple sites for competitive metal binding. Nontheless, we pursued attempts to synthesize 4' and 7' substituted luciferins through Stille chemistry (Figure 4-1). Collectively, the resulting luciferins showed promising physical characteristics, and are good starting points for future luciferin library development.

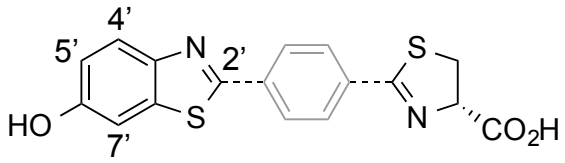

Figure 4-1.Benzothiazole numbering scheme to indicate sites of desired modification. A sample extended chromophore is also shown.

4.1 Extending the lucifeirn pi system with 2'-substitutents

Extending the luciferin pi system was a natural step to build brighter and multi-color luciferins. Indeed, some extended pi scaffolds were predicted to be approximately 2-fold brighter than D-lucfierns (Figure 4-1). This prediction is based on the consensus in the field that the light emitting oxyluciferin accesses the singlet excited state. The electronic structure change in the excited state is analogus to many fluorophores, and therefore we can apply the extensive knowledge about them to our (considerably less studied) system. Furthermore, luciferin itself is fluorescent (see Chapter 3). Although the identity of the light-emitting oxyluciferin species is still debated, most groups believe it is the keto form oxyluciferin (Figure 4-2). This is the structure on which we have based our predictions.

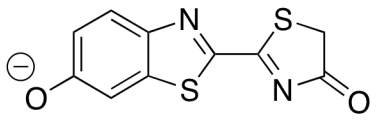

Figure 4-2. Structure of the putative light-emitting species used in our calculations.

Native oxyluciferin has a dipole, similar to most fluorophores, with the donor (D) and acceptor (A) separated by a conjugated system (Figure 4-3) Calculations suggested that by increasing the distance of the D and A in a conjugated molecule, you could, up to a limit, increase the oscillator strength of the molecule and thus the intensity of the emission. Based on this fact, we proposed oxyluciferins from parent luciferins **2** and **3**. As mentioned above, the calculations predicted the oxyluciferins would be approximately fold more than D-luc, respectively. Armed with these data we set about synthesizing the intervening phenyl and intervening alkenyl luciferins.

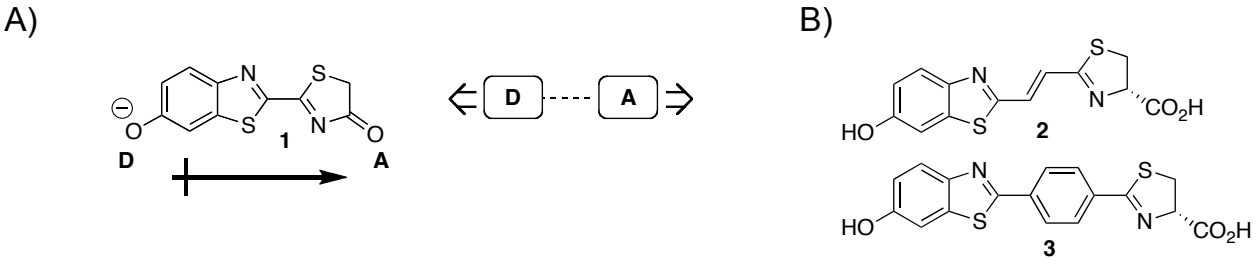

Figure 4-3. A) Oxyluciferin dipole and the separated D and A concept. B) Structures of possible hyperemissive luciferins.

Armed with the computational insights, we set about synthesizing the intervening phenyl and intervening alkenyl luciferins. The challenge posed by the intervening alkenyl luciferin was that we could not proceed with our customary route of thiazole installation by condensing D-cysteine with a nitrile. This is due to the fact that the heteroaryl acrylonitrile (Figure 4-4) is a Michael-type system susceptible to attack by sulfur nucleophiles. Attempts to lithiate the 2'position of the benzothaizole ring were also complicated due to a possible ring opening mechanism as shown by Hilf *et al,* [1].

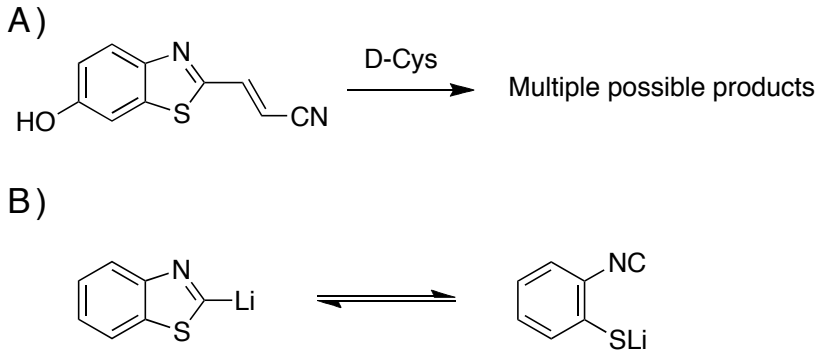

Figure 4-4. Design considerations for intervening alkenyl luciferin.

Inspired by work on the total synthesis of thiangazole [2], we attempted to install the intervening alkene via a Horner-Wadsworth-Emmons reaction with a thiazole unit (Figure 4-5 A). Toward this end, we began studies toward forming the required phosphonate (Figure 4-5 B). While promising, we halted this synthesis when the desired luciferin was reported by another

group [3]. Interestingly, the spectral properties mentioned in the report seem to support those predicted in our computational data.

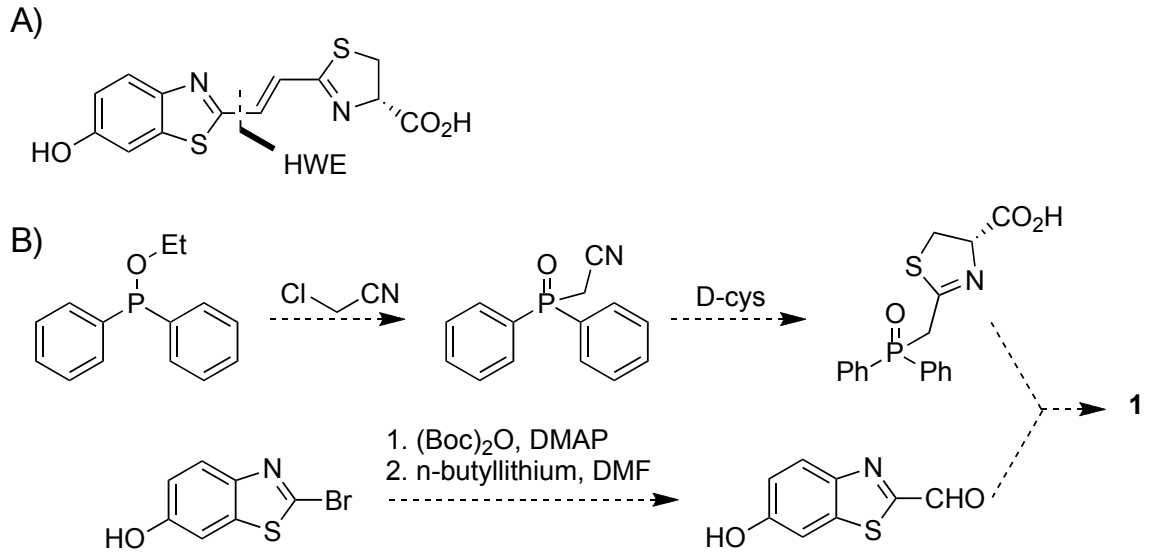

Figure 4-5. Efforts toward alkenyl luciferin. A) Disconnection of alkenyl luciferin. B) Possible synthetic route.

We next focused on an alternative extended chromophore: intervening phenyl luciferin **2**. The key step in the synthesis of this molecule was a Suzuki–Miayaura coupling a known bromobenzothiazole and boronic ester (Scheme 4-1). Traditional Suzuki-Miayaura couplings rely on boronic acids; interestingly, these molecules did not couple well in our hands. Aryl thiazoline synthesis is not as facile as the synthesis of thiazolines by the condensation of D-

cysteine with 2-cyanobenzothiazoles. In fact, that condensation has even been proposed as a new class of "click" reactions [4]. After a screening various conditions, we ultimately settled on a condensation performed over 12 h in refluxing ethanol. Progress has been made toward an amino-substituted variant as well (Scheme 4-1).

Scheme 4-1. Synthesis of phenyl-substituted luciferins.

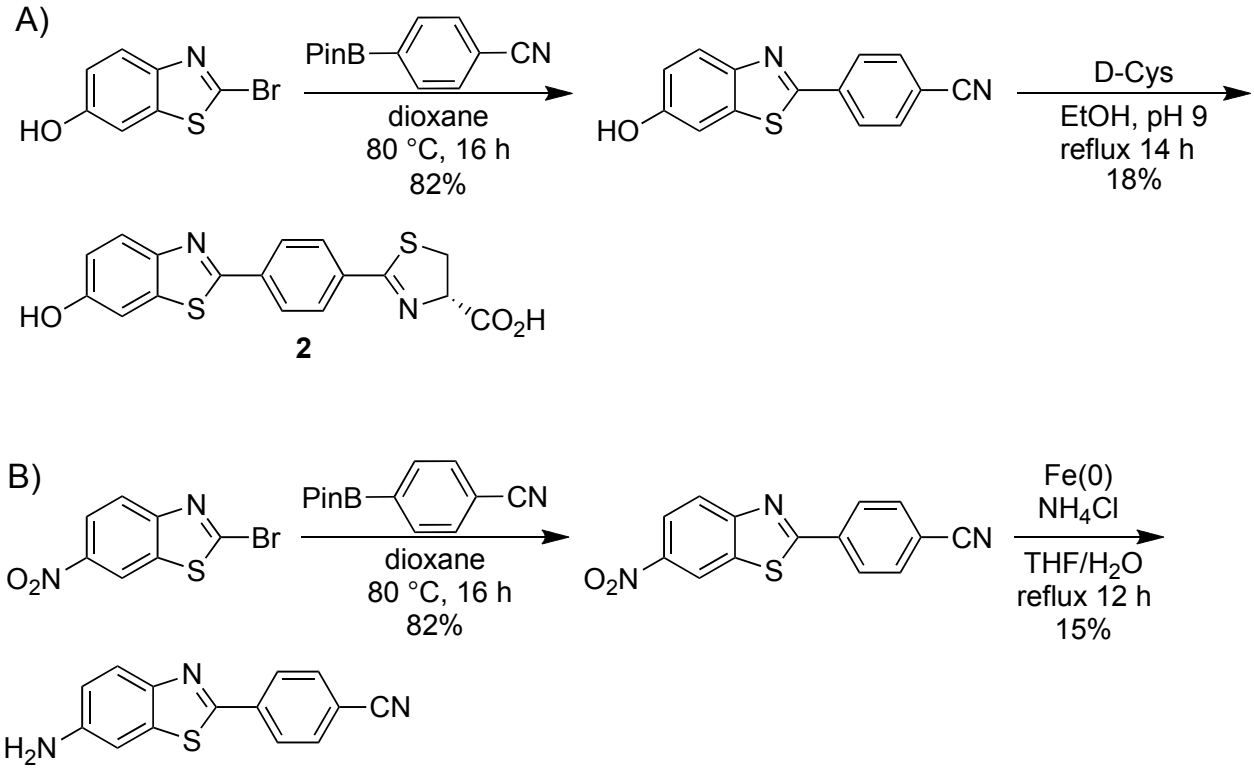

With the luciferin **2** in hand we could test its biochemical properties. The compound **2** does not emit light with Fluc, but rather is a potent inhibitor (Figure 4-6C). This molecule is capable of emitting light, though. The chemilumienscence assay described in Chapter 3 indicated that **2** emitted light at 4% of that reported for D-luc. We were able to further

investigate the fluorescence properties of the molecule. The excitation and emission spectra are shown in Figure 4-6A. Interestingly, the Stokes shift of the molecule was quite large and showed a fairly strong dependance on solvent dielectric (Figure 4-6B) This indicates that the light emitted by **2** is environment dependent, suggesting that the color of light emission of **2** could be modulated by a mutant enzyme.

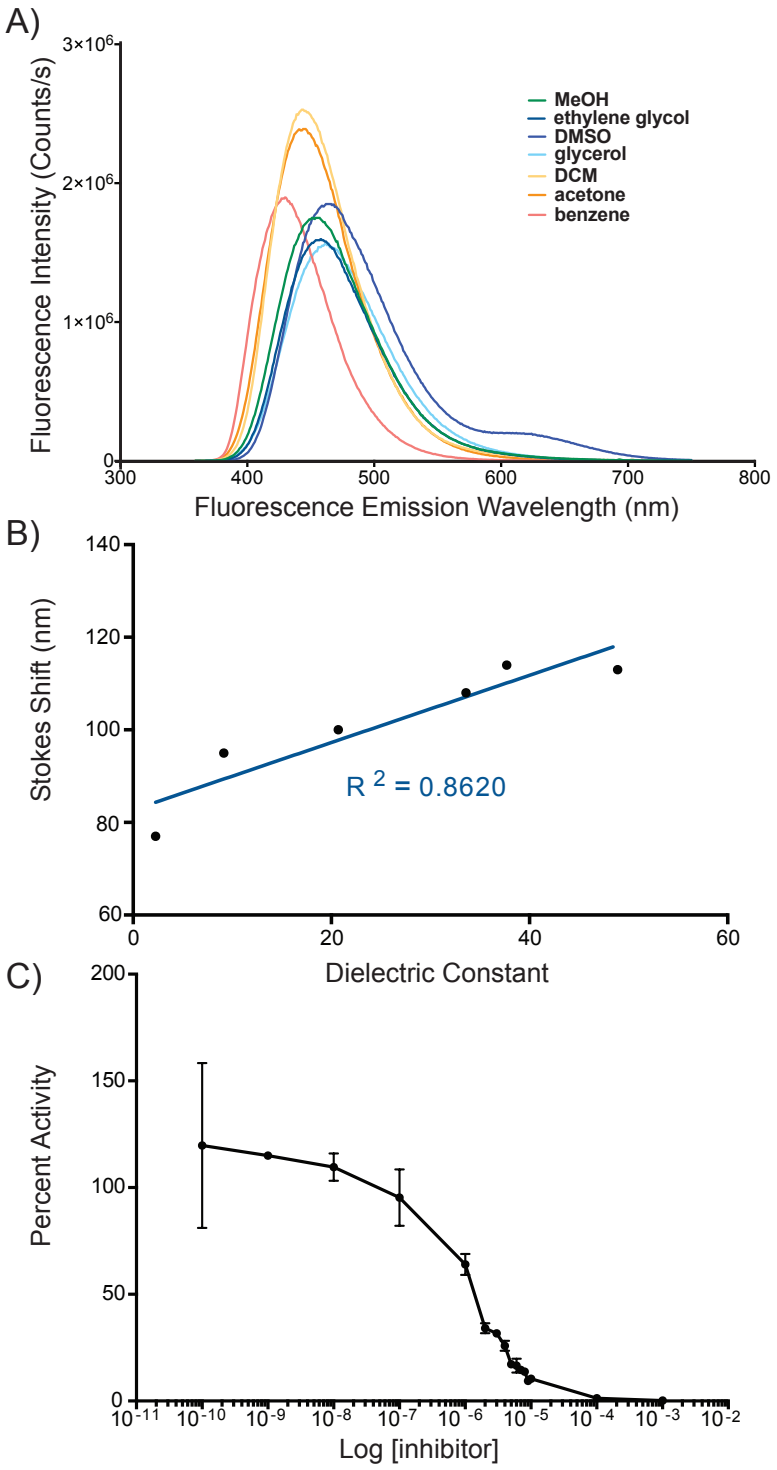

Figure 4-6. Characterization of properties of luciferin **2**. A) Fluorescence intensity of **2** in solvents of varied dielectrics. The excitation wavelength was optimized for each solvent. B) Lippert plot of **2**. C) Concentrations of **2** were varied in reaction mixtures containing 10 μM D-luciferin and 1 μg of Fluc, 25 °C, pH 8.0.

To further test this hypothesis, we added protein to the luciferin solution and re-analzyed the fluorescence data. As shown in Figure 4-7, the fluorescence intensity increased with increasing concentration of protein. These data suggested that phenyl luciferin is capable of robust emission when "bound" in a conformation that prevents non-radiative relaxation or twisting movements. Indeed, we are currently screening for a mutant enzyme that emits light with **2**, likely enforcing a planar conformation.

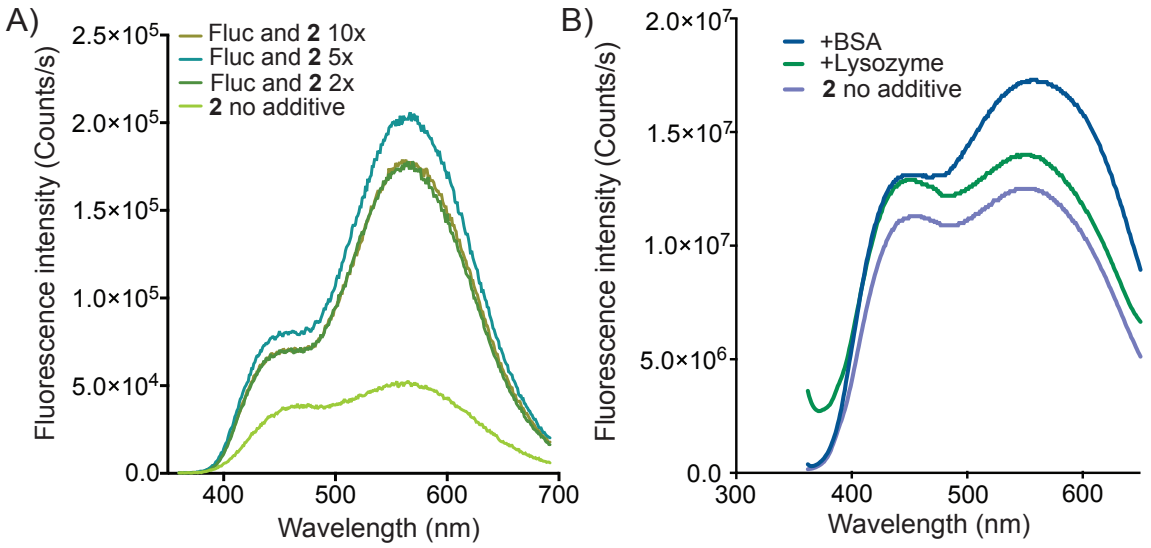

Figure 4-7. Fluorescence of **2** in the presence of protein. A) Fluorescence of **2** in the presence of Fluc. B) Fluorescence of **2** in the presence of the relatively nonpolar protein, BSA, and the relatively polar protein, lysozyme.

One logical extension from these data is that unique luciferases could be identified based to discriminate among luciferins with distinct rotational states. These lucifeirns would be analogous to molecular rotors [5]. Such systems comprise two units with a non-trivial rotational energy barrier to relative rotation. The molecules display many interesting properties, such as high polarity and viscosity sensitivity [6,7].

Applying these ideas to the lucifeirn system, we performed rotational energy barrier calculations on substituted phenyl luciferins. We modeled known molecular rotor fluorophores via semi-emperical PM3 calculations [8], and found the predicted rotational barrier to be 4-6 kcal/mol (Figure 4-8). When we modeled methylated phenyl luciferins **3** and **4** we found the energy barrier to be similar (Figure 4-9), suggesting these molecules are good candidates for molecular rotor luciferins.

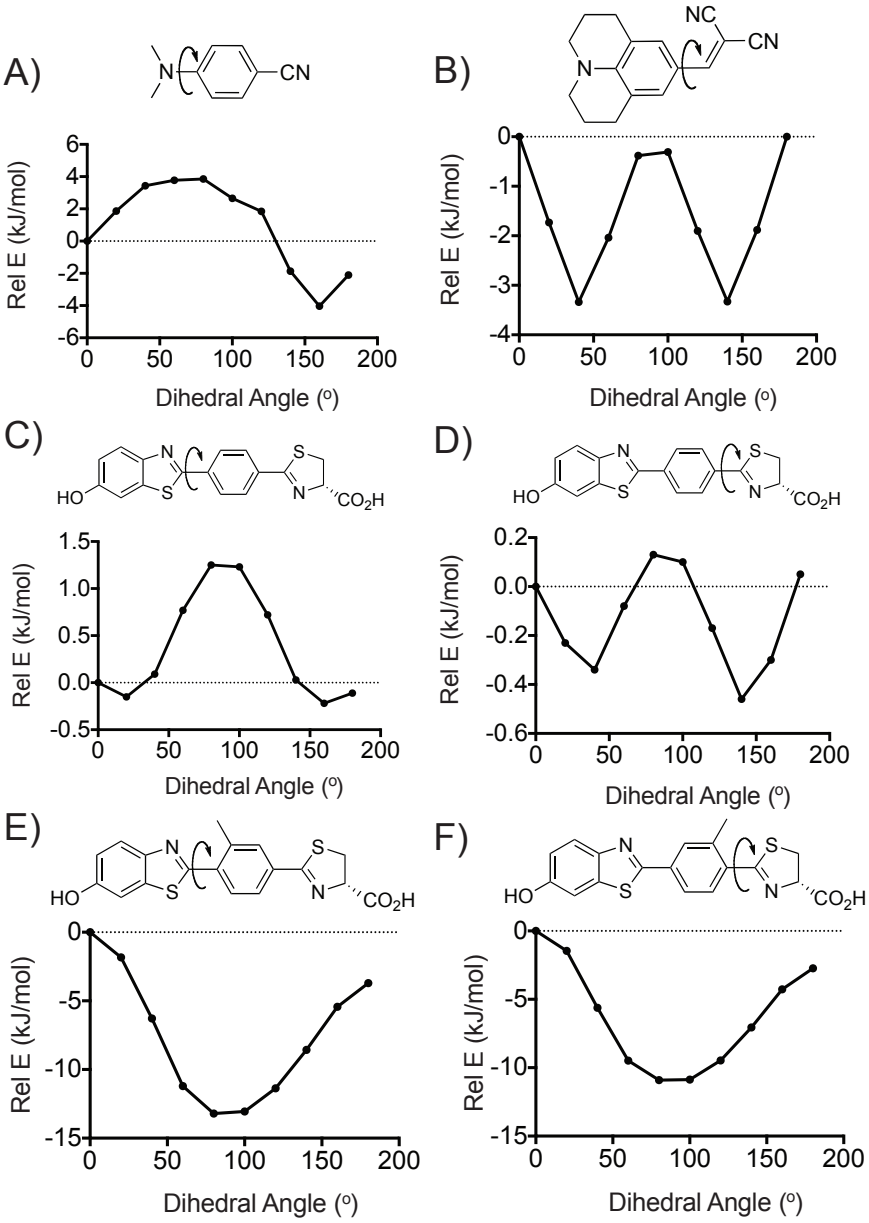

Figure 4-8. Rotational energy barrier calculations for known and novel molecular rotors. All calculations are semi-empirical PM3. A) Known molecular rotor DMABN. B) Known molecular rotor DCVJ. C) Phenyl luciferin **2**. D) Phenyl luciferin **2**. E) Methylated phenyl luciferin **3**. F) Methylated phenyl luciferin **4**.

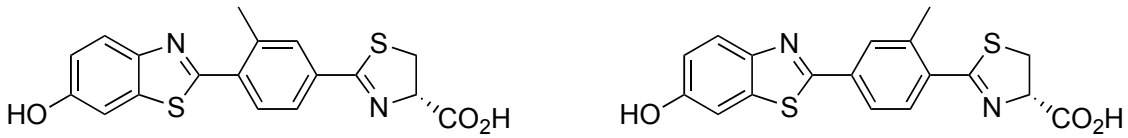

3 **4**

Figure 4-9. Structures of two methyl-substituted luciferins.

Initial attempts to synthesize luciferin **3** using analogous conditions to access **2** were unsuccessful. Thus, a second route was devised and is pictured in Scheme 4-2. In this route, the bromobenzonitrile was lithiated and then quenched with solid CO_2 to provide known carboxylic acid. This molecule was then converted to the acid chloride and reacted with 4-isopropoxyanline to afford the amide in 20% yield over two steps. The amide was treated with Lawesson's reagent [9] to provide the thioamide, which was then cyclized to the benzothiazole using the C–H activation chemistry previously mentioned. The aryl benzothiazole phenol was deprotected using boron trichloride, and the thiazoline installed via the same general method used to install the thiazoline on phenyl luciferin (Scheme 4-2A).

By contrast, methyluciferin **4** could be accessed using Suzuki-Miyaura methodology. The requisite boronic ester was installed with a Miyaura reaction in modest yield. The boronic ester was then coupled to the bromobenzothiazole via a Suzuki-Miyaura reaction. This material was then condensed with cysteine to access the desired molecule (Scheme 4-2B). This compound was assayed as described for **2** above. Luciferin **4** was also found to inhibit Fluc, with an approximate IC_{50} in the high micromolar range. Studies of the fluorescence properties of **3** and **4** are ongoing.

Applying the same procedure mentioned earlier, luciferin **4** is an inhibitor of the native luciferase enzyme, with an approximate IC_{50} in the high micromolar range. Studies of the fluorescence properties of **3** and **4** are ongoing.

In conclusion, intervening phenyl luciferins have been synthesized, and their biochemical and fluorescence behavior characterized. Phenylluciferin **2** shows some promise as an orthogonal luciferin candidate, and methylluciferins **3** and **4** establish groundwork for future work on molecular rotor luciferins.

Scheme 4-2. Synthesis of methyl-substituted phenyl luciferins **3** and **4**.

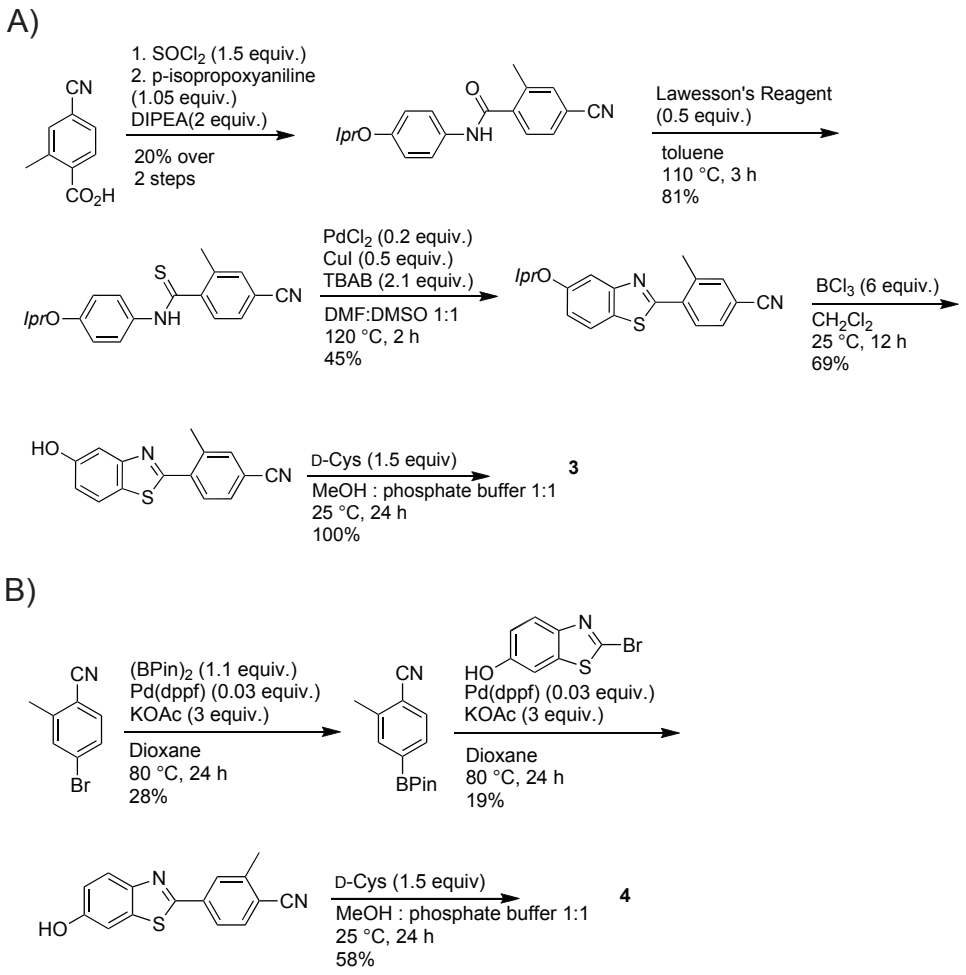

4.2 Building sterically modified luciferins via 4' and 7' substitution

In parallel with the work above, we examined cross coupling to add steric substitutions on the luciferin benzothiazole ring. Broadly, we utilized the bromo luciferins described in chapter 3 as the cross coupling partner, and then surveyed a number of cross coupling methodologies. The 4′- and 7′-bromo scaffolds were particularly attractive for derivatization based on their measured k_{cat} and K_m values with Fluc (Chapter 3). These data suggested that the 4' and 7' positions were "hot spots" for orthogonal probe development and could serve as foci for steric disruptions of luciferin-luciferase binding (Figure 4-1).

Our "holy grail" remained a luciferin synthesis that would allow late-stage diversification to a library of modified luciferins. Cross-coupling was chosen as the best candidate methodology to create such a library. This is because it allows the additional installation of diverse functional groups. Additionally, data from the bromo derivatives and others indicated that the extra "grease" added by the all carbon functionalization may likely increase cell permeability, as opposed to dervitization methodologies adding additional H-bond donors and acceptors. A further goal was to connect any functional group to the luciferin molecule through an sp^3 carbon as opposed to an sp^2 or sp carbon. This is due to the fact that extending the conjugation of the luciferin chromophores would likely alter the frontier molecule orbitals, and possibly quench light emission.

The main challenges with cross-coupling reactions on luciferin substrates are twofold: 1. Late-stage luciferin intermediates are densely functionalized with sensitive moieties, notably the highly reactive nitrile and electrophilic C2' carbon of the benzothiazole (Figure 4-1). 2. These

molecules contain a number of motifs which are known metal ligands, potentially leading to catalytically unproductive interactions with a metal catalyst.

We chose to focus our studies on the 4' and 7' positions of the luciferin benzothiazole based on preliminary work described in Chapters 2 and 3. Additionally, we analyzed crystal structure data suggesting that the 4' and 7' positions were closely juxtaposed to the luciferase backbone. We therefore selected brominated benzothiazoles **5** and **6** as ideal starting points for our cross-coupling studies.

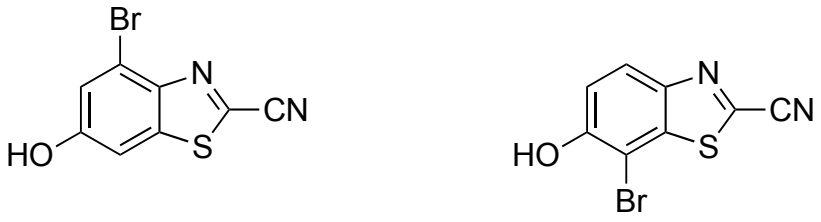

5 **6**

Figure 4-10. Brominated benzothiazoles used as starting points for our cross-coupling study.

Our initial forays into metal-based coupling focused on Negishi methodologies with zinc [10]. These reactions with **5** were unsuccessful, resulting in complex mixtures of products. Mild indium-catalyzed resulted in degradation as well [11]. Fortunately, exploration of Stille protocols [12] showed promise, and we found evidence for the successful coupling of vinyl and phenyl stannanes.

As mentioned above, we had been concerned that conjugated substitions would further complicate the electronic structure of the luciferin chromophore, possibly decreasing light emission. Encouraged by reports of facile allylation using Stille chemistry, we envisioned crafting allylated late-stage intermediates which could then be further derivatized by Suzuki chemistry to create a library of alkyl lucferins. These sterically modified luciferins could provide good starting points for orthogonal luciferin development.

4.3 Synthesis of allylated luciferin intermediates

As mentioned above, we had been concerned that conjugated substitutions would further complicate the electronic structure of the luciferin chromophore, possibly decreasing light emission. Encouraged by reports of facile allylation using Stille chemistry, we envisioned crafting allylated late-stage intermediates which could then be further derivatized sp by Suzuki chemistry to create a library of alkyl luciferins. These sterically modified luciferins could provide good starting points for orthogonal luciferin development.

We decided to focus on synthesizing the 4' and 7' allyl luciferins since our previous data indicated that Fluc was most sensitive to modifications in these areas. The bromo cyanobenzothiazole intermediates were also selected due to their ease of synthesis. The 7' bromobenzothiazole was synthesized according to the method mentioned to Chapter 3, with the exception of increasing catalyst loading on the cyclization reaction from 10 mol % to 20 mol %. The 4'-bromobenzothiazole cyclization protocol was improved by using one equivalent copper iodide and one equivalent pyridine, replacing the low-yielding and capricious cyclization procedure previously used.

With the brominated benzothiazoles in hand, we began screening allylation protocols. The highest yielding in our hands was one reported by Fu *et al.* [13]. This method employed both palladium(0) tri-*t*-butylphosphine and palladium(0) dibenzylidineacetone. Our experiments suggested, though, that this protocol was not catalytic. One explanation could be that the substrate is not interacting with the palladium in a catalytically productive fashion. We further screened conditions, including attempting to pre-coordinate chelating sites, but no improvements in yield were made (Table 4-1).

Table 4-1. Screen of allylation conditions for 4' bromobenzothiazole.

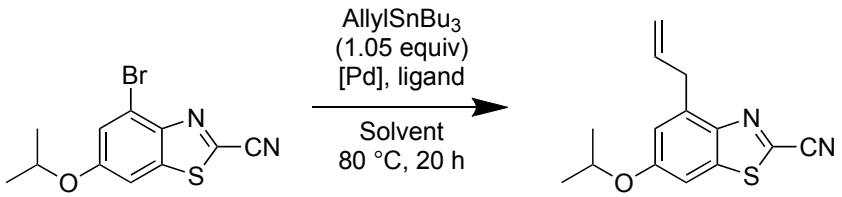

Entry	[Pd]	ligand	additive	solvent	% conversion[1]
1	$Pd(PPh_3)_4$ (5 mol%)		CuI (8 mol%)	dioxane	0%
2	$Pd(PPh_3)_4$ (10 mol%)		LiCl (120 mol%)	dioxane	10%
3	$Pd_2(dba)_3$ (1.5 mol%)	$HP(t\text{-}bu)_3BF_4$ (6 mol%)	CsF (200 mol%)	dioxane	2%
4	$Pd_2(dba)_3$ (15 mol%), $Pd_2(PtBu_3)_6$ (15 mol%)		CsF (200 mol%)	dioxane	20%
5	$Pd(OAc)_2$ (10 mol%)	$P(2\text{-furyl})_3$ (10 mol%)	CsF (200 mol%)	dioxane	9%
6	$Pd_2(dba)_3$ (50 mol%), $Pd_2(PtBu_3)_6$ (50 mol%)		CsF (200 mol%)	dioxane	44%
7	$Pd_2(dba)_3$ (2 mol%)	$AsPh_3$	CsF (200 mol %)	dioxane	0%
8	$Pd_2(dba)_3$ (2 mol%)	$P(Cy)_3$	CsF (200 mol %)	dioxane	redo

1: % conversion determined by NMR

In order to benchmark the disruption of binding with the wild-type enzyme by the addition of steric bulk, we deprotected and condensed the 4' allylated benzothiazole with D-cysteine to provide 4' AllylLuciferin (Scheme 4-3). In an assay with recombinant enzyme, 4' AllylLuciferin emitted light at approximately 1% of D-luc, further supporting our hypothesis that further steric perturbations could quickly disrupt the binding of the alkylated substrate with the native enzyme, providing leads for orthogonal luciferase-luciferin pairs (Figure 4-11)

Scheme 4-3. Synthesis of 4' AllylLuciferin.

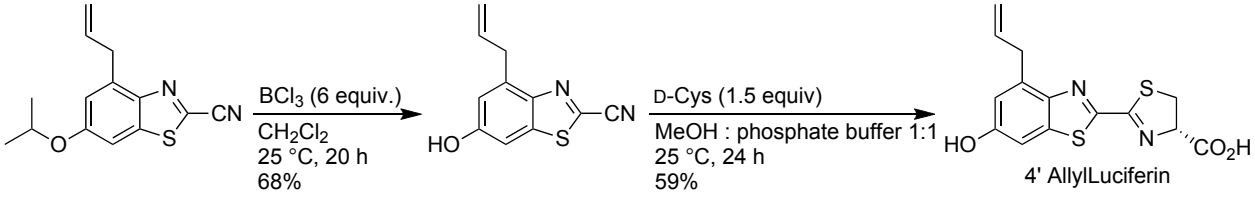

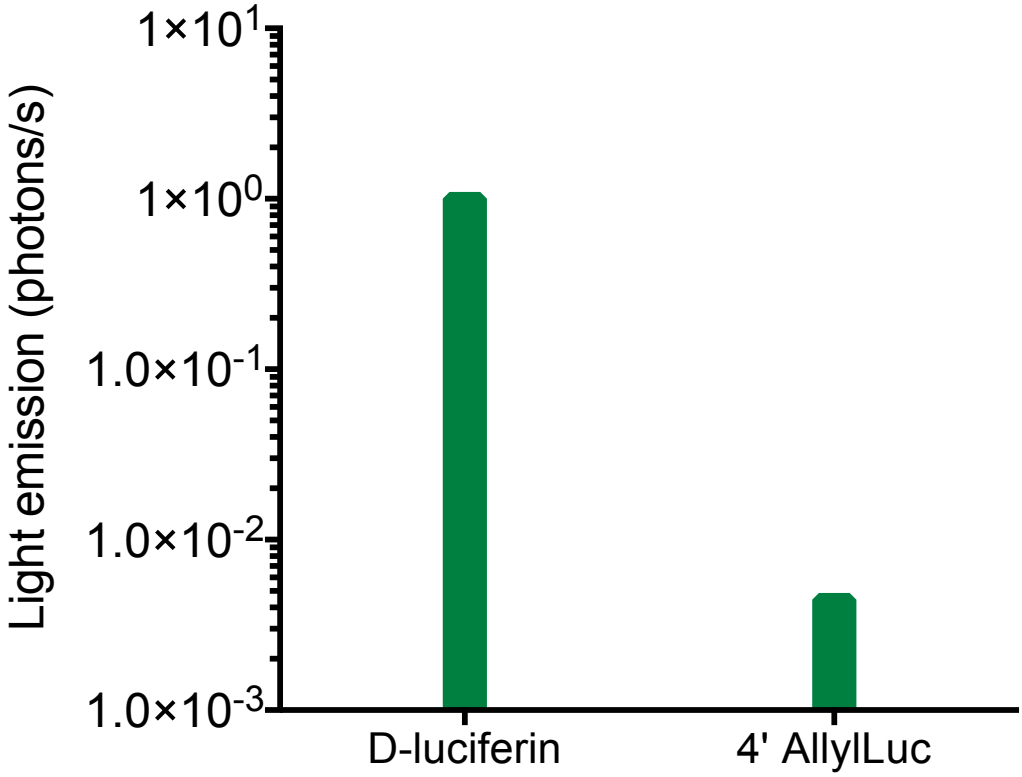

Figure 4-11. Peak light emission for 100 μM concentrations of D-lucferin vs. 4' AllylLuciferin vs. D-lucferin.

4.4 Future directions

4.4a Grubbs metathesis to functionalize allylated intermediates

We hypothesized the terminal alkene present on the allylated benzothiazoles could participate in metathesis reactions to install a variety of functional groups on the late-stage luciferin intermediate. We envisioned two separate modalities for the metathesis reaction: 1. A ring closing metathesis (RCM) route, and 2. A cross metathesis (CM) route.

The RCM route was based on esterifying the metathesis partner to the benzothiazole phenol, performing RCM, and ultimately hydrolyzing the ester to unveil the phenol needed for luciferin light emission (Figure 4-12). To assay this route, we deprotected the allylbenzothiazole and esterified it with two different acid chlorides– the commercially available 4-pentenoyl chloride and the readily synthesized 6-heptenoyl chloride (Figure 4-12). We then attempted to cyclize the pendant alkenes using Hoveyda-Grubbs catalyst II, with or without the inclusion of titanium (IV) isopropoxide (an additive known to assist with macrocylization of esters as well as prevent the chelation of the ruthenium catalyst by the substrate [14]). TLC and NMR evidence indicated the cyclization of the alkenes, as showed that the omission of titanium (IV) isopropoxide resulted in a cleaner reaction. Experiments towards further optimization of this reaction are ongoing.

A CM route has also been investigated. CM can be more complicated than RCM due to the necessity of biasing the reaction towards a productive CM product. One way this can be accomplished is to use an alkene coupling partner that is known to be highly reactive toward CM [15]. TLC and NMR evidence indicates that CM was successful with 1-hexene. Experiments towards further optimization of this exiting result are ongoing.

Another promising avenue may be to borylate the alkene with 9-BBN followed by a Suzuki reaction to cross-couple the borylated intermediate. This avenue has yet to be explored.

4.5 Conclusion

Cross-coupling is a powerful transformation for the rapid diversification of molecules, as well as the formation of carbon-carbon bonds. We have demonstrated the power of this reaction in accessing new luciferins with interesting properties, as well as new steric modifications for luciferin libraries. Overall, this methodology provides possibilities for the study of novel luciferins.

4.6 Materials and methods

4.6a Expression and purification of Fluc

Firefly luciferase was expressed and purified as previously described[16].

4.6b In vitro bioluminescence imaging for peak emission

Imaging was performed using an IVIS Lumina (Xenogen) system equipped with a cooled CCD camera. Reactions were performed in black 96-well flat-bottom plates (Grenier). Bioluminescence buffer [17] (93.5 μL of 20 mM Tris-HCl pH 7.6, 2 mM $MgSO_4$, 2 mM ATP, 0.1 mM EDTA, 1 mM TCEP, 0.5 mg/mL BSA) was added to each well, along with coenzyme A (0.5 μL of a 100 mM solution) and luciferin substrate (1 μL of a 100 mM solution in DMSO). To initiate photon production, Fluc (5 μL of a 1 μg/mL solution in bioluminescence buffer) was added to each well. The plate was then briefly agitated and placed in the IVIS instrument. The bioluminescent output was recorded every 10 s over a 45 min time period. The time point of

peak light emission for each luciferin was determined. Measurements were performed in triplicate.

4.6c In vitro bioluminescence imaging for IC_{50} determination

Imaging was performed using an IVIS Lumina (Xenogen) system equipped with a cooled CCD camera. Reactions were performed in black 96-well flat-bottom plates (Grenier). Bioluminescence buffer (93.5 μL) was added to each well, along with coenzyme A (0.5 μL of a 100 mM solution), D-luciferin (1 μL of a 100 mM solution in DMSO), and varying concentration of inhibitor luciferin. To initiate photon production, Fluc (5 μL of a 1 μg/mL solution in bioluminescence buffer) was added to each well. The plate was then briefly agitated and placed in the IVIS instrument. The bioluminescent output was recorded every 10 s over a 45 min time period. The time point of peak light emission for each luciferin was determined. Measurements were performed in triplicate.

4.6d Fluorescence imaging for Lippert plot

Emission spectra for luciferins were recorded on a FluoroMax-4 spectrometer (Horiba Jobin-Yvon). To 1 mL of each solvent, 2 μL of an 100 mM solution of the luciferin analog in DMSO was added. The solution was then mixed, and added to a 10 mm path length quartz fluorimetry cuvette. Excitation was optimized, and emission was then measured from 450-650 nm (1 nm intervals) at room temperature. The acquisition time was 0.1 s per wavelength.

4.6e Fluorescence imaging for protein binding

Emission spectra for luciferins were recorded on a FluoroMax-4 spectrometer (Horiba Jobin-Yvon).

4.6f General experimental procedures

All reactions were performed in flame- or oven-dried glassware under positive pressure of nitrogen or argon unless otherwise noted. Dichloromethane, dimethylacetamide, *N*,*N*-dimethylformamide, triethylamine, and toluene were dried by columns packed with activated alumina on a solvent purification system. Anhydrous pyridine and DMSO were purchased from Acros Organics in AcroSeal™ bottles. All reagents were used as purchased without further purification. 4,5-Dichloro-1,2,3-dithiazol-1-ium chloride (Appel's salt) was synthesized according to a published procedure[18] and stored in a desiccator. Thin layer chromatography (TLC) was performed on Merck 60 F_{254} pre-coated silica gel plates, and TLC plates were visualized with UV light and ninhydrin stain when appropriate. Flash-column chromatography was performed using silica gel (60 Å, 230-240 mesh, Merck KGA). NMR spectra were recorded with Bruker Advanced spectrometers using deuterated solvents. ^{1}H NMR spectra were recorded at 400 or 500 MHz as indicated. ^{13}C NMR spectra were recorded at 125 MHz. ^{1}H NMR data are reported in the following order: chemical shift (δ ppm), multiplicity, coupling constant (Hz), and integration. ^{13}C NMR data are reported in terms of chemical shift. Infrared spectra were recorded using a Thermo Scientific iD5 ATR infrared spectrophotometer. High-resolution mass spectra were obtained from the UC Irvine Mass Spectrometry Facility. The abbreviations used can be found in the document JOC Standard Abbreviations and Acronyms.

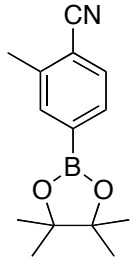

$C_{14}H_{18}BNO_2$
243.11

2-Methyl-4-(4,4,5,5-tetramethyl-1,3,2-dioxaborolan-2-yl)benzonitrile

To an oven-dried round bottomed flask was added 4-bromo-2-methylbenzonitrile (0.22 g, 1.1 mmol), 1,1'-bis(diphenylphosphino)ferrocene]palladium(II) dichloride dichloromethane complex (28 mg, 33 μmol), bis(pinocolato)diboron (0.31 g, 1.1 mmol), and potassium acetate (0.33 g, 3.3 mmol). The flask was then flushed with argon, and anhydrous dioxane (30 mL) was added. The flask was sealed and heated to 70 °C for 16 h. The flask was then diluted with ethyl acetate (100 mL), and washed with water (2 x 100 mL), sat. NH_4Cl (1 x 100 mL) and brine (1 x 100 mL). The organic layer was then dried with $MgSO_4$, filtered and concentrated *in vacuo.* The residue was purified via flash-column chromatography (eluting with 1:9 Et_2O:pet. ether) to yield 2-methyl-4-(4,4,5,5-tetramethyl-1,3,2-dioxaborolan-2-yl)benzonitrile as a colorless solid (68 mg, 0.28 mmol, 25%). Spectra matched those reported in [19].

4.6h General protocol for Suzuki coupling

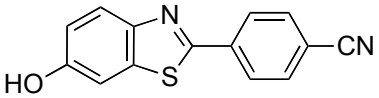

$C_{14}H_8N_2OS$
Mol.Wt.: 252.29

4-(6-Hydroxybenzo[*d*]thiazol-2-yl)benzonitrile

To an oven-dried sealed tube was added 2-bromobenzo[*d*]thiazol-6-ol (117 mg, 0.5 mmol), 4-(4,4,5,5-tetramethyl-1,3,2-dioxaborolan-2-yl)benzonitrile (116 mg, 0.5 mmol), 1,1'-bis(diphenylphosphino)ferrocene]palladium(II) dichloride dichlormethane complex (12 mg, 15 μmol), and tripotassium phosphate (322 mg, 1.5 mmol). Dry dioxane (15 mL) was then added and the reaction was heated to 70 °C for 24 h. The mixture was then diluted with ethyl acetate

(60 mL) and washed with water (2 x 60 mL), saturated ammonium chloride (1 x 60 mL), and brine (1 x 60 mL). The organic phase was dried with $MgSO_4$, filtered, and concentrated *in vacuo.* The mixture was then purified with flash column chromatography (eluting with 7:3 → 6:4 hexanes:ethyl acetate) to provide 4-(6-hydroxybenzo[*d*]thiazol-2-yl)benzonitrile as a colorless solid (63 mg, 0.3 mmol, 49%).

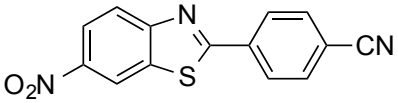

$C_{14}H_7N_3O_2S$
Mol. Wt. 281.29

4-(6-Nitrobenzo[*d*]thiazol-2-yl)benzonitrile

Synthesized according to the general procedure to provide 0.18 g, 0.6 mmol, 81 %. This product was used in the reduction reaction to synthesize 4-(6-aminobenzo[*d*]thiazol-2-yl)benzonitrile. Characterization of this product is ongoing.

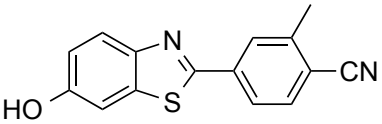

$C_{15}H_{10}N_2OS$
Mol. Wt.: 266.32

4-(6-Hydroxybenzo[*d*]thiazol-2-yl)-2-methylbenzonitrile

Synthesized according to the general procedure to provide 0.14 g, 51 μmol, 19 %. Characterization of this product is ongoing.

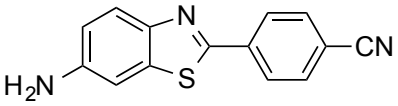

$C_{14}H_9N_3S$
Mol. Wt. 251.31

4-(6-Aminobenzo[*d*]thiazol-2-yl)benzonitrile

To a flask of 4-(6-nitrobenzo[*d*]thiazol-2-yl)benzonitrile (0.18 g, 0.6 mmol), was added iron shavings (0.10 g, 1.9

mmol), ammonium chloride (0.20 g, 3.7 mmol), acetone (10 mL), and water (10 mL). The mixture was then heated to reflux for one hour. The reaction mixture was neutralized with a saturated sodium carbonate solution and extracted with EtOAc (50 mL). The organic layer was washed with saturated sodium carbonate (2 x 50 ml), followed by water (1 x 50 mL) and brine (1 x 50 mL). The organic layer was dried with $MgSO_4$, filtered, and concentrated *in vacuo.* The mixture was then purified with flash column chromatography (eluting with 7:3 → 6:4 hexanes:ethyl acetate) to provide 4-(6-aminobenzo[*d*]thiazol-2-yl)benzonitrile (18 mg, 70 μmol, 11 %). Diagnostic peaks: ^{1}H NMR (400 MHz, $CDCl_3$) δ 8.10 (d, *J* = 8.32 Hz, 2H), 7.85 (d, *J* = 8.7 Hz, 1H), 7.73 (d, *J* = 8.3 Hz, 1H), 7.12 (d, *J* = 2.2 Hz, 1H), 6.86 (dd, *J* = 8.7 Hz, 2.2Hz, 1H). ^{13}C NMR (125 MHz, $CDCl_3$) δ 145.44, 134.3, 133.0, 132.7, 128.4, 127.4, 124.1, 122.3, 118.5, 116.4, 113.2, 106.4.

4.6i General procedure for the synthesis of aryl thiazolines

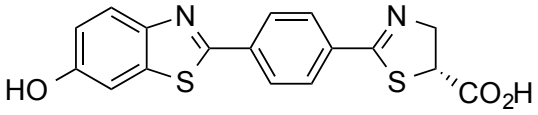

$C_{17}H_{12}N_2O_3S_2$
Mol. Wt.: 356.41

(*R*)-2-(4-(6-Hydroxybenzo[*d*]thiazol-2-yl)phenyl)-4,5-dihydrothiazole-5-carboxylic acid

Following the general procedure of [20]. To a flask of 4-(6-hydroxybenzo[*d*]thiazol-2-yl)benzonitrile (28 mg, 0.1 mmol), was added D-cysteine (58 mg, 0.3 mmol), sodium bicarbonate (28 mg, 0.3 mmol) and absolute ethanol (10 mL). The mixture was heated at reflux for 30 min, and then piperidine (approximately 4 drops) was added until the pH was ~9. The mixture was then heated at reflux for a further 12 h. The mixture was then acidified to pH ~4 with 1 M sodium hydrogen sulfate, diluted with ethyl acetate (50 mL), washed with 1 M sodium hydrogen sulfate (2 x 50 mL), and brine (1 x 50 mL).

The organics were dried with magnesium sulfate, filtered, and concentrated *in vacuo* to provide (*R*)-2-(4-(6-hydroxybenzo[*d*]thiazol-2-yl)phenyl)-4,5-dihydrothiazole-5-carboxylic acid (7 mg, 2 μmol, 18 %). Characterization of this product is ongoing.

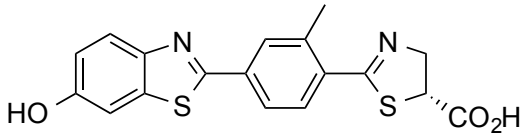

$C_{18}H_{14}N_2O_3S_2$
Mol. Wt.: 370.44

(*R*)-2-(4-(6-Hydroxybenzo[*d*]thiazol-2-yl)-2-methylphenyl)-4,5-dihydrothiazole-5-carboxylic acid

Synthesized according to the general method to provide 0.11 g, 30 μmol, 58%. Characterization of this compound is ongoing.

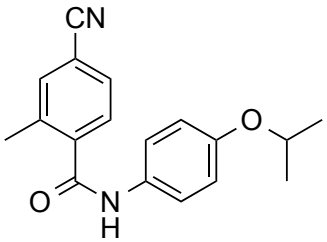

$C_{18}H_{18}N_2O_2$
Mol. Wt 294.35

4-Cyano-*N*-(4-isopropoxyphenyl)-2-methylbenzamide

To a flask of 4-cyano-2-methylbenzoic acid (0.29 g, 1.8 mmol) was added an argon flush followed by anhydrous CH_2Cl_2 (15 mL). To this was added $SOCl_2$ (0.65 mL, 2.7 mmol) followed by approximately 200 μL of anhydrous DMF. The reaction proceeded for 3 h at 25 °C and then was concentrated *in vacuo* to provide a light yellow oil which was used immediately in the following reaction. To a flask containing the crude 4-cyano-2-methylbenzoyl chloride was added an argon flush, 4-isopropoxyaniline (0.29 mL, 1.9 mmol) and anhydrous CH_2Cl_2 (15 mL). Anhydrous Hünig's base (0.52 mL, 3.6 mmol) was added dropwise, and the reaction was allowed to proceed for 18 h. The mixture was then diluted with ethyl acetate (50 mL) and washed with water (50 mL), saturated ammonium chloride (2 x 50 mL), and brine (50 mL). The organics were then dried with magnesium sulfate, filtered, and concentrated *in vacuo*.

The mixture was then purified with flash column chromatography (eluting with 8:2 → 7:3 hexanes:ethyl acetate) to provide 4-cyano-*N*-(4-isopropoxyphenyl)-2-methylbenzamide (0.53 g, 0.4 mmol, 20 % over two steps). ^{1}H NMR (400 MHz, $CDCl_3$) δ 7.50 (m, 5H), 6.90 (d, *J* = 8.9 Hz, 2H), 4.54 (septet, *J* = 6.0 Hz, 1H), 2.53 (s, 3H), 1.35 (d, 6.0 Hz, 6H). ^{13}C NMR (125 MHz, $CDCl_3$) δ 166.1, 155.3, 140.7, 137.8, 134.6, 130.2, 129.8, 127.4, 122.0, 118.2, 116.5, 113.8, 70.4, 22.0, 19.6. HRMS (ESI+) *m/z* calcd for $C_{18}H_{18}N_2O_2Na$ $[M+Na]^+$ 317.1267, found 317.1266.

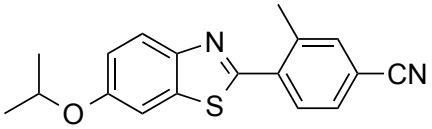

$C_{18}H_{16}N_2OS$
Mol. Wt. 308.40

4-(6-Isopropoxybenzo[*d*]thiazol-2-yl)-3-methylbenzonitrile

To a flask of 4-cyano-*N*-(4-isopropoxyphenyl)-2-methylbenzamide (85 mg, 0.2 mmol) was added Lawesson's reagent (46 mg, 0.1 mmol) and anhydrous toluene (5 mL). The mixture was then heated to reflux for 3 h under argon. The mixture was then diluted with ethyl acetate (20 mL) and washed with water (2 x 20 mL), saturated ammonium chloride (2 x 20 mL), and brine (20 mL). The organics were dried with magnesium sulfate, filtered, and concentrated *in vacuo*. The residue was then purified with flash column chromatography (eluting with 8:2 hexanes:ethyl acetate), however, some of the Lawesson's reagent remained. This mixture was then taken on to be used in the next step (approximate yield: 58 mg, 190 μmol, 81%).

To the mixture of 4-cyano-*N*-(4-isopropoxyphenyl)-2-methylbenzothioamide and residual Lawesson's reagent was added palladium(II) chloride (7 mg, 37 μmol), copper(I) iodide (18 mg, 93 μmol), and tetrabutylammonium bromide (0.13 g, 04 mmol), followed by an argon flush. Anhydrous DMF (10 mL) and DMSO (10 mL) were then added. The reaction was heated at 120 ˚C for 3h. The mixture was diluted with ethyl acetate (50 mL) washed with NH_4Cl (2 x 50 mL),

water (1 x 50 mL), and brine (1 x 50 mL), dried by $MgSO_4$, filtered, and concentrated *in vacuo*. The concentrated mixture was purified by flash column chromatography (eluting with 8:2 hexanes:EtOAc) to afford 4-(6-isopropoxybenzo[*d*]thiazol-2-yl)-3-methylbenzonitrile (26 mg, 83 μmol 36% over two steps). ^{1}H NMR (500 MHz, $CDCl_3$) δ 8.04 (d, J = 8.9 Hz, 1H), 7.91 (d, J = 8.0 Hz, 1H), 7.66 (m, 2H), 7.45 (m, 1H), 7.18 (m, 1H), 4.70 (septet, J = 6.0 Hz), 2.77 (s, 3H), 1.46 (d, J = 6.0 Hz, 6H). ^{13}C NMR (125 MHz, $CDCl_3$) δ 162.8, 156.5, 148.2, 138.5, 137.4, 137.0, 135.0, 130.9, 129.7, 124.4, 118.6, 117.7, 113.0, 106.2, 70.9, 22.0, 21.5. HRMS (ESI+) *m/z* calcd for $C_{18}H_{17}N_2OSNa$ $[M+Na]^+$ 331.0881, found 331.0876.

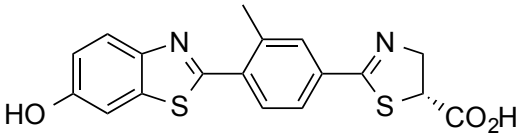

$C_{18}H_{14}N_2O_3S_2$
Mol. Wt. 370.44

(*R*)-2-(4-(6-Hydroxybenzo[*d*]thiazol-2-yl)-3-methylphenyl)-4,5-dihydrothiazole-5-carboxylic acid

To a flask of 4-(6-isopropoxybenzo[*d*]thiazol-2-yl)-3-methylbenzonitrile (31 mg, 0.1 mmol) was added anhydrous CH_2Cl_2 (5 mL) and a 1.0 M solution of BCl_3 in hexanes (0.6 mmol, 0.62 mL) was added slowly. The mixture was stirred at room temperature under nitrogen for 24 h. The reaction was then quenched with a saturated solution of ammonium chloride (10 mL), extracted into ethyl acetate (30 mL), washed with saturated ammonium chloride (2 x 30 mL) and brine (1 x 30 mL). The organic layer was dried with $MgSO_4$, filtered, and concentrated *in vacuo*. The concentrate was then purified with flash-column chromatography (eluting with 1:1 hexanes:ethyl acetate) to yield the title compound which was immediately subjected to the method for aryl thiazoline synthesis mentioned above to provide (*R*)-2-(4-(6-hydroxybenzo[*d*]thiazol-2-yl)-3-methylphenyl)-4,5-dihydrothiazole-5-carboxylic acid (69 % crude yield over two steps). Note: attempts at isolating an analytical

standard of this compound are ongoing. Diagnostic peaks: ^{1}H NMR (400 MHz, CD_3OD) δ 8.8 (m, 4H), 7.0 (m, 1H), 6.8 (m, 1H), 5.1 (m, 1H), 3.3 (m, 2H) 2.6 (s, 3H).

4.6j General procedure for Stille allylation

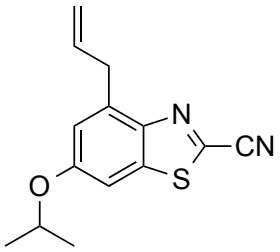

$C_{14}H_{14}N_2OS$
Mol. Wt. 258.34

4-Allyl-6-isopropoxybenzo[*d*]thiazole-2-carbonitrile

Synthesized following the procedure of Fu *et al.* [13]. To a flask of 4-bromo-6-isopropoxybenzo[*d*]thiazole-2-carbonitrile (75 mg, 250 μmol) was added palladium(0) tri-*t*-butylphosphine (20 mg), palladium(0) dibenzylidineacetone (30 mg), cesium fluoride (75 mg), and allyltributylstannane (75 μl). The flask was then flushed with argon, and anhydrous dioxane was added. The mixture was then heated to 80 °C for 24 h. The mixture was then filtered over a pad of celite, which was rinsed with 2 x 50 mL of diethyl ether. The combined organics were washed with water (100 mL), saturated ammonium chloride (2 x 100 mL), and brine (100 mL). The organics were dried with magnesium sulfate, filtered, and concentrated via rotary evaporated. The crude mixture was purified via flash column chromatography (eluting with 9.5:0.5 → 9:1 pet. ether:diethyl ether) to provide 4-allyl-6-isopropoxybenzo[*d*]thiazole-2-carbonitrile (26 mg, 0.1 mmol, 40 %). ^{1}H NMR (400 MHz, $CDCl_3$) δ 7.19 (d, J = 2.0 Hz, 1H), 7.02 (d, J = 1.6 Hz, 1H), 6.09 (m, 1H), 5.16 (m, 2H), 4.64 (m, 1H), 3.88 (d, J = 6.6 Hz, 2H), 1.40 (d, J = 6.0 Hz, 6H); ^{13}C NMR (125 MHz, $CDCl_3$) δ 158.9, 145.9, 138.6, 137.7, 135.6, 132.0,

119.0, 117.1, 113.6, 102.6, 70.8, 36.3, 21.9; HRMS (ESI+) *m/z* calcd for $C_{14}H_{14}N_2OSNa$ $[M+Na]^+$ 281.0724, found 281.0734.

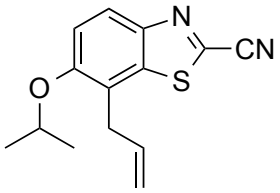

$C_{14}H_{14}N_2OS$
Mol. Wt. 258.34

4-Allyl-6-isopropoxybenzo[*d*]thiazole-2-carbonitrile

Synthesized according to the general method 4.6j. Diagnostic peaks: ^{1}H NMR (500 MHz, $CDCl_3$) δ 8.04 (d, J = 9.0 Hz, 1H), 7.29 (m, 1H), 5.88 (m, 1H), 5.12 (m, 0.5H), 4.70 (septet, J = 6.0 Hz), 3.60 (d, 6.45 Hz), 1.40 (d, J = 6.0 Hz, 8H).

4.7 References

(1) Hilf, C.; Bosold, F.; Harms, K.; Marsch, M.; Boche, G. The equilibrium between 2-lithium-oxazole(-thiazole, -imidazole) derivatives and their acyclic isomers – a structural investigation. *Chem. Ber.* **1997**, *130*, 1213.

(2) Ehrler, J.; Farooq, S. F. Total synthesis of Thiangazole. *Synlett* **1994**, *1994*, 720.

(3) Jathoul, A. P.; Grounds, H.; Anderson, J. C.; Pule, M. A. A dual-color far-red to near-infrared firefly luciferin analogue designed for multiparametric bioluminescence imaging. *Angew. Chem. Int. Ed.* **2014**, *53*, 13059.

(4) Jeon, J.; Shen, B.; Xiong, L.; Miao, Z.; Lee, K. H.; Rao, J.; Chin, F. T. An efficient method for site-specific (18)f-labeling of biomolecules using the rapid condensation reaction between 2-cyanobenzothiazole and cysteine. *Bioconj. Chem.* **2012**, *23*, 1902.

(5) Haidekker, M.; Nipper, M.; Mustafic, A.; Lichlyter, D.; Dakanali, M.; Theodorakis, E. In *Advanced Fluorescence Reporters in Chemistry and Biology I*; Demchenko, A. P., Ed.; Springer Berlin Heidelberg: 2010; Vol. 8, p 267.

(6) Haidekker, M. A.; Theodorakis, E. A. Molecular rotors-fluorescent biosensors for viscosity and flow. *Org. Biomol. Chem.* **2007**, *5*, 1669.

(7) Haidekker, M. A.; Theodorakis, E. A. Environment-sensitive behavior of fluorescent molecular rotors. *J. Biol. Eng.* **2010**, *4*, 11.

(8) Stewart, J. J. P. Optimization of parameters for semiempirical methods I. Method. *J. Comp. Chem.* **1989**, *10*, 209.

(9) Cava, M. P.; Levinson, M. I. Thionation reactions of lawesson's reagents. *Tetrahedron* **1985**, *41*, 5061.

(10) King, A. O.; Okukado, N.; Negishi, E.-i. Highly general stereo-, regio-, and chemo-selective synthesis of terminal and internal conjugated enynes by the Pd-catalysed reaction of alkynylzinc reagents with alkenyl halides. *J. Chem. Soc., Chem. Commun.* **1977**, 683.

(11) Lee, P. H.; Sung, S.-y.; Lee, K. Palladium-catalyzed cross-coupling reactions of in situ generated allylindium reagents with aryl halides. *Org. Lett.* **2001**, *3*, 3201.

(12) Stille, J. K. The palladium-catalyzed cross-coupling reactions of organotin reagents with organic electrophiles. *Angew. Chem. Int. Ed.* **1986**, *25*, 508.

(13) Littke, A. F.; Schwarz, L.; Fu, G. C. Pd/P(t-Bu)3: a mild and general catalyst for stille reactions of aryl chlorides and aryl bromides. *J. Am. Chem. Soc.* **2002**, *124*, 6343.

(14) Prunet, J. l. Progress in metathesis through natural product synthesis. *Eur. J. Org. Chem.* **2011**, 3634.

(15) Chatterjee, A. K.; Choi, T.-L.; Sanders, D. P.; Grubbs, R. H. A general model for selectivity in olefin cross metathesis. *J. Am. Chem. Soc.* **2003**, *125*, 11360.

(16) McCutcheon, D. C.; Paley, M. A.; Steinhardt, R. C.; Prescher, J. A. Expedient synthesis of electronically modified luciferins for bioluminescence imaging. *J. Am. Chem. Soc*. **2012**, *134*, 7604.

(17) Reddy, G. R.; Thompson, W. C.; Miller, S. C. Robust light emission from cyclic alkylaminoluciferin substrates for firefly luciferase. *J. Am. Chem. Soc.* **2010**, *132*, 13586.

(18) Appel, R.; Janssen, H.; Siray, M.; Knoch, F. Synthese und Reaktionen des 4,5-Dichlor-1,2,3-dithiazolium-chlorids. *Chem. Ber.* **1985**, *118*, 1632.

(19) Partridge, B. M.; Thomas, S. P.; Aggarwal, V. K. Enantioenriched synthesis of Escitalopram using lithiation-borylation methodology. *Tetrahedron* **2011**, *67*, 10082.

(20) Loughlin, W. A.; Knevitt, S. A.; Hosking, R. E.; Marshall, R. L. Approaches to the high-throughput synthesis of analogues of dihydroaeruginoic acid. *Aust. J. Chem.* **2000**, *53*, 457.

Appendix A: NMR spectra for Chapter 2

1H spectrum

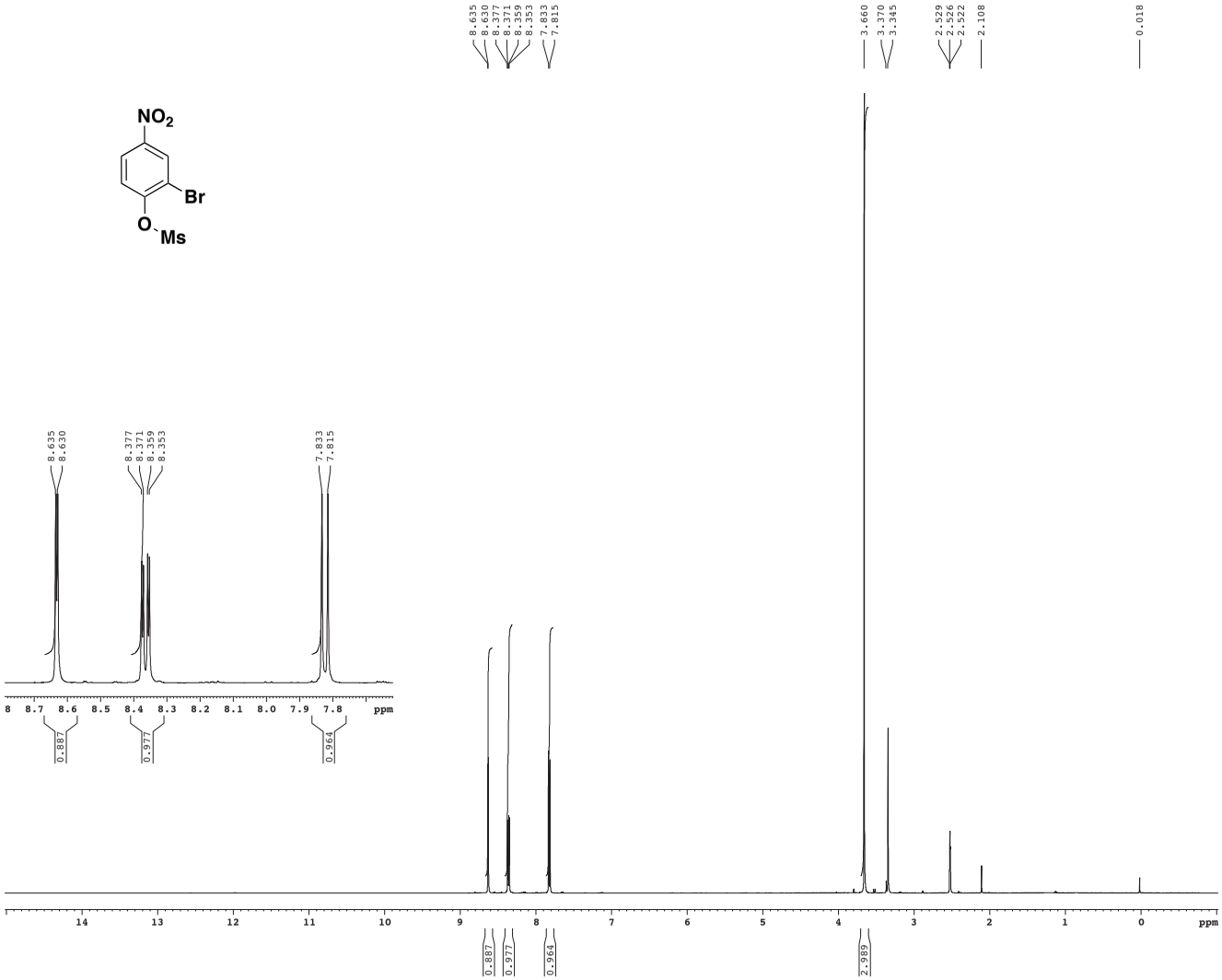


```
Current Data Parameters
USER                rachel
NAME            RD227_iv39
EXPNO                    2
PROCNO                   1

F2 - Acquisition Parameters
Date_             20121123
Time                 21.21
INSTRUM              gm500
PROBHD    5 mm broadband
PULPROG               zg30
TD                   81728
SOLVENT               DMSO
NS                       8
DS                       2
SWH             8012.820 Hz
FIDRES          0.098043 Hz
AQ              5.0998774 sec
RG                  645.1
DW                 62.400 usec
DE                  6.00 usec
TE                 298.0 K
D1              0.10000000 sec
MCREST          0.00000000 sec
MCWRK           0.01500000 sec

======= CHANNEL f1 =======
NUC1                   1H
P1                  12.20 usec
PL1                 -5.00 dB
SFO1          499.4034958 MHz

F2 - Processing parameters
SI                  65536
SF            499.4000000 MHz
WDW                    EM
SSB                     0
LB                   0.30 Hz
GB                      0
PC                   1.00
```

Z-restored spin-echo 13C spectrum with 1H decoupling

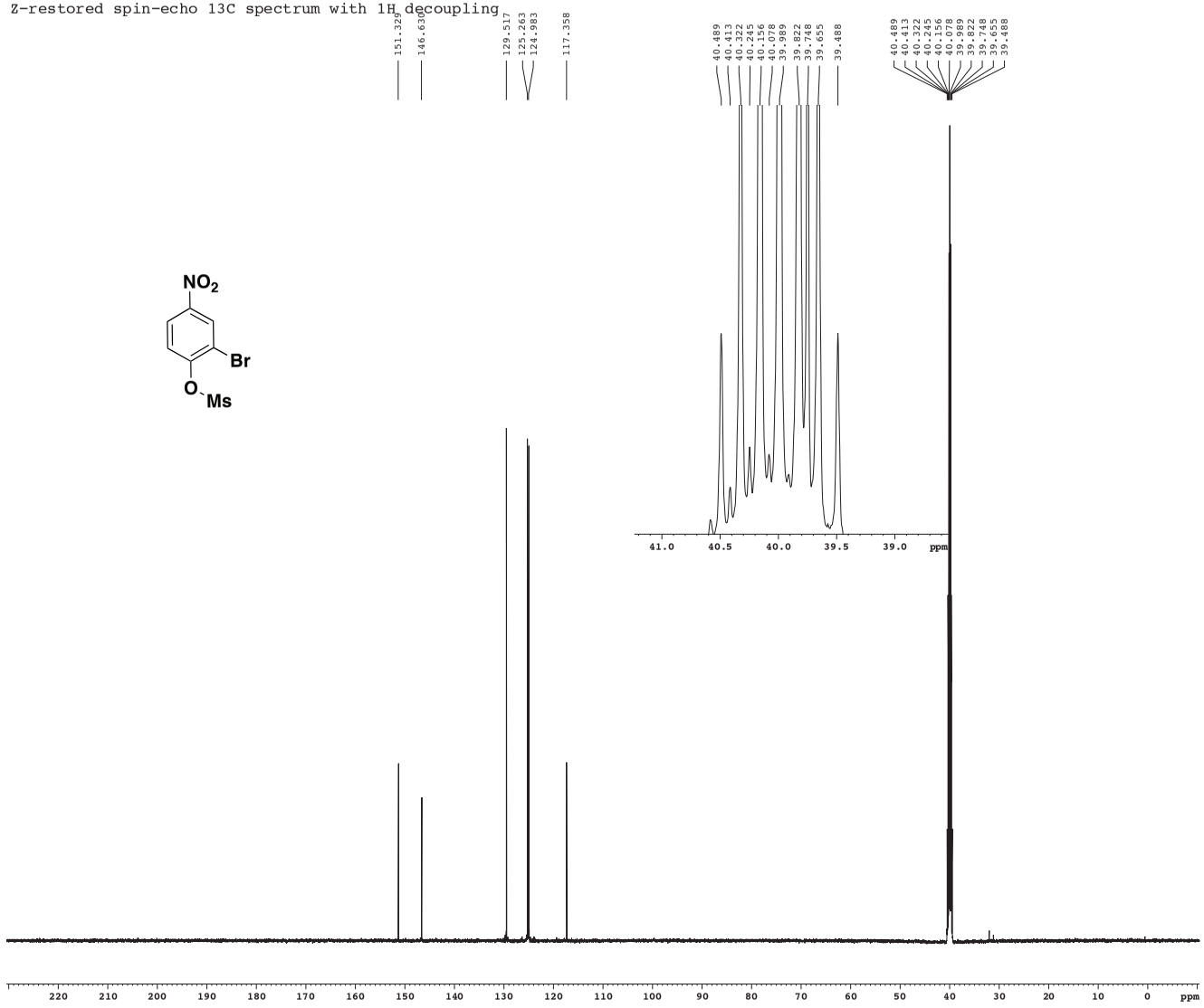


```
Current Data Parameters
USER                rachel
NAME             RD227_iv39
EXPNO                    1
PROCNO                   1

F2 - Acquisition Parameters
Date_             20121123
Time                 22.07
INSTRUM            cryo500
PROBHD     5 mm CPTCI 1H-
PULPROG    SpinEchopg30gp.prd
TD                   65536
SOLVENT               DMSO
NS                     1024
DS                       16
SWH             30303.031 Hz
FIDRES           0.462388 Hz
AQ              1.0813940 sec
RG                 10321.3
DW                  16.500 usec
DE                   6.00 usec
TE                  298.0 K
D1             0.25000000 sec
d11            0.03000000 sec
D16            0.00020000 sec
d17            0.00019600 sec
MCREST         0.00000000 sec
MCWRK          0.01500000 sec
P2                  31.00 usec

======== CHANNEL f1 ========
NUC1                  13C
P1                  15.50 usec
P11                500.00 usec
P12               2000.00 usec
PL0                120.00 dB
PL1                 -1.00 dB
SFO1          125.7942548 MHz
SP1                  3.20 dB
SP2                  3.20 dB
SPNAM1     Crp60,0.5,20.1
SPNAM2       Crp60comp.4
SPOFF1               0.00 Hz
SPOFF2               0.00 Hz

======== CHANNEL f2 ========
CPDPRG2            waltz16
NUC2                    1H
PCPD2              100.00 usec
PL2                  1.60 dB
PL12                24.60 dB
SFO2          500.2225011 MHz

===== GRADIENT CHANNEL =====
GPNAM1           SINE.100
GPNAM2           SINE.100
GPX1                 0.00 %
GPX2                 0.00 %
GPY1                 0.00 %
GPY2                 0.00 %
GPZ1                30.00 %
GPZ2                50.00 %
p15                500.00 usec
p16               1000.00 usec

F2 - Processing parameters
SI                   65536
SF            125.7804190 MHz
WDW                     EM
SSB                      0
LB                    1.00 Hz
GB                       0
PC                    2.00
```

1H spectrum

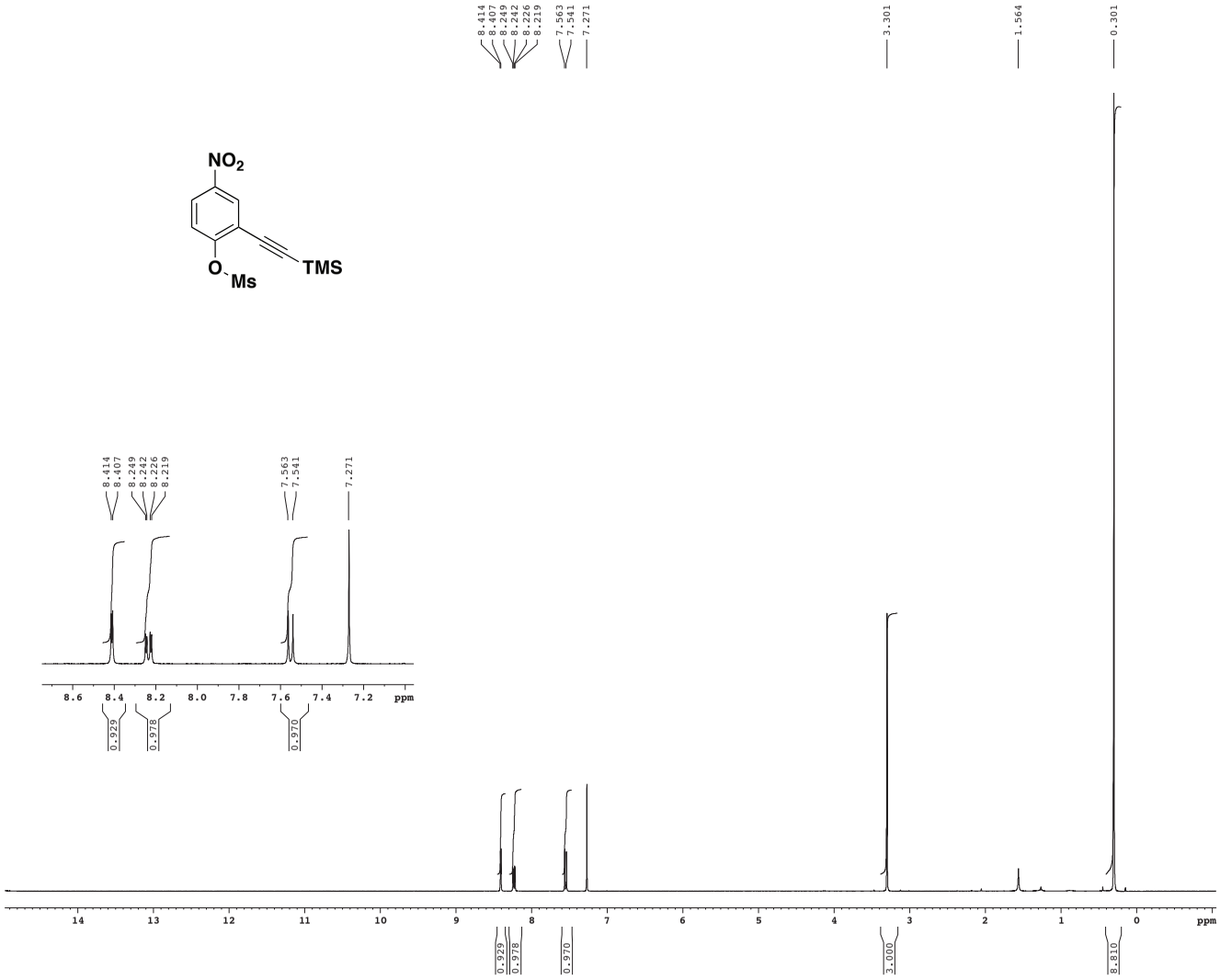


```
Current Data Parameters
USER                rachel
NAME             RB015_vi95
EXPNO                    2
PROCNO                   1

F2 - Acquisition Parameters
Date_             20131203
Time                 15.05
INSTRUM             drx400
PROBHD    5 mm QNP H/F/P
PULPROG              zg30
TD                   65536
SOLVENT              CDCl3
NS                       8
DS                       2
SWH              6410.256 Hz
FIDRES           0.097813 Hz
AQ               5.1118579 sec
RG                   812.7
DW                  78.000 usec
DE                   4.50 usec
TE                  298.0 K
D1               0.10000000 sec
MCREST           0.00000000 sec
MCWRK            0.01500000 sec

======= CHANNEL f1 =======
NUC1                    1H
P1                   12.00 usec
PL1                   0.00 dB
SFO1            400.1328009 MHz

F2 - Processing parameters
SI                   65536
SF              400.1300175 MHz
WDW                     EM
SSB                      0
LB                    0.30 Hz
GB                       0
PC                    2.00
```

Z-restored spin-echo 13C spectrum with 1H decoupling

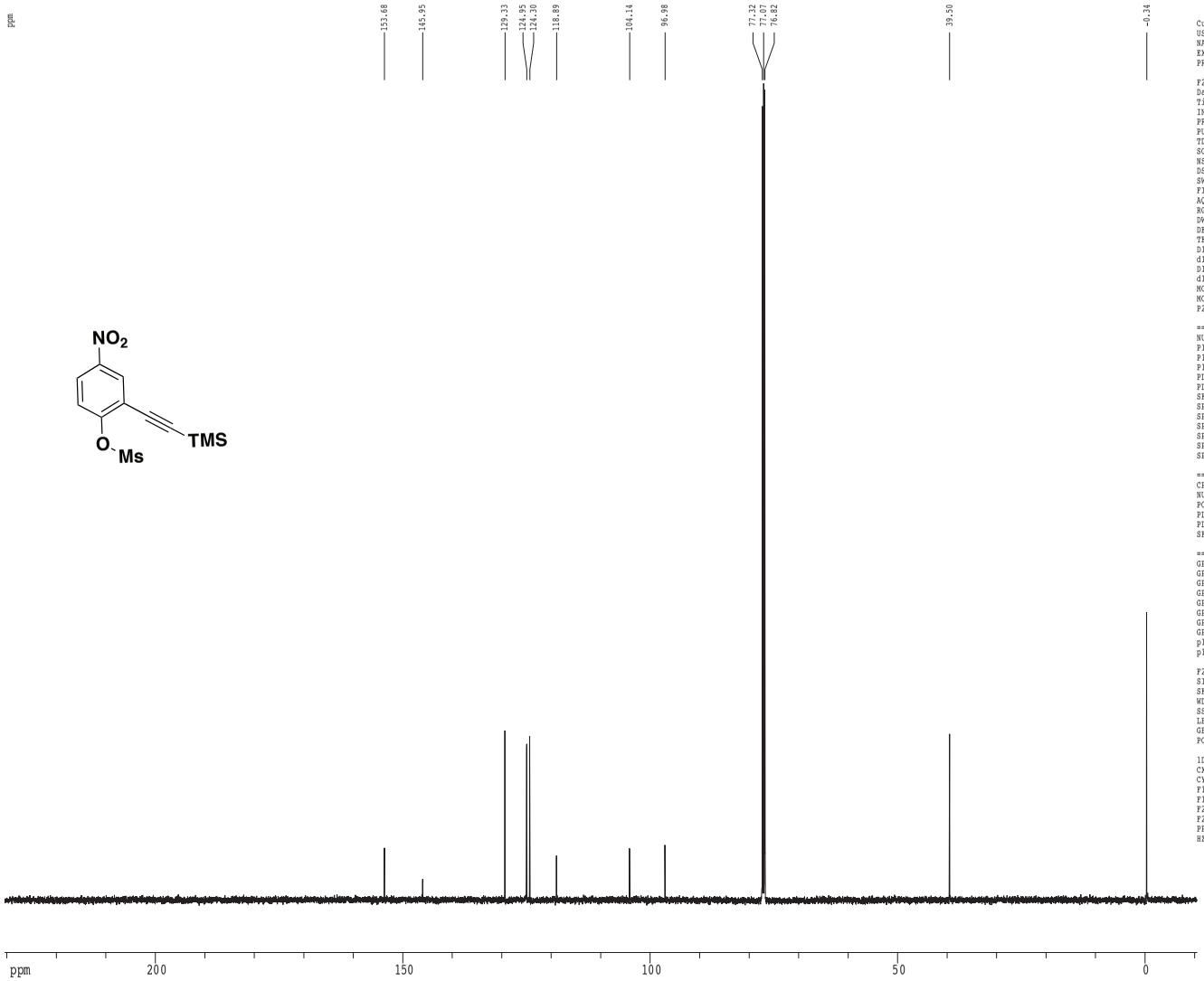


```
Current Data Parameters
USER            rachel
NAME      RB015_vi9513c
EXPNO                 1
PROCNO                1

F2 - Acquisition Parameters
Date_          20131203
Time             21.20
INSTRUM         cryo500
PROBHD   5 mm CPTCI 1H-
PULPROG  SpinEchopg30gp.prd
TD              65536
SOLVENT          CDCl3
NS                1024
DS                  16
SWH           30303.031 Hz
FIDRES         0.462388 Hz
AQ           1.0813940 sec
RG              7298.2
DW              16.500 usec
DE               6.00 usec
TE              298.0 K
D1          0.25000000 sec
d11         0.03000000 sec
D16         0.00020000 sec
d17         0.00019600 sec
MCREST      0.00000000 sec
MCWRK       0.01500000 sec
P2               31.00 usec

======= CHANNEL f1 =======
NUC1               13C
P1               15.50 usec
P11             500.00 usec
P12            2000.00 usec
PL0             120.00 dB
PL1              -1.00 dB
SFO1        125.7942548 MHz
SP1              3.20 dB
SP2              3.20 dB
SPNAM1   Crp60,0.5,20.1
SPNAM2     Crp60comp.4
SPOFF1           0.00 Hz
SPOFF2           0.00 Hz

======= CHANNEL f2 =======
CPDPRG2        waltz16
NUC2               1H
PCPD2           100.00 usec
PL2               1.60 dB
PL12             24.60 dB
SFO2       500.2225011 MHz

===== GRADIENT CHANNEL ====
GPNAM1         SINE.100
GPNAM2         SINE.100
GPX1             0.00 %
GPX2             0.00 %
GPY1             0.00 %
GPY2             0.00 %
GPZ1            30.00 %
GPZ2            50.00 %
p15             500.00 usec
p16            1000.00 usec

F2 - Processing parameters
SI                65536
SF         125.7804190 MHz
WDW                 EM
SSB                  0
LB               1.00 Hz
GB                   0
PC               2.00

1D NMR plot parameters
CX               22.80 cm
CY               15.65 cm
F1P             230.460 ppm
F1            28987.37 Hz
F2P             -10.460 ppm
F2           -1315.66 Hz
PPMCM          10.56667 ppm/cm
HZCM         1329.08032 Hz/cm
```

1H spectrum

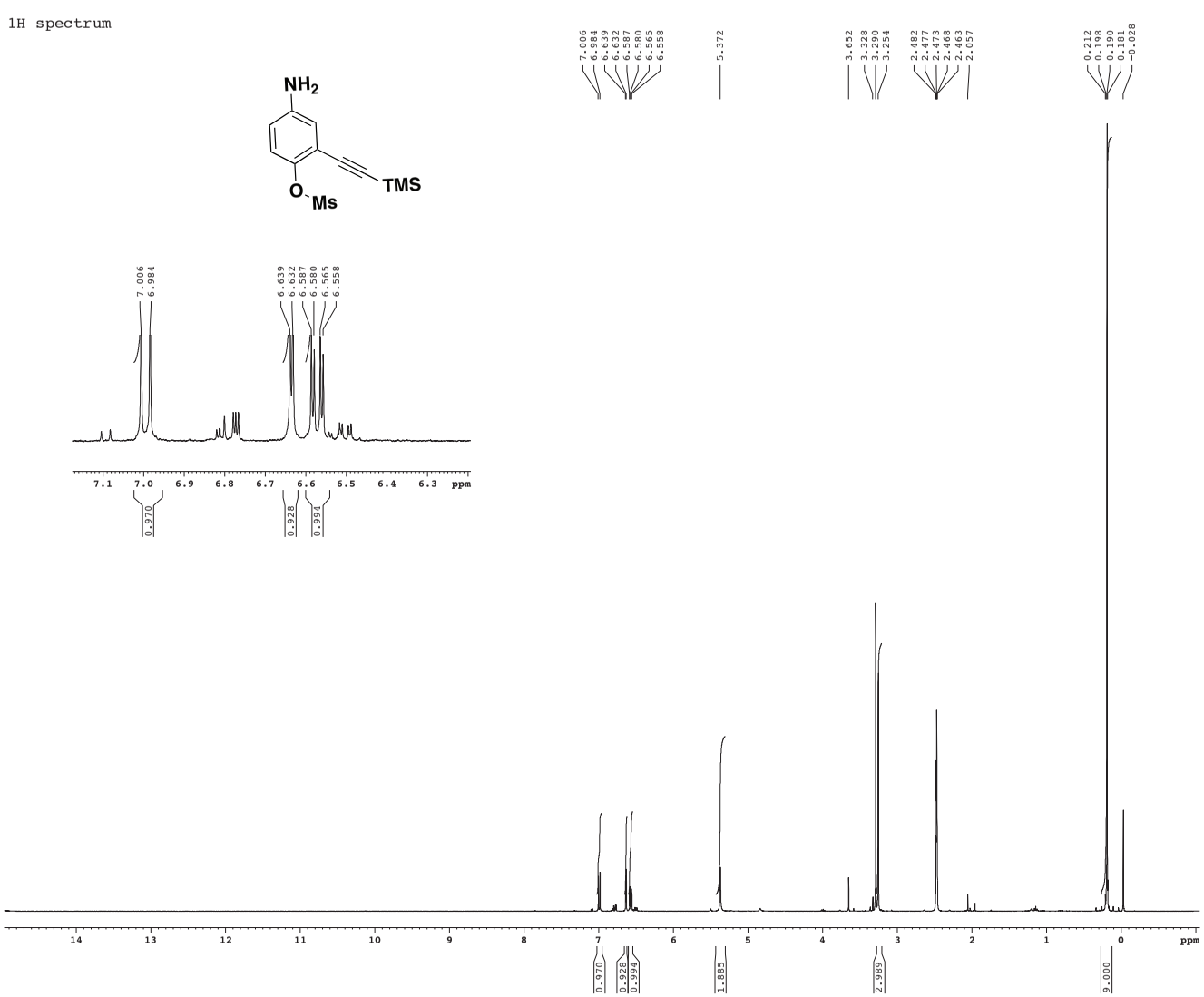


```
Current Data Parameters
USER                rachel
NAME          RD323_iv179
EXPNO                   1
PROCNO                  1

F2 - Acquisition Parameters
Date_            20130417
Time               23.06
INSTRUM            drx400
PROBHD   5 mm QNP H/F/P
PULPROG             zg30
TD                 65536
SOLVENT             DMSO
NS                     8
DS                     2
SWH             6410.256 Hz
FIDRES          0.097813 Hz
AQ              5.1118579 sec
RG                 645.1
DW                78.000 usec
DE                 4.50 usec
TE                298.0 K
D1           0.10000000 sec
MCREST       0.00000000 sec
MCWRK        0.01500000 sec

======= CHANNEL f1 =======
NUC1                  1H
P1                12.00 usec
PL1               -0.60 dB
SFO1         400.1328009 MHz

F2 - Processing parameters
SI                 65536
SF           400.1300175 MHz
WDW                   EM
SSB                    0
LB                  0.30 Hz
GB                     0
PC                  2.00
```

13C spectrum with 1H decoupling

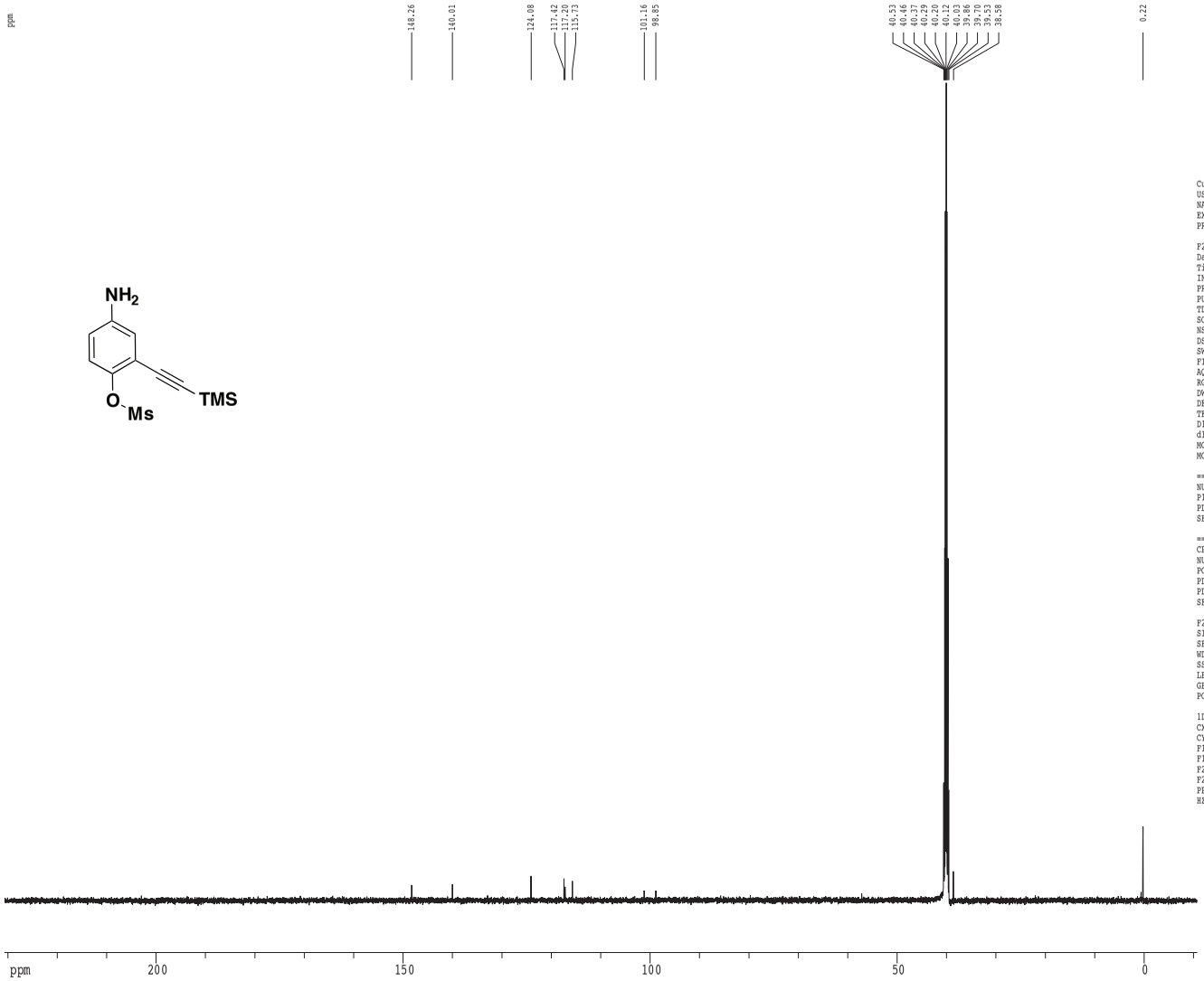


```
Current Data Parameters
USER                rachel
NAME          RD323_iv179
EXPNO                   2
PROCNO                  1

F2 - Acquisition Parameters
Date_           20130417
Time              23.51
INSTRUM           qn500
PROBHD   5 mm broadband
PULPROG          zgdc30
TD                65536
SOLVENT            DMSO
NS                  1024
DS                     4
SWH            30303.031 Hz
FIDRES          0.462388 Hz
AQ             1.0813940 sec
RG                 16384
DW                16.500 usec
DE                 4.50 usec
TE                298.0 K
D1            0.25000000 sec
d11           0.03000000 sec
MCREST        0.00000000 sec
MCWRK         0.01500000 sec

======== CHANNEL f1 ========
NUC1                 13C
P1                  7.70 usec
PL1                 0.00 dB
SFO1         125.5880432 MHz

======== CHANNEL f2 ========
CPDPRG2          waltz16
NUC2                  1H
PCPD2             80.00 usec
PL2               -3.00 dB
PL12              13.20 dB
SFO2         499.4024970 MHz

F2 - Processing parameters
SI                 65536
SF           125.5742300 MHz
WDW                   EM
SSB                    0
LB                  1.00 Hz
GB                     0
PC                  2.00

1D NMR plot parameters
CX                 22.80 cm
CY                 15.65 cm
F1P               230.658 ppm
F1              28964.67 Hz
F2P               -10.658 ppm
F2              -1338.36 Hz
PPMCM            10.58402 ppm/cm
HZCM          1329.08032 Hz/cm
```

1H spectrum

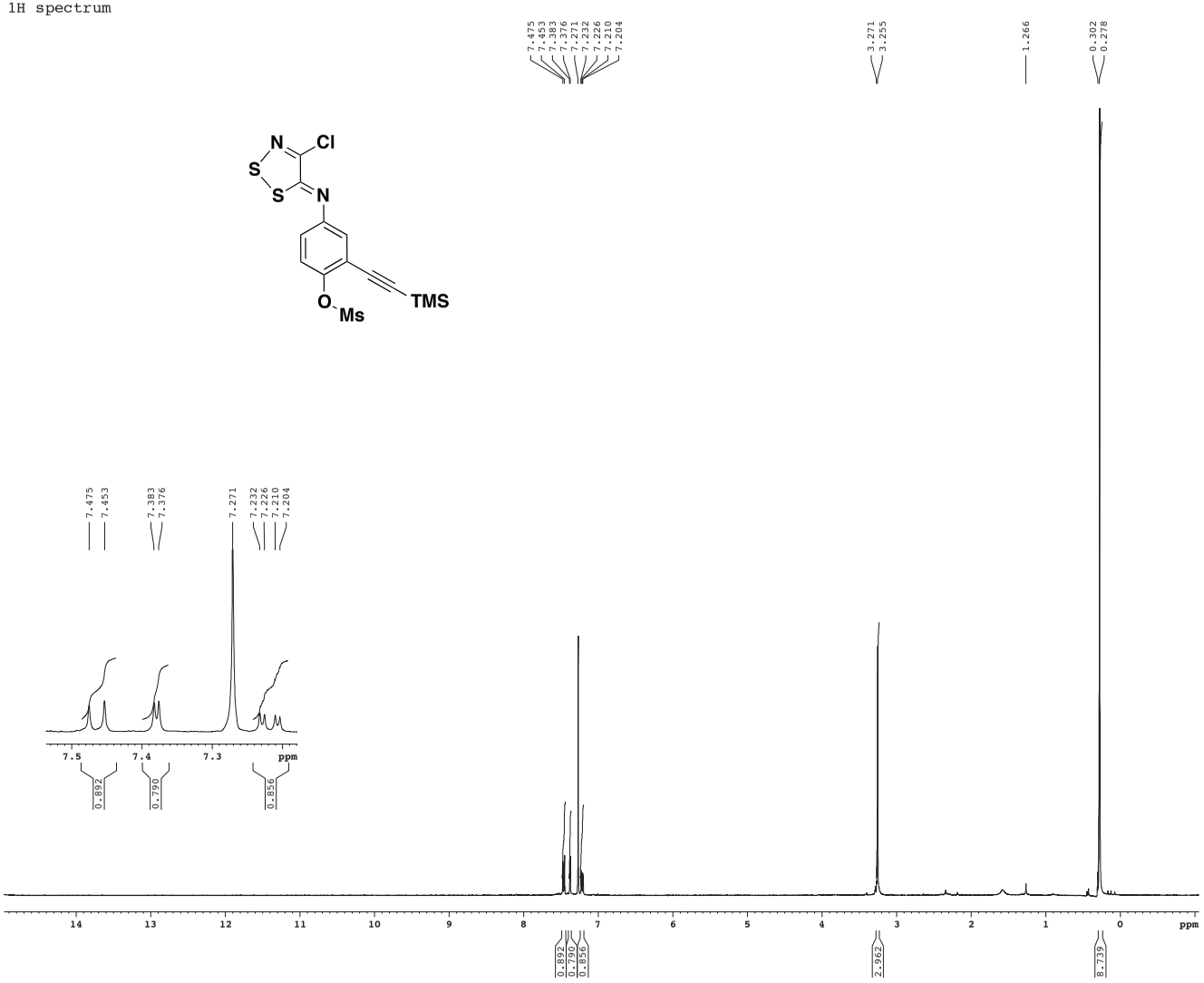


```
Current Data Parameters
USER                rachel
NAME          RB017_try3
EXPNO                    2
PROCNO                   1

F2 - Acquisition Parameters
Date_            20131204
Time                13.34
INSTRUM            drx400
PROBHD   5 mm QNP H/F/P
PULPROG             zg30
TD                  65536
SOLVENT             CDCl3
NS                      8
DS                      2
SWH             6410.256 Hz
FIDRES          0.097813 Hz
AQ              5.1118579 sec
RG                   1024
DW                 78.000 usec
DE                  4.50 usec
TE                 298.0 K
D1            0.10000000 sec
MCREST        0.00000000 sec
MCWRK         0.01500000 sec

======== CHANNEL f1 ========
NUC1                   1H
P1                  12.00 usec
PL1                  0.00 dB
SFO1          400.1328009 MHz

F2 - Processing parameters
SI                  65536
SF            400.1300175 MHz
WDW                    EM
SSB                     0
LB                   0.30 Hz
GB                      0
PC                   2.00
```

Z-restored spin-echo 13C spectrum with 1H decoupling

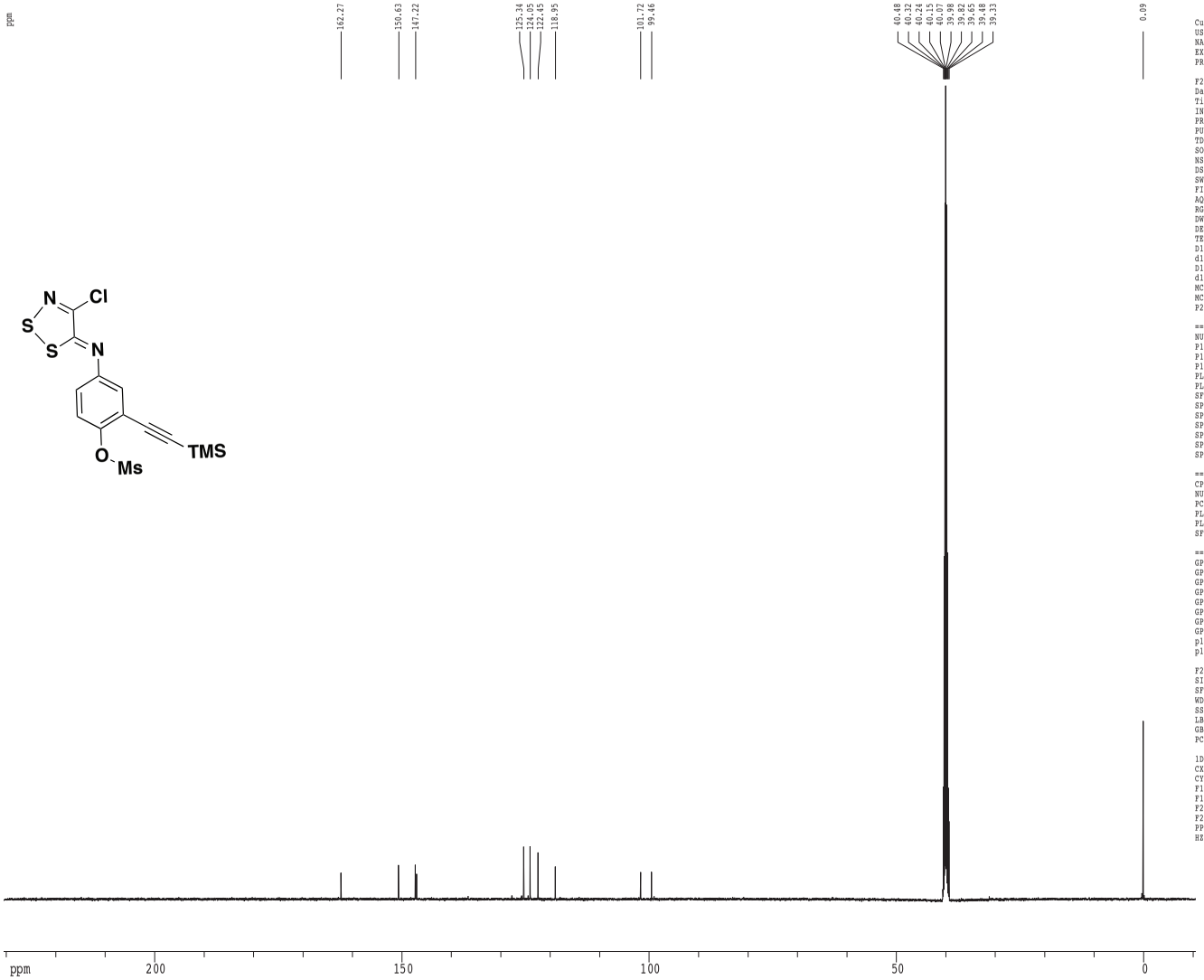


```
Current Data Parameters
USER            rachel
NAME        RD225_iv32
EXPNO                1
PROCNO               1

F2 - Acquisition Parameters
Date_         20121123
Time             21.40
INSTRUM        cryo500
PROBHD   5 mm CPTCI 1H-
PULPROG  SpinEchopg30gp.prd
TD              65536
SOLVENT          DMSO
NS                1024
DS                  16
SWH           30303.031 Hz
FIDRES         0.462388 Hz
AQ            1.0813940 sec
RG               7298.2
DW               16.500 usec
DE                6.00 usec
TE               298.0 K
D1           0.25000000 sec
d11          0.03000000 sec
D16          0.00020000 sec
d17          0.00019600 sec
MCREST       0.00000000 sec
MCWRK        0.01500000 sec
P2                31.00 usec

======= CHANNEL f1 =======
NUC1                13C
P1                15.50 usec
P11              500.00 usec
P12             2000.00 usec
PL0              120.00 dB
PL1               -1.00 dB
SFO1         125.7942548 MHz
SP1                3.20 dB
SP2                3.20 dB
SPNAM1   Crp60,0.5,20.1
SPNAM2      Crp60comp.4
SPOFF1              0.00 Hz
SPOFF2              0.00 Hz

======= CHANNEL f2 =======
CPDPRG2          waltz16
NUC2                 1H
PCPD2            100.00 usec
PL2                1.60 dB
PL12              24.60 dB
SFO2        500.2225011 MHz

===== GRADIENT CHANNEL =====
GPNAM1         SINE.100
GPNAM2         SINE.100
GPX1               0.00 %
GPX2               0.00 %
GPY1               0.00 %
GPY2               0.00 %
GPZ1              30.00 %
GPZ2              50.00 %
p15              500.00 usec
p16             1000.00 usec

F2 - Processing parameters
SI                  65536
SF          125.7804190 MHz
WDW                    EM
SSB                     0
LB                   1.00 Hz
GB                      0
PC                   2.00

1D NMR plot parameters
CX                  22.80 cm
CY                  15.65 cm
F1P               230.460 ppm
F1               28987.37 Hz
F2P               -10.460 ppm
F2               -1315.66 Hz
PPMCM            10.56667 ppm/cm
HZCM           1329.08032 Hz/cm
```

1H spectrum

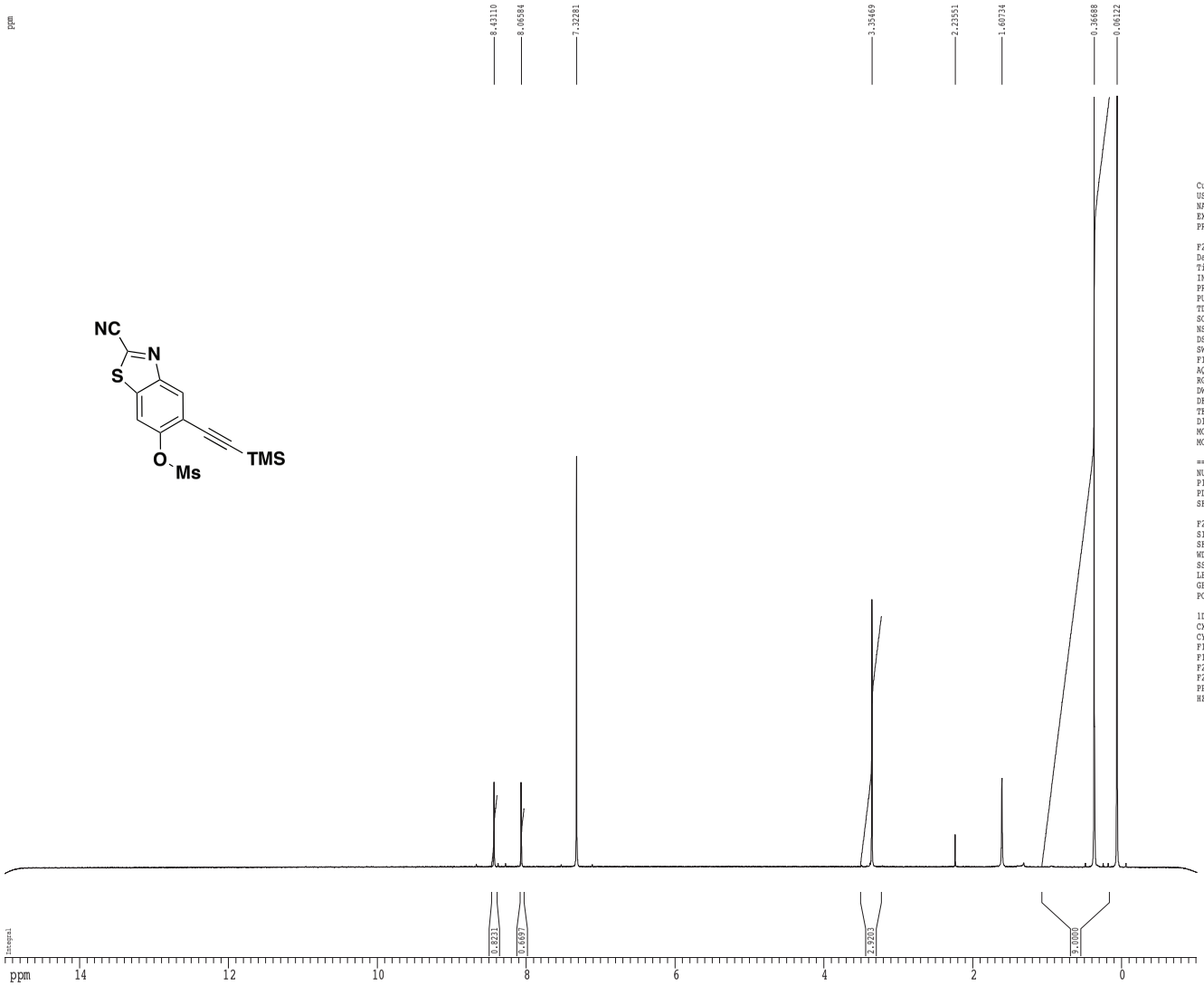


```
Current Data Parameters
USER            rachel
NAME      RD268_iv84hex
EXPNO               1
PROCNO              1

F2 - Acquisition Parameters
Date_          20130117
Time             21.23
INSTRUM        cryo500
PROBHD   5 mm CPTCI 1H-
PULPROG          zg30
TD               81728
SOLVENT          CDCl3
NS                   8
DS                   2
SWH            8012.820 Hz
FIDRES         0.098043 Hz
AQ           5.0998774 sec
RG                 5.7
DW              62.400 usec
DE               6.00 usec
TE              298.0 K
D1           0.10000000 sec
MCREST       0.00000000 sec
MCWRK        0.01500000 sec

======== CHANNEL f1 ========
NUC1                1H
P1                7.50 usec
PL1               1.60 dB
SFO1       500.2235015 MHz

F2 - Processing parameters
SI               65536
SF         500.2200000 MHz
WDW                EM
SSB                 0
LB               0.30 Hz
GB                  0
PC               4.00

1D NMR plot parameters
CX               22.80 cm
CY               15.00 cm
F1P             15.009 ppm
F1             7507.95 Hz
F2P             -1.009 ppm
F2             -504.87 Hz
PPMCM          0.70257 ppm/cm
HZCM         351.43951 Hz/cm
```

Z-restored spin-echo 13C spectrum with 1H decoupling

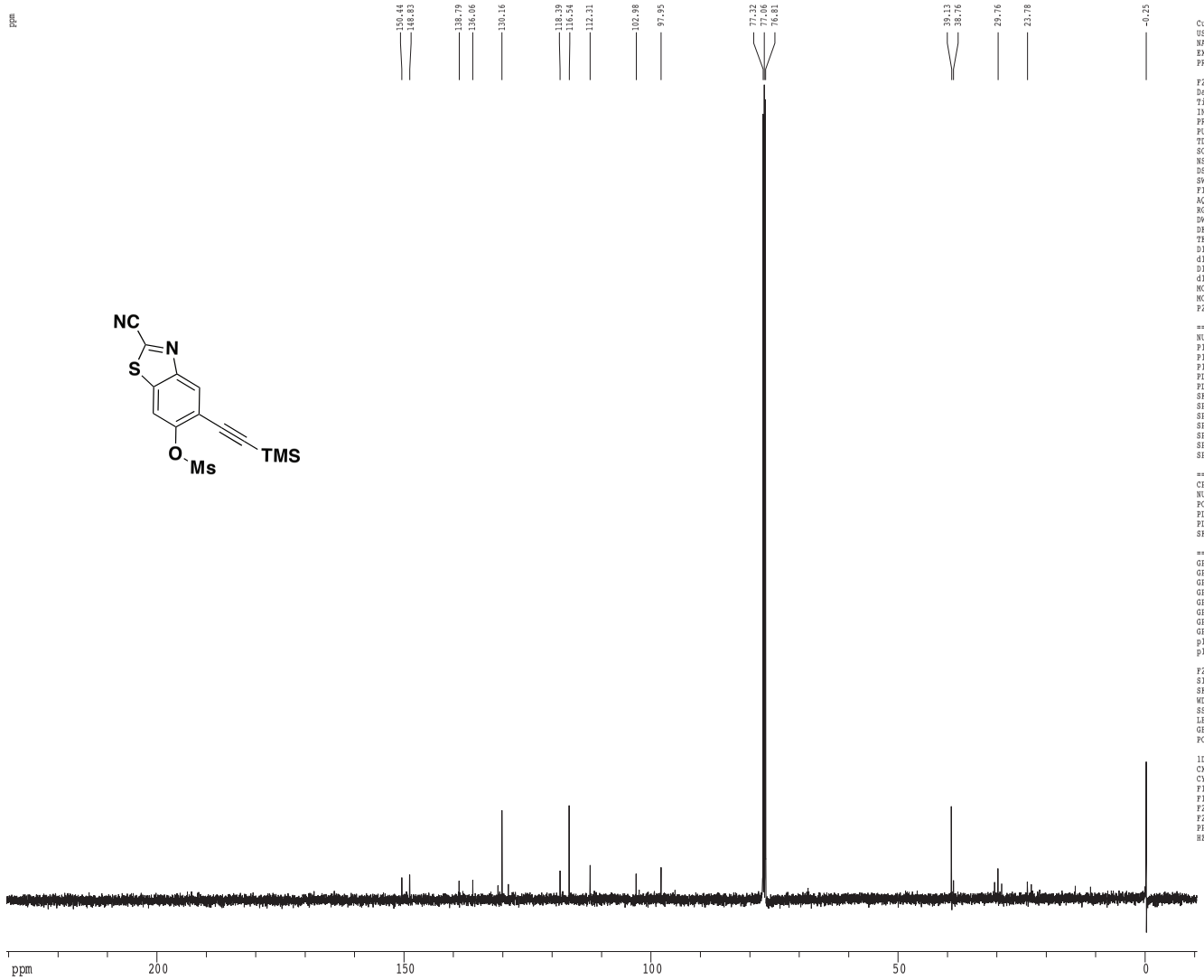


```
Current Data Parameters
USER            rachel
NAME       RB038_cf213C
EXPNO               1
PROCNO              1

F2 - Acquisition Parameters
Date_          20140117
Time             14.08
INSTRUM         cryo500
PROBHD   5 mm CPTCI 1H-
PULPROG  SpinEchopg30gp.prd
TD              65536
SOLVENT          CDCl3
NS                1024
DS                  16
SWH           30303.031 Hz
FIDRES         0.462388 Hz
AQ            1.0813940 sec
RG               2580.3
DW               16.500 usec
DE                6.00 usec
TE               298.0 K
D1          0.25000000 sec
d11         0.03000000 sec
D16         0.00020000 sec
d17         0.00019600 sec
MCREST      0.00000000 sec
MCWRK       0.01500000 sec
P2                31.00 usec

======= CHANNEL f1 =======
NUC1               13C
P1                15.50 usec
P11              500.00 usec
P12             2000.00 usec
PL0              120.00 dB
PL1               -1.00 dB
SFO1        125.7942548 MHz
SP1               3.20 dB
SP2               3.20 dB
SPNAM1   Crp60,0.5,20.1
SPNAM2     Crp60comp.4
SPOFF1            0.00 Hz
SPOFF2            0.00 Hz

======= CHANNEL f2 =======
CPDPRG2         waltz16
NUC2               1H
PCPD2            100.00 usec
PL2                1.60 dB
PL12              24.60 dB
SFO2        500.2225011 MHz

===== GRADIENT CHANNEL ====
GPNAM1         SINE.100
GPNAM2         SINE.100
GPX1              0.00 %
GPX2              0.00 %
GPY1              0.00 %
GPY2              0.00 %
GPZ1             30.00 %
GPZ2             50.00 %
p15              500.00 usec
p16             1000.00 usec

F2 - Processing parameters
SI                65536
SF          125.7804190 MHz
WDW                 EM
SSB                  0
LB                1.00 Hz
GB                   0
PC                2.00

1D NMR plot parameters
CX                22.80 cm
CY                15.65 cm
F1P            230.460 ppm
F1             28987.37 Hz
F2P             -10.460 ppm
F2             -1315.66 Hz
PPMCM          10.56667 ppm/cm
HZCM         1329.08032 Hz/cm
```

1H spectrum

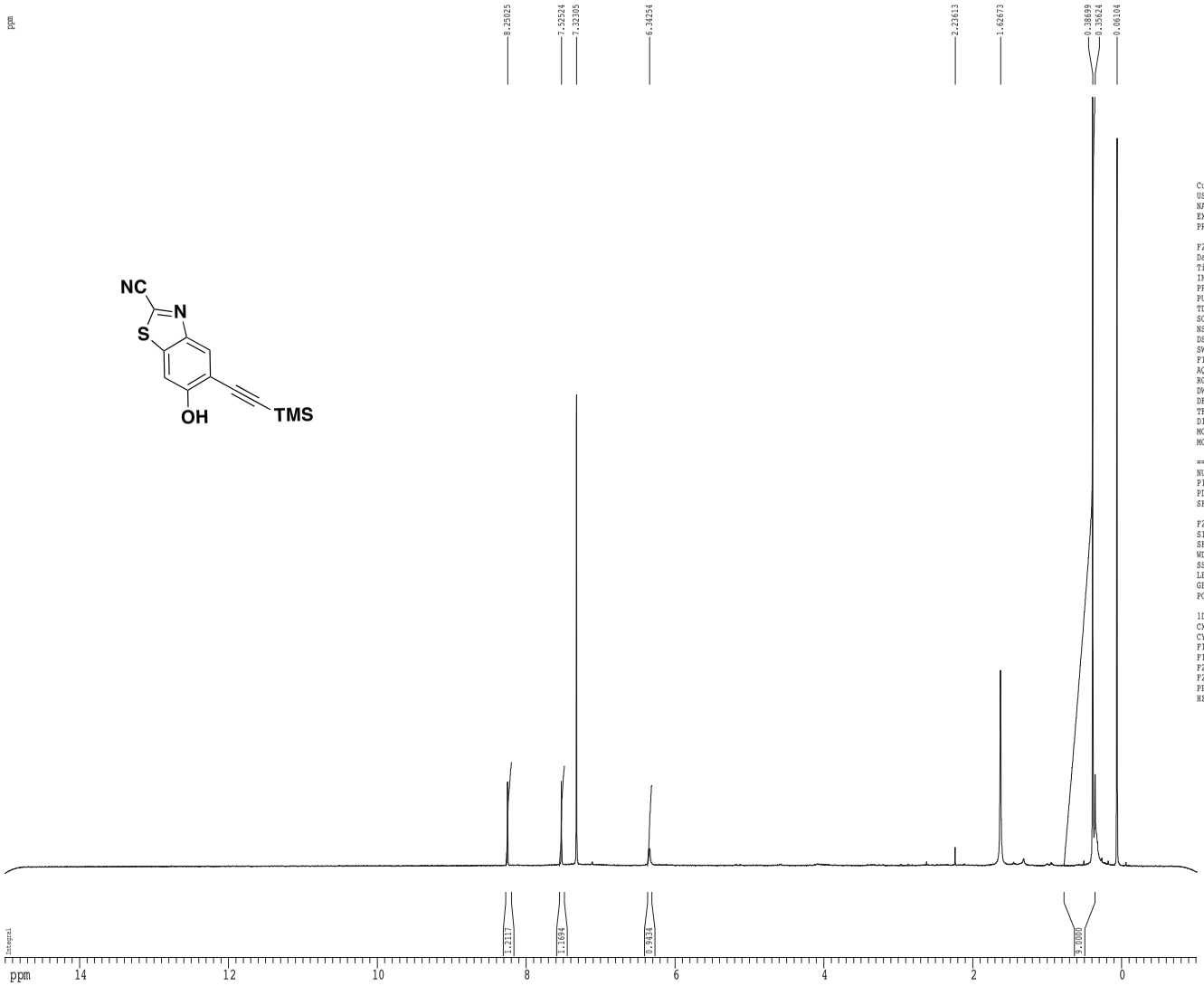


```
Current Data Parameters
USER            rachel
NAME     RD426_tritpent
EXPNO                 2
PROCNO                1

F2 - Acquisition Parameters
Date_          20130807
Time             16.34
INSTRUM        cryo500
PROBHD   5 mm CPTCI 1H-
PULPROG           zg30
TD                81728
SOLVENT           CDCl3
NS                    8
DS                    2
SWH            8012.820 Hz
FIDRES         0.098043 Hz
AQ           5.0998774 sec
RG                  5.7
DW               62.400 usec
DE                6.00 usec
TE                298.0 K
D1           0.10000000 sec
MCREST       0.00000000 sec
MCWRK        0.01500000 sec

======== CHANNEL f1 ========
NUC1                 1H
P1                7.50 usec
PL1               1.60 dB
SFO1       500.2235015 MHz

F2 - Processing parameters
SI                65536
SF         500.2200000 MHz
WDW                  EM
SSB                   0
LB                 0.30 Hz
GB                    0
PC                 4.00

1D NMR plot parameters
CX                22.80 cm
CY                15.00 cm
F1P              15.009 ppm
F1              7507.95 Hz
F2P              -1.009 ppm
F2              -504.87 Hz
PPMCM           0.70257 ppm/cm
HZCM         351.43951 Hz/cm
```

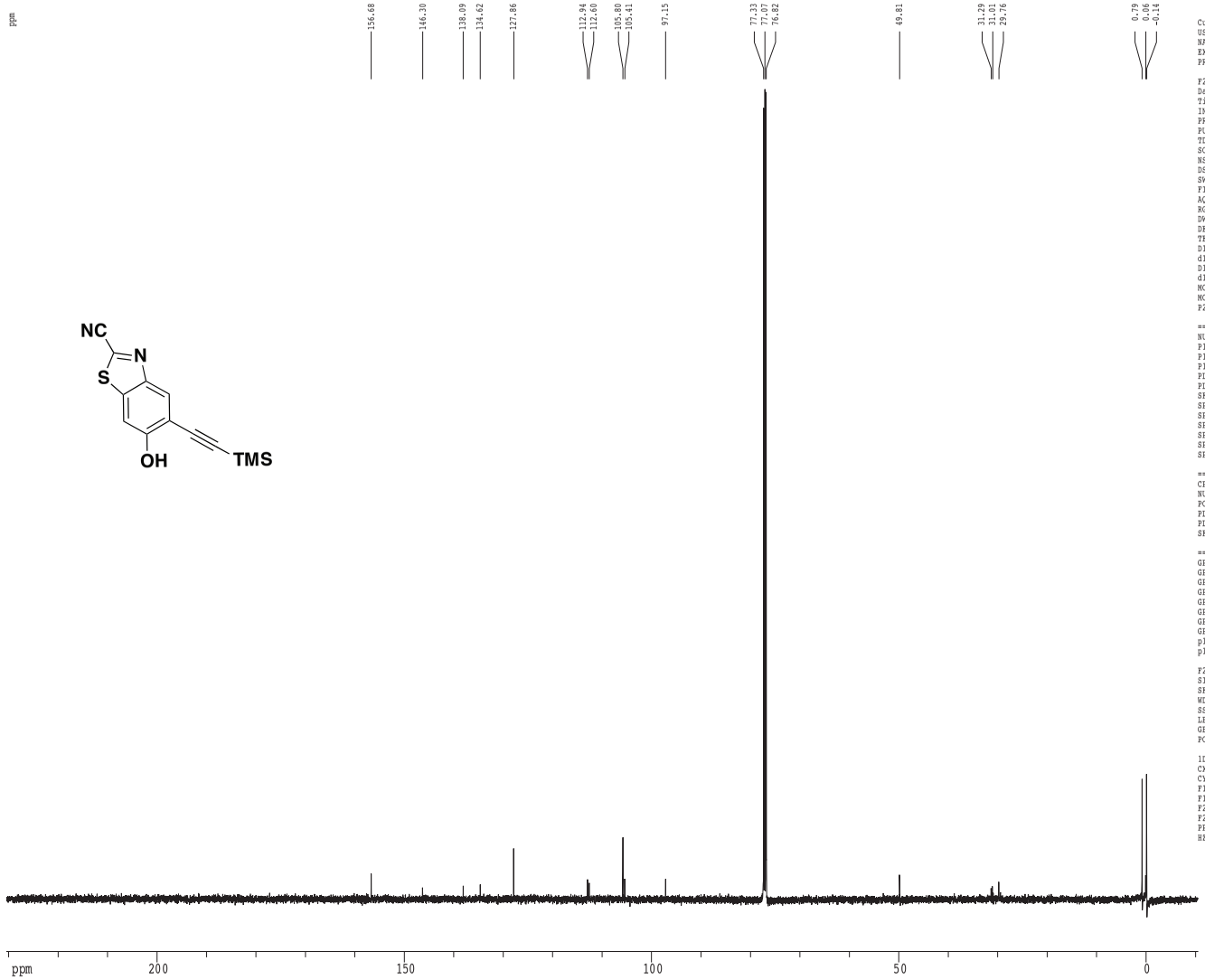


```
Current Data Parameters
USER            rachel
NAME      RD426_v1413C
EXPNO                 2
PROCNO                1

F2 - Acquisition Parameters
Date_        20130802
Time            18.59
INSTRUM        cryo500
PROBHD   5 mm CPTCI 1H-
PULPROG  SpinEchopg30gp.prd
TD             65536
SOLVENT        CDCl3
NS              1024
DS                16
SWH        30303.031 Hz
FIDRES      0.462388 Hz
AQ        1.0813940 sec
RG           7298.2
DW           16.500 usec
DE            6.00 usec
TE            298.0 K
D1        0.25000000 sec
d11       0.03000000 sec
D16       0.00020000 sec
d17       0.00019600 sec
MCREST    0.00000000 sec
MCWRK     0.01500000 sec
P2           31.00 usec

======= CHANNEL f1 =======
NUC1            13C
P1            15.50 usec
P11          500.00 usec
P12         2000.00 usec
PL0          120.00 dB
PL1           -1.00 dB
SFO1     125.7942548 MHz
SP1            3.20 dB
SP2            3.20 dB
SPNAM1   Crp60,0.5,20.1
SPNAM2     Crp60comp.4
SPOFF1         0.00 Hz
SPOFF2         0.00 Hz

======= CHANNEL f2 =======
CPDPRG2      waltz16
NUC2            1H
PCPD2        100.00 usec
PL2            1.60 dB
PL12          24.60 dB
SFO2     500.2225011 MHz

===== GRADIENT CHANNEL ====
GPNAM1       SINE.100
GPNAM2       SINE.100
GPX1           0.00 %
GPX2           0.00 %
GPY1           0.00 %
GPY2           0.00 %
GPZ1          30.00 %
GPZ2          50.00 %
p15         500.00 usec
p16        1000.00 usec

F2 - Processing parameters
SI             65536
SF     125.7804190 MHz
WDW              EM
SSB               0
LB             1.00 Hz
GB                0
PC             1.50

1D NMR plot parameters
CX             22.80 cm
CY             15.65 cm
F1P         230.460 ppm
F1        28987.37 Hz
F2P         -10.460 ppm
F2       -1315.66 Hz
PPMCM       10.56667 ppm/cm
HZCM     1329.08032 Hz/cm
```

1H spectrum

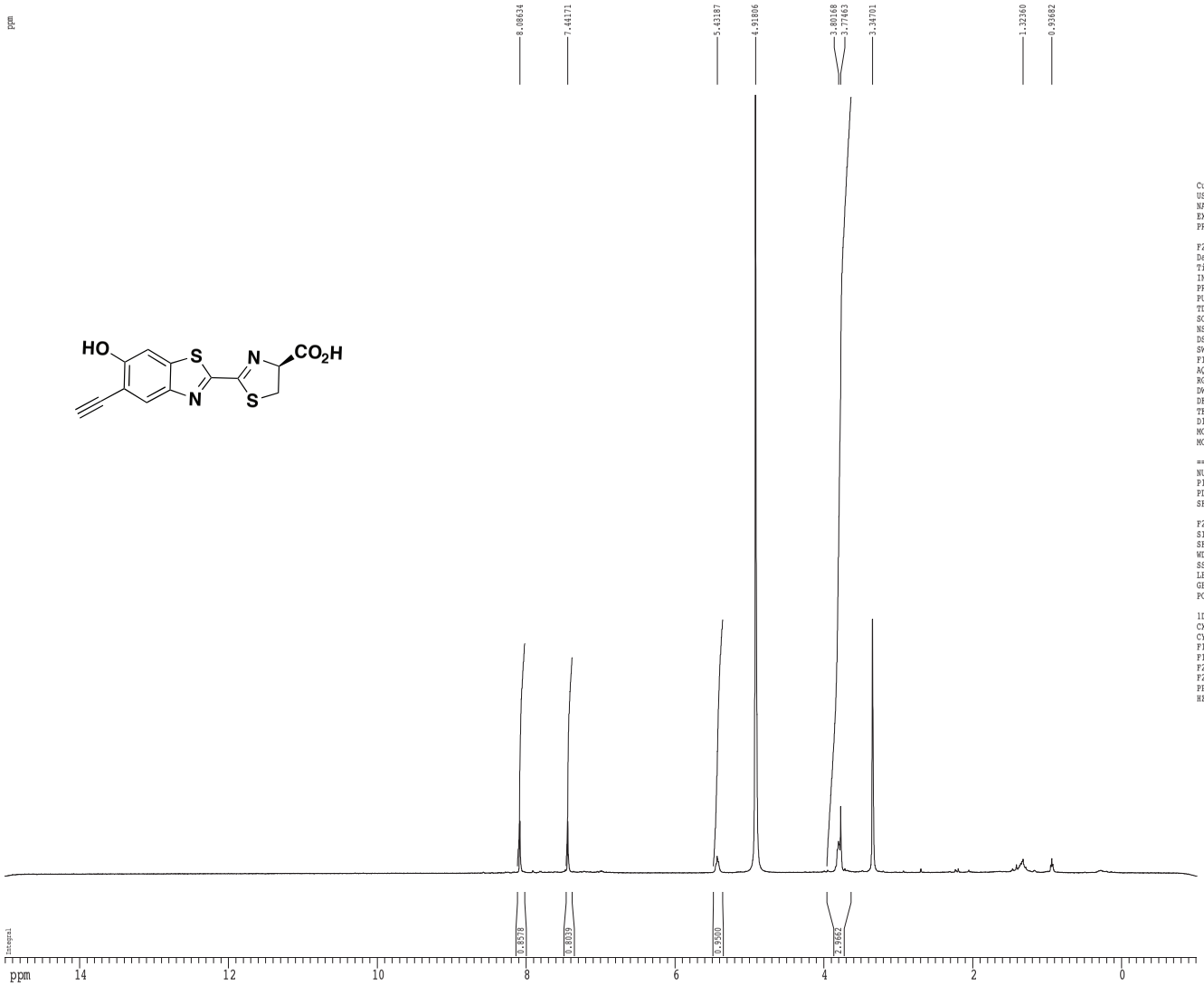


```
Current Data Parameters
USER            rachel
NAME        RD483_trpen
EXPNO                 2
PROCNO                1

F2 - Acquisition Parameters
Date_          20131015
Time             17.21
INSTRUM        cryo500
PROBHD   5 mm CPTCI 1H-
PULPROG          zg30
TD               81728
SOLVENT          CDCl3
NS                   8
DS                   2
SWH            8012.820 Hz
FIDRES         0.098043 Hz
AQ           5.0998774 sec
RG                10.1
DW              62.400 usec
DE               6.00 usec
TE              298.0 K
D1           0.10000000 sec
MCREST       0.00000000 sec
MCWRK        0.01500000 sec

======== CHANNEL f1 ========
NUC1                 1H
P1                7.50 usec
PL1               1.60 dB
SFO1        500.2235015 MHz

F2 - Processing parameters
SI               65536
SF          500.2200000 MHz
WDW                 EM
SSB                  0
LB                0.30 Hz
GB                   0
PC                4.00

1D NMR plot parameters
CX               22.80 cm
CY               15.00 cm
F1P             15.009 ppm
F1             7507.95 Hz
F2P             -1.009 ppm
F2             -504.87 Hz
PPMCM          0.70257 ppm/cm
HZCM         351.43951 Hz/cm
```

Z-restored spin-echo 13C spectrum with 1H decoupling

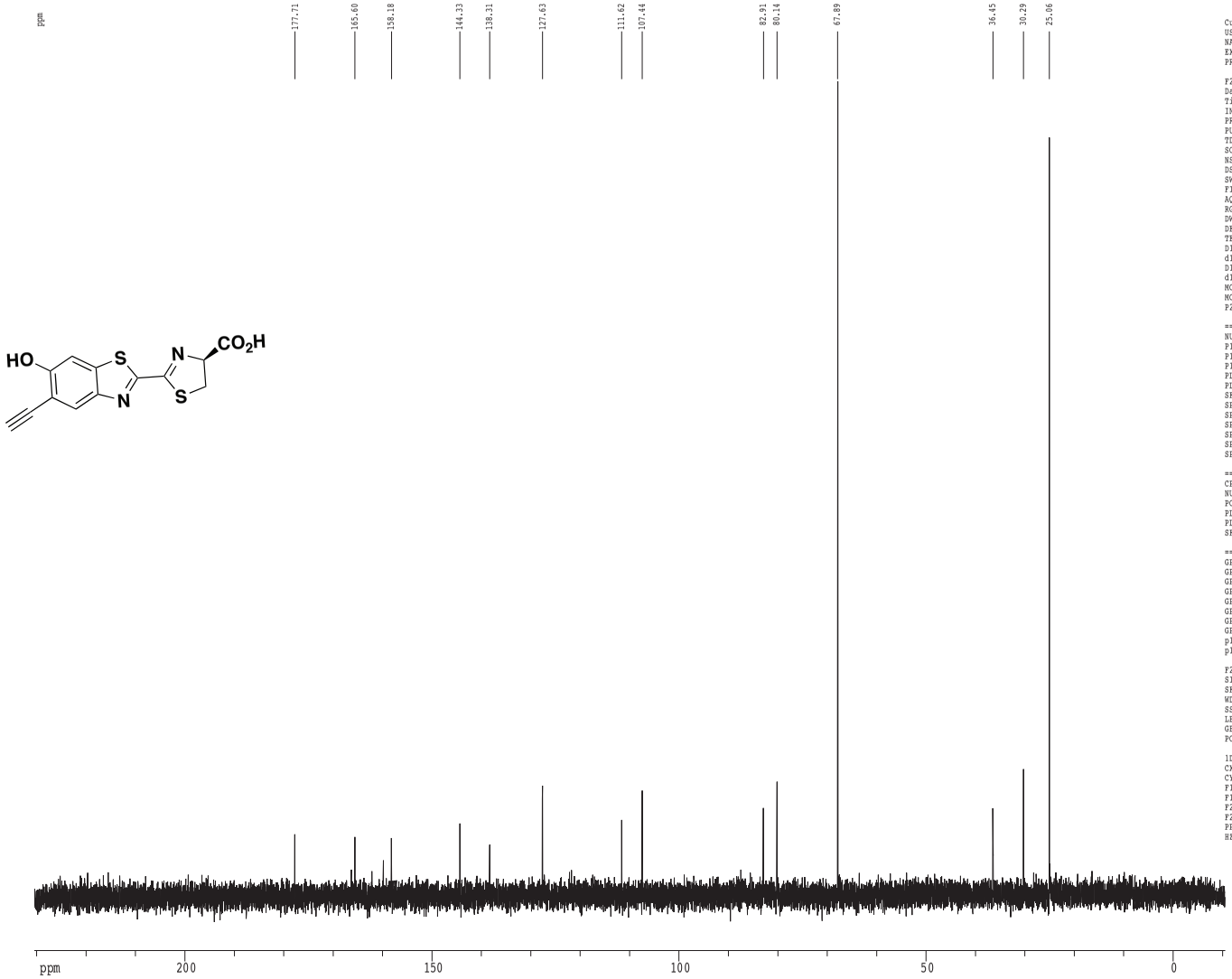


```
Current Data Parameters
USER            rachel
NAME        RD483_d203
EXPNO                2
PROCNO               1

F2 - Acquisition Parameters
Date_          20131015
Time             21.56
INSTRUM        cryo500
PROBHD   5 mm CPTCI 1H-
PULPROG  SpinEchopg30gp.prd
TD              65536
SOLVENT          CDCl3
NS                2048
DS                  16
SWH           30303.031 Hz
FIDRES         0.462388 Hz
AQ           1.0813940 sec
RG              7298.2
DW              16.500 usec
DE               6.00 usec
TE              298.0 K
D1          0.25000000 sec
d11         0.03000000 sec
D16         0.00020000 sec
d17         0.00019600 sec
MCREST      0.00000000 sec
MCWRK       0.01500000 sec
P2               31.00 usec

======= CHANNEL f1 =======
NUC1               13C
P1               15.50 usec
P11             500.00 usec
P12            2000.00 usec
PL0             120.00 dB
PL1              -1.00 dB
SFO1        125.7942548 MHz
SP1              3.20 dB
SP2              3.20 dB
SPNAM1   Crp60,0.5,20.1
SPNAM2     Crp60comp.4
SPOFF1           0.00 Hz
SPOFF2           0.00 Hz

======= CHANNEL f2 =======
CPDPRG2         waltz16
NUC2               1H
PCPD2           100.00 usec
PL2               1.60 dB
PL12             24.60 dB
SFO2        500.2225011 MHz

===== GRADIENT CHANNEL ====
GPNAM1         SINE.100
GPNAM2         SINE.100
GPX1             0.00 %
GPX2             0.00 %
GPY1             0.00 %
GPY2             0.00 %
GPZ1            30.00 %
GPZ2            50.00 %
p15            500.00 usec
p16           1000.00 usec

F2 - Processing parameters
SI              65536
SF         125.7804190 MHz
WDW                EM
SSB                 0
LB               1.00 Hz
GB                  0
PC               2.00

1D NMR plot parameters
CX              22.80 cm
CY              15.65 cm
F1P            230.460 ppm
F1           28987.37 Hz
F2P             -10.460 ppm
F2           -1315.66 Hz
PPMCM          10.56667 ppm/cm
HZCM         1329.08032 Hz/cm
```

1H spectrum

S-1

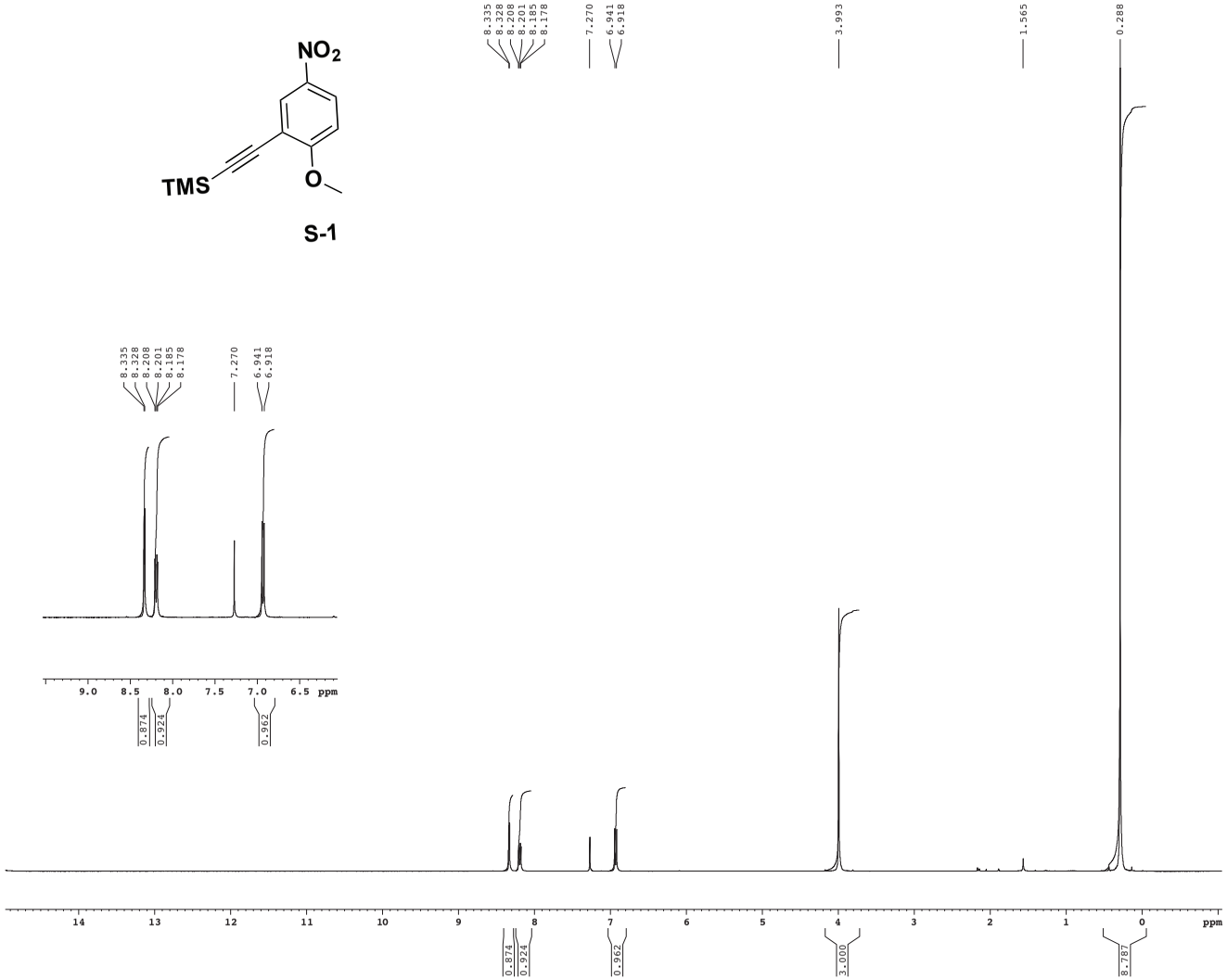


```
Current Data Parameters
USER              rachel
NAME      RD019_ii44_colfrac1
EXPNO                  1
PROCNO                 1

F2 - Acquisition Parameters
Date_          20111026
Time              23.21
INSTRUM         drx400
PROBHD   5 mm QNP H/F/P
PULPROG           zg30
TD               65536
SOLVENT          CDCl3
NS                   8
DS                   2
SWH           6410.256 Hz
FIDRES        0.097813 Hz
AQ            5.1118579 sec
RG               287.4
DW               78.000 usec
DE                4.50 usec
TE               298.0 K
D1          0.10000000 sec
MCREST      0.00000000 sec
MCWRK       0.01500000 sec

======= CHANNEL f1 =======
NUC1                1H
P1               12.00 usec
PL1              -0.60 dB
SFO1       400.1328009 MHz

F2 - Processing parameters
SI               65536
SF         400.1300175 MHz
WDW                EM
SSB                 0
LB               0.30 Hz
GB                  0
PC               2.00
```

Z-restored spin-echo 13C spectrum with 1H decoupling

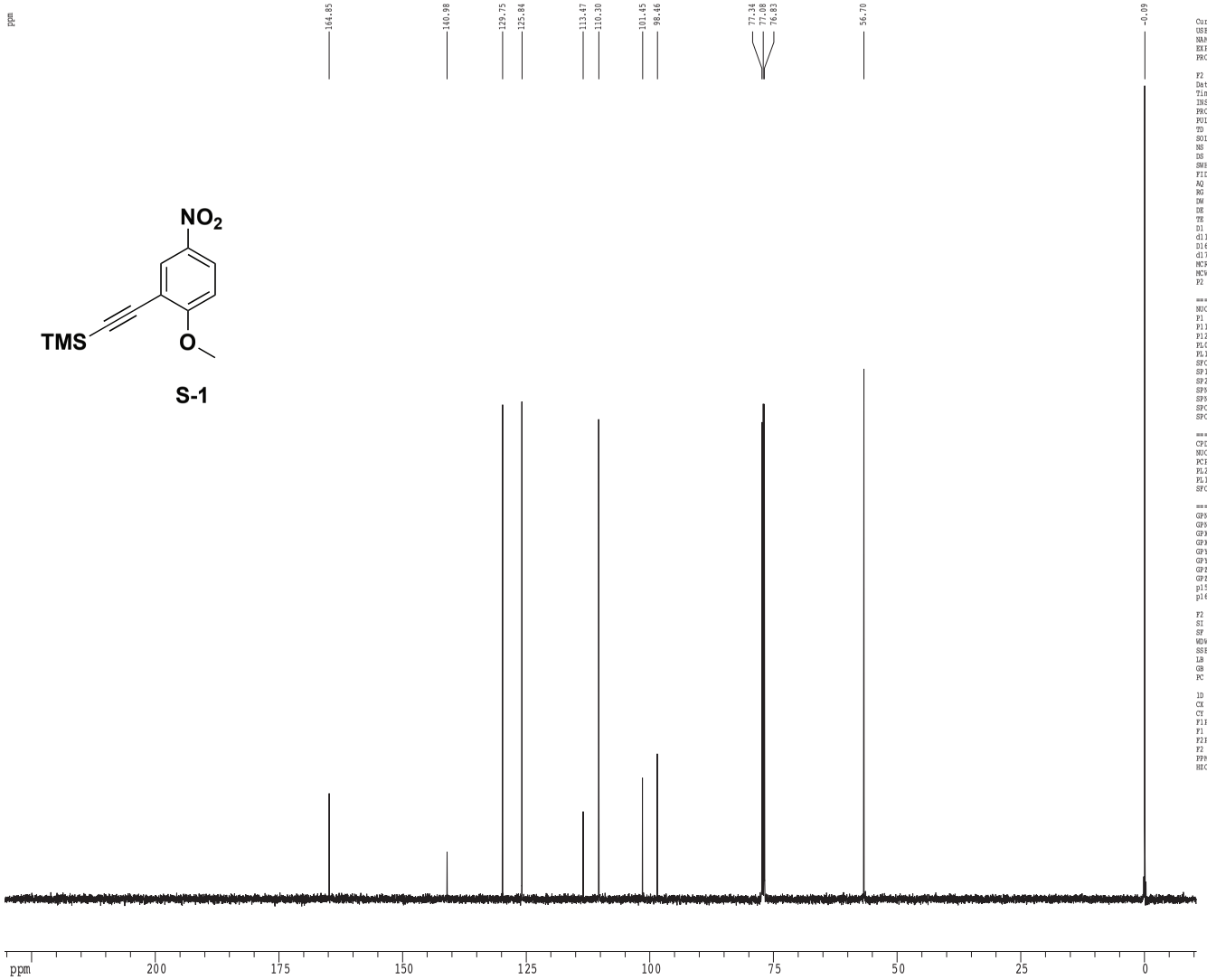


```
Current Data Parameters
USER            rachel
NAME      RD019_ii44_colfracl13C
EXPNO                1
PROCNO               1

F2 - Acquisition Parameters
Date_          20111027
Time               12.03
INSTRUM         cryo500
PROBHD   5 mm CPTCI 1H-
PULPROG  SpinEchopg30gp.prd
TD                65536
SOLVENT           CDCl3
NS                  613
DS                   16
SWH            30303.031 Hz
FIDRES          0.462388 Hz
AQ             1.0813940 sec
RG                2298.8
DW               16.500 usec
DE                6.00 usec
TE               298.0 K
D1           0.25000000 sec
d11          0.03000000 sec
D16          0.00020000 sec
d17          0.00019600 sec
MCREST       0.00000000 sec
MCWRK        0.01500000 sec
P2              31.00 usec

====== CHANNEL f1 ======
NUC1                13C
P1               15.50 usec
P11             500.00 usec
P12            2000.00 usec
PL0             120.00 dB
PL1              -1.00 dB
SFO1        125.7942548 MHz
SP1               3.20 dB
SP2               3.20 dB
SPNAM1    Crp60,0.5,20.1
SPNAM2      Crp60comp.4
SPOFF1            0.00 Hz
SPOFF2            0.00 Hz

====== CHANNEL f2 ======
CPDPRG2         waltz16
NUC2                 1H
PCPD2           100.00 usec
PL2               1.60 dB
PL12             24.60 dB
SFO2        500.2225011 MHz

===== GRADIENT CHANNEL =====
GPNAM1          SINE.100
GPNAM2          SINE.100
GPX1              0.00 %
GPX2              0.00 %
GPY1              0.00 %
GPY2              0.00 %
GPZ1             30.00 %
GPZ2             50.00 %
p15             500.00 usec
p16            1000.00 usec

F2 - Processing parameters
SI                65536
SF          125.7804190 MHz
WDW                  EM
SSB                   0
LB                 1.00 Hz
GB                    0
PC                 2.00

1D NMR plot parameters
CX               22.80 cm
CY               15.65 cm
F1P             230.460 ppm
F1            28987.37 Hz
F2P            -10.460 ppm
F2            -1315.66 Hz
PPMCM          10.56667 ppm/cm
HZCM        1329.08032 Hz/cm
```

Appendix B: NMR spectra for Chapter 3

1H spectrum

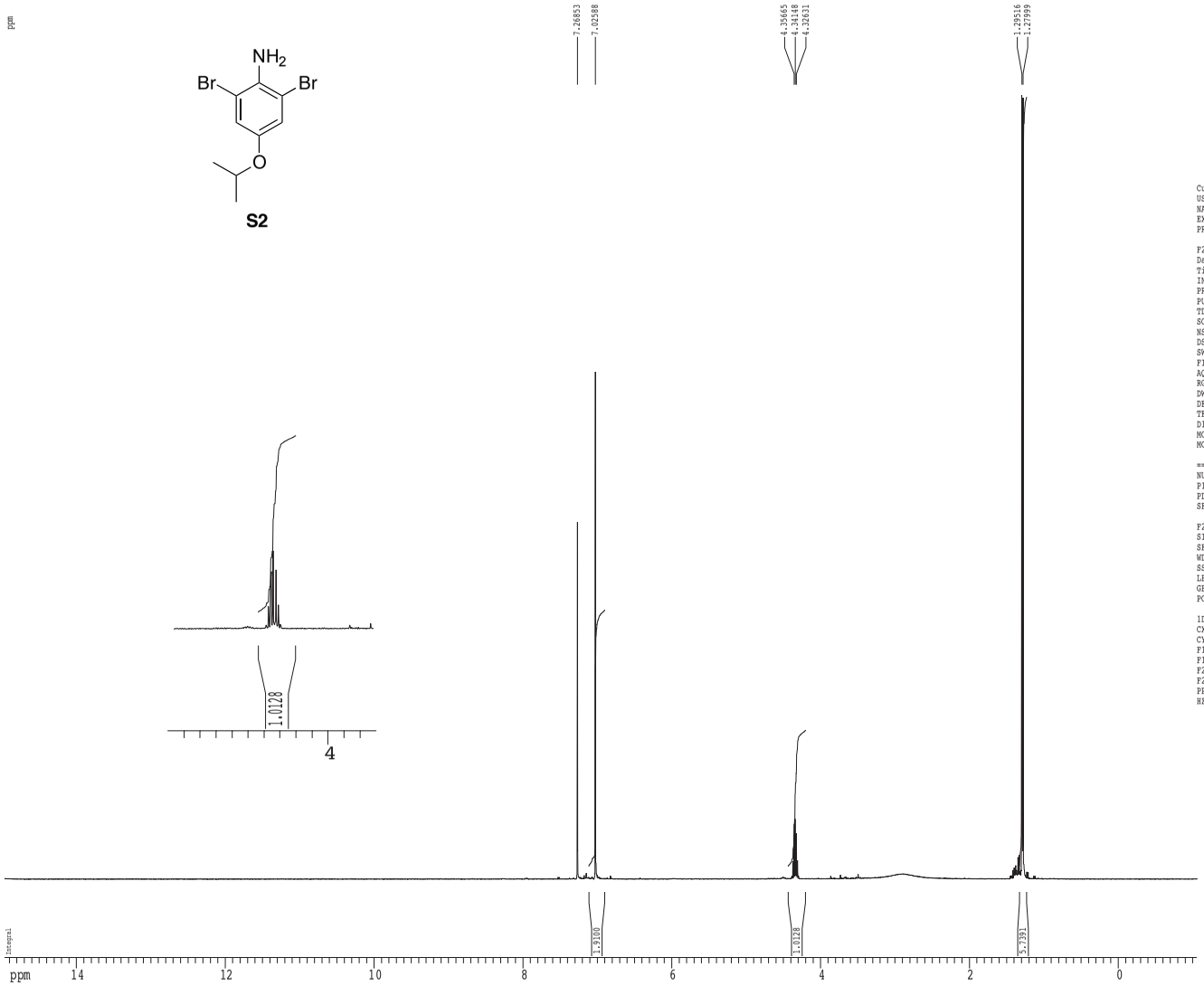


```
Current Data Parameters
USER            rachel
NAME         RB152_try2
EXPNO                 2
PROCNO                1

F2 - Acquisition Parameters
Date_        20140603
Time            12.15
INSTRUM         drx400
PROBHD   5 mm QNP H/F/P
PULPROG          zg30
TD              65536
SOLVENT         CDCl3
NS                  8
DS                  2
SWH          6410.256 Hz
FIDRES       0.097813 Hz
AQ          5.1118579 sec
RG              812.7
DW             78.000 usec
DE              4.50 usec
TE             298.0 K
D1          0.10000000 sec
MCREST      0.00000000 sec
MCWRK       0.01500000 sec

======== CHANNEL f1 ========
NUC1               1H
P1             12.00 usec
PL1             0.00 dB
SFO1      400.1328009 MHz

F2 - Processing parameters
SI              65536
SF        400.1300175 MHz
WDW               EM
SSB                0
LB              0.30 Hz
GB                 0
PC              2.00

1D NMR plot parameters
CX              22.80 cm
CY              15.00 cm
F1P            14.966 ppm
F1             5988.51 Hz
F2P             -1.054 ppm
F2             -421.74 Hz
PPMCM          0.70265 ppm/cm
HZCM        281.15158 Hz/cm
```

Z-restored spin-echo 13C spectrum with 1H decoupling

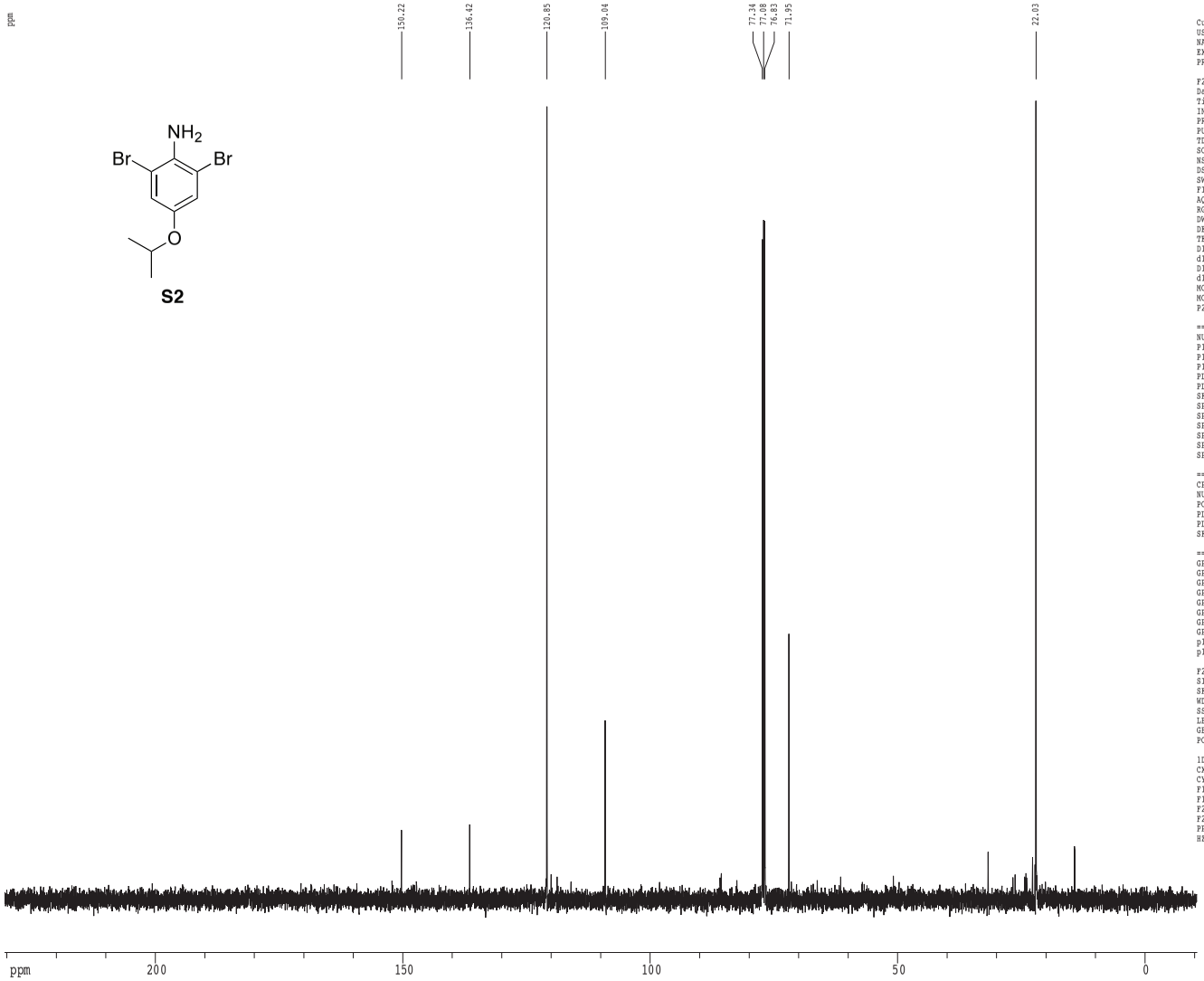


```
Current Data Parameters
USER            rachel
NAME          RB131_13C
EXPNO               1
PROCNO              1

F2 - Acquisition Parameters
Date_         20140512
Time             21.42
INSTRUM        cryo500
PROBHD   5 mm CPTCI 1H-
PULPROG  SpinEchopg30gp.prd
TD              65536
SOLVENT          CDCl3
NS                 260
DS                  16
SWH           30303.031 Hz
FIDRES         0.462388 Hz
AQ            1.0813940 sec
RG              16384
DW             16.500 usec
DE              6.00 usec
TE             298.0 K
D1          0.25000000 sec
d11         0.03000000 sec
D16         0.00020000 sec
d17         0.00019600 sec
MCREST      0.00000000 sec
MCWRK       0.01500000 sec
P2             31.00 usec

======= CHANNEL f1 =======
NUC1              13C
P1             15.50 usec
P11           500.00 usec
P12          2000.00 usec
PL0           120.00 dB
PL1            -1.00 dB
SFO1        125.7942548 MHz
SP1            3.20 dB
SP2            3.20 dB
SPNAM1   Crp60,0.5,20.1
SPNAM2     Crp60comp.4
SPOFF1         0.00 Hz
SPOFF2         0.00 Hz

======= CHANNEL f2 =======
CPDPRG2        waltz16
NUC2              1H
PCPD2         100.00 usec
PL2             1.60 dB
PL12           24.60 dB
SFO2       500.2225011 MHz

===== GRADIENT CHANNEL ====
GPNAM1        SINE.100
GPNAM2        SINE.100
GPX1            0.00 %
GPX2            0.00 %
GPY1            0.00 %
GPY2            0.00 %
GPZ1           30.00 %
GPZ2           50.00 %
p15           500.00 usec
p16          1000.00 usec

F2 - Processing parameters
SI              65536
SF         125.7804190 MHz
WDW               EM
SSB                0
LB              1.00 Hz
GB                 0
PC              2.00

1D NMR plot parameters
CX             22.80 cm
CY             15.65 cm
F1P           230.460 ppm
F1          28987.37 Hz
F2P            -10.460 ppm
F2          -1315.66 Hz
PPMCM         10.56667 ppm/cm
HZCM        1329.08032 Hz/cm
```

1H spectrum

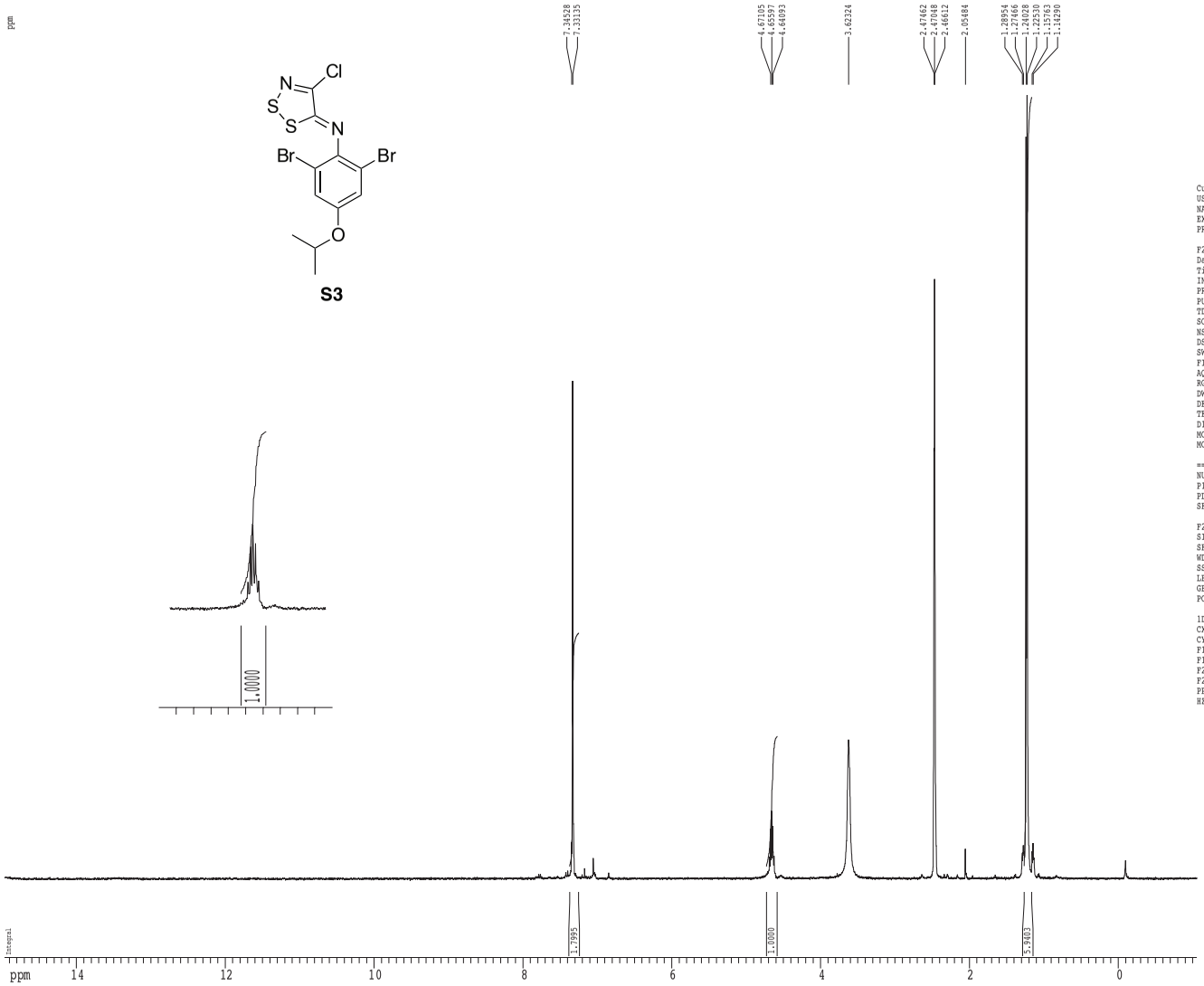

S3

```
Current Data Parameters
USER                rachel
NAME          rb255_pump2
EXPNO                   1
PROCNO                  1

F2 - Acquisition Parameters
Date_            20141001
Time               10.52
INSTRUM           drx400
PROBHD   5 mm QNP H/F/P
PULPROG            zg30
TD                65536
SOLVENT            DMSO
NS                    8
DS                    2
SWH            6410.256 Hz
FIDRES         0.097813 Hz
AQ             5.1118579 sec
RG                 1024
DW               78.000 usec
DE                4.50 usec
TE               297.9 K
D1            0.10000000 sec
MCREST        0.00000000 sec
MCWRK         0.01500000 sec

======== CHANNEL f1 ========
NUC1                 1H
P1                12.00 usec
PL1                0.00 dB
SFO1        400.1328009 MHz

F2 - Processing parameters
SI                 65536
SF          400.1300175 MHz
WDW                  EM
SSB                   0
LB                 0.30 Hz
GB                    0
PC                 2.00

1D NMR plot parameters
CX                22.80 cm
CY                15.00 cm
F1P              14.966 ppm
F1             5988.51 Hz
F2P              -1.054 ppm
F2             -421.74 Hz
PPMCM           0.70265 ppm/cm
HZCM          281.15158 Hz/cm
```

Z-restored spin-echo 13C spectrum with 1H decoupling

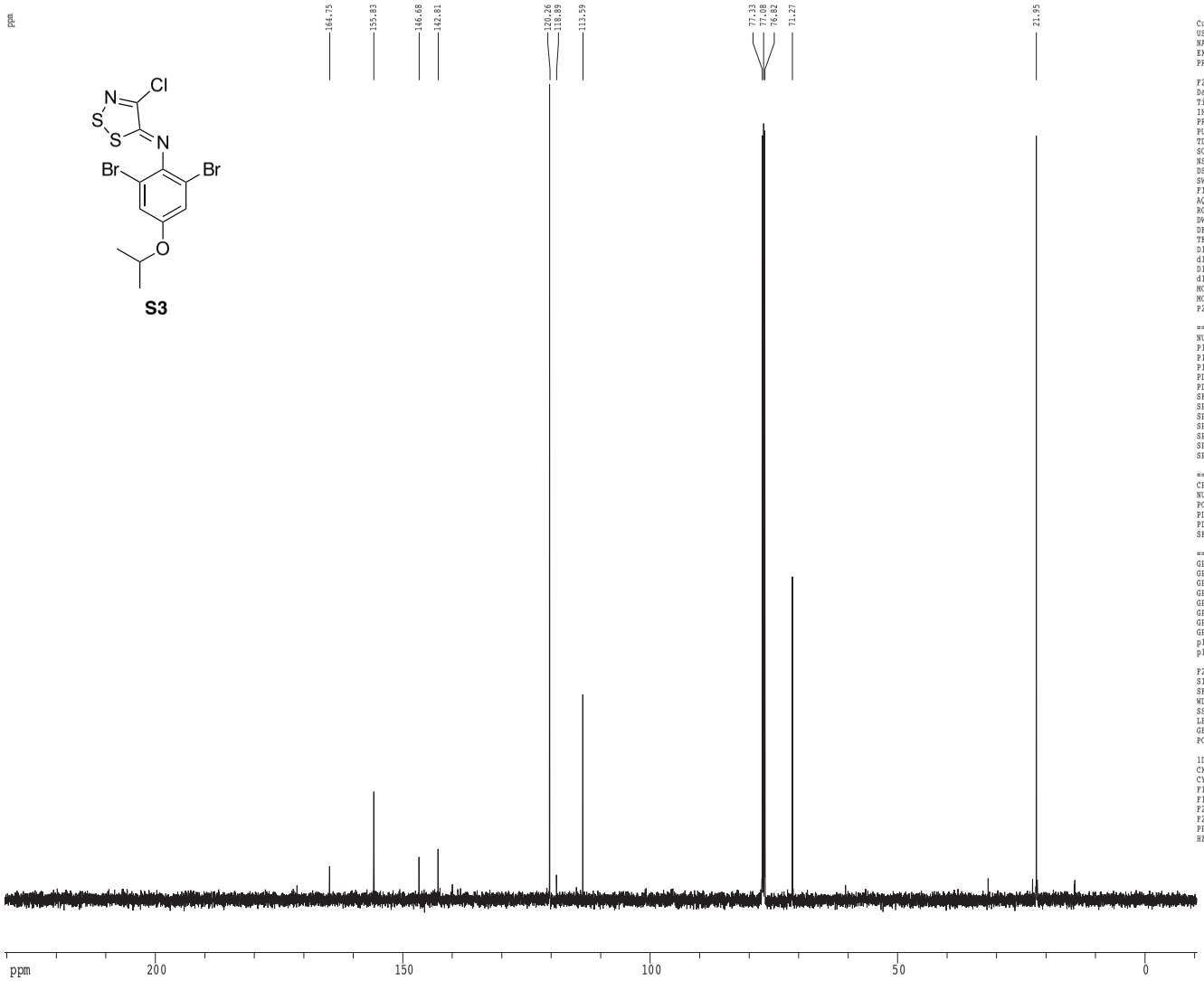


```
Current Data Parameters
USER            rachel
NAME      RB171_cryo13c
EXPNO               2
PROCNO              1

F2 - Acquisition Parameters
Date_         20140624
Time             22.18
INSTRUM        cryo500
PROBHD   5 mm CPTCI 1H-
PULPROG  SpinEchopg30gp.prd
TD              65536
SOLVENT          CDCl3
NS                 568
DS                  16
SWH           30303.031 Hz
FIDRES         0.462388 Hz
AQ            1.0813940 sec
RG                6502
DW              16.500 usec
DE               6.00 usec
TE              298.0 K
D1          0.25000000 sec
d11         0.03000000 sec
D16         0.00020000 sec
d17         0.00019600 sec
MCREST      0.00000000 sec
MCWRK       0.01500000 sec
P2               31.00 usec

======= CHANNEL f1 =======
NUC1               13C
P1               15.50 usec
P11             500.00 usec
P12            2000.00 usec
PL0             120.00 dB
PL1              -1.00 dB
SFO1        125.7942548 MHz
SP1              3.20 dB
SP2              3.20 dB
SPNAM1   Crp60,0.5,20.1
SPNAM2     Crp60comp.4
SPOFF1           0.00 Hz
SPOFF2           0.00 Hz

======= CHANNEL f2 =======
CPDPRG2        waltz16
NUC2               1H
PCPD2           100.00 usec
PL2               1.60 dB
PL12             24.60 dB
SFO2       500.2225011 MHz

===== GRADIENT CHANNEL ====
GPNAM1         SINE.100
GPNAM2         SINE.100
GPX1             0.00 %
GPX2             0.00 %
GPY1             0.00 %
GPY2             0.00 %
GPZ1            30.00 %
GPZ2            50.00 %
p15            500.00 usec
p16           1000.00 usec

F2 - Processing parameters
SI              65536
SF         125.7804190 MHz
WDW                EM
SSB                 0
LB               1.00 Hz
GB                  0
PC               2.00

1D NMR plot parameters
CX              22.80 cm
CY              15.65 cm
F1P            230.460 ppm
F1           28987.37 Hz
F2P             -10.460 ppm
F2           -1315.66 Hz
PPMCM          10.56667 ppm/cm
HZCM         1329.08032 Hz/cm
```

1H spectrum

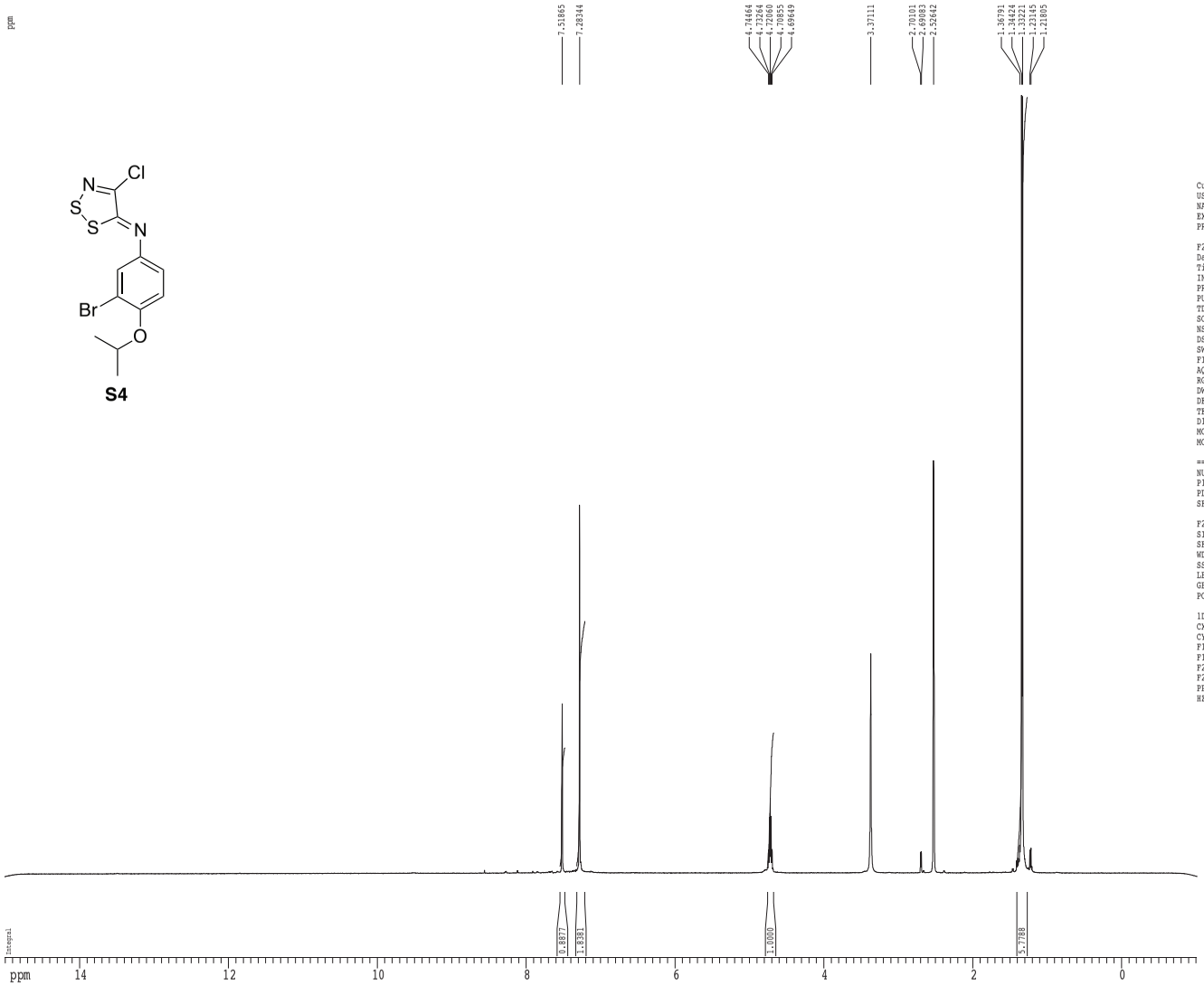

S4

```
Current Data Parameters
USER              rachel
NAME       HB282_1hcryo
EXPNO                  2
PROCNO                 1

F2 - Acquisition Parameters
Date_           20141108
Time              16.33
INSTRUM         cryo500
PROBHD   5 mm CPTCI 1H-
PULPROG            zg30
TD                81728
SOLVENT            DMSO
NS                     8
DS                     2
SWH             8012.820 Hz
FIDRES          0.098043 Hz
AQ            5.0998774 sec
RG                    16
DW               62.400 usec
DE                6.00 usec
TE                298.0 K
D1            0.10000000 sec
MCREST        0.00000000 sec
MCWRK         0.01500000 sec

======== CHANNEL f1 ========
NUC1                  1H
P1                 7.50 usec
PL1                1.60 dB
SFO1        500.2235015 MHz

F2 - Processing parameters
SI                65536
SF          500.2200000 MHz
WDW                  EM
SSB                   0
LB                 0.30 Hz
GB                    0
PC                 4.00

1D NMR plot parameters
CX                22.80 cm
CY                15.00 cm
F1P               15.009 ppm
F1               7507.95 Hz
F2P               -1.009 ppm
F2               -504.87 Hz
PPMCM            0.70257 ppm/cm
HZCM          351.43951 Hz/cm
```

Z-restored spin-echo 13C spectrum with 1H decoupling

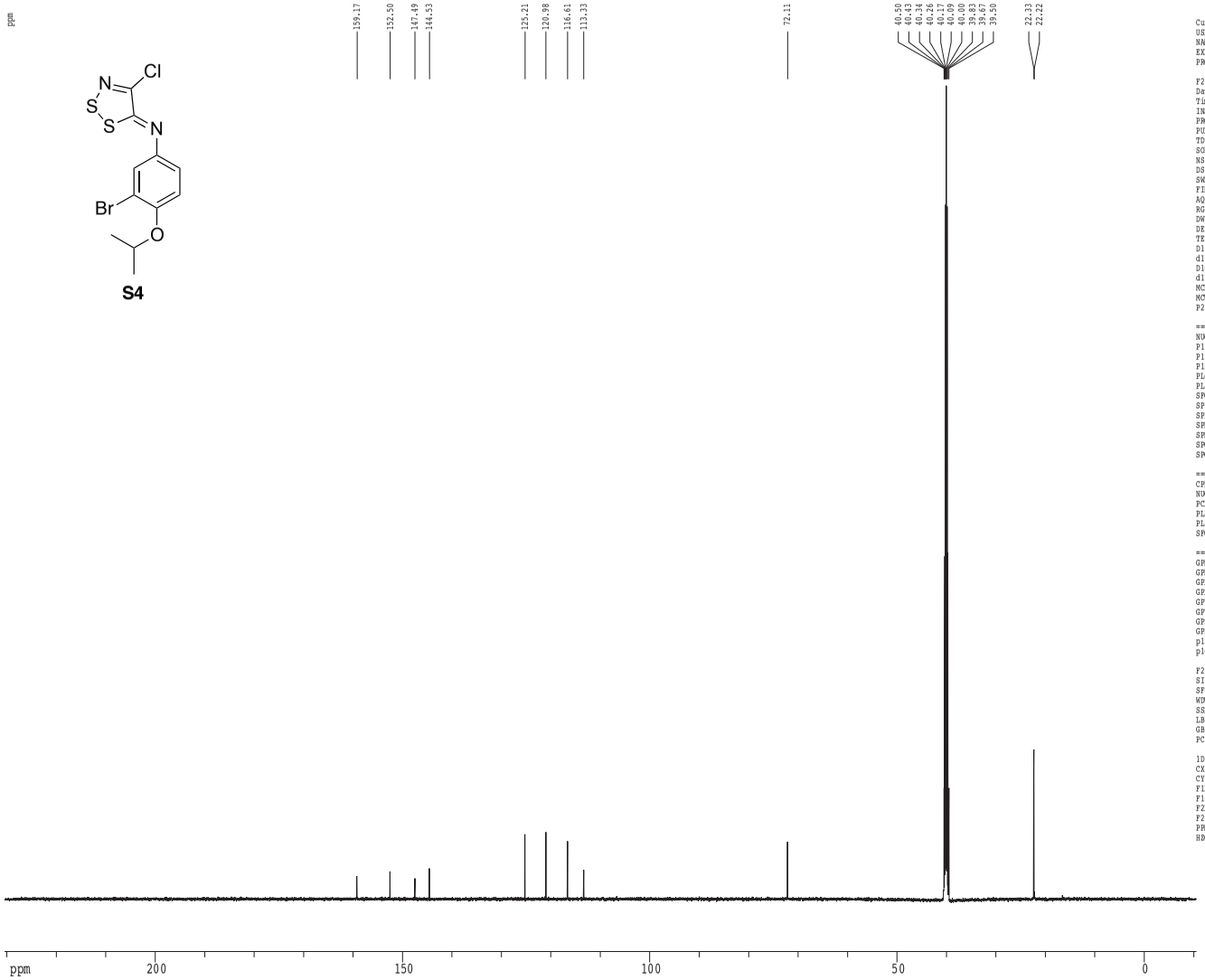


```
Current Data Parameters
USER            rachel
NAME      rb282_13cCryo
EXPNO                 2
PROCNO                1

F2 - Acquisition Parameters
Date_          20141108
Time             16.39
INSTRUM        cryo500
PROBHD   5 mm CPTCI 1H-
PULPROG  SpinEchopg30gp.prd
TD             65536
SOLVENT          CDCl3
NS                1003
DS                  16
SWH           30303.031 Hz
FIDRES         0.462388 Hz
AQ           1.0813940 sec
RG              7298.2
DW              16.500 usec
DE               6.00 usec
TE              298.0 K
D1          0.25000000 sec
d11         0.03000000 sec
D16         0.00020000 sec
d17         0.00019600 sec
MCREST      0.00000000 sec
MCWRK       0.01500000 sec
P2               31.00 usec

======= CHANNEL f1 =======
NUC1               13C
P1               15.50 usec
P11             500.00 usec
P12            2000.00 usec
PL0             120.00 dB
PL1              -1.00 dB
SFO1        125.7942548 MHz
SP1              3.20 dB
SP2              3.20 dB
SPNAM1   Crp60,0.5,20.1
SPNAM2      Crp60comp.4
SPOFF1           0.00 Hz
SPOFF2           0.00 Hz

======= CHANNEL f2 =======
CPDPRG2         waltz16
NUC2               1H
PCPD2           100.00 usec
PL2               1.60 dB
PL12             24.60 dB
SFO2        500.2225011 MHz

===== GRADIENT CHANNEL ====
GPNAM1         SINE.100
GPNAM2         SINE.100
GPX1              0.00 %
GPX2              0.00 %
GPY1              0.00 %
GPY2              0.00 %
GPZ1             30.00 %
GPZ2             50.00 %
p15             500.00 usec
p16            1000.00 usec

F2 - Processing parameters
SI                65536
SF         125.7804190 MHz
WDW                  EM
SSB                   0
LB                1.00 Hz
GB                    0
PC                2.00

1D NMR plot parameters
CX               22.80 cm
CY               15.65 cm
F1P             230.460 ppm
F1            28987.37 Hz
F2P             -10.460 ppm
F2           -1315.66 Hz
PPMCM          10.56667 ppm/cm
HZCM         1329.08032 Hz/cm
```

1H spectrum

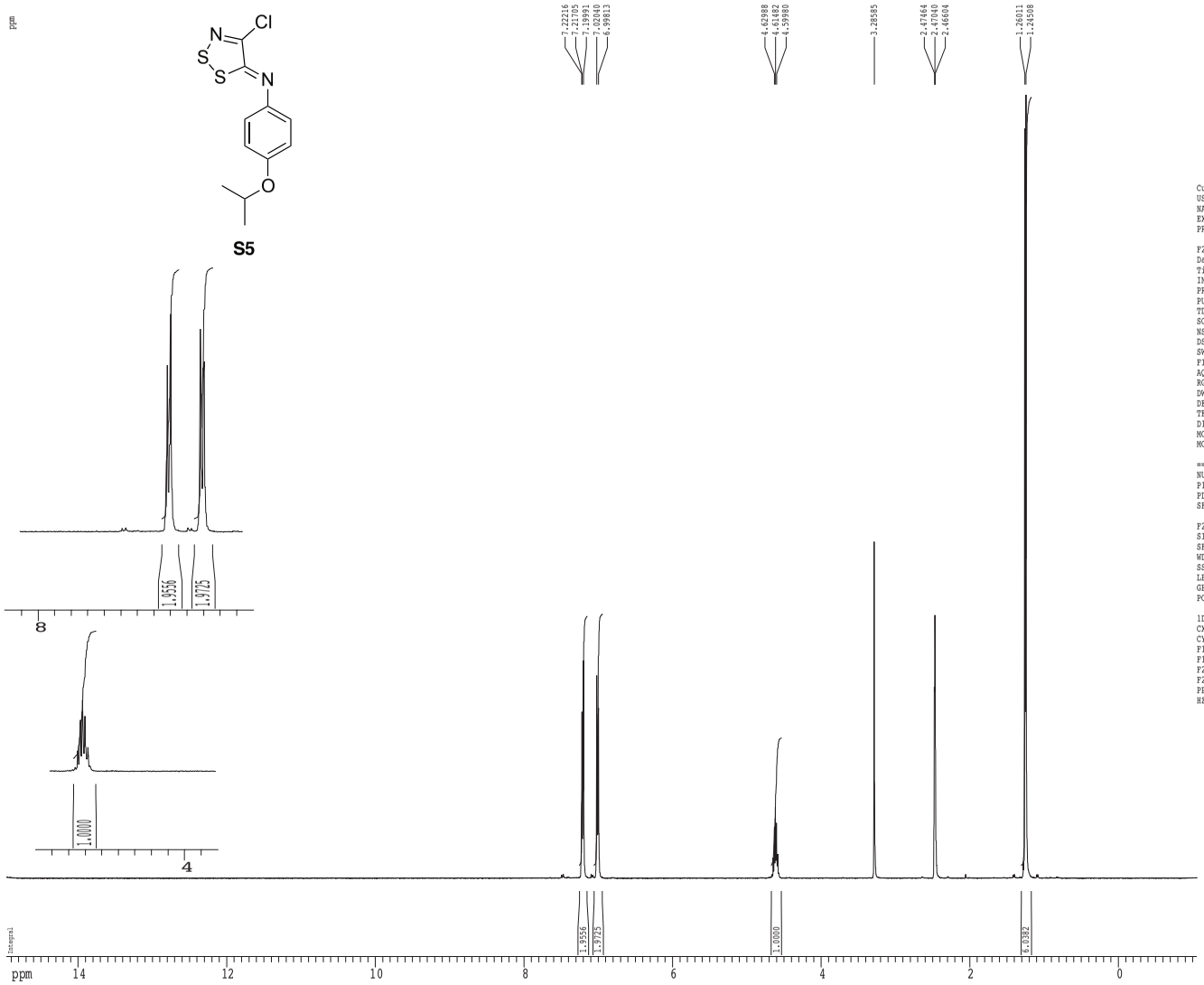


```
Current Data Parameters
USER            rachel
NAME          rb257_dmso
EXPNO                 1
PROCNO                1

F2 - Acquisition Parameters
Date_          20140925
Time               13.33
INSTRUM           drx400
PROBHD   5 mm QNP H/F/P
PULPROG            zg30
TD                65536
SOLVENT            DMSO
NS                    8
DS                    2
SWH            6410.256 Hz
FIDRES         0.097813 Hz
AQ            5.1118579 sec
RG                645.1
DW               78.000 usec
DE                4.50 usec
TE               298.0 K
D1           0.10000000 sec
MCREST       0.00000000 sec
MCWRK        0.01500000 sec

======== CHANNEL f1 ========
NUC1                 1H
P1                12.00 usec
PL1                0.00 dB
SFO1        400.1328009 MHz

F2 - Processing parameters
SI                65536
SF          400.1300175 MHz
WDW                  EM
SSB                   0
LB                 0.30 Hz
GB                    0
PC                 2.00

1D NMR plot parameters
CX                22.80 cm
CY                15.00 cm
F1P              14.966 ppm
F1             5988.51 Hz
F2P              -1.054 ppm
F2             -421.74 Hz
PPMCM          0.70265 ppm/cm
HZCM         281.15158 Hz/cm
```

Z-restored spin-echo 13C spectrum with 1H decoupling

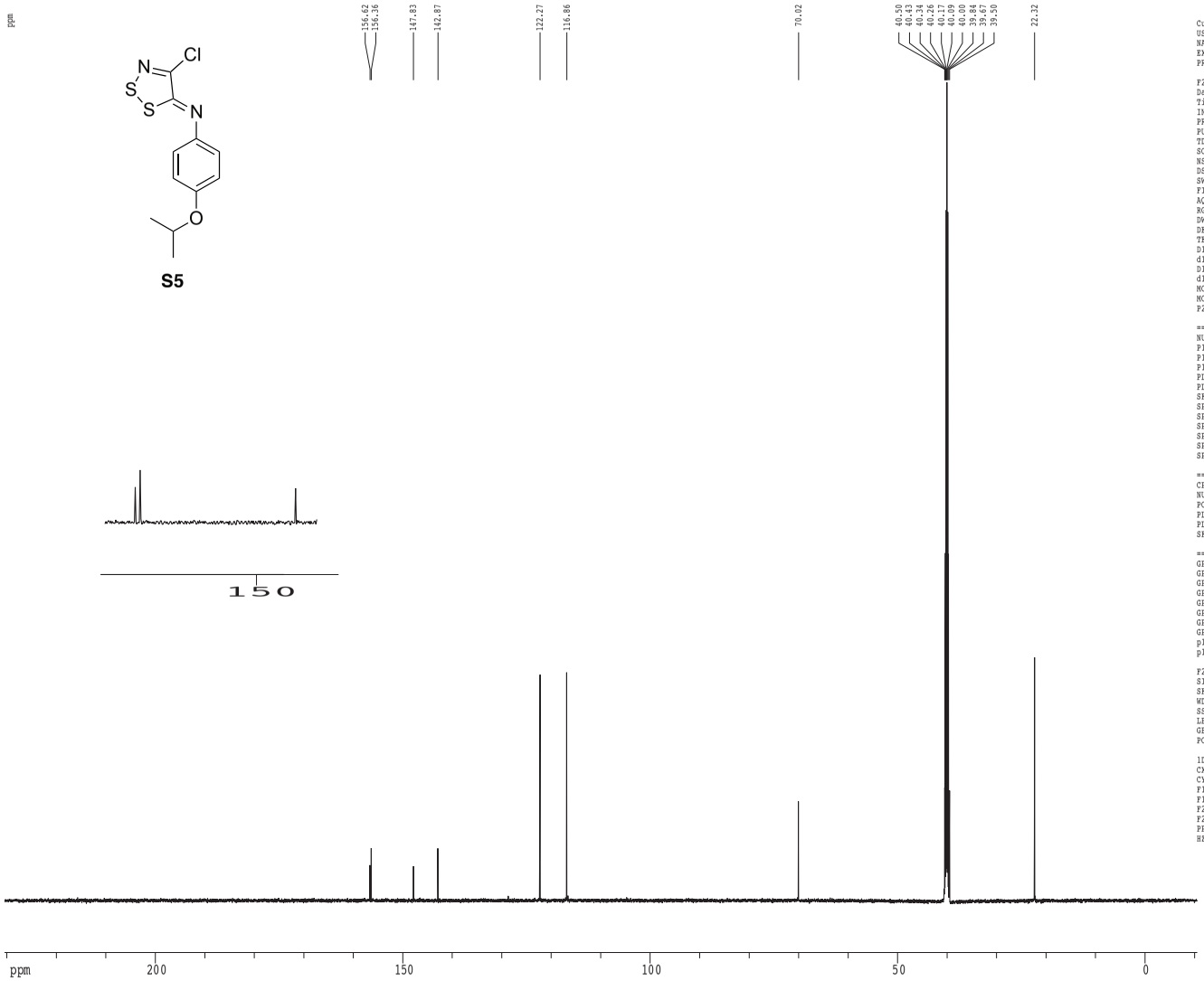


```
Current Data Parameters
USER            rachel
NAME          RB257_13c
EXPNO                 2
PROCNO                1

F2 - Acquisition Parameters
Date_          20140925
Time              15.17
INSTRUM         cryo500
PROBHD   5 mm CPTCI 1H-
PULPROG  SpinEchopg30gp.prd
TD                65536
SOLVENT            DMSO
NS                   837
DS                    16
SWH           30303.031 Hz
FIDRES         0.462388 Hz
AQ            1.0813940 sec
RG               2896.3
DW               16.500 usec
DE                6.00 usec
TE               298.0 K
D1           0.25000000 sec
d11          0.03000000 sec
D16          0.00020000 sec
d17          0.00019600 sec
MCREST       0.00000000 sec
MCWRK        0.01500000 sec
P2                31.00 usec

======= CHANNEL f1 =======
NUC1                13C
P1                15.50 usec
P11              500.00 usec
P12             2000.00 usec
PL0              120.00 dB
PL1               -1.00 dB
SFO1         125.7942548 MHz
SP1                3.20 dB
SP2                3.20 dB
SPNAM1   Crp60,0.5,20.1
SPNAM2      Crp60comp.4
SPOFF1             0.00 Hz
SPOFF2             0.00 Hz

======= CHANNEL f2 =======
CPDPRG2         waltz16
NUC2                 1H
PCPD2            100.00 usec
PL2                1.60 dB
PL12              24.60 dB
SFO2         500.2225011 MHz

===== GRADIENT CHANNEL ====
GPNAM1          SINE.100
GPNAM2          SINE.100
GPX1               0.00 %
GPX2               0.00 %
GPY1               0.00 %
GPY2               0.00 %
GPZ1              30.00 %
GPZ2              50.00 %
p15              500.00 usec
p16             1000.00 usec

F2 - Processing parameters
SI                 65536
SF         125.7804190 MHz
WDW                   EM
SSB                    0
LB                  1.00 Hz
GB                     0
PC                  2.00

1D NMR plot parameters
CX                 22.80 cm
CY                 15.65 cm
F1P               230.460 ppm
F1               28987.37 Hz
F2P               -10.460 ppm
F2              -1315.66 Hz
PPMCM            10.56667 ppm/cm
HZCM           1329.08032 Hz/cm
```

1H spectrum

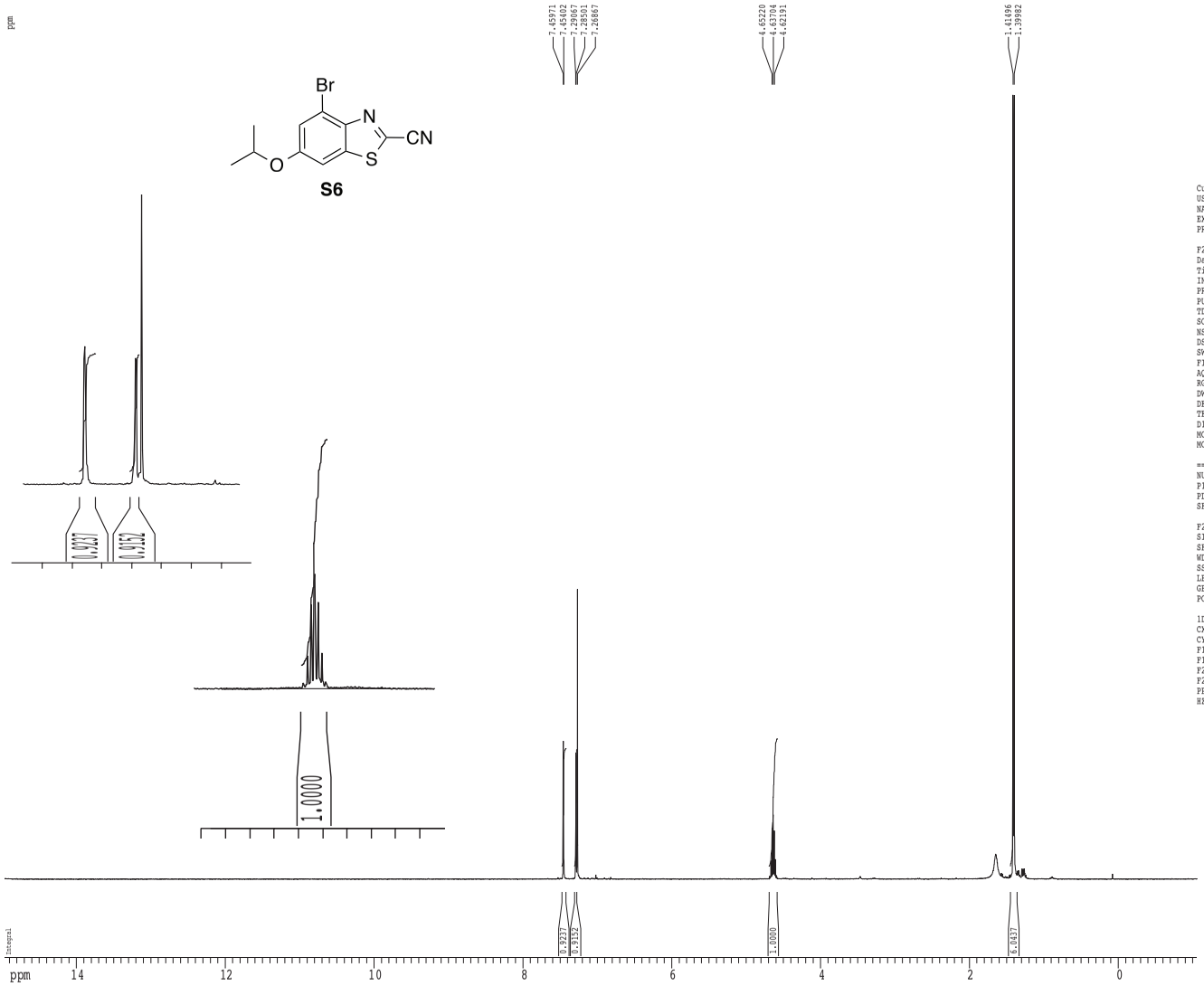

Current Data Parameters
USER rachel
NAME RB156
EXPNO 1
PROCNO 1

F2 - Acquisition Parameters
Date_ 20140605
Time 10.16
INSTRUM drx400
PROBHD 5 mm QNP H/F/P
PULPROG zg30
TD 65536
SOLVENT CDCl3
NS 8
DS 2
SWH 6410.256 Hz
FIDRES 0.097813 Hz
AQ 5.1118579 sec
RG 812.7
DW 78.000 usec
DE 4.50 usec
TE 298.0 K
D1 0.10000000 sec
MCREST 0.00000000 sec
MCWRK 0.01500000 sec

======== CHANNEL f1 ========
NUC1 1H
P1 12.00 usec
PL1 0.00 dB
SFO1 400.1328009 MHz

F2 - Processing parameters
SI 65536
SF 400.1300175 MHz
WDW EM
SSB 0
LB 0.30 Hz
GB 0
PC 2.00

1D NMR plot parameters
CX 22.80 cm
CY 15.00 cm
F1P 14.966 ppm
F1 5988.51 Hz
F2P -1.054 ppm
F2 -421.74 Hz
PPMCM 0.70265 ppm/cm
HZCM 281.15158 Hz/cm

Z-restored spin-echo 13C spectrum with 1H decoupling

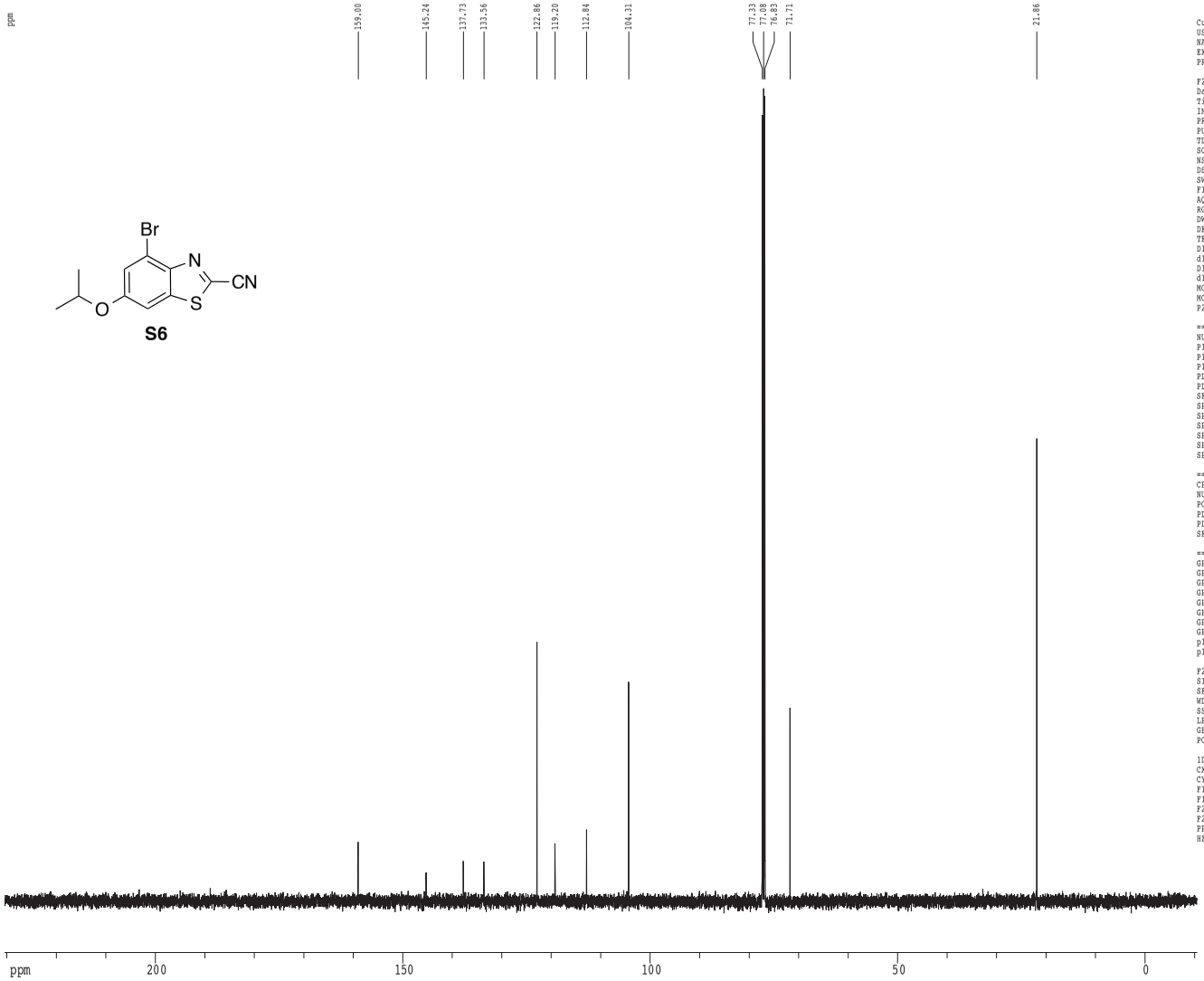


```
Current Data Parameters
USER            rachel
NAME      Rb156_cryo13c
EXPNO               2
PROCNO              1

F2 - Acquisition Parameters
Date_        20140605
Time           11.13
INSTRUM        cryo500
PROBHD   5 mm CPTCI 1H-
PULPROG  SpinEchopg30gp.prd
TD            65536
SOLVENT       CDCl3
NS              613
DS               16
SWH        30303.031 Hz
FIDRES      0.462388 Hz
AQ         1.0813940 sec
RG             6502
DW           16.500 usec
DE            6.00 usec
TE           298.0 K
D1        0.25000000 sec
d11       0.03000000 sec
D16       0.00020000 sec
d17       0.00019600 sec
MCREST    0.00000000 sec
MCWRK     0.01500000 sec
P2           31.00 usec

======= CHANNEL f1 =======
NUC1            13C
P1           15.50 usec
P11         500.00 usec
P12        2000.00 usec
PL0         120.00 dB
PL1          -1.00 dB
SFO1     125.7942548 MHz
SP1          3.20 dB
SP2          3.20 dB
SPNAM1   Crp60,0.5,20.1
SPNAM2     Crp60comp.4
SPOFF1       0.00 Hz
SPOFF2       0.00 Hz

======= CHANNEL f2 =======
CPDPRG2      waltz16
NUC2            1H
PCPD2       100.00 usec
PL2           1.60 dB
PL12         24.60 dB
SFO2     500.2225011 MHz

===== GRADIENT CHANNEL ====
GPNAM1      SINE.100
GPNAM2      SINE.100
GPX1         0.00 %
GPX2         0.00 %
GPY1         0.00 %
GPY2         0.00 %
GPZ1        30.00 %
GPZ2        50.00 %
p15        500.00 usec
p16       1000.00 usec

F2 - Processing parameters
SI            65536
SF     125.7804190 MHz
WDW             EM
SSB              0
LB            1.00 Hz
GB               0
PC            2.00

1D NMR plot parameters
CX           22.80 cm
CY           15.65 cm
F1P        230.460 ppm
F1       28987.37 Hz
F2P        -10.460 ppm
F2       -1315.66 Hz
PPMCM      10.56667 ppm/cm
HZCM    1329.08032 Hz/cm
```

1H spectrum

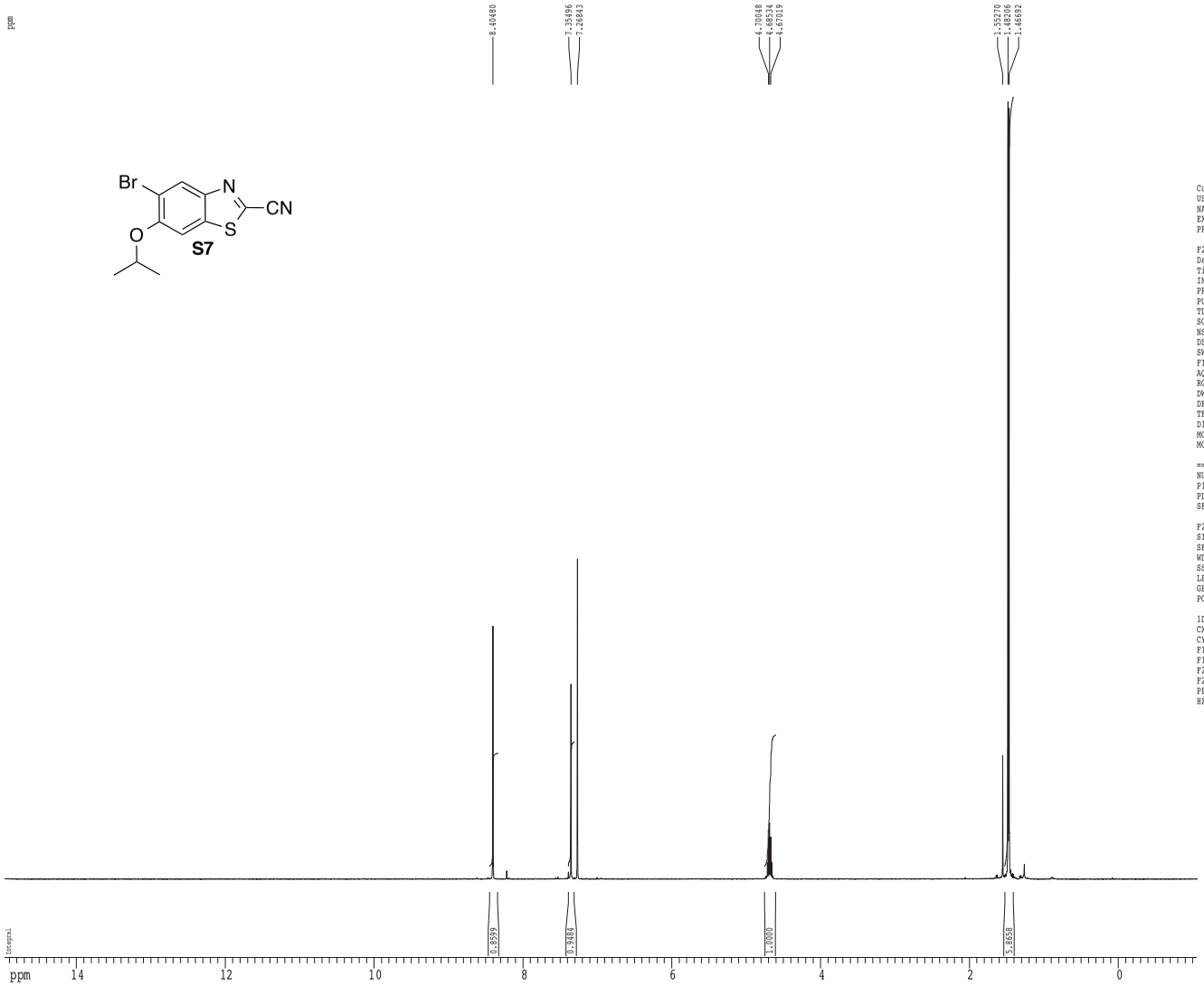


```
Current Data Parameters
USER            rachel
NAME            rb_294
EXPNO                1
PROCNO               1

F2 - Acquisition Parameters
Date_        20141121
Time            12.05
INSTRUM        drx400
PROBHD   5 mm QNP H/F/P
PULPROG          zg30
TD              65536
SOLVENT         CDCl3
NS                  8
DS                  2
SWH          6410.256 Hz
FIDRES       0.097813 Hz
AQ          5.1118579 sec
RG               1024
DW             78.000 usec
DE              4.50 usec
TE             298.0 K
D1         0.10000000 sec
MCREST     0.00000000 sec
MCWRK      0.01500000 sec

======== CHANNEL f1 ========
NUC1               1H
P1             12.00 usec
PL1             0.00 dB
SFO1      400.1328009 MHz

F2 - Processing parameters
SI              65536
SF        400.1300175 MHz
WDW               EM
SSB                0
LB              0.30 Hz
GB                 0
PC              2.00

1D NMR plot parameters
CX              22.80 cm
CY              15.00 cm
F1P            14.966 ppm
F1             5988.51 Hz
F2P            -1.054 ppm
F2             -421.74 Hz
PPMCM          0.70265 ppm/cm
HZCM        281.15158 Hz/cm
```

Z-restored spin-echo 13C spectrum with 1H decoupling

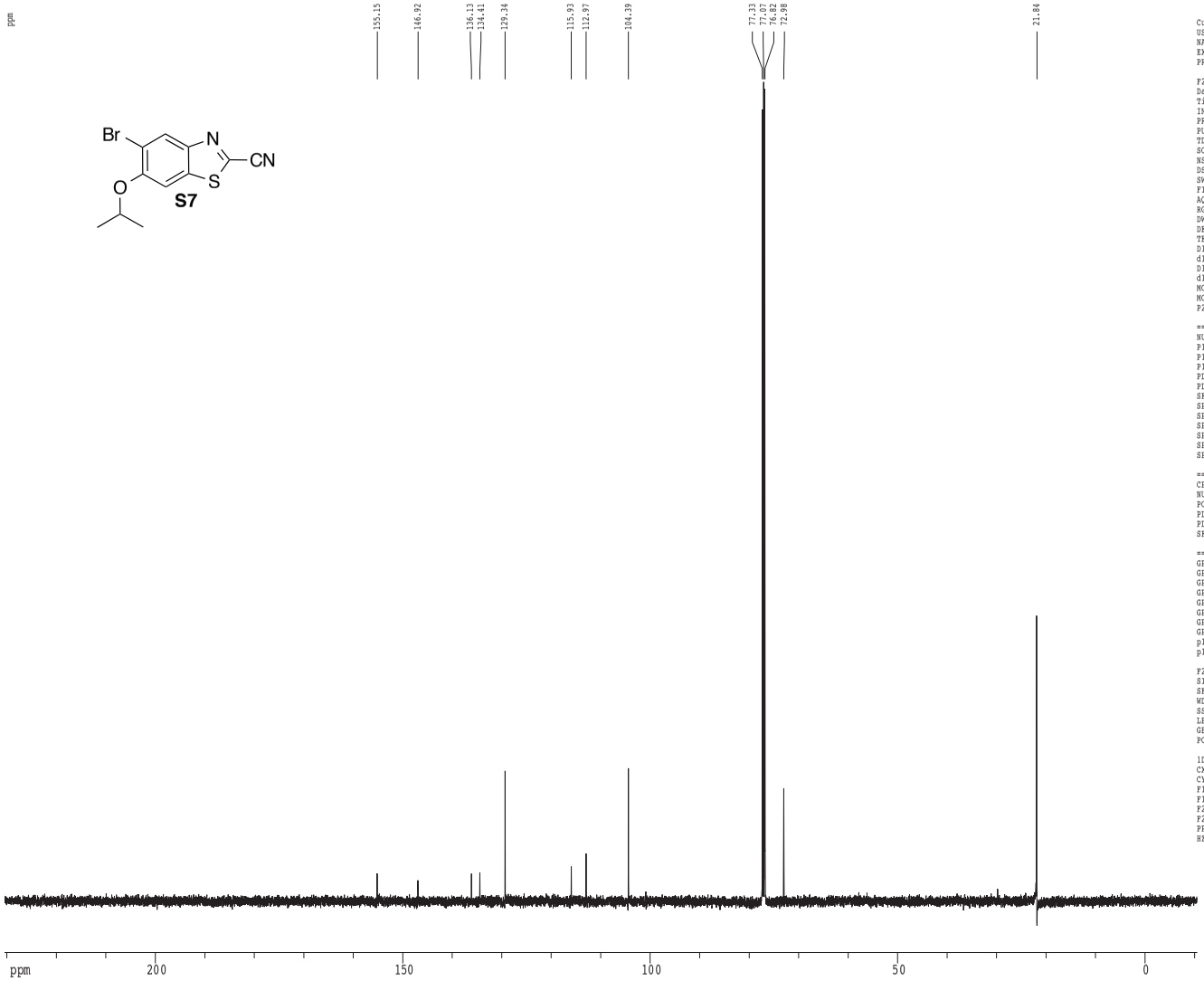


```
Current Data Parameters
USER            rachel
NAME          RB269_13c
EXPNO               2
PROCNO              1

F2 - Acquisition Parameters
Date_         20141010
Time             14.05
INSTRUM        cryo500
PROBHD   5 mm CPTCI 1H-
PULPROG  SpinEchopg30gp.prd
TD              65536
SOLVENT          CDCl3
NS                1024
DS                  16
SWH           30303.031 Hz
FIDRES         0.462388 Hz
AQ            1.0813940 sec
RG               7298.2
DW               16.500 usec
DE                6.00 usec
TE               298.0 K
D1           0.25000000 sec
d11          0.03000000 sec
D16          0.00020000 sec
d17          0.00019600 sec
MCREST       0.00000000 sec
MCWRK        0.01500000 sec
P2                31.00 usec

======= CHANNEL f1 =======
NUC1                13C
P1                15.50 usec
P11              500.00 usec
P12             2000.00 usec
PL0              120.00 dB
PL1               -1.00 dB
SFO1         125.7942548 MHz
SP1                3.20 dB
SP2                3.20 dB
SPNAM1   Crp60,0.5,20.1
SPNAM2      Crp60comp.4
SPOFF1             0.00 Hz
SPOFF2             0.00 Hz

======= CHANNEL f2 =======
CPDPRG2         waltz16
NUC2                 1H
PCPD2            100.00 usec
PL2                1.60 dB
PL12              24.60 dB
SFO2         500.2225011 MHz

===== GRADIENT CHANNEL ====
GPNAM1          SINE.100
GPNAM2          SINE.100
GPX1               0.00 %
GPX2               0.00 %
GPY1               0.00 %
GPY2               0.00 %
GPZ1              30.00 %
GPZ2              50.00 %
p15              500.00 usec
p16             1000.00 usec

F2 - Processing parameters
SI                 65536
SF          125.7804190 MHz
WDW                   EM
SSB                    0
LB                 1.00 Hz
GB                     0
PC                  2.00

1D NMR plot parameters
CX                 22.80 cm
CY                 15.65 cm
F1P             230.460 ppm
F1             28987.37 Hz
F2P             -10.460 ppm
F2             -1315.66 Hz
PPMCM           10.56667 ppm/cm
HZCM         1329.08032 Hz/cm
```

1H spectrum

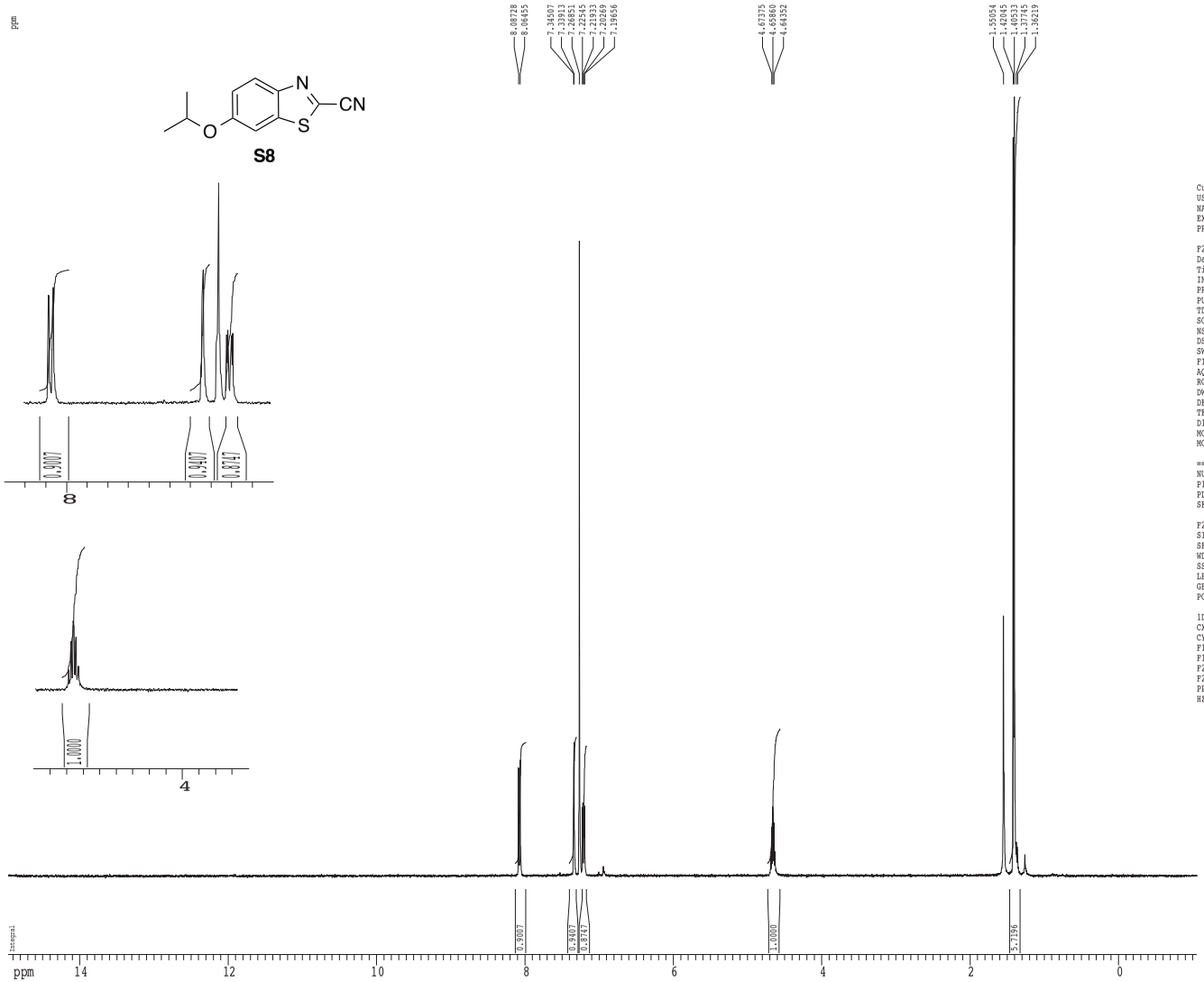


```
Current Data Parameters
USER            rachel
NAME         rb259_try4
EXPNO                 1
PROCNO                1

F2 - Acquisition Parameters
Date_        20141016
Time            14.57
INSTRUM         drx400
PROBHD   5 mm QNP H/F/P
PULPROG          zg30
TD              65536
SOLVENT         CDCl3
NS                  8
DS                  2
SWH          6410.256 Hz
FIDRES       0.097813 Hz
AQ          5.1118579 sec
RG             1290.2
DW             78.000 usec
DE              4.50 usec
TE             298.0 K
D1          0.10000000 sec
MCREST      0.00000000 sec
MCWRK       0.01500000 sec

======== CHANNEL f1 ========
NUC1              1H
P1             12.00 usec
PL1             0.00 dB
SFO1      400.1328009 MHz

F2 - Processing parameters
SI              65536
SF        400.1300175 MHz
WDW               EM
SSB                0
LB              0.30 Hz
GB                 0
PC              2.00

1D NMR plot parameters
CX              22.80 cm
CY              15.00 cm
F1P            14.966 ppm
F1             5988.51 Hz
F2P             -1.054 ppm
F2             -421.74 Hz
PPMCM         0.70265 ppm/cm
HZCM        281.15158 Hz/cm
```

Z-restored spin-echo 13C spectrum with 1H decoupling

S8

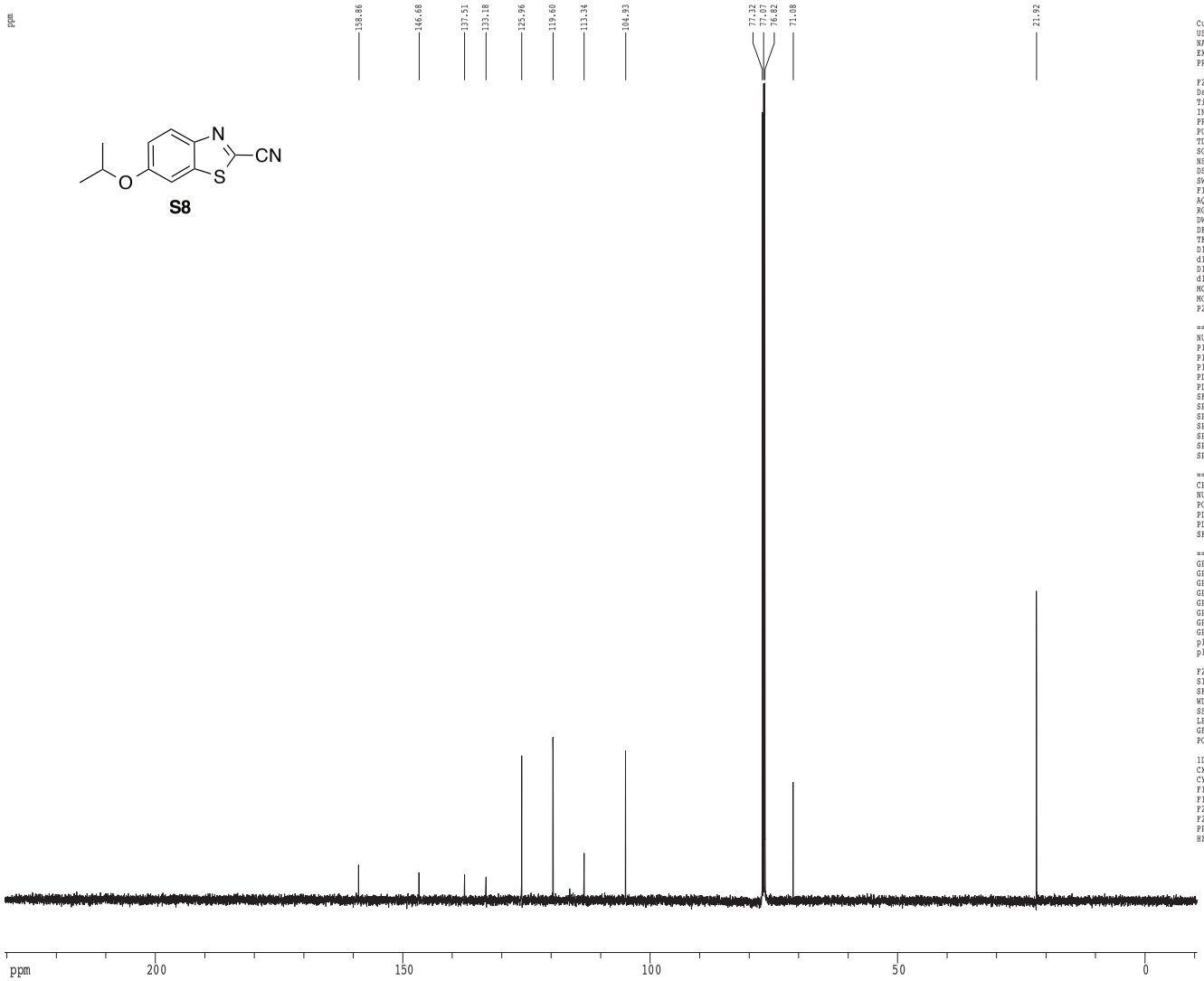


```
Current Data Parameters
USER            rachel
NAME          RB259_13c
EXPNO               2
PROCNO              1

F2 - Acquisition Parameters
Date_        20140929
Time            17.12
INSTRUM       cryo500
PROBHD   5 mm CPTCI 1H-
PULPROG  SpinEchopg30gp.prd
TD              65536
SOLVENT          CDCl3
NS                1024
DS                  16
SWH          30303.031 Hz
FIDRES        0.462388 Hz
AQ           1.0813940 sec
RG              7298.2
DW             16.500 usec
DE              6.00 usec
TE              298.0 K
D1          0.25000000 sec
d11         0.03000000 sec
D16         0.00020000 sec
d17         0.00019600 sec
MCREST      0.00000000 sec
MCWRK       0.01500000 sec
P2             31.00 usec

======= CHANNEL f1 =======
NUC1              13C
P1             15.50 usec
P11           500.00 usec
P12          2000.00 usec
PL0           120.00 dB
PL1            -1.00 dB
SFO1       125.7942548 MHz
SP1             3.20 dB
SP2             3.20 dB
SPNAM1   Crp60,0.5,20.1
SPNAM2     Crp60comp.4
SPOFF1          0.00 Hz
SPOFF2          0.00 Hz

======= CHANNEL f2 =======
CPDPRG2       waltz16
NUC2              1H
PCPD2         100.00 usec
PL2             1.60 dB
PL12           24.60 dB
SFO2       500.2225011 MHz

===== GRADIENT CHANNEL ====
GPNAM1        SINE.100
GPNAM2        SINE.100
GPX1            0.00 %
GPX2            0.00 %
GPY1            0.00 %
GPY2            0.00 %
GPZ1           30.00 %
GPZ2           50.00 %
p15           500.00 usec
p16          1000.00 usec

F2 - Processing parameters
SI              65536
SF         125.7804190 MHz
WDW               EM
SSB                0
LB              1.00 Hz
GB                 0
PC              2.00

1D NMR plot parameters
CX             22.80 cm
CY             15.65 cm
F1P           230.460 ppm
F1          28987.37 Hz
F2P           -10.460 ppm
F2          -1315.66 Hz
PPMCM         10.56667 ppm/cm
HZCM        1329.08032 Hz/cm
```

1H spectrum

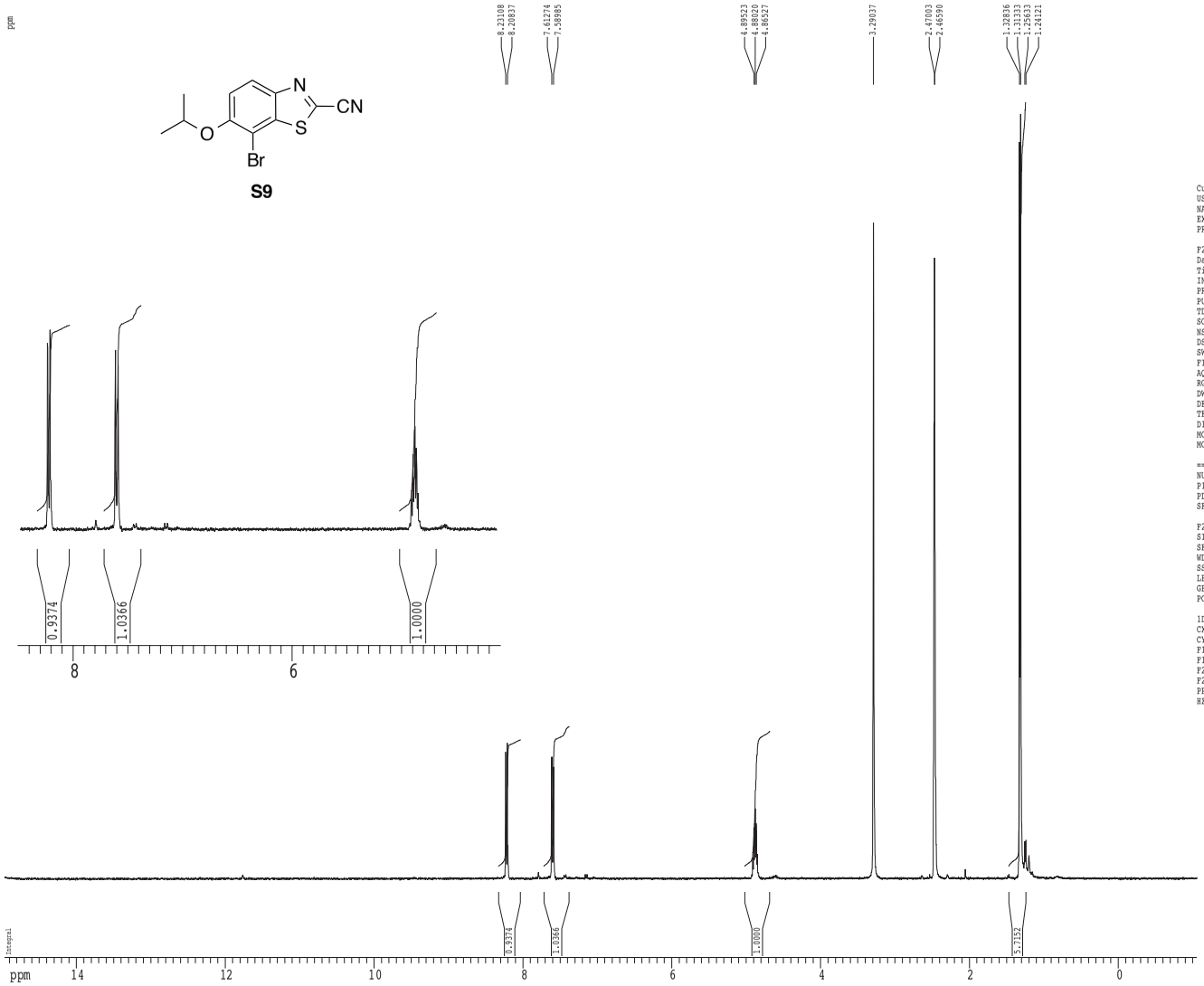

Current Data Parameters
USER rachel
NAME rb261_dmso
EXPNO 1
PROCNO 1

F2 - Acquisition Parameters
Date_ 20141007
Time 16.55
INSTRUM drx400
PROBHD 5 mm QNP H/F/P
PULPROG zg30
TD 65536
SOLVENT DMSO
NS 8
DS 2
SWH 6410.256 Hz
FIDRES 0.097813 Hz
AQ 5.1118579 sec
RG 1149.4
DW 78.000 usec
DE 4.50 usec
TE 298.0 K
D1 0.10000000 sec
MCREST 0.00000000 sec
MCWRK 0.01500000 sec

======== CHANNEL f1 ========
NUC1 1H
P1 12.00 usec
PL1 0.00 dB
SFO1 400.1328009 MHz

F2 - Processing parameters
SI 65536
SF 400.1300175 MHz
WDW EM
SSB 0
LB 0.30 Hz
GB 0
PC 2.00

1D NMR plot parameters
CX 22.80 cm
CY 15.00 cm
F1P 14.966 ppm
F1 5988.51 Hz
F2P -1.054 ppm
F2 -421.74 Hz
PPMCM 0.70265 ppm/cm
HZCM 281.15158 Hz/cm

Z-restored spin-echo 13C spectrum with 1H decoupling

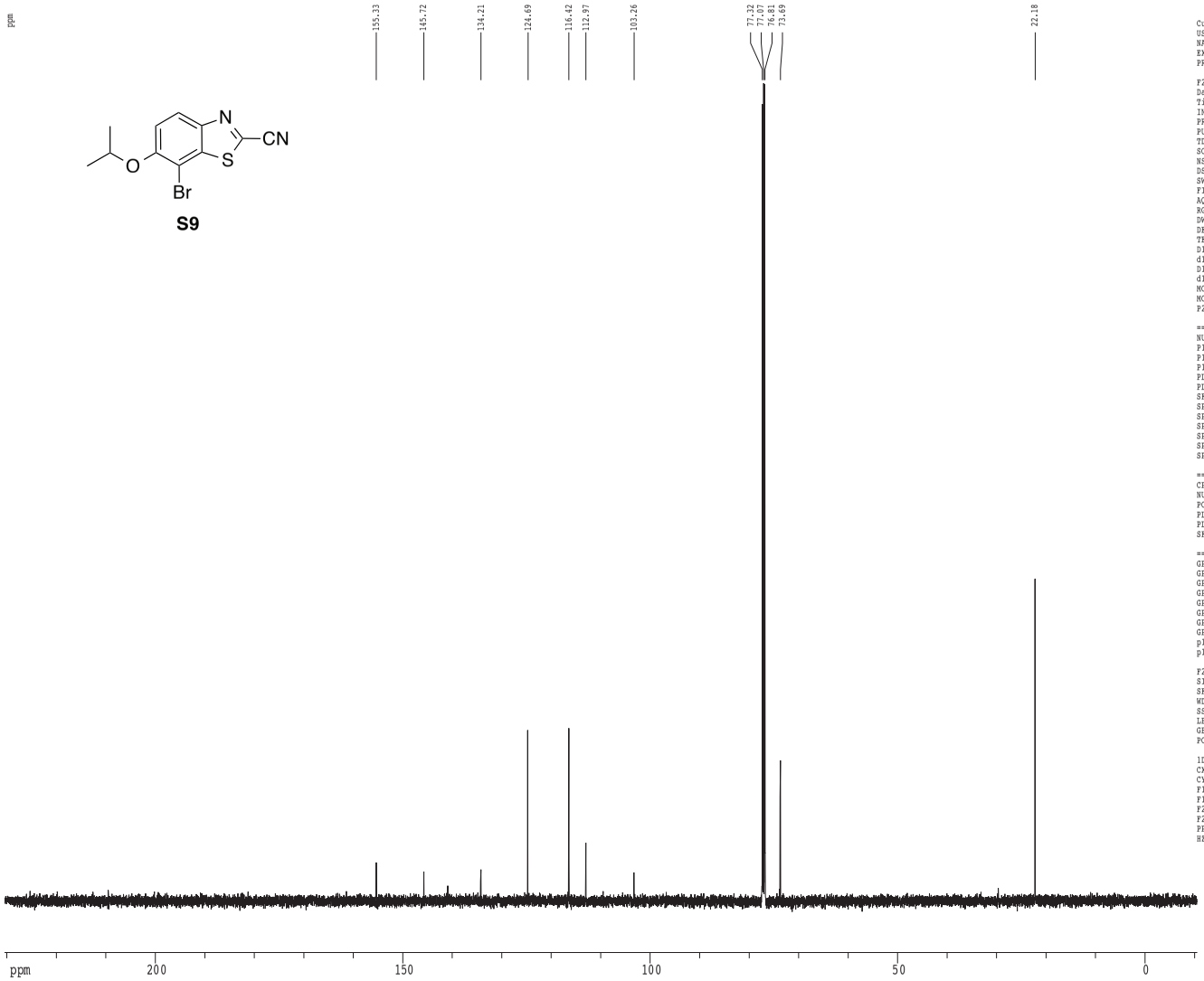


```
Current Data Parameters
USER            rachel
NAME      RB190_cryo13c
EXPNO                 2
PROCNO                1

F2 - Acquisition Parameters
Date_          20140712
Time             19.28
INSTRUM        cryo500
PROBHD   5 mm CPTCI 1H-
PULPROG  SpinEchopg30gp.prd
TD             65536
SOLVENT        CDCl3
NS              1024
DS                16
SWH          30303.031 Hz
FIDRES        0.462388 Hz
AQ           1.0813940 sec
RG              7298.2
DW              16.500 usec
DE               6.00 usec
TE              298.0 K
D1          0.25000000 sec
d11         0.03000000 sec
D16         0.00020000 sec
d17         0.00019600 sec
MCREST      0.00000000 sec
MCWRK       0.01500000 sec
P2               31.00 usec

======= CHANNEL f1 =======
NUC1               13C
P1               15.50 usec
P11             500.00 usec
P12            2000.00 usec
PL0             120.00 dB
PL1              -1.00 dB
SFO1        125.7942548 MHz
SP1              3.20 dB
SP2              3.20 dB
SPNAM1   Crp60,0.5,20.1
SPNAM2     Crp60comp.4
SPOFF1           0.00 Hz
SPOFF2           0.00 Hz

======= CHANNEL f2 =======
CPDPRG2        waltz16
NUC2               1H
PCPD2           100.00 usec
PL2               1.60 dB
PL12             24.60 dB
SFO2       500.2225011 MHz

===== GRADIENT CHANNEL ====
GPNAM1         SINE.100
GPNAM2         SINE.100
GPX1              0.00 %
GPX2              0.00 %
GPY1              0.00 %
GPY2              0.00 %
GPZ1             30.00 %
GPZ2             50.00 %
p15             500.00 usec
p16            1000.00 usec

F2 - Processing parameters
SI                65536
SF         125.7804190 MHz
WDW                  EM
SSB                   0
LB               1.00 Hz
GB                    0
PC               2.00

1D NMR plot parameters
CX               22.80 cm
CY               15.65 cm
F1P             230.460 ppm
F1            28987.37 Hz
F2P             -10.460 ppm
F2            -1315.66 Hz
PPMCM          10.56667 ppm/cm
HZCM         1329.08032 Hz/cm
```

1H spectrum

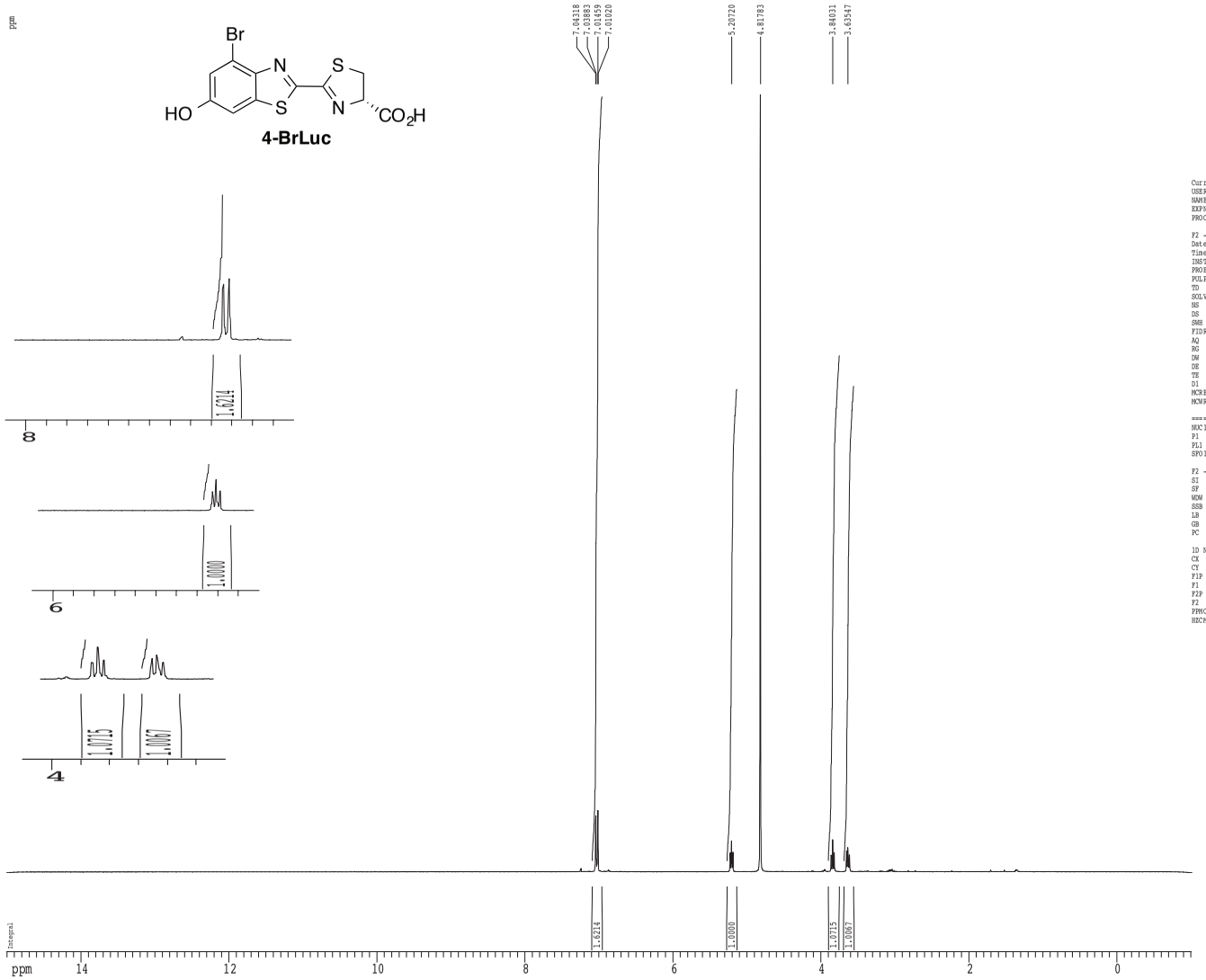


```
Current Data Parameters
USER              rachel
NAME      rb4xbromoluciferin_cryo
EXPNO                  1
PROCNO                 1

F2 - Acquisition Parameters
Date_          20141117
Time               19.28
INSTRUM         cryo500
PROBHD   5 mm CPPCI 1H-
PULPROG            zg30
TD                81728
SOLVENT             D2O
NS                    8
DS                    2
SWH            8012.820 Hz
FIDRES         0.098043 Hz
AQ           5.0998774 sec
RG                   16
DW               62.400 usec
DE                6.00 usec
TE               298.0 K
D1           0.10000000 sec
MCREST       0.00000000 sec
MCWRK        0.01500000 sec

======== CHANNEL f1 =======
NUC1                 1H
P1                 7.50 usec
PL1                1.60 dB
SFO1       500.2235015 MHz

F2 - Processing parameters
SI                65536
SF         500.2200000 MHz
WDW                  EM
SSB                   0
LB                 0.30 Hz
GB                    0
PC                 4.00

1D NMR plot parameters
CX                22.80 cm
CY                15.00 cm
F1P               15.009 ppm
F1                7507.95 Hz
F2P               -1.009 ppm
F2                -504.87 Hz
PPMCM          0.70257 ppm/cm
HZCM         351.43951 Hz/cm
```

Z-restored spin-echo 13C spectrum with 1H decoupling

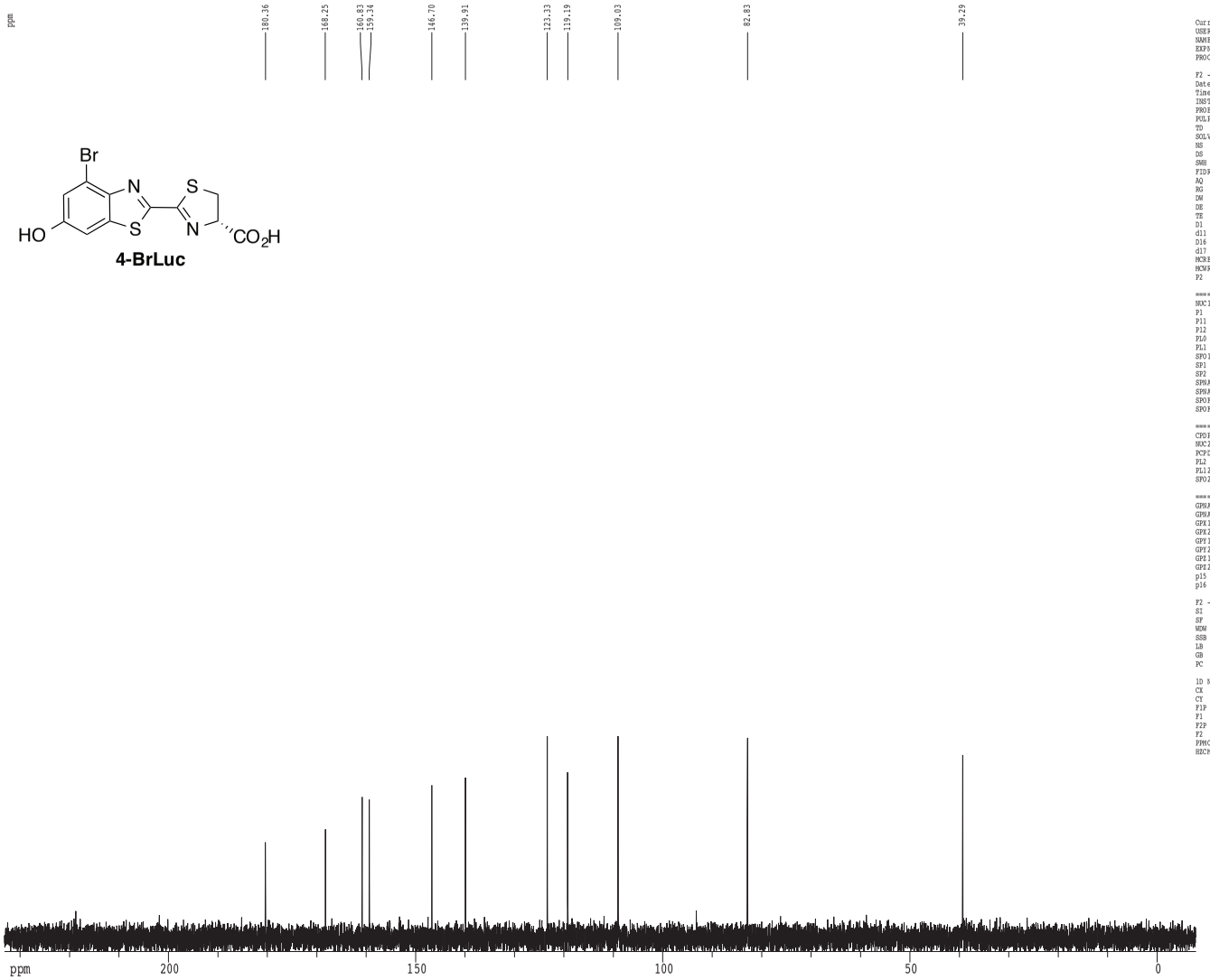


```
Current Data Parameters
USER                rachel
NAME     rb4xbromoluciferin_cryo
EXPNO                    2
PROCNO                   1

F2 - Acquisition Parameters
Date_            20141117
Time                19.39
INSTRUM           cryo500
PROBHD    5 mm CPTCI 1H-
PULPROG   SpinEchopg13cp.prd
TD                  65536
SOLVENT             CDCl3
NS                    489
DS                     16
SWH             30303.031 Hz
FIDRES           0.462388 Hz
AQ               1.0813940 sec
RG                   13004
DW                  16.500 usec
DE                   6.00 usec
TE                  298.0 K
D1             0.25000000 sec
d11            0.03000000 sec
D16            0.00020000 sec
d17            0.00019600 sec
MCREST         0.00000000 sec
MCWRK          0.01500000 sec
P2                  33.10 usec

======== CHANNEL f1 ========
NUC1                  13C
P1                  16.55 usec
P11                500.00 usec
P12               2000.00 usec
PL0                120.00 dB
PL1                 -1.00 dB
SFO1          125.7942548 MHz
SP1                  2.70 dB
SP2                  2.70 dB
SPNAM1     Crp60,0.5,20.1
SPNAM2       Crp60comp.4
SFOFF1                0.00 Hz
SFOFF2                0.00 Hz

======== CHANNEL f2 ========
CPDPRG2            waltz16
NUC2                    1H
PCPD2              100.00 usec
PL2                  1.60 dB
PL12                24.50 dB
SFO2          500.2225011 MHz

===== GRADIENT CHANNEL =====
GPNAM1            SINE.100
GPNAM2            SINE.100
GPX1                  0.00 %
GPX2                  0.00 %
GPY1                  0.00 %
GPY2                  0.00 %
GPZ1                 30.00 %
GPZ2                 50.00 %
p15                 500.00 usec
p16                1000.00 usec

F2 - Processing parameters
SI                  65536
SF            125.7800839 MHz
WDW                    EM
SSB                     0
LB                   1.00 Hz
GB                      0
PC                   2.00

1D NMR plot parameters
CX                  22.80 cm
CY                  15.65 cm
F1P                233.125 ppm
F1               29322.47 Hz
F2P                 -7.796 ppm
F2               -980.56 Hz
PPMCM            10.56670 ppm/cm
HZCM           1329.08032 Hz/cm
```

1H spectrum

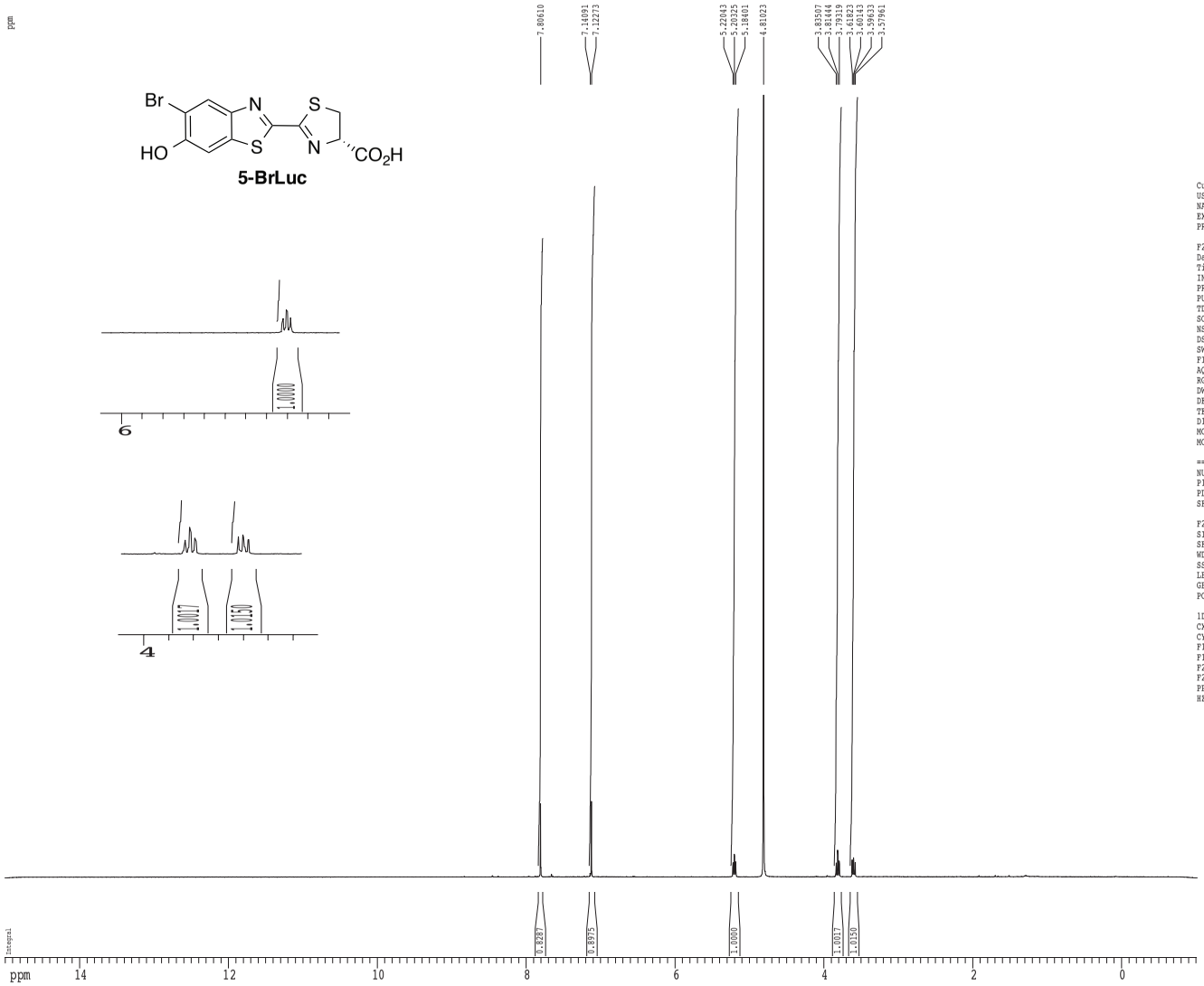


```
Current Data Parameters
USER            rachel
NAME          rl_5bromo
EXPNO               1
PROCNO              1

F2 - Acquisition Parameters
Date_         20150118
Time             17.11
INSTRUM        cryo500
PROBHD   5 mm CPTCI 1H-
PULPROG          zg30
TD              81728
SOLVENT           D2O
NS                  8
DS                  2
SWH            8012.820 Hz
FIDRES         0.098043 Hz
AQ            5.0998774 sec
RG                  6.3
DW               62.400 usec
DE                6.00 usec
TE               298.0 K
D1            0.10000000 sec
MCREST        0.00000000 sec
MCWRK         0.01500000 sec

======== CHANNEL f1 ========
NUC1                1H
P1                7.50 usec
PL1               1.60 dB
SFO1        500.2235015 MHz

F2 - Processing parameters
SI                65536
SF          500.2200000 MHz
WDW                 EM
SSB                  0
LB                0.30 Hz
GB                   0
PC                4.00

1D NMR plot parameters
CX               22.80 cm
CY               15.00 cm
F1P             15.009 ppm
F1             7507.95 Hz
F2P             -1.009 ppm
F2             -504.87 Hz
PPMCM          0.70257 ppm/cm
HZCM         351.43951 Hz/cm
```

Z-restored spin-echo 13C spectrum with 1H decoupling

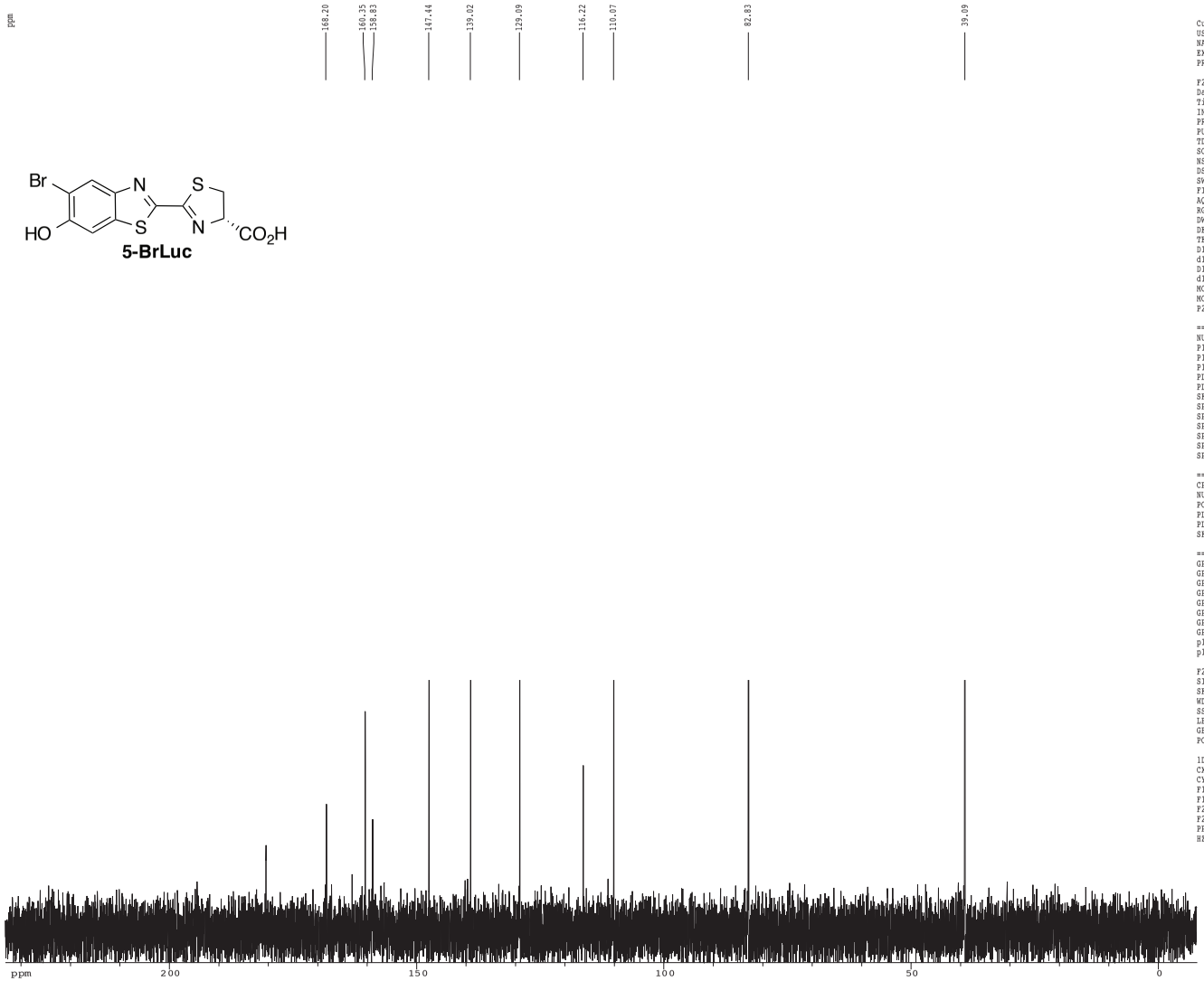


```
Current Data Parameters
USER            rachel
NAME          rl_5bromo
EXPNO               2
PROCNO              1

F2 - Acquisition Parameters
Date_          20150118
Time             17.18
INSTRUM        cryo500
PROBHD   5 mm CPTCI 1H-
PULPROG  SpinEchopg30gp.prd
TD              65536
SOLVENT          CDCl3
NS                1024
DS                  16
SWH           30303.031 Hz
FIDRES         0.462388 Hz
AQ            1.0813940 sec
RG               13004
DW              16.500 usec
DE               6.00 usec
TE              298.0 K
D1          0.25000000 sec
d11         0.03000000 sec
D16         0.00020000 sec
d17         0.00019600 sec
MCREST      0.00000000 sec
MCWRK       0.01500000 sec
P2              33.10 usec

======= CHANNEL f1 =======
NUC1              13C
P1              16.55 usec
P11            500.00 usec
P12           2000.00 usec
PL0            120.00 dB
PL1             -1.00 dB
SFO1        125.7942548 MHz
SP1              2.70 dB
SP2              2.70 dB
SPNAM1   Crp60,0.5,20.1
SPNAM2     Crp60comp.4
SPOFF1           0.00 Hz
SPOFF2           0.00 Hz

======= CHANNEL f2 =======
CPDPRG2        waltz16
NUC2              1H
PCPD2          100.00 usec
PL2              1.60 dB
PL12            24.50 dB
SFO2       500.2225011 MHz

===== GRADIENT CHANNEL ====
GPNAM1        SINE.100
GPNAM2        SINE.100
GPX1             0.00 %
GPX2             0.00 %
GPY1             0.00 %
GPY2             0.00 %
GPZ1            30.00 %
GPZ2            50.00 %
p15            500.00 usec
p16           1000.00 usec

F2 - Processing parameters
SI              65536
SF         125.7800839 MHz
WDW                EM
SSB                 0
LB               1.00 Hz
GB                  0
PC               2.00

1D NMR plot parameters
CX              22.80 cm
CY              15.65 cm
F1P            233.125 ppm
F1           29322.47 Hz
F2P             -7.796 ppm
F2           -980.56 Hz
PPMCM          10.56670 ppm/cm
HZCM        1329.08032 Hz/cm
```

1H spectrum

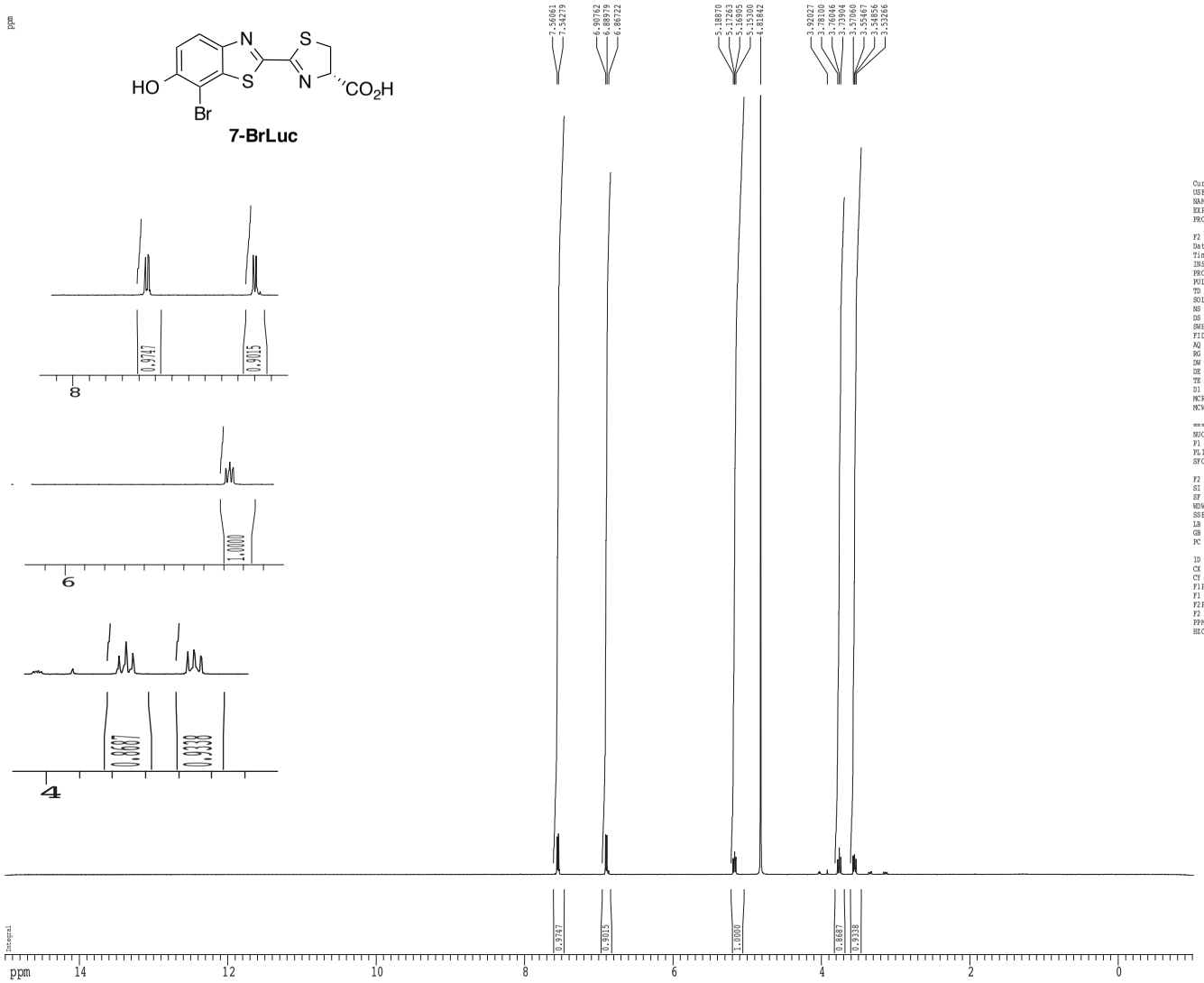

Current Data Parameters
USER rachel
NAME rb7bromoluciferin_cryo
EXPNO 1
PROCNO 1

F2 - Acquisition Parameters
Date_ 20141117
Time 19.01
INSTRUM cryo500
PROBHD 5 mm CPTCI 1H-
PULPROG zg30
TD 81728
SOLVENT D2O
NS 8
DS 2
SWH 8012.820 Hz
FIDRES 0.098043 Hz
AQ 5.0998774 sec
RG 12.7
DW 62.400 usec
DE 6.00 usec
TE 298.0 K
D1 0.10000000 sec
MCREST 0.00000000 sec
MCWRK 0.01500000 sec

======= CHANNEL f1 =======
NUC1 1H
P1 7.50 usec
PL1 1.60 dB
SFO1 500.2235015 MHz

F2 - Processing parameters
SI 65536
SF 500.2200000 MHz
WDW EM
SSB 0
LB 0.30 Hz
GB 0
PC 4.00

1D NMR plot parameters
CX 22.80 cm
CY 15.00 cm
F1P 15.009 ppm
F1 7507.95 Hz
F2P -1.009 ppm
F2 -504.87 Hz
PPMCM 0.70257 ppm/cm
HZCM 351.43951 Hz/cm

Z-restored spin-echo 13C spectrum with 1H decoupling

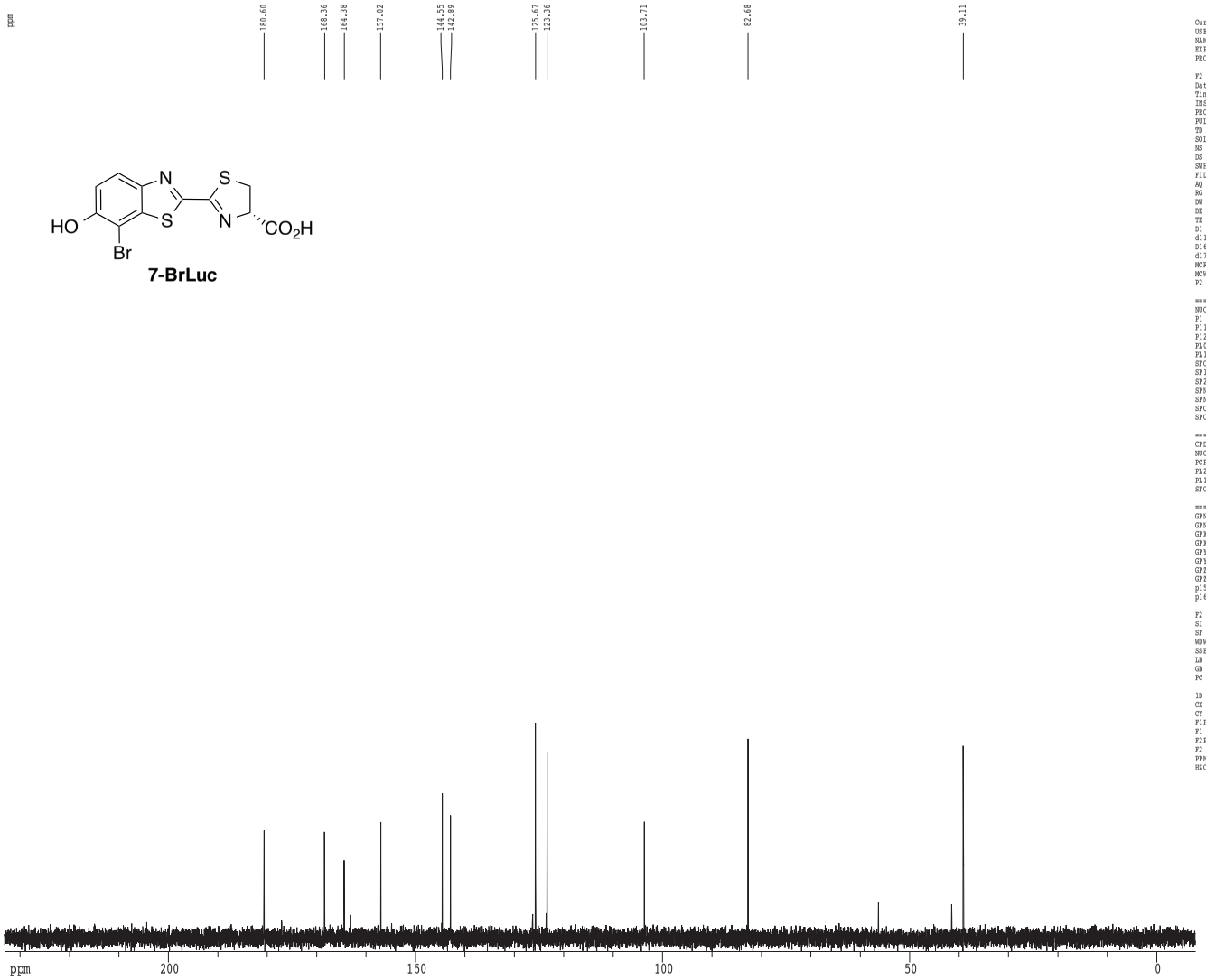


```
Current Data Parameters
USER                 rachel
NAME     rb7bromoluciferin_cryo
EXPNO                     2
PROCNO                    1

F2 - Acquisition Parameters
Date_           20141117
Time                 19.03
INSTRUM          cryo500
PROBHD   5 mm CPTCI 1H-
PULPROG  SpinEchopg30gp.prd
TD                  65536
SOLVENT             CDCl3
NS                    883
DS                     16
SWH            30303.031 Hz
FIDRES          0.462388 Hz
AQ             1.0813940 sec
RG                   8192
DW                16.500 usec
DE                 6.00 usec
TE                298.0 K
D1            0.25000000 sec
d11           0.03000000 sec
D16           0.00020000 sec
d17           0.00019600 sec
MCREST        0.00000000 sec
MCWRK         0.01500000 sec
P2                33.10 usec

====== CHANNEL f1 ======
NUC1                 13C
P1                 16.55 usec
P11               500.00 usec
P12              2000.00 usec
PL0               120.00 dB
PL1                -1.00 dB
SFO1         125.7942548 MHz
SP1                 2.70 dB
SP2                 2.70 dB
SPNAM1    Crp60,0.5,20.1
SPNAM2      Crp60comp.4
SPOFF1              0.00 Hz
SPOFF2              0.00 Hz

====== CHANNEL f2 ======
CPDPRG2          waltz16
NUC2                  1H
PCPD2             100.00 usec
PL2                 1.60 dB
PL12               24.50 dB
SFO2         500.2225011 MHz

===== GRADIENT CHANNEL =====
GPNAM1           SINE.100
GPNAM2           SINE.100
GPX1                0.00 %
GPX2                0.00 %
GPY1                0.00 %
GPY2                0.00 %
GPZ1               30.00 %
GPZ2               50.00 %
p15               500.00 usec
p16              1000.00 usec

F2 - Processing parameters
SI                  65536
SF           125.7800839 MHz
WDW                    EM
SSB                     0
LB                   1.00 Hz
GB                      0
PC                   2.00

1D NMR plot parameters
CX                  22.80 cm
CY                  15.65 cm
F1P               233.125 ppm
F1              29322.47 Hz
F2P                -7.796 ppm
F2               -980.56 Hz
PPMCM            10.56670 ppm/cm
HZCM           1329.08032 Hz/cm
```

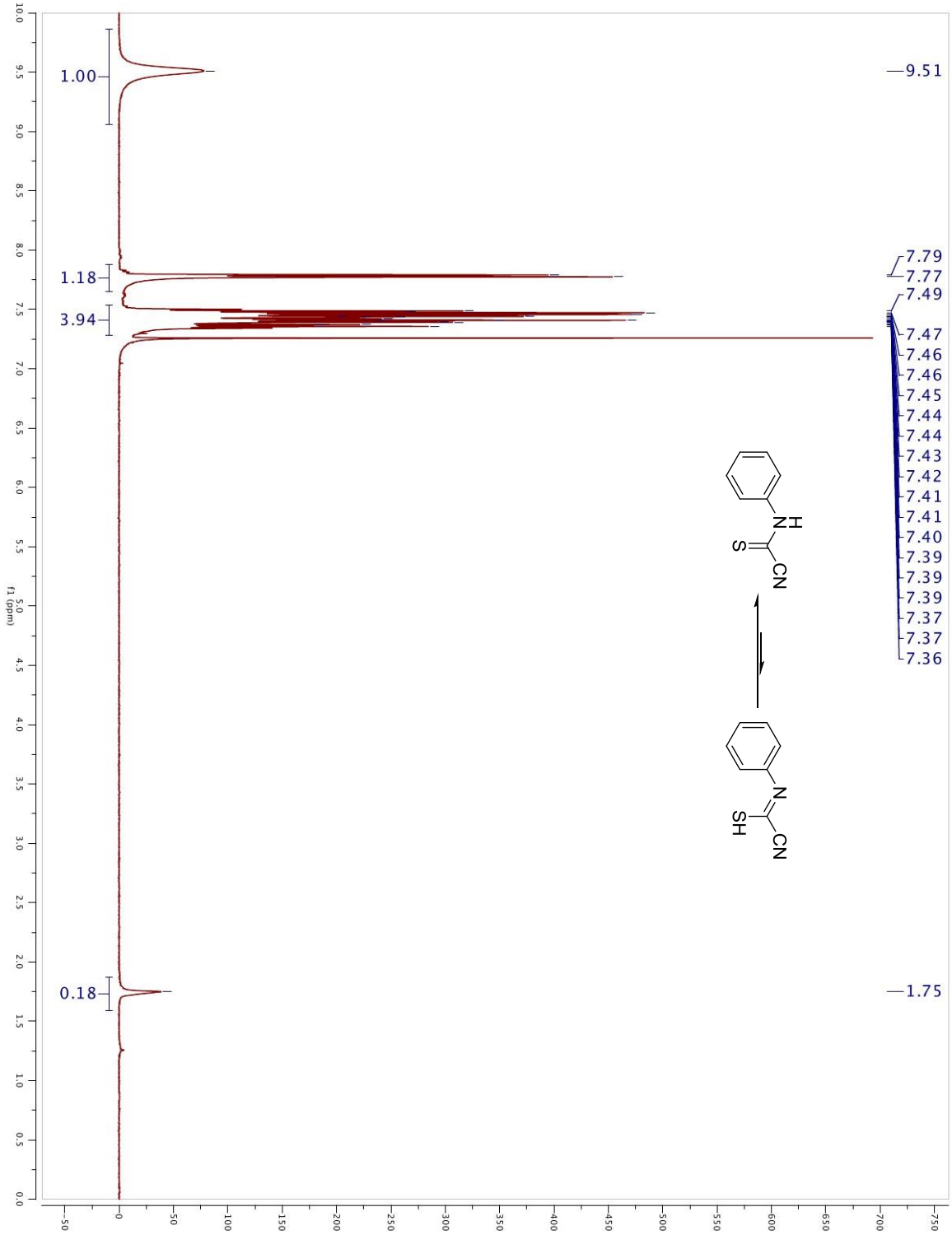
9.51
7.79
7.77
7.49
7.47
7.46
7.46
7.45
7.44
7.44
7.43
7.42
7.41
7.41
7.40
7.39
7.39
7.39
7.37
7.37
7.36
1.75
1.00
1.18
3.94
0.18
f1 (ppm)
H
N
S
CN
N
SH
CN

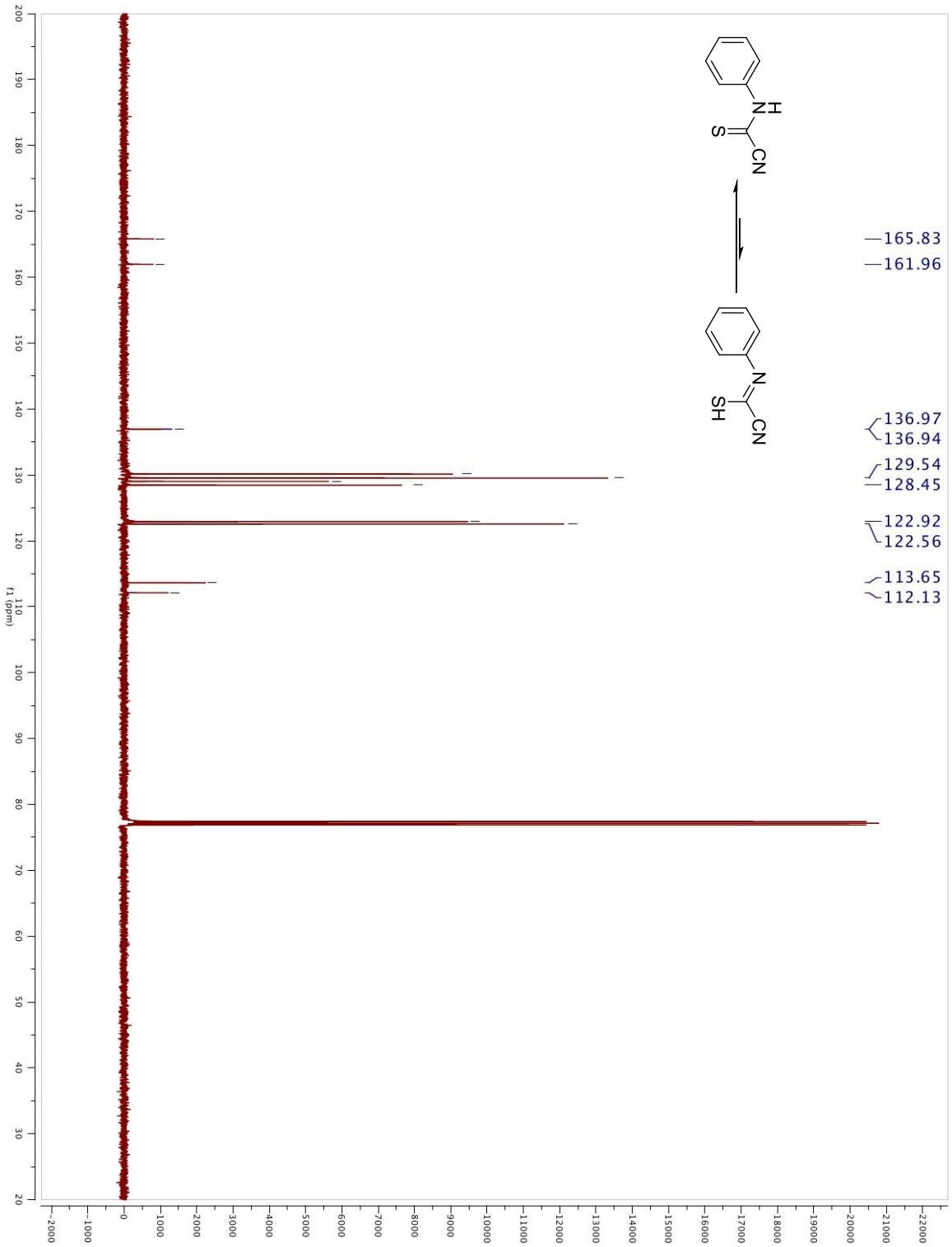
165.83
161.96
136.97
136.94
129.54
128.45
122.92
122.56
113.65
112.13
f1 (ppm)

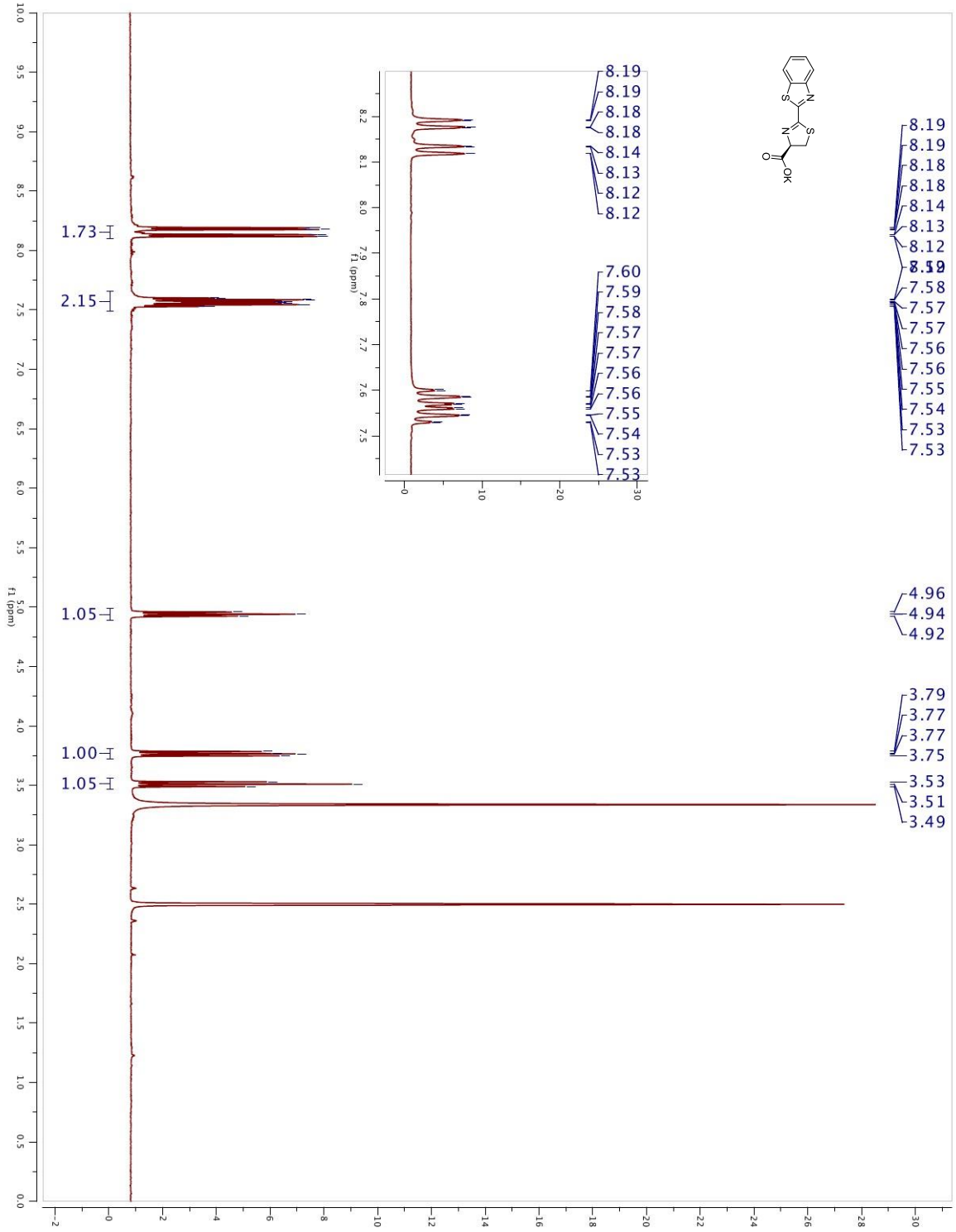
1.73
2.15
1.05
1.00
1.05
8.19
8.19
8.18
8.18
8.14
8.13
8.12
8.12
7.60
7.59
7.58
7.57
7.57
7.56
7.56
7.55
7.54
7.53
7.53
4.96
4.94
4.92
3.79
3.77
3.77
3.75
3.53
3.51
3.49
f1 (ppm)

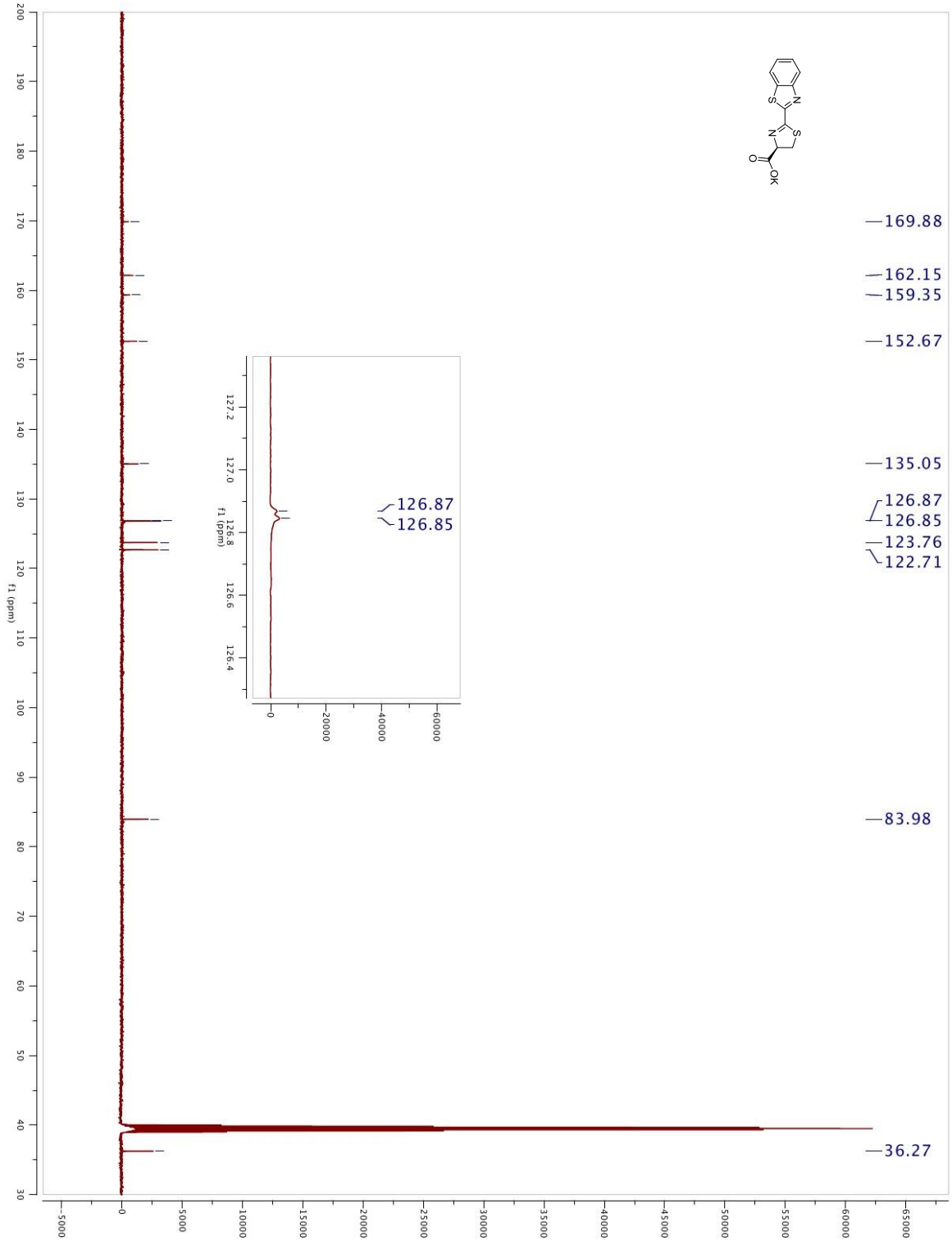
169.88
162.15
159.35
152.67
135.05
126.87
126.85
123.76
122.71
83.98
36.27
126.87
126.85
f1 (ppm)

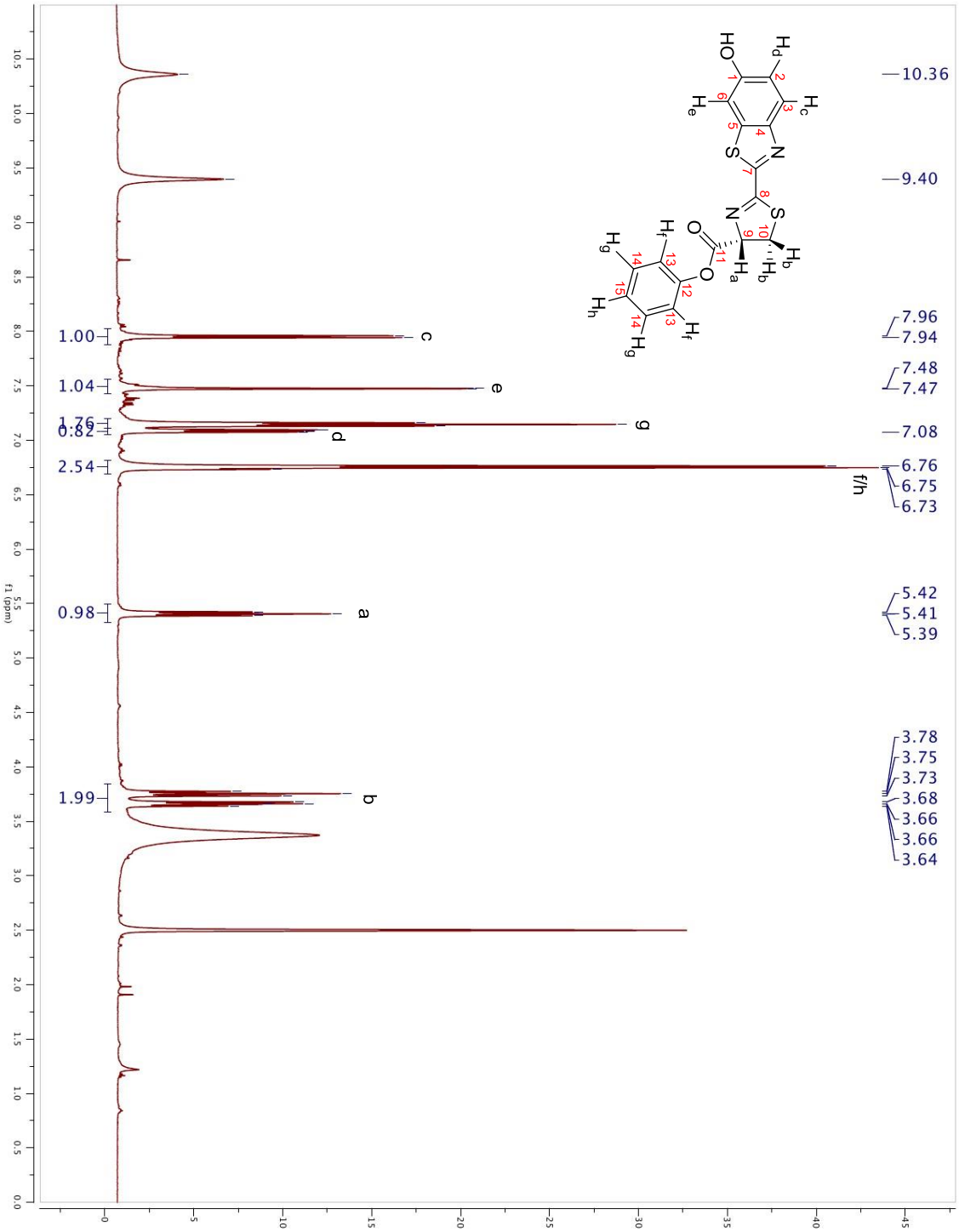
10.36
9.40
7.96
7.94
7.48
7.47
7.08
6.76
6.75
6.73
5.42
5.41
5.39
3.78
3.75
3.73
3.68
3.66
3.66
3.64
1.00
1.04
1.76
0.82
2.54
0.98
1.99
c
e
g
d
f/h
a
b
f1 (ppm)

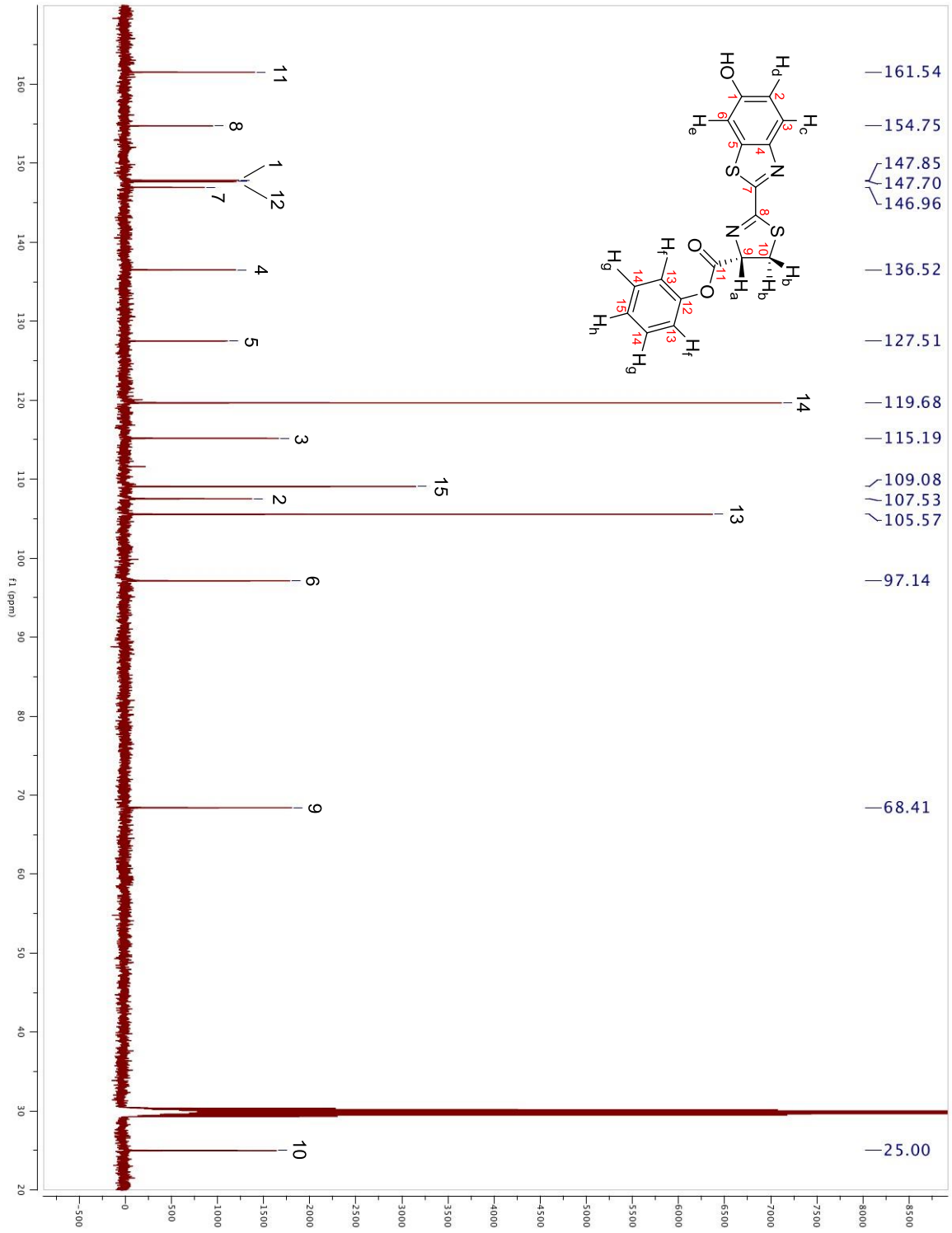
161.54
154.75
147.85
147.70
146.96
136.52
127.51
119.68
115.19
109.08
107.53
105.57
97.14
68.41
25.00
f1 (ppm)

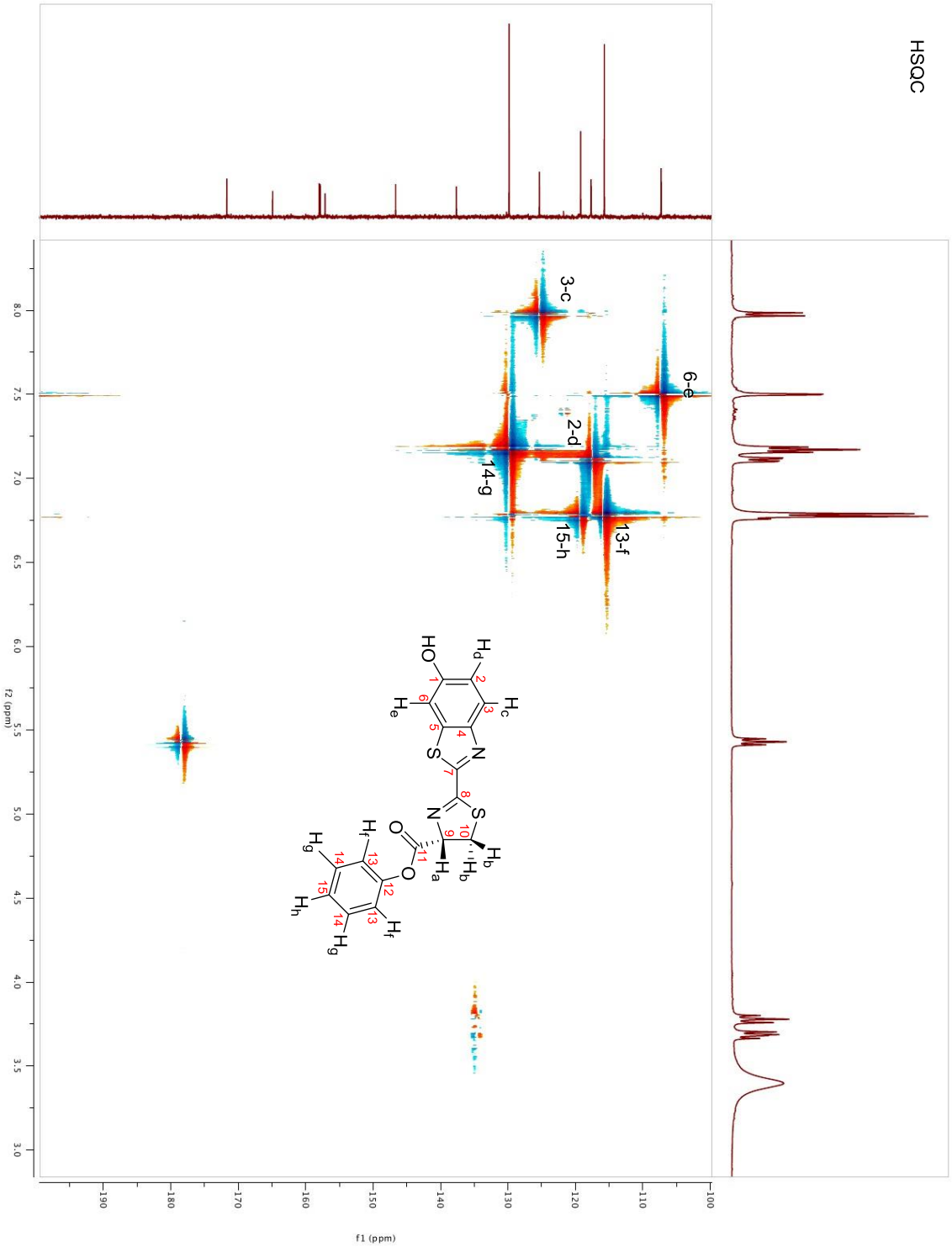
HSQC
6-e
3-c
2-d
14-g
13-f
15-h
f2 (ppm)
f1 (ppm)

HMBC optimized for
2 Hz coupling

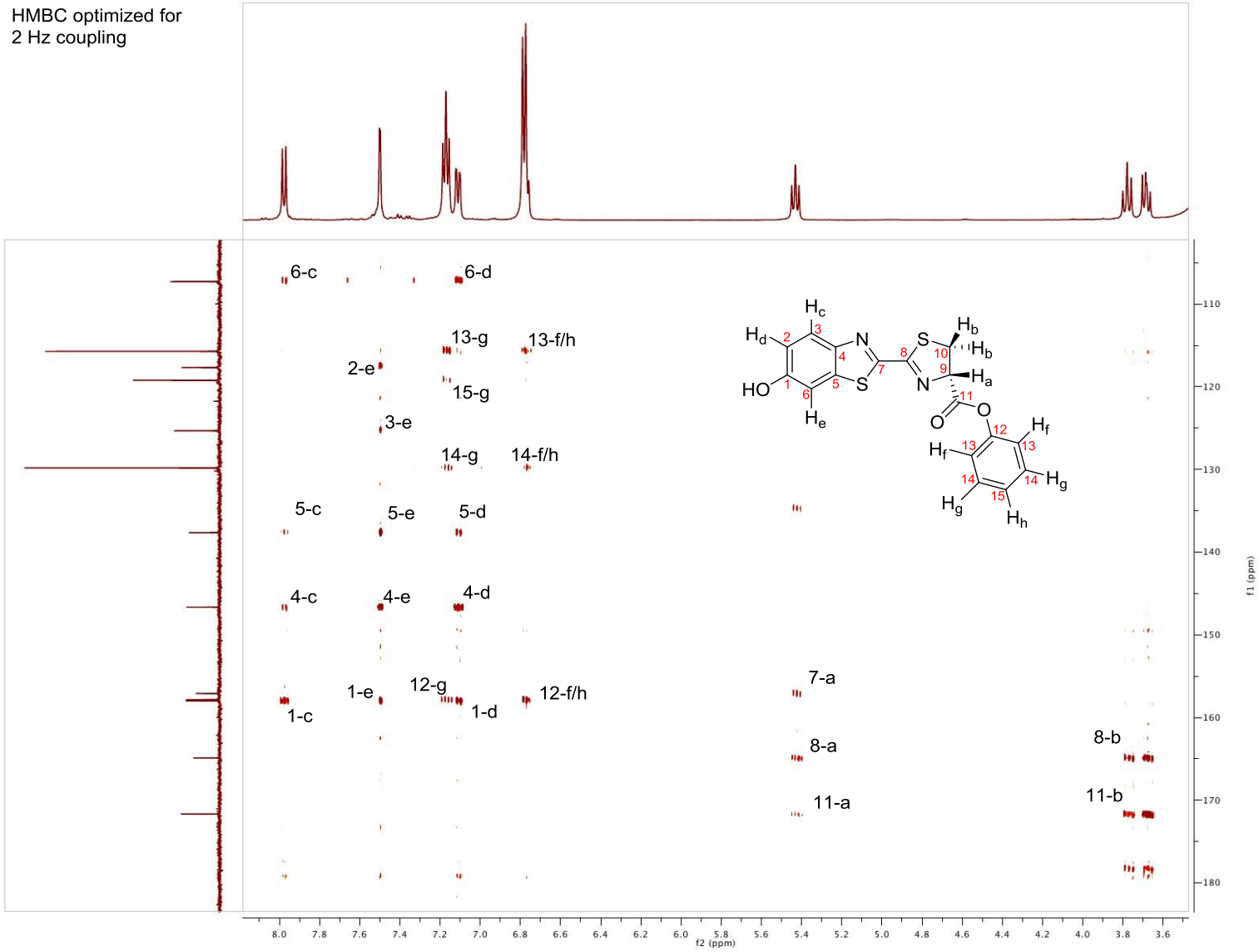

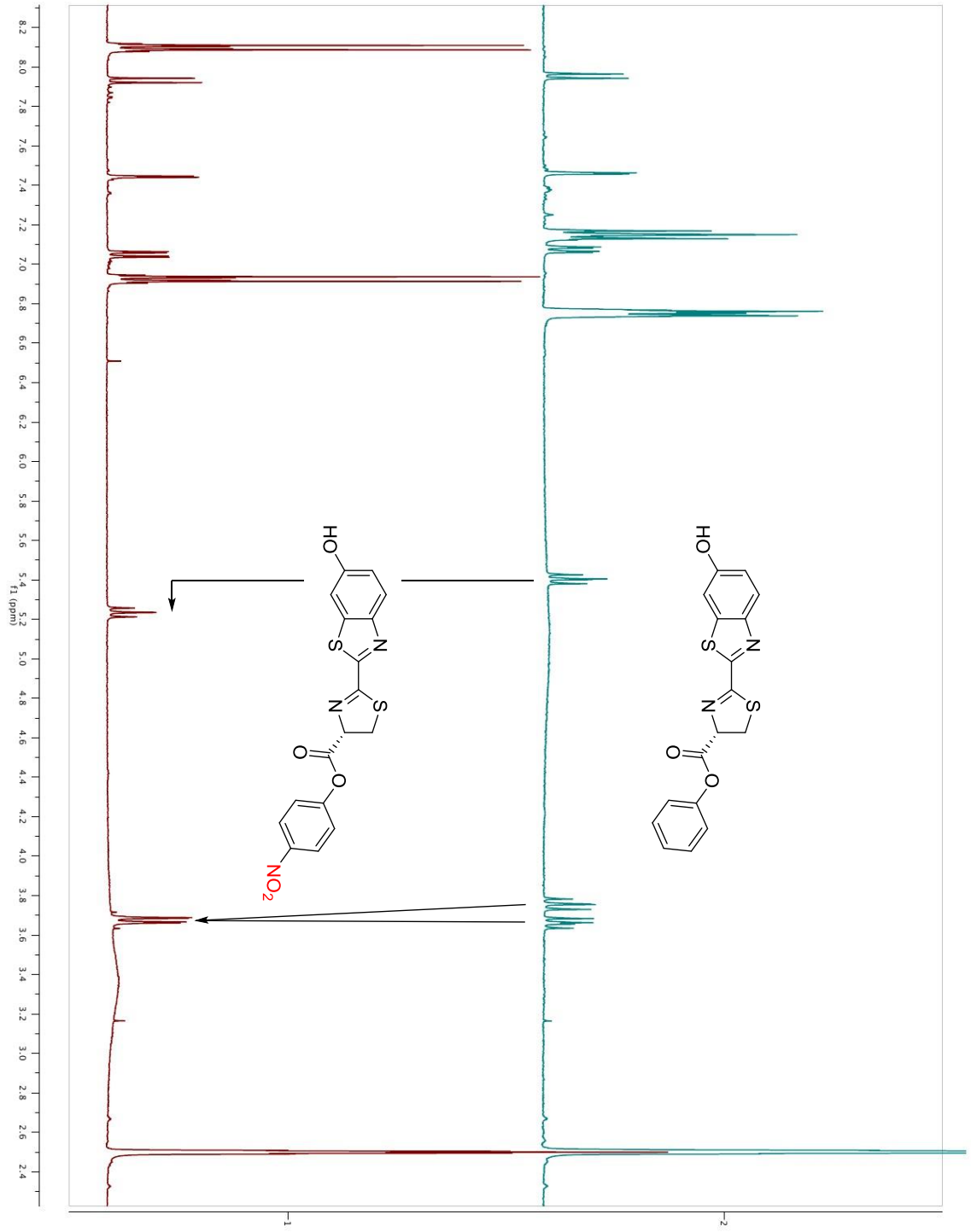
f1 (ppm)
8.2
8.0
7.8
7.6
7.4
7.2
7.0
6.8
6.6
6.4
6.2
6.0
5.8
5.6
5.4
5.2
5.0
4.8
4.6
4.4
4.2
4.0
3.8
3.6
3.4
3.2
3.0
2.8
2.6
2.4
1
2
HO
S
N
N
S
O
O
NO2
HO
S
N
N
S
O
O

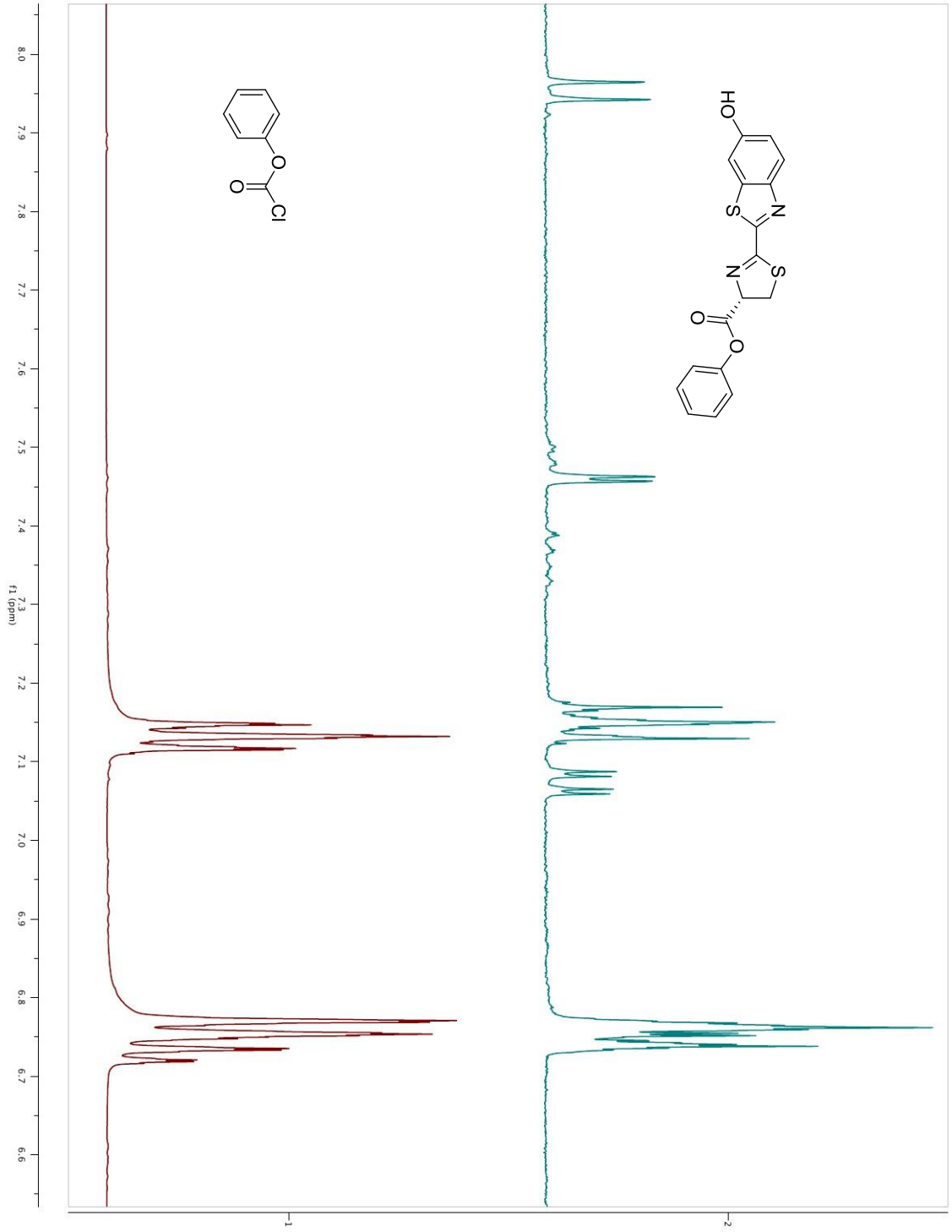
HO
S
N
N
S
O
O
Cl
O
8.0
7.9
7.8
7.7
7.6
7.5
7.4
7.3
f1 (ppm)
7.2
7.1
7.0
6.9
6.8
6.7
6.6
1
2

Appendix C: NMR spectra for Chapter 4

1H spectrum

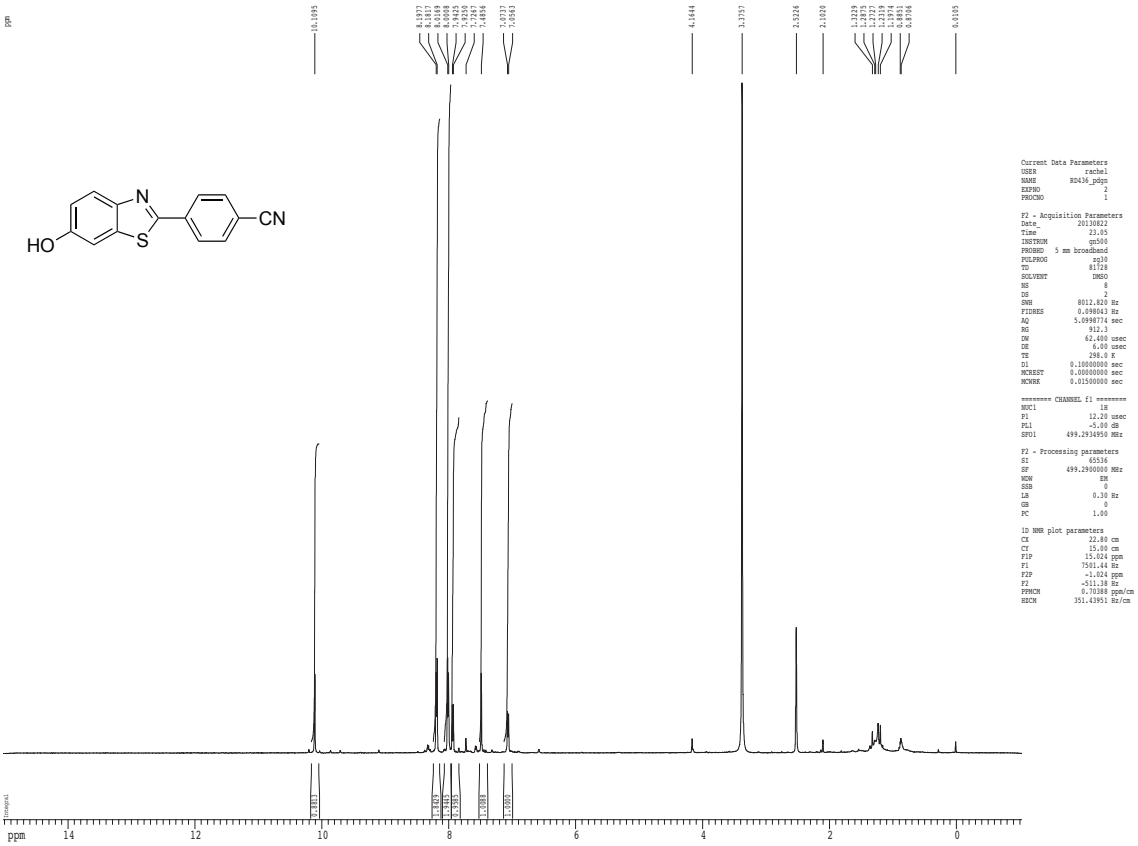
ppm
10.1995
8.8977
8.8817
8.8649
8.8088
8.8008
7.8425
7.8305
7.7909
7.7249
7.4894
7.0737
7.0563
4.1844
3.3757
2.5226
2.1020
1.3229
1.2875
1.2737
1.2577
1.2374
1.2143
0.8451
0.8356
0.8195
Integral
1.0403
1.0485
1.0485
1.0485
1.0485
1.0088
1.0080
ppm
14
12
10
8
6
4
2
0
HO
N
S
CN
Current Data Parameters
USER rachel
NAME RD436_pdqn
EXPNO 2
PROCNO 1
F2 - Acquisition Parameters
Date_ 20130822
Time 23.05
INSTRUM qnp500
PROBHD 5 mm broadband
PULPROG zg30
TD 81728
SOLVENT DMSO
NS 8
DS 2
SWH 8012.820 Hz
FIDRES 0.098043 Hz
AQ 5.0980774 sec
RG 912.3
DW 62.400 usec
DE 6.00 usec
TE 298.0 K
D1 0.10000000 sec
MCREST 0.00000000 sec
MCWRK 0.01500000 sec
======== CHANNEL f1 ========
NUC1 1H
P1 12.20 usec
PL1 -5.00 dB
SFO1 499.2934950 MHz
F2 - Processing parameters
SI 65536
SF 499.2900000 MHz
WDW EM
SSB 0
LB 0.30 Hz
GB 0
PC 1.00
1D NMR plot parameters
CX 22.80 cm
CY 15.00 cm
F1P 15.024 ppm
F1 7501.44 Hz
F2P -1.024 ppm
F2 -511.38 Hz
PPMCM 0.70388 ppm/cm
HZCM 351.43951 Hz/cm

Z-restored spin-echo 13C spectrum with 1H decoupling

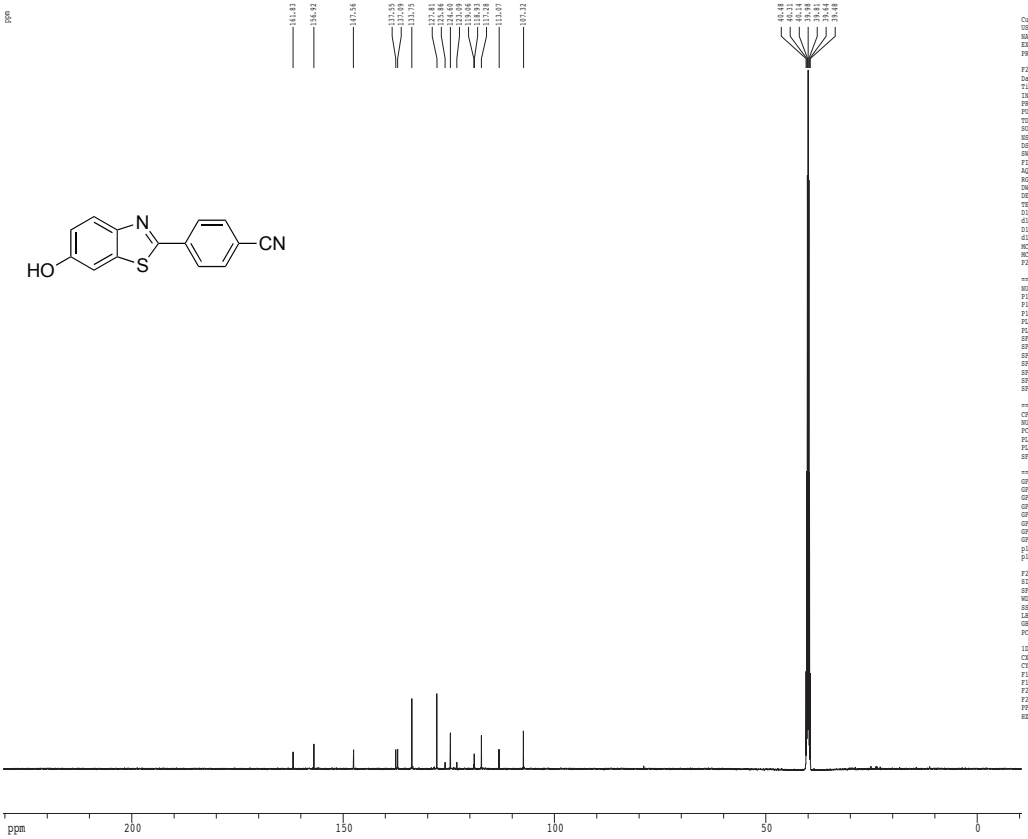


```
Current Data Parameters
USER            rachel
NAME        RD436_pd13c
EXPNO               2
PROCNO              1

F2 - Acquisition Parameters
Date_        20130822
Time           22.58
INSTRUM      cryo500
PROBHD   5 mm CPTCI 1H-
PULPROG  Spin2chopp3fsp.prd
TD            65536
SOLVENT        DMSO
NS              760
DS               16
SWH        30303.031 Hz
FIDRES      0.462388 Hz
AQ          1.0813940 sec
RG            9195.2
DW            16.500 usec
DE             6.00 usec
TE            298.0 K
D1         0.25000000 sec
d11        0.03000000 sec
D16        0.00020000 sec
d17        0.00019600 sec
MCREST     0.00000000 sec
MCWRK      0.01500000 sec
P2            31.00 usec

======== CHANNEL f1 ========
NUC1            13C
P1            15.50 usec
P11          500.00 usec
P12         2000.00 usec
PL0          120.00 dB
PL1           -1.00 dB
SFO1      125.7942548 MHz
SP1           3.20 dB
SP2           3.20 dB
SPNAM1   Crp60,0.5,20.1
SPNAM2     Crp60comp.4
SPOFF1        0.00 Hz
SPOFF2        0.00 Hz

======== CHANNEL f2 ========
CPDPRG2       waltz16
NUC2            1H
PCPD2        100.00 usec
PL2           1.60 dB
PL12         24.60 dB
SFO2     500.2225011 MHz

===== GRADIENT CHANNEL =====
GPNAM1       SINE.100
GPNAM2       SINE.100
GPX1          0.00 %
GPX2          0.00 %
GPY1          0.00 %
GPY2          0.00 %
GPZ1         30.00 %
GPZ2         50.00 %
p15        500.00 usec
p16       1000.00 usec

F2 - Processing parameters
SI            65536
SF      125.7804190 MHz
WDW            EM
SSB             0
LB            1.00 Hz
GB              0
PC            2.00

1D NMR plot parameters
CX           22.80 cm
CY           15.65 cm
F1P         230.460 ppm
F1        28987.37 Hz
F2P        -10.460 ppm
F2       -1315.66 Hz
PPMCM     10.56667 ppm/cm
HZCM    1329.08032 Hz/cm
```

1H spectrum

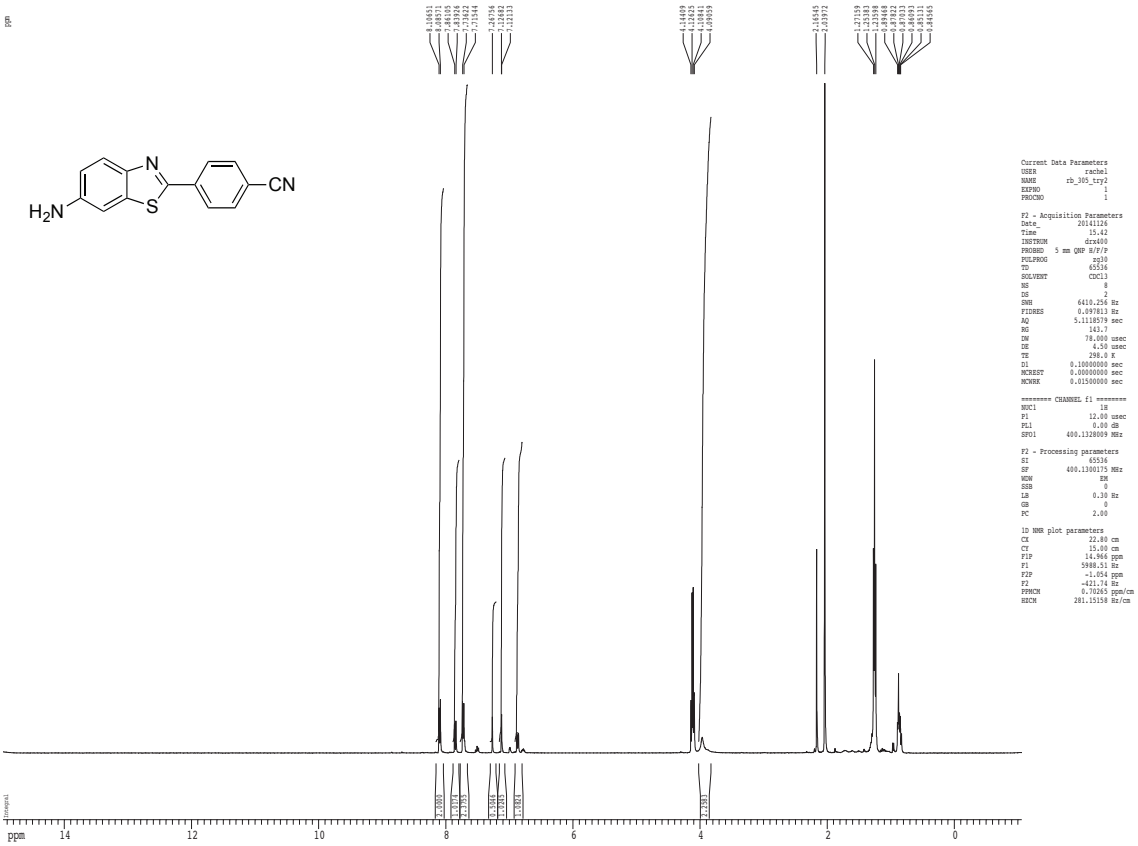
ppm
8.13651
8.13375
8.05935
7.85926
7.85648
7.77594
7.77344
7.26756
7.13682
7.13133
4.14409
4.12625
4.10841
4.09059
2.16545
2.03972
1.27139
1.25389
1.23598
1.21848
1.08646
0.87922
0.87033
0.86093
0.85311
0.84595
Integral
2.0880
1.0974
2.1195
3.3664
3.3295
1.0824
2.2590
ppm
14
12
10
8
6
4
2
0
Current Data Parameters
USER rachel
NAME rb_305_try2
EXPNO 1
PROCNO 1
F2 - Acquisition Parameters
Date_ 20141126
Time 15.42
INSTRUM drx400
PROBHD 5 mm QNP H/P/P
PULPROG zg30
TD 65536
SOLVENT CDCl3
NS 8
DS 2
SWH 6410.256 Hz
FIDRES 0.097813 Hz
AQ 5.1118579 sec
RG 143.7
DW 78.000 usec
DE 4.50 usec
TE 298.0 K
D1 0.10000000 sec
MCREST 0.00000000 sec
MCWRK 0.01500000 sec
======== CHANNEL f1 ========
NUC1 1H
P1 12.00 usec
PL1 0.00 dB
SFO1 400.1328009 MHz
F2 - Processing parameters
SI 65536
SF 400.1300175 MHz
WDW EM
SSB 0
LB 0.30 Hz
GB 0
PC 2.00
1D NMR plot parameters
CX 22.80 cm
CY 15.00 cm
F1P 14.966 ppm
F1 5988.51 Hz
F2P -1.054 ppm
F2 -421.74 Hz
PPMCM 0.70265 ppm/cm
HZCM 281.15158 Hz/cm

13C spectrum with 1H decoupling

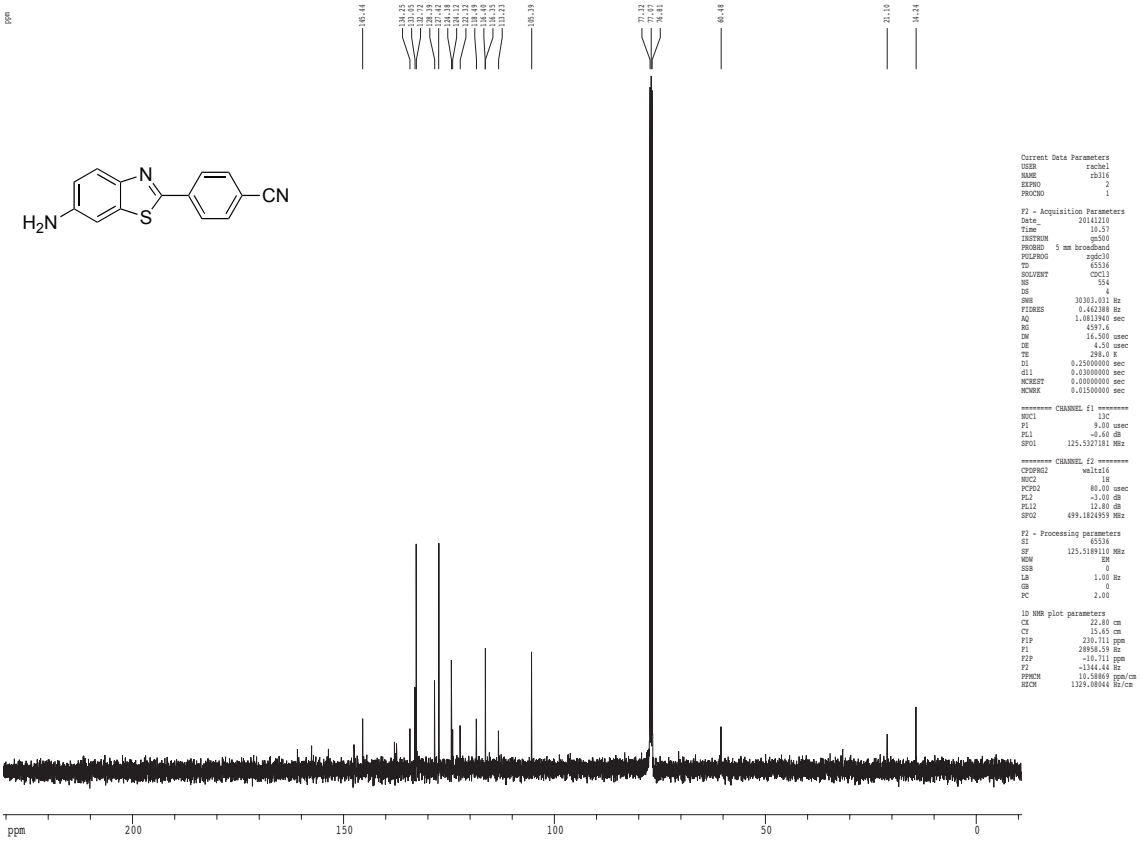


```
Current Data Parameters
USER              rachel
NAME              rb316
EXPNO                 2
PROCNO                1

F2 - Acquisition Parameters
Date_          20141210
Time              10.57
INSTRUM           spc500
PROBHD   5 mm broadband
PULPROG           zgdc30
TD                65536
SOLVENT           CDCl3
NS                  554
DS                    4
SWH           30303.031 Hz
FIDRES         0.462388 Hz
AQ             1.0813940 sec
RG               4597.6
DW               16.500 usec
DE                4.50 usec
TE               298.0 K
D1            0.25000000 sec
d11           0.03000000 sec
MCREST        0.00000000 sec
MCWRK         0.01500000 sec

======== CHANNEL f1 ========
NUC1                13C
P1                 9.00 usec
PL1               -0.60 dB
SFO1        125.5327181 MHz

======= CHANNEL f2 =======
CPDPRG2          waltz16
NUC2                 1H
PCPD2             80.00 usec
PL2               -3.00 dB
PL12              12.80 dB
SFO2        499.1824959 MHz

F2 - Processing parameters
SI                  65536
SF          125.5189110 MHz
WDW                    EM
SSB                     0
LB                   1.00 Hz
GB                      0
PC                   2.00

1D NMR plot parameters
CX                  22.80 cm
CY                  15.65 cm
F1P              230.711 ppm
F1               28958.59 Hz
F2P              -10.711 ppm
F2               -1344.44 Hz
PPMCM            10.58869 ppm/cm
HZCM          1329.08044 Hz/cm
```

1H spectrum

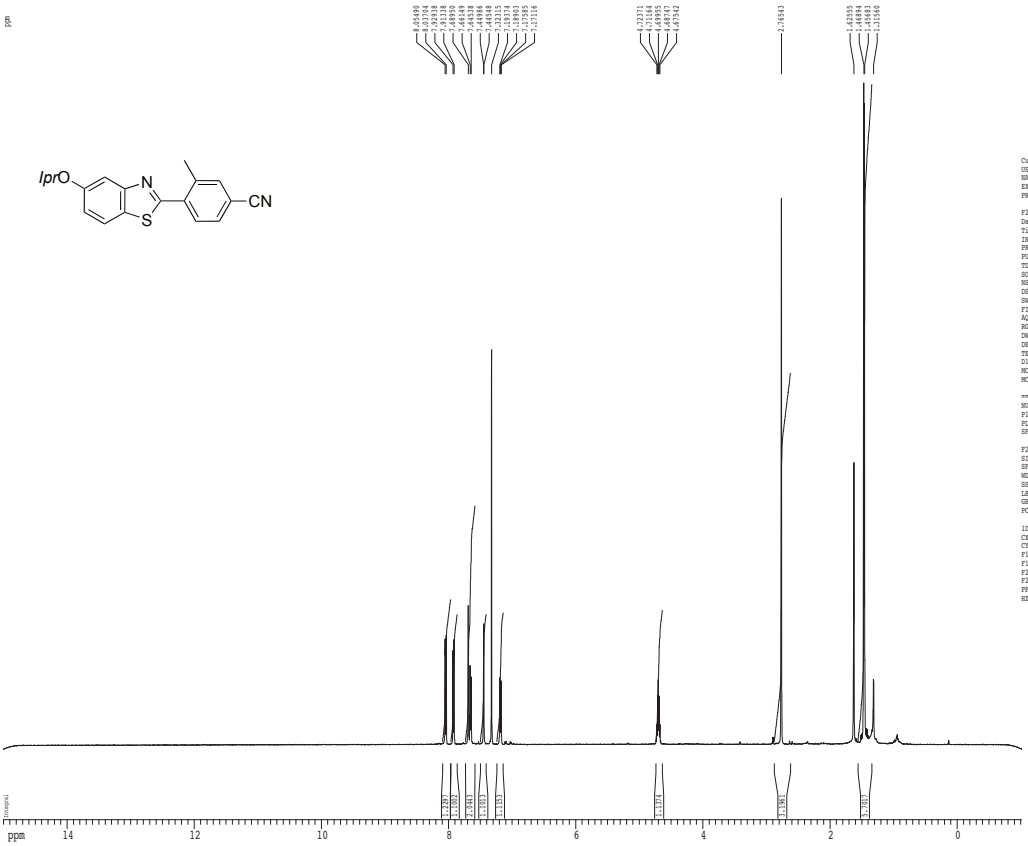


```
Current Data Parameters
USER            rachel
NAME        RL204_cryo
EXPNO               2
PROCNO              1

F2 - Acquisition Parameters
Date_        20150715
Time            17.53
INSTRUM       cryo500
PROBHD   5 mm CPTCI 1H-
PULPROG         zg30
TD              81728
SOLVENT         CDCl3
NS                  8
DS                  2
SWH           8012.820 Hz
FIDRES        0.098043 Hz
AQ          5.0998774 sec
RG                5.7
DW             62.400 usec
DE              6.00 usec
TE             298.0 K
D1          0.10000000 sec
MCREST      0.00000000 sec
MCWRK       0.01500000 sec

======== CHANNEL f1 ========
NUC1              1H
P1              7.50 usec
PL1             1.40 dB
SFO1       500.2235015 MHz

F2 - Processing parameters
SI             65536
SF         500.2200000 MHz
WDW              EM
SSB               0
LB             0.30 Hz
GB                0
PC             4.00

1D NMR plot parameters
CX             22.80 cm
CY             15.00 cm
F1P            15.009 ppm
F1             7507.95 Hz
F2P            -1.009 ppm
F2             -504.87 Hz
PPMCM        0.70257 ppm/cm
HZCM       351.43951 Hz/cm
```

Z-restored spin-echo 13C spectrum with 1H decoupling

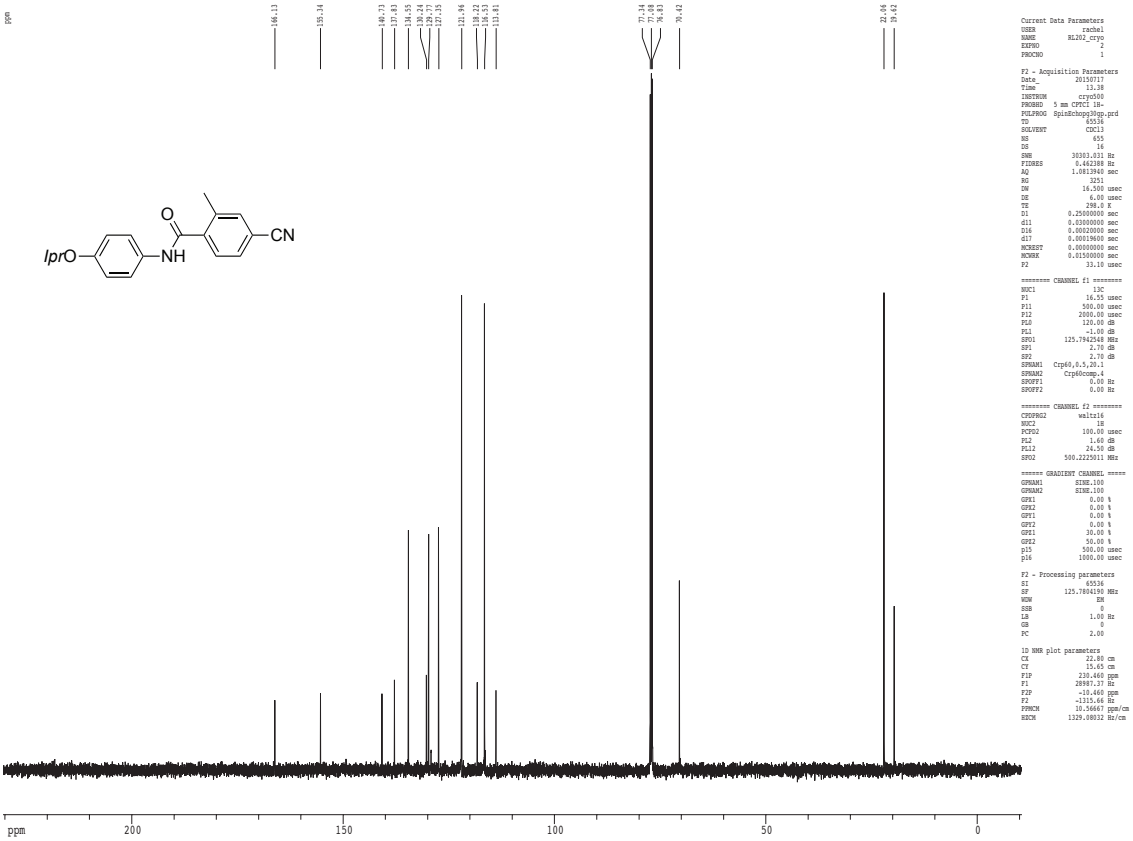


```
Current Data Parameters
USER            rachel
NAME         RL202_cryo
EXPNO                2
PROCNO               1

F2 - Acquisition Parameters
Date_         20150717
Time             13.38
INSTRUM        cryo500
PROBHD   5 mm CPTCI 1H-
PULPROG  SpinEchopg30gp.prd
TD              65536
SOLVENT          CDCl3
NS                 655
DS                  16
SWH           30303.031 Hz
FIDRES        0.462388 Hz
AQ            1.0813940 sec
RG                 3251
DW               16.500 usec
DE                6.00 usec
TE               298.0 K
D1            0.25000000 sec
d11           0.03000000 sec
D16           0.00020000 sec
d17           0.00019600 sec
MCREST        0.00000000 sec
MCWRK         0.01500000 sec
P2               33.10 usec

======== CHANNEL f1 ========
NUC1                 13C
P1                 16.55 usec
P11               500.00 usec
P12              2000.00 usec
PL0               120.00 dB
PL1                -1.00 dB
SFO1         125.7942548 MHz
SP1                 2.70 dB
SP2                 2.70 dB
SPNAM1    Crp60,0.5,20.1
SPNAM2      Crp60comp.4
SPOFF1              0.00 Hz
SPOFF2              0.00 Hz

======== CHANNEL f2 ========
CPDPRG2          waltz16
NUC2                  1H
PCPD2             100.00 usec
PL2                 1.60 dB
PL12               24.50 dB
SFO2        500.2225011 MHz

====== GRADIENT CHANNEL =====
GPNAM1         SINE.100
GPNAM2         SINE.100
GPX1                0.00 %
GPX2                0.00 %
GPY1                0.00 %
GPY2                0.00 %
GPZ1               30.00 %
GPZ2               50.00 %
p15               500.00 usec
p16              1000.00 usec

F2 - Processing parameters
SI                 65536
SF          125.7804190 MHz
WDW                   EM
SSB                    0
LB                  1.00 Hz
GB                     0
PC                  2.00

1D NMR plot parameters
CX                 22.80 cm
CY                 15.65 cm
F1P               230.460 ppm
F1                28987.37 Hz
F2P               -10.460 ppm
F2                -1315.66 Hz
PPMCM            10.56667 ppm/cm
HZCM          1329.08032 Hz/cm
```

Z-restored spin-echo 13C spectrum with 1H decoupling

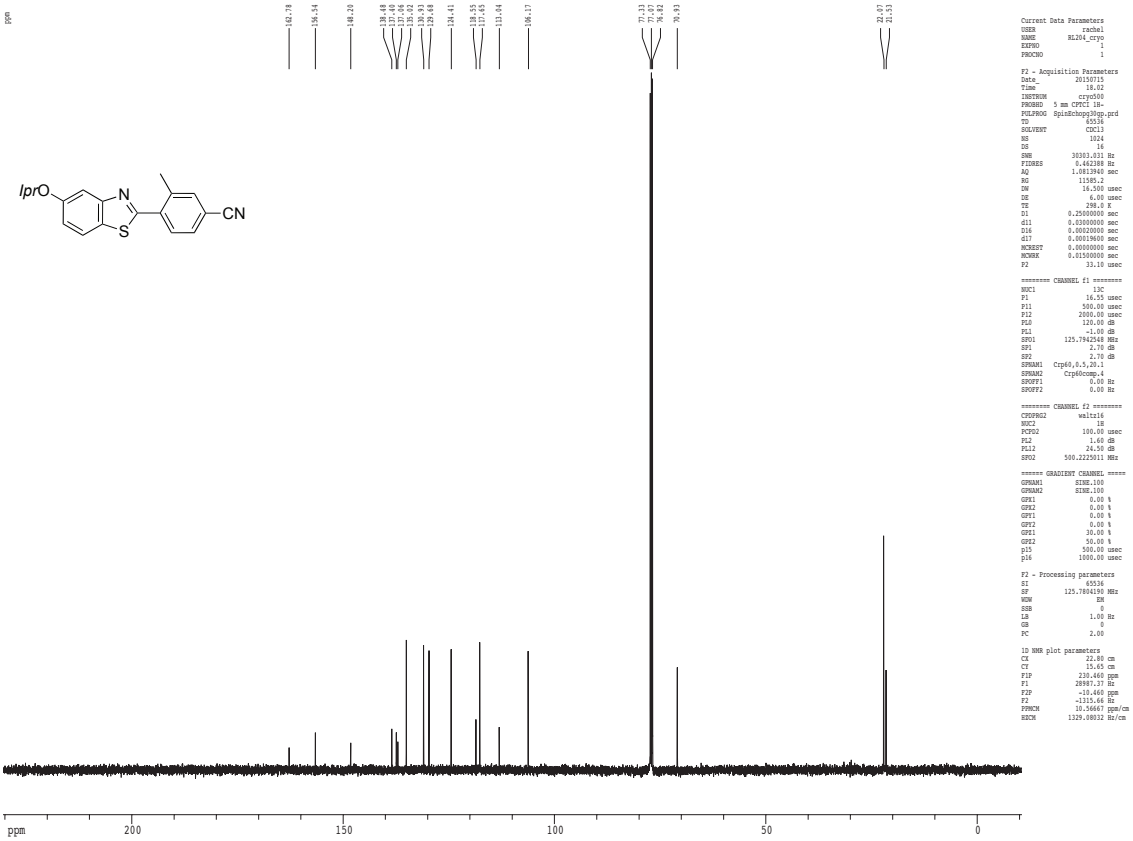


```
Current Data Parameters
USER          rachel
NAME        RL204_cryo
EXPNO             1
PROCNO            1

F2 - Acquisition Parameters
Date_        20150715
Time           18.02
INSTRUM      cryo500
PROBHD   5 mm CPTCI 1H-
PULPROG  SpinEchopg30gp.prd
TD            65536
SOLVENT       CDCl3
NS             1024
DS               16
SWH        30303.031 Hz
FIDRES      0.462388 Hz
AQ          1.0813940 sec
RG           11585.2
DW           16.500 usec
DE            6.00 usec
TE           298.0 K
D1         0.25000000 sec
d11        0.03000000 sec
D16        0.00020000 sec
d17        0.00019600 sec
MCREST     0.00000000 sec
MCWRK      0.01500000 sec
P2           33.10 usec

======== CHANNEL f1 ========
NUC1            13C
P1            16.55 usec
P11          500.00 usec
P12         2000.00 usec
PL0          120.00 dB
PL1           -1.00 dB
SFO1      125.7942548 MHz
SP1           2.70 dB
SP2           2.70 dB
SPNAM1   Crp40,0.5,20.1
SPNAM2    Crp60comp.4
SPOFF1        0.00 Hz
SPOFF2        0.00 Hz

======== CHANNEL f2 ========
CPDPRG2      waltz16
NUC2            1H
PCPD2       100.00 usec
PL2           1.60 dB
PL12         24.50 dB
SFO2     500.2225011 MHz

====== GRADIENT CHANNEL =====
GPNAM1       SINE.100
GPNAM2       SINE.100
GPX1          0.00 %
GPX2          0.00 %
GPY1          0.00 %
GPY2          0.00 %
GPZ1         30.00 %
GPZ2         50.00 %
p15        500.00 usec
p16       1000.00 usec

F2 - Processing parameters
SI            65536
SF      125.7804190 MHz
WDW             EM
SSB              0
LB            1.00 Hz
GB               0
PC            2.00

1D NMR plot parameters
CX           22.80 cm
CY           15.65 cm
F1P        230.460 ppm
F1       28987.37 Hz
F2P        -10.460 ppm
F2       -1315.66 Hz
PPMCM     10.56667 ppm/cm
HZCM    1329.08032 Hz/cm
```

Z-restored spin-echo 13C spectrum with 1H decoupling

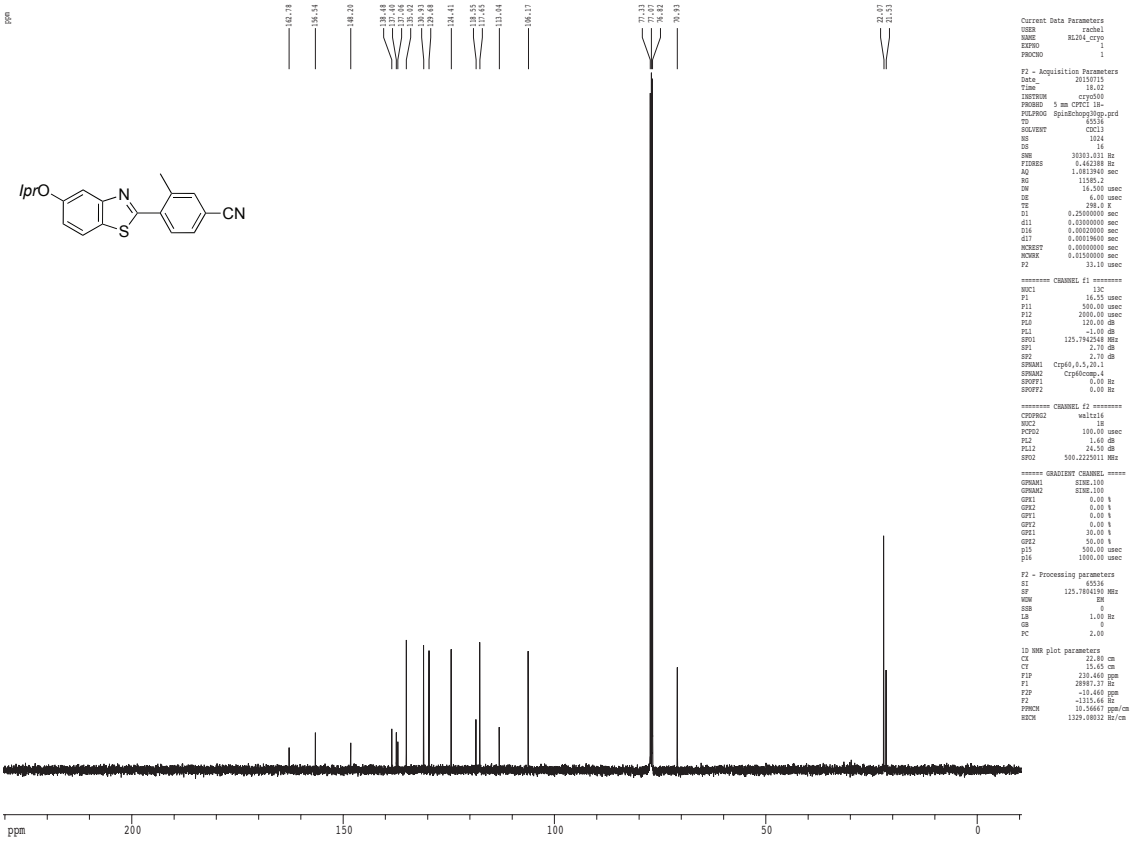


```
Current Data Parameters
USER          rachel
NAME        RL204_cryo
EXPNO             1
PROCNO            1

F2 - Acquisition Parameters
Date_        20150715
Time            18.02
INSTRUM       cryo500
PROBHD   5 mm CPTCI 1H-
PULPROG  SpinEchopg30gp.prd
TD            65536
SOLVENT         CDCl3
NS              1024
DS                16
SWH         30303.031 Hz
FIDRES       0.462388 Hz
AQ          1.0813940 sec
RG            11585.2
DW             16.500 usec
DE              6.00 usec
TE            298.0 K
D1          0.25000000 sec
d11         0.03000000 sec
D16         0.00020000 sec
d17         0.00019600 sec
MCREST      0.00000000 sec
MCWRK       0.01500000 sec
P2             33.10 usec

======== CHANNEL f1 ========
NUC1             13C
P1             16.55 usec
P11           500.00 usec
P12          2000.00 usec
PL0           120.00 dB
PL1            -1.00 dB
SFO1       125.7942548 MHz
SP1            2.70 dB
SP2            2.70 dB
SPNAM1   Crp40,0.5,20.1
SPNAM2    Crp60comp.4
SPOFF1         0.00 Hz
SPOFF2         0.00 Hz

======== CHANNEL f2 ========
CPDPRG2       waltz16
NUC2             1H
PCPD2        100.00 usec
PL2            1.60 dB
PL12          24.50 dB
SFO2      500.2225011 MHz

====== GRADIENT CHANNEL =====
GPNAM1       SINE.100
GPNAM2       SINE.100
GPX1           0.00 %
GPX2           0.00 %
GPY1           0.00 %
GPY2           0.00 %
GPZ1          30.00 %
GPZ2          50.00 %
p15          500.00 usec
p16         1000.00 usec

F2 - Processing parameters
SI            65536
SF       125.7804190 MHz
WDW             EM
SSB              0
LB            1.00 Hz
GB               0
PC            2.00

1D NMR plot parameters
CX            22.80 cm
CY            15.65 cm
F1P         230.460 ppm
F1        28987.37 Hz
F2P         -10.460 ppm
F2        -1315.66 Hz
PPMCM       10.56667 ppm/cm
HZCM      1329.08032 Hz/cm
```

1H spectrum

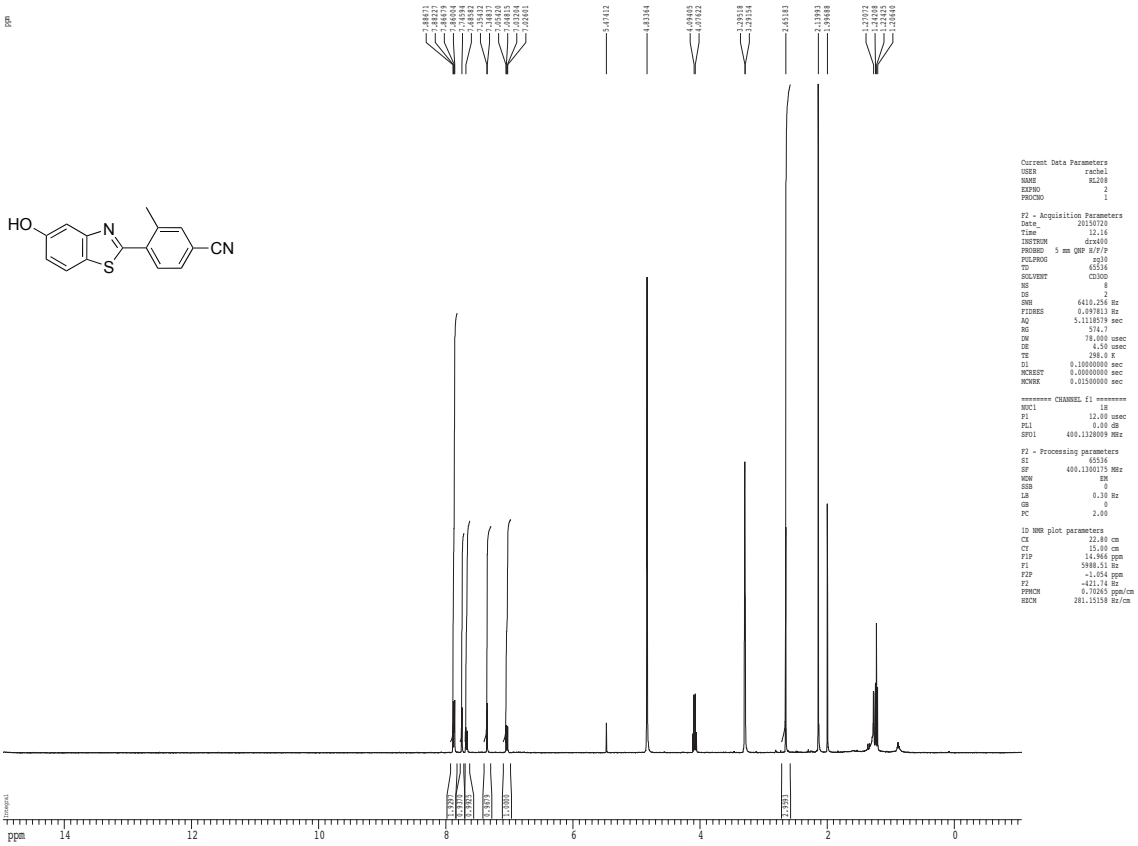

Current Data Parameters
USER rachel
NAME RL208
EXPNO 2
PROCNO 1

F2 - Acquisition Parameters
Date_ 20150720
Time 12.16
INSTRUM drx400
PROBHD 5 mm QNP H/P/F
PULPROG zg30
TD 65536
SOLVENT CD3OD
NS 8
DS 2
SWH 6410.256 Hz
FIDRES 0.097813 Hz
AQ 5.1118579 sec
RG 574.7
DW 78.000 usec
DE 4.50 usec
TE 298.0 K
D1 0.10000000 sec
MCREST 0.00000000 sec
MCWRK 0.01500000 sec

======== CHANNEL f1 ========
NUC1 1H
P1 12.00 usec
PL1 0.00 dB
SFO1 400.1328009 MHz

F2 - Processing parameters
SI 65536
SF 400.1300175 MHz
WDW EM
SSB 0
LB 0.30 Hz
GB 0
PC 2.00

1D NMR plot parameters
CX 22.80 cm
CY 15.00 cm
F1P 14.966 ppm
F1 5988.51 Hz
F2P -1.054 ppm
F2 -421.74 Hz
PPMCM 0.70265 ppm/cm
HZCM 281.15158 Hz/cm

1H spectrum

3

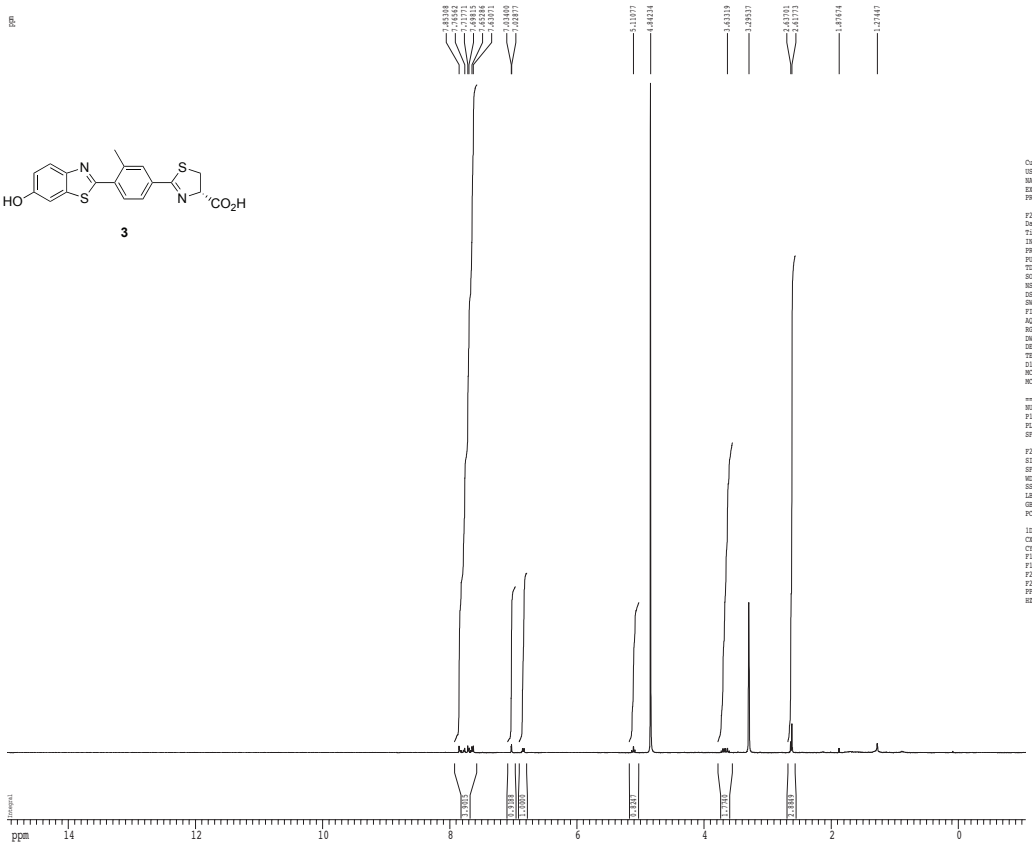


```
Current Data Parameters
USER            rachel
NAME        RL211_lyoph
EXPNO             2
PROCNO            1

F2 - Acquisition Parameters
Date_       20150723
Time          18.13
INSTRUM       drx400
PROBHD   5 mm QNP H/P/F
PULPROG        zg30
TD            65536
SOLVENT       CD3OD
NS               8
DS               2
SWH        6410.256 Hz
FIDRES     0.097813 Hz
AQ       5.1118579 sec
RG           812.7
DW          78.000 usec
DE           4.50 usec
TE          298.0 K
D1       0.10000000 sec
MCREST   0.00000000 sec
MCWRK    0.01500000 sec

======== CHANNEL f1 =======
NUC1           1H
P1          12.00 usec
PL1          0.00 dB
SFO1     400.1328009 MHz

F2 - Processing parameters
SI          65536
SF     400.1300175 MHz
WDW           EM
SSB            0
LB          0.30 Hz
GB             0
PC          2.00

1D NMR plot parameters
CX          22.80 cm
CY          15.00 cm
F1P        14.966 ppm
F1        5988.51 Hz
F2P        -1.054 ppm
F2        -421.74 Hz
PPMCM     0.70265 ppm/cm
HZCM     281.15158 Hz/cm
```

1H spectrum

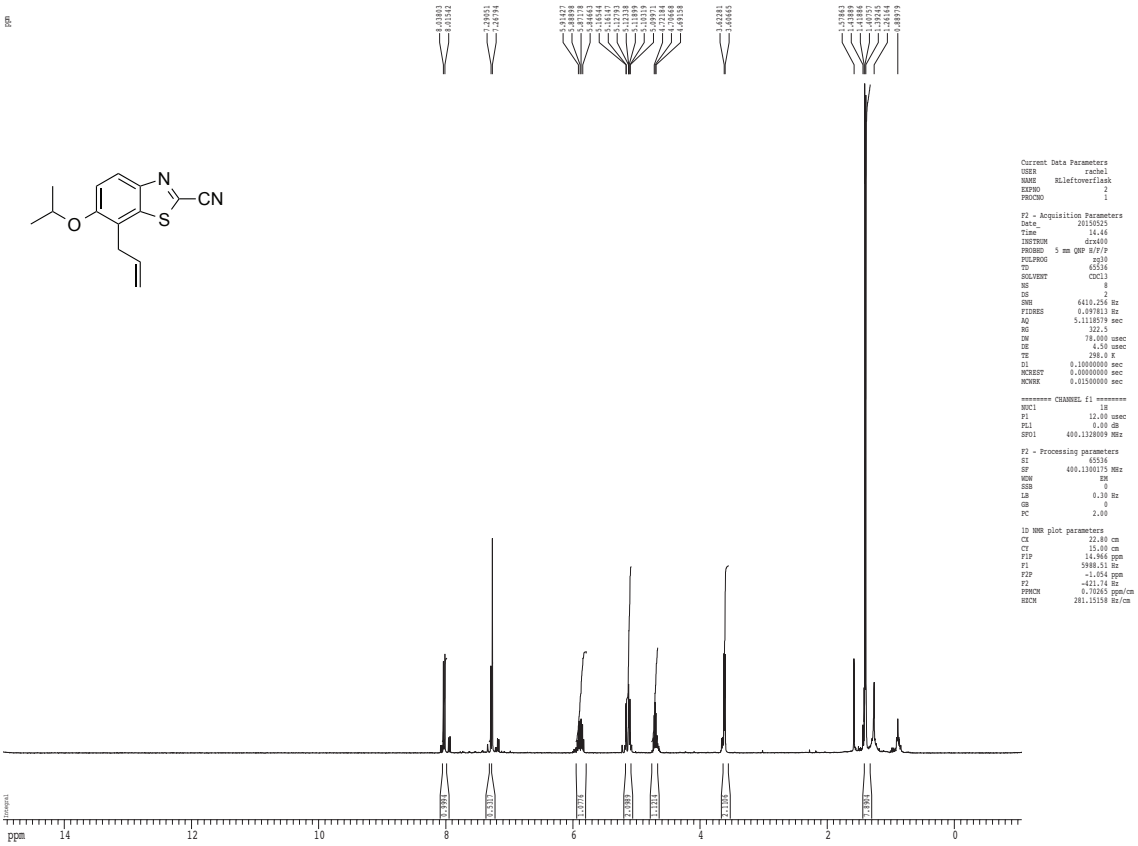
ppm
8.00812
8.00316
7.29051
7.26794
5.81427
5.80898
5.80728
5.80199
5.16544
5.16347
5.15239
5.13338
5.13139
5.12939
5.12739
5.05971
5.05754
4.75544
4.75488
4.65538
3.62281
3.60495
1.57843
1.46889
1.46386
1.46072
1.32425
1.26544
1.26019
Integral
2.9891
9.3357
1.0791
2.0889
1.1214
2.1285
7.3804
ppm
14
12
10
8
6
4
2
0
N
CN
S
O
Current Data Parameters
USER rachel
NAME RLleftoverflask
EXPNO 2
PROCNO 1
F2 - Acquisition Parameters
Date_ 20150525
Time 14.46
INSTRUM drx400
PROBHD 5 mm QNP H/P/F
PULPROG zg30
TD 65536
SOLVENT CDCl3
NS 8
DS 2
SWH 6410.256 Hz
FIDRES 0.097813 Hz
AQ 5.1118579 sec
RG 322.5
DW 78.000 usec
DE 4.50 usec
TE 298.0 K
D1 0.10000000 sec
MCREST 0.00000000 sec
MCWRK 0.01500000 sec
======== CHANNEL f1 ========
NUC1 1H
P1 12.00 usec
PL1 0.00 dB
SFO1 400.1328009 MHz
F2 - Processing parameters
SI 65536
SF 400.1300175 MHz
WDW EM
SSB 0
LB 0.30 Hz
GB 0
PC 2.00
1D NMR plot parameters
CX 22.80 cm
CY 15.00 cm
F1P 14.966 ppm
F1 5988.51 Hz
F2P -1.054 ppm
F2 -421.74 Hz
PPMCM 0.70265 ppm/cm
HZCM 281.15158 Hz/cm

1H spectrum

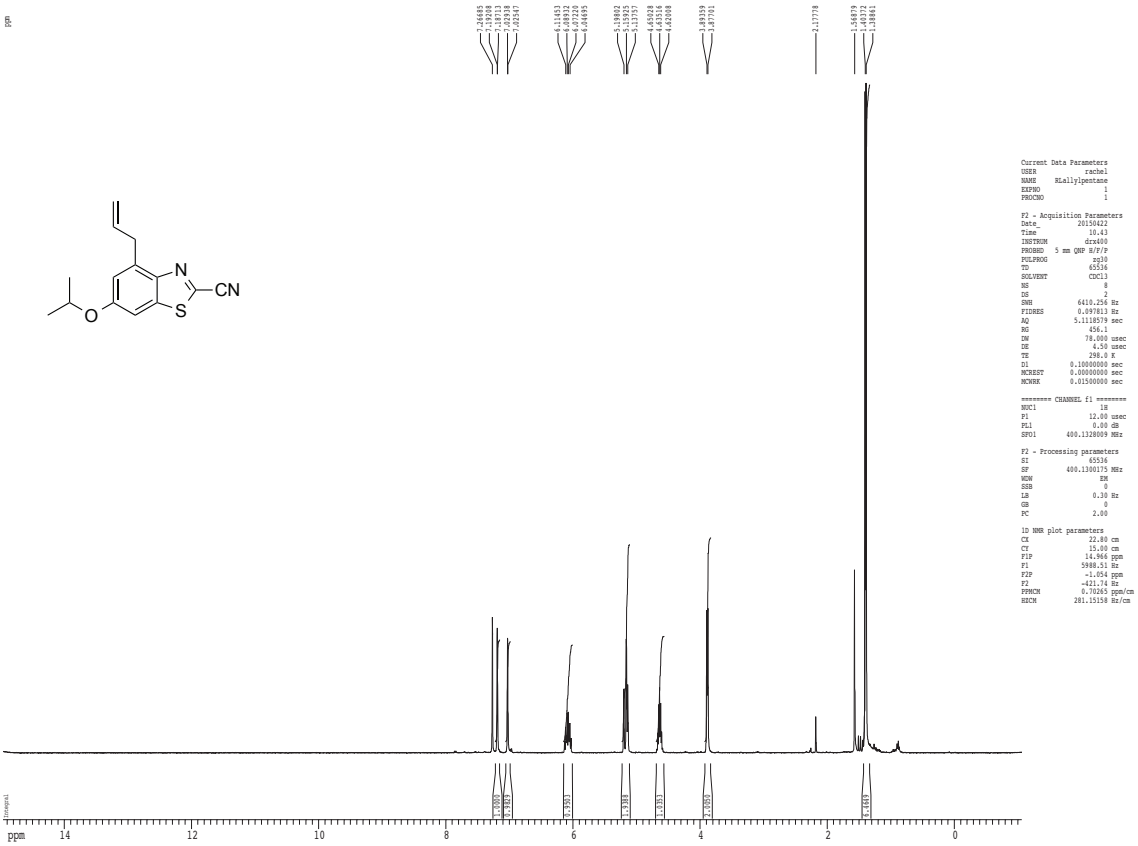


```
Current Data Parameters
USER              rachel
NAME      RLallylpentane
EXPNO                  1
PROCNO                 1

F2 - Acquisition Parameters
Date_          20150422
Time              10.43
INSTRUM        drx400
PROBHD   5 mm QNP H/P/P
PULPROG           zg30
TD               65536
SOLVENT          CDCl3
NS                   8
DS                   2
SWH           6410.256 Hz
FIDRES        0.097813 Hz
AQ            5.1118579 sec
RG               456.1
DW               78.000 usec
DE                4.50 usec
TE               298.0 K
D1           0.10000000 sec
MCREST       0.00000000 sec
MCWRK        0.01500000 sec

======== CHANNEL f1 =======
NUC1               1H
P1               12.00 usec
PL1               0.00 dB
SFO1        400.1328009 MHz

F2 - Processing parameters
SI               65536
SF          400.1300175 MHz
WDW              EM
SSB               0
LB               0.30 Hz
GB                0
PC               2.00

1D NMR plot parameters
CX              22.80 cm
CY              15.00 cm
F1P             14.966 ppm
F1             5988.51 Hz
F2P             -1.054 ppm
F2              -421.74 Hz
PPMCM          0.70265 ppm/cm
HZCM          281.15158 Hz/cm
```

Z-restored spin-echo 13C spectrum with 1H decoupling

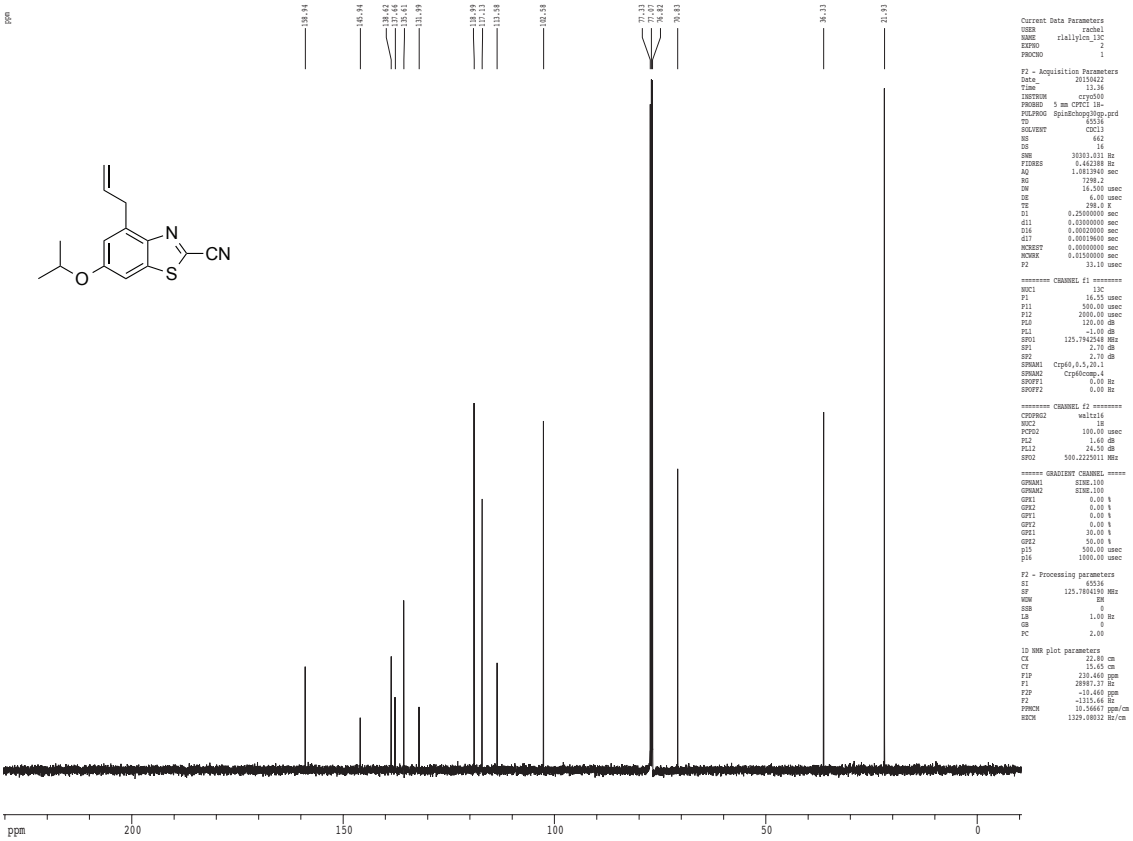


```
Current Data Parameters
USER              rachel
NAME      rlallylcn_13C
EXPNO               2
PROCNO              1

F2 - Acquisition Parameters
Date_          20150422
Time             13.36
INSTRUM        cryo500
PROBHD   5 mm CPTCI 1H-
PULPROG  SpinEchopg30gp.prd
TD             65536
SOLVENT          CDCl3
NS               662
DS                16
SWH          30303.031 Hz
FIDRES       0.462388 Hz
AQ           1.0813940 sec
RG             7298.2
DW             16.500 usec
DE              6.00 usec
TE             298.0 K
D1          0.25000000 sec
d11         0.03000000 sec
D16         0.00020000 sec
d17         0.00019600 sec
MCREST      0.00000000 sec
MCWRK       0.01500000 sec
P2             33.10 usec

======== CHANNEL f1 ========
NUC1             13C
P1             16.55 usec
P11           500.00 usec
P12          2000.00 usec
PL0            120.00 dB
PL1             -1.00 dB
SFO1       125.7942548 MHz
SP1             2.70 dB
SP2             2.70 dB
SPNAM1   Crp60,0.5,20.1
SPNAM2     Crp60comp.4
SPOFF1          0.00 Hz
SPOFF2          0.00 Hz

======== CHANNEL f2 ========
CPDPRG2        waltz16
NUC2              1H
PCPD2          100.00 usec
PL2             1.60 dB
PL12           24.50 dB
SFO2       500.2225011 MHz

====== GRADIENT CHANNEL =====
GPNAM1        SINE.100
GPNAM2        SINE.100
GPX1            0.00 %
GPX2            0.00 %
GPY1            0.00 %
GPY2            0.00 %
GPZ1           30.00 %
GPZ2           50.00 %
p15           500.00 usec
p16          1000.00 usec

F2 - Processing parameters
SI               65536
SF         125.7804190 MHz
WDW               EM
SSB                0
LB              1.00 Hz
GB                 0
PC              2.00

1D NMR plot parameters
CX              22.80 cm
CY              15.65 cm
F1P           230.460 ppm
F1            28987.37 Hz
F2P           -10.460 ppm
F2            -1315.66 Hz
PPMCM        10.56667 ppm/cm
HZCM       1329.08032 Hz/cm
```

Appendix D: Additional computational data for Chapter 3

D-Luc

S0 Energy = -1438.843074343

C	-1.2813373	4.2620165	0.9672691
C	-0.5639216	3.0090061	1.0785824
C	0.8064982	3.0073406	1.1731258
C	1.5866350	4.2210546	1.1679940
C	0.8995049	5.4641204	1.0601380
C	-0.4599930	5.4801449	0.9650070
S	1.9038716	1.6557876	1.3136942
C	3.2596334	2.7958787	1.3508706
N	2.9068526	4.0653135	1.2658870
C	4.5972422	2.3599630	1.4611518
S	5.8813591	3.5980542	1.4854097
N	4.9702370	1.1080088	1.5469792
C	6.3234754	0.9454358	1.6461948
C	7.1002788	2.2773794	1.6302748
O	6.9126056	-0.1140081	1.7399920
O	-2.5220026	4.3248825	0.8775392
H	-1.0078312	6.4213743	0.8805400
H	1.4886068	6.3838958	1.0560990
H	-1.1523024	2.0906698	1.0827860
H	7.7967781	2.2782298	0.7806943
H	7.6821334	2.3670627	2.5575835

S1 Energy = -1438.837364170

C	-1.3077364	4.2411522	0.9742593
C	-0.5251260	3.0144489	1.0853816
C	0.8732071	3.0787400	1.1717981
C	1.5811853	4.2982977	1.1571969
C	0.8343348	5.4909973	1.0477456
C	-0.5449927	5.4702381	0.9599381
S	1.9763984	1.7519350	1.3077014
C	3.3014484	2.9069091	1.3384698
N	2.9533467	4.1697306	1.2536181
C	4.6384353	2.4025237	1.4553801
S	5.9626301	3.5791753	1.4991833
N	4.9516785	1.1310834	1.5337424
C	6.2915119	0.9031962	1.6420835
C	7.1250283	2.2021387	1.6445183
O	6.8391147	-0.1862002	1.7311552
O	-2.5568109	4.1882638	0.8988577
H	-1.1121422	6.3987922	0.8751294
H	1.3781167	6.4389700	1.0335322
H	-1.0664676	2.0675599	1.0986238
H	7.8317080	2.1872338	0.8022538
H	7.7034552	2.2664248	2.5772437

6'-aminoLuc

S0 Energy = -1419.531486458

C	-4.4714246	0.6994008	-0.0531430
C	-3.3692188	1.5614488	-0.0974595
C	-4.2658215	-0.7069461	0.0061684
C	-3.0009735	-1.2492622	0.0244840
C	-2.0921667	1.0063512	-0.0803884
C	0.2163665	0.2382510	-0.0579573
S	-0.5584490	1.8136621	-0.1235692
C	1.6607835	0.1366511	-0.0622214
C	3.7786309	0.8331079	-0.1041887
C	4.0076765	-0.6855881	-0.0437758
S	2.3821488	-1.4681121	-0.0009116
H	4.5888990	-0.9326787	0.8545634
H	4.5767526	-1.0051463	-0.9269342
N	2.4274703	1.1729047	-0.1094693
N	-0.5788406	-0.7855947	-0.0088251
C	-1.8823847	-0.3974068	-0.0192836
H	-3.5184629	2.6409029	-0.1456867
H	-2.8488274	-2.3279379	0.0711795
H	-5.1385883	-1.3622747	0.0351306
O	4.6868831	1.6208778	-0.1420452
N	-5.7511204	1.1900916	-0.1014747
H	-5.9101560	2.1741553	0.0461581
H	-6.5173909	0.5846211	0.1462701

S1 Energy = -1419.527675377

C	-4.4803789	0.6851627	-0.0178088
C	-3.3266056	1.5285508	-0.0610676
C	-4.3249978	-0.7152743	0.0290246
C	-3.0598503	-1.2789556	0.0336751
C	-2.0683707	0.9377477	-0.0550975
C	0.2198206	0.1264484	-0.0523619
S	-0.5154815	1.7232744	-0.1001641
C	1.6501356	0.0722123	-0.0638300
C	3.7302659	0.8922127	-0.1104362
C	4.0432301	-0.6194627	-0.0588742
S	2.4601755	-1.4950325	-0.0164827
H	4.6396163	-0.8437868	0.8364763
H	4.6276427	-0.9073218	-0.9438741
N	2.3864681	1.1573965	-0.1079582
N	-0.6099309	-0.9016371	-0.0076986
C	-1.9050211	-0.4652489	-0.0080012
H	-3.4498270	2.6122753	-0.0984732
H	-2.9332101	-2.3617129	0.0698932
H	-5.2111955	-1.3504931	0.0610567

O	4.6238033	1.7152787	-0.1476353
N	-5.7079766	1.2648930	-0.0238185
H	-5.8180548	2.2669642	-0.0557480
H	-6.5484712	0.7079876	0.0058242

6'-MeNHLH2

S0 Energy = -1458.761653271

C	-4.4872976	0.6696379	-0.0489409
C	-3.3824353	1.5327374	-0.1473878
C	-4.2720884	-0.7304882	0.0981780
C	-2.9995231	-1.2591416	0.1461942
C	-2.1052672	0.9900004	-0.0985360
C	0.2091789	0.2348838	-0.0417864
S	-0.5742369	1.8011763	-0.1969441
C	1.6531610	0.1391059	-0.0510849
C	3.7681740	0.8399187	-0.1370161
C	4.0035162	-0.6744100	-0.0183228
S	2.3812831	-1.4597322	0.0727991
H	4.5957110	-0.8835664	0.8824064
H	4.5639884	-1.0267934	-0.8945450
N	2.4162632	1.1749752	-0.1482248
N	-0.5804386	-0.7877926	0.0730776
C	-1.8861072	-0.4084055	0.0475822
H	-3.5376057	2.6067408	-0.2618215
H	-2.8411273	-2.3321072	0.2603661
H	-5.1294213	-1.3979398	0.1745117
O	4.6738481	1.6285687	-0.2099286
N	-5.7542279	1.1765487	-0.0942315
C	-6.9503067	0.3858882	-0.0248385
H	-5.8519107	2.1722670	-0.2066495
H	-7.0154443	-0.3411765	-0.8521188
H	-7.8189738	1.0492230	-0.0928716
H	-7.0241598	-0.1697600	0.9249636

S1 Energy = -1458.758090104

C	-4.4940452	0.6138937	-0.0458721
C	-3.3500759	1.4627083	-0.1364094
C	-4.3265676	-0.7776759	0.0912730
C	-3.0503608	-1.3241779	0.1393935
C	-2.0836445	0.8894190	-0.0874074
C	0.2132737	0.1040229	-0.0300020
S	-0.5432916	1.6872872	-0.1817513
C	1.6443727	0.0696163	-0.0445610
C	3.7108312	0.9173472	-0.1637966
C	4.0492132	-0.5815949	-0.0108331
S	2.4807752	-1.4770004	0.1024370
H	4.6543218	-0.7338128	0.8936643
H	4.6333114	-0.9197773	-0.8779575
N	2.3633530	1.1606597	-0.1676050
N	-0.6032185	-0.9254865	0.0826763
C	-1.9065876	-0.5057360	0.0515846
H	-3.4831241	2.5410358	-0.2431797
H	-2.9132055	-2.4009690	0.2454444
H	-5.1955703	-1.4295292	0.1595461
O	4.5903845	1.7502028	-0.2662265
N	-5.7219068	1.2035500	-0.0986606
C	-6.9633152	0.4926620	-0.0284835
H	-5.7527764	2.2078640	-0.1987465
H	-7.0532381	-0.2347449	-0.8530727
H	-7.7923929	1.2032438	-0.0971100
H	-7.0519632	-0.0626493	0.9204859

6'-Me2NLH2

S0 Energy = -1497.990421989

C	-4.4861974	0.7491604	-0.0910281
C	-3.3611606	1.5968276	-0.1029254
C	-4.2810704	-0.6653136	-0.0660703
C	-3.0199584	-1.2164225	-0.0494197
C	-2.0926843	1.0261819	-0.0865954
C	0.2120281	0.2425126	-0.0606940
S	-0.5521773	1.8244503	-0.0965605
C	1.6546717	0.1319701	-0.0515171
C	3.7772472	0.8162629	-0.0572887
C	3.9971041	-0.7046679	-0.0201194
S	2.3667505	-1.4782345	-0.0106258
H	4.5657277	-0.9700488	0.8810927
H	4.5755926	-1.0121816	-0.9014106
N	2.4291049	1.1640647	-0.0717082
N	-0.5910980	-0.7771687	-0.0435917
C	-1.8908190	-0.3788969	-0.0578753
H	-3.4715258	2.6777862	-0.1257107
H	-2.8823335	-2.2979416	-0.0301953
H	-5.1408846	-1.3315481	-0.0599715
O	4.6912395	1.5987041	-0.0718205
N	-5.7553110	1.2633106	-0.1035751
C	-6.9004261	0.3869323	-0.1106124
H	-6.9294967	-0.2594303	0.7820583
H	-6.9190932	-0.2614487	-1.0026626
H	-7.8138926	0.9887326	-0.1156257
C	-5.9470514	2.6908924	-0.1349602
H	-5.5047395	3.1446984	-1.0383141
H	-5.4994370	3.1821005	0.7455521

H	-7.0177921	2.9136213	-0.1359343

S1 Energy = -1497.987259200

C	-4.4966845	0.7060184	-0.0951344
C	-3.3379064	1.5324563	-0.1030681
C	-4.3377266	-0.7006779	-0.0714968
C	-3.0750048	-1.2718974	-0.0554425
C	-2.0812256	0.9327865	-0.0856622
C	0.2064057	0.1197652	-0.0591166
S	-0.5299475	1.7200821	-0.0907584
C	1.6380950	0.0676805	-0.0498289
C	3.7165129	0.8948966	-0.0549151
C	4.0342412	-0.6157478	-0.0211218
S	2.4534342	-1.4965669	-0.0141354
H	4.6189543	-0.8505449	0.8791625
H	4.6322186	-0.8879359	-0.9019022
N	2.3720938	1.1552380	-0.0672201
N	-0.6200908	-0.9069333	-0.0462647
C	-1.9188294	-0.4680740	-0.0610814
H	-3.4222004	2.6165555	-0.1228028
H	-2.9600356	-2.3561791	-0.0384609
H	-5.2079783	-1.3521217	-0.0662337
O	4.6074021	1.7221357	-0.0680827
N	-5.7431889	1.2882624	-0.1110534
C	-6.9170887	0.4558623	-0.1048516
H	-6.9465014	-0.1815247	0.7945456
H	-6.9379717	-0.2073221	-0.9857761
H	-7.8124491	1.0821284	-0.1182652
C	-5.8948431	2.7218790	-0.1370610
H	-5.4332203	3.1604881	-1.0369026
H	-5.4356909	3.1923887	0.7476793
H	-6.9584563	2.9718076	-0.1428581

CycloLuc-1

S0 Energy = -1496.809364595

C	-4.5332049	0.8700070	0.1884754
C	-3.4533613	1.7437545	0.1266118
C	-4.3651522	-0.5455850	0.2133999
C	-3.1167863	-1.1115332	0.1776570
C	-2.1843145	1.1564577	0.0896171
C	0.1120877	0.3549146	0.0035415
S	-0.6418683	1.9392121	0.0022762
C	1.5514649	0.2322211	-0.0585663
C	3.6773770	0.8961032	-0.1735707
C	3.8849595	-0.6267986	-0.1410293
S	2.2501354	-1.3848422	-0.0472983
H	4.4949910	-0.8940398	0.7320955
H	4.4162729	-0.9430566	-1.0485217
N	2.3340119	1.2567174	-0.1214294
N	-0.6993542	-0.6578692	0.0621271
C	-1.9952502	-0.2539636	0.1118390
H	-3.5905528	2.8247393	0.1037956
H	-2.9647913	-2.1914208	0.1969222
O	4.5971562	1.6694522	-0.2374958
N	-5.8720096	1.1721768	0.2532084
C	-6.6725631	-0.0121654	-0.0344857
H	-6.2017164	2.0817157	-0.0338749
C	-5.7307858	-1.1718301	0.3314280
H	-6.9422776	-0.0552014	-1.1051920
H	-7.6014056	-0.0146429	0.5505426
H	-5.8687522	-2.0462145	-0.3170772
H	-5.9041856	-1.4993389	1.3695036

S1 Energy = -1496.805965042

C	-4.5188303	0.8448987	0.0649123
C	-3.4057626	1.7038943	-0.0120338
C	-4.3933374	-0.5645303	0.1453505
C	-3.1441156	-1.1508470	0.1515579
C	-2.1554606	1.0885034	-0.0049445
C	0.1249134	0.2489555	-0.0108181
S	-0.5914225	1.8572849	-0.0896190
C	1.5596392	0.1717704	-0.0422211
C	3.6502853	0.9576060	-0.1443735
C	3.9407244	-0.5561388	-0.0564846
S	2.3452184	-1.4049256	0.0351680
H	4.5484552	-0.7654240	0.8349124
H	4.5062645	-0.8768773	-0.9425104
N	2.3087500	1.2431367	-0.1275050
N	-0.7045317	-0.7689543	0.0710004
C	-2.0034705	-0.3225669	0.0759388
H	-3.5234551	2.7860514	-0.0737316
H	-3.0096882	-2.2313761	0.2125619
O	4.5534279	1.7670832	-0.2187222
N	-5.8340155	1.1946670	0.0757037
C	-6.7191482	0.0498699	0.1600770
H	-6.1648151	2.1465673	0.0261097
C	-5.7705014	-1.1687788	0.2125729
H	-7.3916321	0.0217248	-0.7129199
H	-7.3574459	0.1257051	1.0554184
H	-5.9546457	-1.8571504	-0.6255961
H	-5.9152757	-1.7511800	1.1346954

CycloLuc-2

S0 Energy = -1536.043936818

C	-4.5177037	0.8825209	0.2240439
C	-3.4339598	1.7519734	0.1364294
C	-4.3507512	-0.5346255	0.2477281
C	-3.1064844	-1.1051381	0.2004083
C	-2.1669125	1.1588914	0.0932334
C	0.1268617	0.3503597	-0.0067657
S	-0.6231183	1.9365082	-0.0107615
C	1.5647602	0.2224707	-0.0772111
C	3.6933664	0.8773770	-0.1950317
C	3.8939476	-0.6468396	-0.1793518
S	2.2563345	-1.3979752	-0.0803654
H	4.5101054	-0.9258714	0.6856685
H	4.4161248	-0.9561856	-1.0945647
N	2.3521888	1.2437481	-0.1368690
N	-0.6880078	-0.6596411	0.0640315
C	-1.9813369	-0.2512773	0.1234451
H	-3.5607052	2.8327060	0.0962407
H	-2.9588448	-2.1855981	0.2200439
O	4.6171515	1.6467845	-0.2510712
N	-5.8518777	1.1947327	0.3023929
C	-6.6485020	0.0088926	0.0171091
C	-5.7166292	-1.1573484	0.3722052
H	-6.9228079	-0.0181674	-1.0557101
H	-7.5794186	0.0173775	0.6002205
H	-5.8611150	-2.0270291	-0.2809260
H	-5.8872431	-1.4891083	1.4092008
C	-6.3644971	2.4939682	-0.0182548
H	-5.8029838	3.2695056	0.5186751
H	-7.4126624	2.5630680	0.2996060
H	-6.3145398	2.7136773	-1.1018496

S1 Energy = -1536.040963107

C	-4.5096600	0.8542040	0.1497455
C	-3.3959787	1.7067676	0.0687325
C	-4.3833063	-0.5567709	0.2088052
C	-3.1369889	-1.1493234	0.1908217
C	-2.1462485	1.0860860	0.0494318
C	0.1319822	0.2400044	-0.0070415
S	-0.5826276	1.8524619	-0.0552789
C	1.5658464	0.1595740	-0.0649257
C	3.6562055	0.9426315	-0.1939619
C	3.9451256	-0.5726231	-0.1355150
S	2.3496750	-1.4194086	-0.0268745
H	4.5691531	-0.7966795	0.7408769
H	4.4932948	-0.8801285	-1.0369966
N	2.3158528	1.2304861	-0.1474074
N	-0.6976121	-0.7754734	0.0767525
C	-1.9962040	-0.3247174	0.1097975
H	-3.4995787	2.7898275	0.0147012
H	-3.0080556	-2.2311926	0.2376484
O	4.5593568	1.7517801	-0.2726379
N	-5.8321243	1.2122105	0.1885602
C	-6.6848755	0.0439584	0.0684711
C	-5.7582083	-1.1528831	0.3347588
H	-7.1099440	0.0065919	-0.9532229
H	-7.5318000	0.1168724	0.7668801
H	-5.9361312	-1.9759780	-0.3701055
H	-5.9174814	-1.5574133	1.3477642
C	-6.3383710	2.5335888	-0.0053534
H	-5.6983115	3.2686290	0.4987506
H	-7.3487701	2.6066709	0.4168807
H	-6.3934748	2.8000035	-1.0781078

NMeBenzLuc

S0 Energy = -1135.399753938

C	-1.2375449	4.3192697	0.9962674
C	-0.4291839	3.1348193	1.1216527
C	0.9443563	3.2706318	1.2010201
C	1.6150501	4.5430098	1.1635154
C	0.8378917	5.7288952	1.0400824
C	-0.5179048	5.6093513	0.9611894
N	1.9576406	2.3551952	1.3231419
C	3.1544686	3.0707689	1.3539433
N	2.9375752	4.3880752	1.2571934
C	4.4438684	2.5185508	1.4699009
S	5.8229820	3.6547542	1.4821962
N	4.7301631	1.2386532	1.5699342
C	6.0642714	0.9785272	1.6692306
C	6.9386156	2.2469089	1.6391193
O	6.5736526	-0.1233549	1.7732947
O	-2.4841720	4.2994069	0.9184069
H	-1.1548781	6.4917420	0.8650602
H	1.3375206	6.6997692	1.0111411
H	-0.9352195	2.1688883	1.1502326
H	7.6327425	2.1853652	0.7896568
H	7.5282210	2.3002674	2.5645180
C	1.7922907	0.9278022	1.3994518
H	0.7219850	0.7032482	1.3445312
H	2.2034190	0.5317288	2.3366408
H	2.3157012	0.4246350	0.5764295

S1 Energy = -1135.392767424

C	-1.2697770	4.3170913	0.9924328
C	-0.4065855	3.1465368	1.1205726
C	0.9918151	3.3271635	1.2005843
C	1.6018254	4.5962767	1.1619881
C	0.7781299	5.7292504	1.0391205
C	-0.6017663	5.5991948	0.9571558
N	1.9941187	2.4141495	1.3226699
C	3.1821287	3.1413153	1.3550917
N	2.9700840	4.4493477	1.2607930
C	4.4658335	2.5246643	1.4740042
S	5.8668476	3.6162170	1.4850740
N	4.7105919	1.2333453	1.5753908
C	6.0328826	0.9289858	1.6731358
C	6.9437794	2.1723608	1.6407074
O	6.5140263	-0.1932310	1.7774979
O	-2.5124690	4.1635050	0.9200294
H	-1.2392930	6.4792365	0.8609364
H	1.2413250	6.7190183	1.0086065
H	-0.8846781	2.1666191	1.1494226
H	7.6369856	2.0968506	0.7903603
H	7.5396985	2.2154232	2.5637056
C	1.8352167	0.9832688	1.3974546
H	0.7677426	0.7475944	1.3387873
H	2.2581147	0.5986480	2.3327155
H	2.3769349	0.4940774	0.5795138

4-BrLuc

S0 Energy = -4011.790393777

O	-6.8448625	3.5066263	0.0000277
C	-5.7550987	2.8962422	-0.0001237
C	-4.4743511	3.5689170	-0.0003715
C	-3.3128202	2.8399157	-0.0005227
C	-3.2717813	1.3958513	-0.0004524
C	-4.5269237	0.7361945	-0.0002101
C	-5.7085744	1.4350660	-0.0000525
S	-1.6680617	3.4417652	-0.0008231
C	-1.0904728	1.7475828	-0.0008238
N	-2.0679365	0.8190991	-0.0006187
C	0.2372386	1.4631867	-0.0010187
S	0.7687657	-0.3190377	-0.0010166
N	1.2835062	2.2978614	-0.0012224
C	2.4933628	1.7402297	-0.0013884
C	2.4823412	0.1899125	-0.0013115
H	3.0104887	-0.1843149	0.8905541
H	3.0102020	-0.1844092	-0.8933036
O	3.5877124	2.3056246	-0.0015908
H	-4.4739261	4.6604285	-0.0004295
H	-6.6651359	0.9136911	0.0001339
Br	-4.5378820	-1.1629725	-0.0001056

S1 Energy = -4011.710603849723

O	-6.7829107	3.6274877	-0.0000102
C	-5.7500840	2.9238810	-0.0001261
C	-4.4317689	3.5471242	-0.0003866
C	-3.2788420	2.7497812	-0.0005274
C	-3.3110194	1.3393784	-0.0004453
C	-4.5919987	0.7416342	-0.0001902
C	-5.7608189	1.4779501	-0.0000238
S	-1.6406106	3.3008724	-0.0008041
C	-1.1150913	1.6245661	-0.0007993
N	-2.0771422	0.7305339	-0.0006072
C	0.2923759	1.3577569	-0.0010236
S	0.8186614	-0.3320233	-0.0011378
N	1.2191917	2.2868683	-0.0011642
C	2.4891504	1.7898465	-0.0013885
C	2.5314880	0.2469192	-0.0013424
H	3.0703789	-0.1065825	0.8892589
H	3.0702231	-0.1066770	-0.8920082
O	3.5235144	2.4402342	-0.0015856
H	-4.3849815	4.6365284	-0.0004720
H	-6.7312604	0.9838975	0.0001866
Br	-4.6826752	-1.1525073	-0.0000731

5- BrLuc

S0 Energy = -4011.801518284

O	-6.7891639	3.5566622	-0.0032265
C	-5.7123659	2.9455578	-0.0020496
C	-4.4263046	3.6087163	-0.0048395
C	-3.2568236	2.8885796	-0.0034073
C	-3.2398164	1.4495888	0.0009261
C	-4.4786221	0.7552349	0.0037855
C	-5.6411938	1.4692353	0.0023466
S	-1.6061438	3.4546740	-0.0061729
C	-1.0610640	1.7704864	-0.0014388
N	-2.0314378	0.8797553	0.0018765
C	0.3135098	1.4331837	-0.0013169
S	0.7500242	-0.2931721	0.0036376
N	1.2894669	2.3021346	-0.0046127
C	2.5322110	1.7265635	-0.0037090
C	2.4881321	0.1859963	0.0010092
H	3.0086956	-0.1874802	0.8932456

H	3.0074937	-0.1929026	-0.8896401
O	3.5923193	2.3188898	-0.0062399
H	-4.4424913	4.6989112	-0.0081132
Br	-7.2975886	0.5503267	0.0061108
H	-4.4737861	-0.3346915	0.0070588

S1 Energy = -4011.796387194

O	-6.7437212	3.6772546	-0.0031658
C	-5.7186254	2.9697383	-0.0018696
C	-4.3954213	3.5818131	-0.0044834
C	-3.2377910	2.7950392	-0.0030318
C	-3.2846579	1.3868124	0.0009242
C	-4.5476541	0.7623570	0.0035154
C	-5.7058689	1.5174540	0.0022117
S	-1.5935900	3.3370327	-0.0058902
C	-1.0840590	1.6554509	-0.0015344
N	-2.0491522	0.7671677	0.0016384
C	0.3244271	1.3753295	-0.0014447
S	0.8310340	-0.3204403	0.0041211
N	1.2604039	2.2930692	-0.0052328
C	2.5258156	1.7815085	-0.0041678
C	2.5505003	0.2384339	0.0013366
H	3.0856052	-0.1180970	0.8930933
H	3.0847145	-0.1245141	-0.8883520
O	3.5668260	2.4206560	-0.0070476
H	-4.3611156	4.6716393	-0.0076101
Br	-7.3876280	0.6456411	0.0056586
H	-4.5949914	-0.3270960	0.0065609

7-BrLuc

S0 Energy = -4011.759897560

O	-6.8117381	3.4595796	0.0029335
C	-5.7216478	2.8707448	0.0013385
C	-4.4348731	3.5452103	0.0045764
C	-3.2531015	2.8403188	0.0026474
C	-3.2340551	1.4008789	-0.0027133
C	-4.4737326	0.7034700	-0.0060358
C	-5.6422345	1.4048733	-0.0040951
S	-1.6157756	3.4241695	0.0058077
C	-1.0583751	1.7446135	-0.0001276
N	-2.0207710	0.8437951	-0.0040662
C	0.3182677	1.4165633	-0.0005116
S	0.7643403	-0.3082045	-0.0066373
N	1.2897944	2.2900858	0.0033428
C	2.5355001	1.7211731	0.0020153
C	2.4996733	0.1802397	-0.0037318
H	3.0212415	-0.1961605	0.8866843
H	3.0223923	-0.1895294	-0.8962514
O	3.5926833	2.3185410	0.0048960
Br	-4.4145662	5.4330358	0.0116693
H	-4.4573940	-0.3881333	-0.0100862
H	-6.6069278	0.8930852	-0.0065650

S1 Energy = -4011.795056788

O	-6.7843515	3.5880324	0.0033296
C	-5.7447304	2.9044070	0.0014106
C	-4.4133815	3.5294764	0.0045355
C	-3.2306306	2.7536740	0.0023402
C	-3.2794805	1.3475690	-0.0029263
C	-4.5444281	0.7235825	-0.0060107
C	-5.7124689	1.4607122	-0.0039673
S	-1.5979460	3.3016099	0.0053605
C	-1.0783132	1.6198572	-0.0006018
N	-2.0425238	0.7318175	-0.0044872
C	0.3286271	1.3500736	-0.0007245
S	0.8529965	-0.3429053	-0.0066833
N	1.2604692	2.2750099	0.0033161
C	2.5278859	1.7751634	0.0022345
C	2.5671773	0.2317636	-0.0034626
H	3.1050927	-0.1254000	0.8863331
H	3.1061519	-0.1188499	-0.8952208
O	3.5658623	2.4214073	0.0053212
Br	-4.3248798	5.3856081	0.0115190
H	-4.5783246	-0.3683564	-0.0101170
H	-6.6841035	0.9640973	-0.0064089

4- MeLuc

S0 Energy = -1478.088011145

O	-6.7289911	3.6696745	0.1913071
C	-5.6462956	3.0556790	0.1448748
C	-4.3628723	3.7243125	0.1703403
C	-3.2120188	2.9786822	0.1159915
C	-3.2188915	1.5384587	0.0332927
C	-4.4734377	0.8442514	0.0057794
C	-5.6163495	1.5904697	0.0601384
S	-1.5496031	3.5138645	0.1303052
C	-1.0300675	1.8237117	0.0282129
N	-2.0236779	0.9534131	-0.0120204
C	0.3317961	1.4617994	-0.0055679
S	0.7361893	-0.2737558	-0.1086860
N	1.3317126	2.3070498	0.0332729
C	2.5582984	1.7081919	-0.0125856

C	2.4835405	0.1702327	-0.0997177
H	3.0048742	-0.2654432	0.7634767
H	2.9882448	-0.1637733	-1.0164602
O	3.6344090	2.2745939	0.0095662
H	-4.3577533	4.8128363	0.2329169
H	-6.5944928	1.1028612	0.0418039
C	-4.4736565	-0.6513604	-0.0804322
H	-3.9323021	-1.0920052	0.7700719
H	-3.9493620	-0.9907338	-0.9862696
H	-5.4982936	-1.0444203	-0.0931215

S1 Energy = -1478.082134380

O	-6.6779253	3.7824044	0.1953789
C	-5.6490293	3.0707318	0.1448208
C	-4.3262277	3.6881794	0.1673760
C	-3.1826178	2.8786365	0.1099713
C	-3.2464733	1.4742763	0.0302688
C	-4.5205391	0.8479191	0.0068018
C	-5.6650538	1.6286263	0.0625463
S	-1.5324555	3.3972284	0.1236619
C	-1.0390233	1.7134407	0.0225788
N	-2.0221457	0.8405881	-0.0178082
C	0.3593483	1.4138128	-0.0081401
S	0.8339124	-0.2913576	-0.1105285
N	1.3180212	2.3095386	0.0338866
C	2.5701496	1.7738355	-0.0090095
C	2.5640177	0.2324909	-0.0974541
H	3.1006792	-0.1871462	0.7654081
H	3.0831631	-0.0848006	-1.0131317
O	3.6265641	2.3888358	0.0160158
H	-4.2707046	4.7754887	0.2290530
H	-6.6489219	1.1548158	0.0449379
C	-4.5722930	-0.6454579	-0.0781855
H	-4.0387859	-1.1020709	0.7704853
H	-4.0551937	-1.0016460	-0.9832228
H	-5.6074663	-1.0097794	-0.0892209

4- NO2Luc

S0 Energy = -1643.004485500

O	-6.6716535	3.7795938	0.0392606
C	-5.6022913	3.1447406	0.0425758
C	-4.3034886	3.7672875	0.1458032
C	-3.1622209	2.9986553	0.1343024
C	-3.1663606	1.5611215	0.0506429
C	-4.4494033	0.9444739	-0.0401944
C	-5.5966781	1.6829409	-0.0642181
S	-1.5016991	3.5322032	0.1925347
C	-0.9882898	1.8467572	0.0781756
N	-1.9672870	0.9748159	0.0095526
C	0.3863382	1.4875774	0.0579656
S	0.7974883	-0.2345817	-0.0702303
N	1.3663416	2.3458318	0.1260171
C	2.6056996	1.7562443	0.0850187
C	2.5415623	0.2221378	-0.0325558
H	3.0544466	-0.2286100	0.8278206
H	3.0577689	-0.0925329	-0.9496267
O	3.6691426	2.3375659	0.1327893
H	-4.2684630	4.8547504	0.2170523
H	-6.5607791	1.1823507	-0.1478717
N	-4.5671021	-0.5134866	-0.0856172
O	-5.4529445	-0.9869424	-0.7741445
O	-3.7948987	-1.1644147	0.5844472

S1 Energy = -1642.996545840

O	-6.6112305	3.7849343	0.0756080
C	-5.5533597	3.1251624	0.0551514
C	-4.2708721	3.7845577	0.1141690
C	-3.1456507	2.9991767	0.0878316
C	-3.1733807	1.5530182	0.0044345
C	-4.4634897	0.8915421	-0.0550061
C	-5.5885375	1.6660192	-0.0291869
S	-1.4918092	3.5435405	0.1467973
C	-0.9898621	1.8685851	0.0591965
N	-1.9613612	0.9884769	-0.0076009
C	0.3929918	1.5039038	0.0617680
S	0.7853808	-0.2144043	-0.0301058
N	1.3664039	2.3662261	0.1278657
C	2.6078416	1.7682956	0.1148656
C	2.5326992	0.2341911	0.0255132
H	3.0286337	-0.2063583	0.9010951
H	3.0590472	-0.1042995	-0.8772949
O	3.6693112	2.3495825	0.1665100
H	-4.2487547	4.8716956	0.1769733
H	-6.5579811	1.1741717	-0.0734083
N	-4.6069636	-0.5289665	-0.1388763
O	-5.7797432	-0.9839310	-0.1839657
O	-3.5740852	-1.2366398	-0.1628346

PhLuc

S0 Energy = -1669.912412725

C	-4.1280261	1.5123750	-0.9205689
C	-2.8911687	2.0724997	-1.1738410
C	-1.7259689	1.3986597	-0.7678764
C	-1.8531346	0.1541857	-0.1046469
C	-3.0992199	-0.4196775	0.1557670
C	-4.2379135	0.2703006	-0.2583526
H	-5.0506768	2.0126871	-1.2243315
H	-2.7989722	3.0331965	-1.6860730
H	-3.1855810	-1.3823779	0.6694253
N	-0.4425174	1.8313777	-0.9522469
S	-0.2753623	-0.4471026	0.2773263
C	0.4221124	0.9963512	-0.4719817
C	6.0909405	1.8401647	-0.7401270
S	6.7339756	3.3128693	-1.4901904
N	6.9286838	0.9832402	-0.2700457
C	8.3985643	2.7311018	-1.1412883
C	8.2584533	1.3665460	-0.4361113
H	8.9348041	3.4353938	-0.4846741
H	8.9798682	2.6118148	-2.0699706
O	9.2106609	0.7284437	-0.0819067
O	-5.4854805	-0.1999840	-0.0541927
H	-5.4483588	-1.0534333	0.4041399
C	1.8704091	1.1956671	-0.5278513
C	2.3718137	2.3602593	-1.1329548
C	2.7744053	0.2606057	0.0014840
C	4.1416482	0.4790868	-0.0717551
C	4.6412507	1.6425490	-0.6773547
C	3.7384483	2.5786060	-1.2053584
H	4.1099944	3.4916067	-1.6817698
H	1.6614130	3.0819078	-1.5419557
H	2.4039707	-0.6529602	0.4775347
H	4.8540286	-0.2420019	0.3356333

S1 Energy = -1669.907790024

C	-4.1345190	1.5161512	-0.9225135
C	-2.9056126	2.0808504	-1.1739263
C	-1.7199988	1.4094482	-0.7693635
C	-1.8365674	0.1457184	-0.1006712
C	-3.0668178	-0.4284533	0.1560677
C	-4.2258457	0.2651143	-0.2601670
H	-5.0640460	2.0061963	-1.2209080
H	-2.8130449	3.0428679	-1.6828595
H	-3.1549091	-1.3928214	0.6665925
N	-0.4653621	1.8581378	-0.9596429
S	-0.2495288	-0.4477775	0.2778284
C	0.4334037	1.0134422	-0.4757310
C	6.0692092	1.8457007	-0.7436104
S	6.7409010	3.3130397	-1.5032677
N	6.9206078	0.9798131	-0.2621570
C	8.3966950	2.7092964	-1.1395569
C	8.2346135	1.3455902	-0.4232917
H	8.9413729	3.4102003	-0.4850867
H	8.9842315	2.5763588	-2.0633095
O	9.2009639	0.7116583	-0.0653842
O	-5.4499490	-0.2186282	-0.0523532
H	-5.4162954	-1.0762703	0.4049800
C	1.8531169	1.2069677	-0.5288917
C	2.3642311	2.3821573	-1.1401224
C	2.7704504	0.2642417	0.0048302
C	4.1274268	0.4801816	-0.0685724
C	4.6413433	1.6564704	-0.6821865
C	3.7242670	2.5988236	-1.2132300
H	4.0999268	3.5098186	-1.6889918
H	1.6564200	3.1064014	-1.5499651
H	2.4012647	-0.6504480	0.4828250
H	4.8451151	-0.2362891	0.3365216

6' – deoxyLuc

S0 Energy = -1364.262556246

C	-3.8887853	0.5411853	0.0180407
C	-3.9813083	-0.8641396	0.0333510
C	-2.8472751	-1.6632313	0.0353918
H	-4.9657325	-1.3351363	0.0428777
C	-2.6586667	1.1731746	0.0050638
H	-4.8026377	1.1368910	0.0154811
C	-1.4949478	0.3864087	0.0077234
H	-2.5681963	2.2595490	-0.0081928
C	-1.6014809	-1.0284963	0.0224105
H	-2.9301269	-2.7502593	0.0459045
N	-0.2139126	0.8614673	-0.0042680
S	-0.0171715	-1.7323308	0.0190287
C	0.6414379	-0.1116984	-0.0006608
C	2.0829149	0.0893377	-0.0129804
S	2.6897696	1.7383480	-0.0324891
N	2.9128232	-0.8948249	-0.0102107
C	4.3652767	1.0675144	-0.0392240
C	4.2416239	-0.4637484	-0.0226020
H	4.9265511	1.3996161	0.8443366
H	4.9118806	1.3813354	-0.9385757
O	5.1979637	-1.1909620	-0.0204063

S1 Energy = -1364.230020612

C	-3.8559532	0.5712146	0.0087144
C	-3.9801107	-0.8276326	-0.0767330
C	-2.8552328	-1.6466446	-0.0950343
H	-4.9723293	-1.2785667	-0.1279337
C	-2.6136292	1.1765583	0.0796964
H	-4.7565146	1.1873864	0.0202942
C	-1.4550570	0.3728865	0.0672685
H	-2.5053782	2.2595641	0.1460202
C	-1.6012735	-1.0435992	-0.0229363
H	-2.9574920	-2.7302281	-0.1616933
N	-0.1826011	0.8234438	0.1372677
S	-0.0334010	-1.7961254	-0.0189254
C	0.6835525	-0.1825684	0.0994154
C	2.0575145	0.0104766	0.1765614
S	2.7004163	1.6696698	0.3979463
N	3.0050565	-0.9447297	0.1866544
C	4.2720697	1.0967426	-0.1928708
C	4.2224603	-0.4725259	0.1487035
H	5.1188655	1.6225679	0.2616548
H	4.3679470	1.0850764	-1.2904330
O	5.3410903	-0.9529663	0.2563626

6'-MethoxyLuc

S0 Energy = -1478.585905861

C	-1.9457970	4.8111594	0.6845139
C	-0.6014930	5.0305282	0.4054565
C	-2.5278098	3.6288309	0.2233707
C	-1.7700652	2.6829162	-0.5062453
C	-0.4334305	2.9108234	-0.7785140
C	0.1743274	4.0905754	-0.3264205
H	-2.2352423	1.7647298	-0.8604312
S	0.3912284	6.3856428	0.8378426
N	1.4763897	4.4471802	-0.5197342
C	1.7296041	5.5970213	0.0209326
C	3.0327088	6.2358887	-0.0217056
N	3.2560264	7.3808234	0.5256109
S	4.3402938	5.4041219	-0.8533971
C	5.4209665	6.7867227	-0.4324256
C	4.5770564	7.7980662	0.3590192
H	5.8164506	7.2677286	-1.3369697
H	6.2664107	6.4530192	0.1838765
O	5.0296732	8.8297438	0.7783827
H	0.1572773	2.1868500	-1.3402255
H	-2.5554427	5.5199750	1.2436690
O	-3.8308072	3.4632503	0.5189803
C	-4.4987251	2.3008076	0.0942555
H	-5.5301848	2.3930159	0.4477822
H	-4.0472212	1.3953547	0.5305478
H	-4.4999112	2.2162513	-1.0043316

S1 Energy = -1478.580085938

C	-1.8830714	4.7861949	0.6530733
C	-0.5388785	4.9784218	0.3602200
C	-2.5226898	3.5843639	0.1975980
C	-1.8064591	2.6305781	-0.5233447
C	-0.4547536	2.8521572	-0.8025455
C	0.2029577	4.0230497	-0.3696471
H	-2.2836720	1.7170192	-0.8717882
S	0.4740507	6.3254358	0.7825550
N	1.5078183	4.3379954	-0.5857000
C	1.8023033	5.5113490	-0.0448518
C	3.0585498	6.1795059	-0.0584263
N	3.2276935	7.3498519	0.5172052
S	4.4434269	5.4342124	-0.8657924
C	5.4314980	6.8726580	-0.3890814
C	4.5033062	7.8273186	0.3954081
H	5.8282793	7.3874346	-1.2750250
H	6.2774763	6.5748132	0.2457066
O	4.9219653	8.8806493	0.8346122
H	0.1181310	2.1142760	-1.3659913
H	-2.4780628	5.5069822	1.2143548
O	-3.8099637	3.4991991	0.5308661
C	-4.5550478	2.3653572	0.1431859
H	-5.5683465	2.5186056	0.5234362
H	-4.1262099	1.4509222	0.5814733
H	-4.5780176	2.2726754	-0.9536606